Non-Geometric Compactifications and String Cosmology in the Swampland

Guoen Nian
念国恩

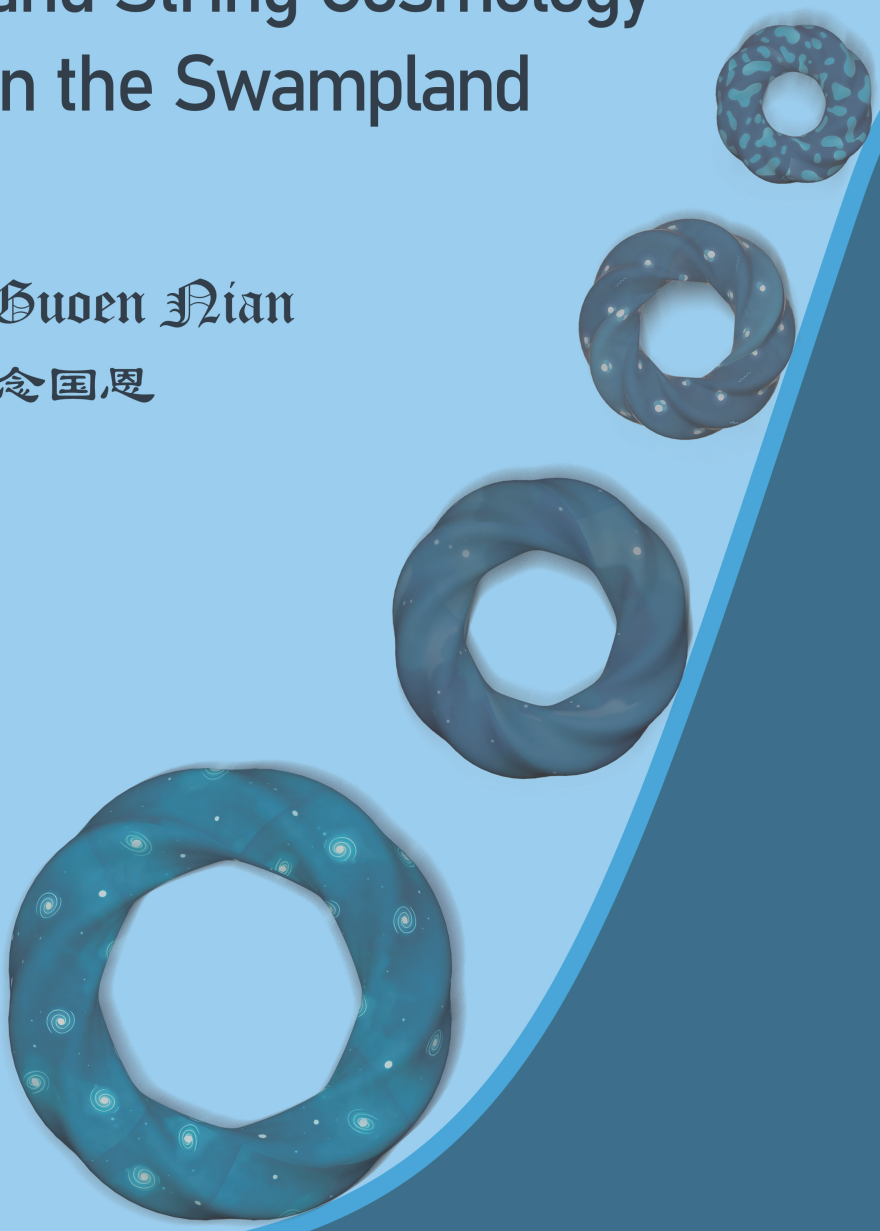

Non-Geometric Compactifications and String Cosmology in the Swampland

Guoen Nian

PhD thesis, Utrecht University, August 2025

ISBN: 978-90-393-7983-7

DOI: 10.33540/3262

About the cover: The picture shows a sequence of twisted tori rolling down a slope that represents a candidate scalar potential on field space. The potential features a de Sitter-like minimum and a nearby maximum in the interior of field space, then decreases exponentially from right to left. The twisted torus schematically symbolizes the non-geometric internal space of string-theory compactifications. As the torus descends, one of its radii grows, encoding the increasing expectation value of a modulus. During this process, the universe evolves in step with this descent, conveyed by patterns on the tori. These patterns trace the universe's history: reheating, Big Bang nucleosynthesis, recombination, the emergence of galaxies, and culminate in the present-day cosmos on the back cover. These cosmic textures are adapted from the "History of the Universe" image on NASA's website.

Non-Geometric Compactifications and String Cosmology in the Swampland

Niet-geometrische compactificaties en
snaarcosmologie in het Swampland

(met een samenvatting in het Nederlands)

Proefschrift

ter verkrijging van de graad van doctor aan de
Universiteit Utrecht
op gezag van de
rector magnificus, prof. dr. ir. W. Hazeleger,
ingevolge het besluit van het college voor promoties
in het openbaar te verdedigen op

dinsdag 2 december 2025 des middags te 12.15 uur

door

Guoen Nian

geboren op 2 februari 1997
te Liaocheng, Shandong, China

Promotoren:

Prof. dr. S.J.G. Vandoren
Prof. dr. T.W. Grimm

Beoordelingscommissie:

Prof. A. Acúcarro
Prof. dr. E.L.M.P. Laenen
Dr. M. Montero
Prof. dr. D. Roest
Prof. dr. ir. H.T.C. Stoof

Publications

Chapter II is based on the work

[1] Julian Freigang, Dieter Lüst, Guo-En Nian and Marco Scalisi,
Cosmic Acceleration and Turns in the Swampland,
JCAP 11 (2023) 080, [**arXiv: 2306.17217**].

Chapter III is based on the work

[2] Guo-En Nian and Stefan Vandoren,
Towards a String Realization of the Dark Dimension via T-folds,
JHEP 08 (2025) 106, [**arXiv: 2411.19216**].

In **Chapter IV**, Section IV.1–Appendix IV.B is based on the work

[3] George Gkountoumis, Chris Hull, Guo-En Nian and Stefan Vandoren,
Duality and Infinite Distance Limits in Asymmetric Freely Acting Orbifolds,
JHEP 09 (2025) 198, [**arXiv: 2506.11699**].

This work also appears in George Gkountoumis's dissertation, *Strings on Freely Acting Orbifolds: Spectra, Moduli Spaces, and Branes*, which is scheduled for publication in the same year as this thesis. The majority of the results were obtained through joint collaboration. In the course of this work, the author focused more on the Swampland conjectures and the decompactification spectra, while George Gkountoumis focused more on the detailed computation of partition functions and the 4D spectrum.

Appendix IV.C–Appendix IV.D is based on the unfinished work

[4] George Gkountoumis, Guo-En Nian and Stefan Vandoren,
Quantum Corrections to the Moduli Space in Asymmetric Freely Acting Orbifolds,
to be published.

Contents

Chapter I

Introduction and Preliminaries

I.1 Introduction

Modern physics has achieved two monumentally successful theoretical frameworks: the Standard Model (SM) of particle physics and the Λ Cold Dark Matter (ΛCDM) model of cosmology.

The Standard Model is a renormalizable quantum field theory of three generations of quarks and leptons interacting via gauge bosons, based on the $\mathrm{SU(3)_c} \times \mathrm{SU(2)_L} \times \mathrm{U(1)_Y}$ gauge group, and excluding gravity. The $\mathrm{SU(2)_L} \times \mathrm{U(1)_Y}$ electroweak sector unifies weak interactions with electromagnetism and is spontaneously broken to $\mathrm{U(1)_{em}}$ when the Higgs doublet acquires a vacuum expectation value at the electroweak scale $\sim 246\,\mathrm{GeV}$, giving masses to the $W^{\pm}$ and Z^0 while leaving the photon massless. The W, Z bosons were discovered in 1983 and the Higgs boson in 2012 [1, 2]. The $\mathrm{SU(3)_c}$ sector is quantum chromodynamics (QCD), accounting for the behavior of quarks and gluons constructing hadrons, exhibiting asymptotic freedom at short interaction distances and color confinement at long distances.

The ΛCDM model is the concordance cosmological framework built on general relativity (GR) and a nearly homogeneous and isotropic universe. It is a simple 6-parameter model that, with the addition of inflation, explains a wide range of cosmic observations. Today's energy density of the Universe is dominated by the dark sector: $\sim 68\%$ dark energy, modeled as a cosmological constant, and $\sim 27\%$ cold dark matter, with the remainder in baryons and radiation [3]. The presence of dark energy drives the observed late-time accelerated expansion. At early times, the model accounts for light-element abundances via Big Bang Nucleosynthesis and predicts the existence and near-blackbody spectrum of the Cosmic Microwave Background (CMB). Given initial conditions inferred from the CMB, ΛCDM also reproduces the statistical properties of large-scale structure and galaxy clustering observed today.

Despite the triumphs of both models, a closer inspection reveals many fundamental problems. The Standard Model contains no particle that accounts for dark matter or dark energy. It features around twenty free parameters, whose values are fixed empirically with no underlying explanation or organizing principle. Furthermore, it suffers from the hierarchy problem, whereby radiative quantum corrections drive the Higgs mass toward the ultraviolet cutoff, whereas the observed value is only about $125\,\mathrm{GeV}$. This requires unnatural fine-tuning of the bare Higgs mass to cancel large quantum contributions. In addition, the matter-antimatter asymmetry in the observable universe cannot be explained by the CP-violating processes present in the SM. Issues such as neutrino masses and the near-vanishing of CP violation in QCD (the strong CP problem) are likewise beyond the framework of the Standard Model.

Similarly, largely because the dark sector lacks a microscopic interpretation, the ΛCDM model faces several outstanding problems. The observed cosmological constant that drives late-time acceleration is much smaller than naive QFT zero-point energy estimates by 10^{122}, requiring an extremely fine-tuned cancellation between the bare Λ in GR and quantum contributions from the Standard

Model. Extrapolating ΛCDM backward in time leads to an initial singularity, and spacetime singularities (the Big Bang and those inside black holes) signal the breakdown of classical general relativity and the need for a quantum theory of gravity. Within inflationary cosmology, puzzles remain, including how to achieve a graceful exit and why the inflationary energy scale is so small compared with the Planck scale. On the observational side, recent analyses [4–7] favor dynamical dark energy over a strict cosmological constant, and some studies [8–10] report possible deviations from isotropy or unusual large-angle alignments in the CMB.

Taken together, these problems indicate that the Standard Model and ΛCDM model are merely low-energy effective approximations of more fundamental laws, valid below their cutoff scales. In addition, perturbative quantization of Einstein gravity in the QFT technique is non-renormalizable and requires an infinite number of counterterms. These facts motivate a consistent, predictive theory of *Quantum Gravity* (QG) that reconciles GR with quantum field theory, and ideally, unifies with fundamental forces in the Standard Model[1].

To date, string theory is the most developed and arguably the only consistent candidate for quantum gravity. Its fundamental objects are one-dimensional strings, open or closed, whose normal modes correspond to particles with definite mass, spin, and charges. The resulting spectrum includes many new states, providing plausible dark matter candidates such as axions or the lightest supersymmetric particles. It offers a unifying framework for all matter and forces, including the graviton, reproducing Einstein gravity as an effective theory. Notably, the spectrum is tightly constrained by the mathematical consistency of string theory, including anomaly cancellation, duality, and compactification setups, so the theory functions as a first principle framework rather than one guided by empirical input. In addition, unlike the Standard Model, the worldsheet description introduces only a single fundamental parameter: the string tension $1/2\pi\alpha'$, while parameters in effective field theories (EFTs) can arise from moduli stabilization in the string spectrum. Problems in QFT, such as short-distance UV singularities, are mitigated by the extended nature of strings.

The mathematical consistency of string theory requires ten spacetime dimensions and supersymmetry[2], neither of which is manifest in our Universe. Consequently, six spatial dimensions must be compactified and spacetime supersymmetry must be broken. Engineering such compactifications and supersymmetry reductions, and deriving the associated low-energy effective theories—including their spectra, interactions, and potentials—falls under the area of *string phenomenology*.

In this framework, a string compactification is specified by choosing a six-dimensional compact manifold and can be systematically enriched by turning on fluxes, imposing orbifold or orientifold projections, and introducing brane configu-

[1] Many researchers also expect the existence of a Grand Unified Theory (GUT), which unifies strong interaction and electroweak interaction.

[2] One can formulate a non-supersymmetric string theory with only bosonic degrees of freedom on the worldsheet, which we introduce in Subsection I.2.1. However, bosonic string theory lives in 26 spacetime dimensions, far from the four of our Universe, and contains no fermion spectrum.

rations, thereby generating a broad class of consistent models. Fixing the moduli at specific expectation values determines a low-energy effective field theory, which defines a *vacuum* of string theory. The collection of these vacua is known as the *Landscape* of string theory. Note that, distinct compactifications can produce the same effective theory, which is known as *duality* (see Subsection I.3.3). Although finite, the string Landscape is extraordinarily large: estimates include $\mathcal{O}\left(10^{500}\right)$ type IIB Calabi–Yau flux vacua [11, 12], and $\mathcal{O}\left(10^{272000}\right)$ F-theory flux vacua for an elliptic Calabi–Yau fourfold [13]. Large though it is, the Landscape remains a small subset of EFTs, since it only consists of those that admit a consistent ultraviolet completion in quantum gravity; whereas the rest lie in the *Swampland* [14].

Characterizing the boundary between the Landscape and the Swampland reveals universal properties of QG-consistent EFTs, thereby guiding model building and offering bottom-up insight into quantum gravity. A set of conjectural criteria that delineate this boundary is collectively known as the *Swampland program*. We will introduce the Swampland conjectures in Section I.5 and investigate string phenomenology in light of them throughout this thesis. Verifying and sharpening these conjectures, particularly through various string compactifications, is an important goal in the research area. In this thesis, we focus on non-geometric compactifications (see Subsection I.3.5), which, compared to geometric compactifications such as Calabi–Yau, have been far less studied, especially in the context of the Swampland program.

Returning to the physics of our Universe, string phenomenology has two principal aims: deriving the observed particle spectrum, including the Standard Model and dark sector states, and realizing cosmology, especially the nature of dark energy. In this thesis we focus on the latter, namely string cosmology (see Section I.4 and Subsection II.3.3). In string compactifications, the cosmic acceleration is governed by the scalar potential, which is determined by the spectrum of scalar fields and their stabilization. While the cosmological constant problem is a deep challenge, the vast Landscape may furnish vacua with a small cosmological constant or appropriate dynamical dark energy. Moreover, the Swampland program imposes nontrivial constraints on such potentials. In our thesis, we will test some Swampland conjectures in cosmological settings and analyze their implications for string cosmology.

I.2 String theory

In this section, we present a concise and formal overview of perturbative string theory, laying the groundwork for the later discussions of compactifications, dualities, and various aspects of string phenomenology. Our presentation is guided by textbooks and lecture notes on string theory collected in [15–22], to which the interested reader is referred for comprehensive treatments. We begin with bosonic string theory to introduce the essential concepts, then transition to type II superstring theory.

I.2.1 Bosonic string theory

The evolution of a point particle in spacetime traces out a one-dimensional worldline. Analogously, the evolution of a one-dimensional string traces out a two-dimensional surface known as the worldsheet embedded in the background spacetime. We can parametrize this $(1+1)$-dimensional worldsheet with coordinates $\{\sigma^\alpha\}$, $\alpha = 0, 1$, where σ^0 is the worldsheet time parameter and σ^1 is the space parameter along the string length. The dynamics of the worldsheet in a flat background is described by the Polyakov action:

$$S_{\mathrm{P}} = -\frac{T}{2}\int_\Sigma \mathrm{d}^2\sigma\sqrt{-h}h^{\alpha\beta}\partial_\alpha X^\mu \partial_\beta X^\nu \eta_{\mu\nu}\,, \tag{I.2.1}$$

where $T \equiv 1/2\pi\alpha'$ is the string tension, with α' being the Regge slope, which defines the string length scale $\ell_s \equiv 2\pi\sqrt{\alpha'}$. $h^{\alpha\beta}$ is the inverse metric of the worldsheet, and X^μ are the embedding functions that map the worldsheet into the spacetime (target space). This action gives simple equations of motion

$$\partial^\alpha\partial_\alpha X^\mu = 0\,. \tag{I.2.2}$$

From this perspective, the spacetime coordinates can be interpreted as 2-dimensional bosonic fields on the worldsheet.

A key feature of the Polyakov action (I.2.1) is its invariance under two local symmetries on the worldsheet: diffeomorphisms (reparameterization invariance)

$$X'^\mu(\sigma') = X^\mu(\sigma)\,, \qquad h'_{\gamma\delta}(\sigma')\frac{\partial\sigma'^\gamma}{\partial\sigma'^\alpha}\frac{\partial\sigma'^\delta}{\partial\sigma'^\beta} = h_{\alpha\beta}(\sigma)\,, \tag{I.2.3}$$

and Weyl invariance

$$X'^\mu(\sigma) = X^\mu(\sigma)\,, \qquad h'_{\gamma\delta}(\sigma) = e^{2\omega(\sigma)}h_{\alpha\beta}(\sigma)\,, \tag{I.2.4}$$

with $\omega(\sigma)$ an arbitrary function. These symmetries imply a redundancy in the degrees of freedom of the worldsheet metric. We can take the conformal gauge to fix it by setting the metric $h_{\alpha\beta}(\sigma) = \eta_{\alpha\beta}$. With this gauge, we can reparametrize to light-cone coordinates $\sigma^+ = \sigma^0 + \sigma^1$, $\sigma^- = \sigma^0 - \sigma^1$, which are holomorphic and anti-holomorphic coordinates respectively. The equations of motion (I.2.2) become

$$\partial_+\partial_- X^\mu = 0\,. \tag{I.2.5}$$

The general solution can then be decomposed into left-moving and right-moving modes:

$$X^\mu(\sigma) = X^\mu_{\mathrm{L}}\left(\sigma^+\right) + X^\mu_{\mathrm{R}}\left(\sigma^-\right)\,, \tag{I.2.6}$$

where X^μ_{L} is the left-moving part of the string which is holomorphic, and X^μ_{R} is the right-moving part of the string which is anti-holomorphic. After fixing to conformal gauge, the residual gauge freedom consists precisely of holomorphic and anti-holomorphic coordinate transformations, which is the infinite-dimensional conformal group on the worldsheet. It is a subgroup of diffeomorphisms, which

can be undone by a Weyl transformation. Thus, bosonic string theory in the conformal gauge is described by a 2-dimensional conformal field theory on the worldsheet.

Within the framework of this CFT, the energy-momentum tensor $T(\sigma)$ in light-cone coordinates has $T_{+-} = 0$. Another two components have mode expansions

$$T_{++}\left(\sigma^{+}\right) = \sum_{n\in\mathbb{Z}} L_n e^{-in\sigma^{+}}, \qquad T_{--}\left(\sigma^{-}\right) = \sum_{n\in\mathbb{Z}} \widetilde{L}_n e^{-in\sigma^{-}}. \tag{I.2.7}$$

The above Fourier coefficients satisfy two independent copies of the Virasoro algebra, which is a quantum extension of the classical algebra of conformal transformations:

$$\begin{aligned} [L_m, L_n] &= (m-n)L_{m+n} + \frac{c}{12} m\left(m^2-1\right)\delta_{m,-n}\,, \\ \left[\widetilde{L}_m, \widetilde{L}_n\right] &= (m-n)\widetilde{L}_{m+n} + \frac{\tilde{c}}{12} m\left(m^2-1\right)\delta_{m,-n}\,, \end{aligned} \tag{I.2.8}$$

where $c, \tilde{c}$ are the central charges, and physical constraints require $c = \tilde{c}$.

To determine the dynamics of the string, the equations of motion must be supplemented with boundary conditions for $X^{\mu}(\sigma)$. The choice of boundary conditions distinguishes between two fundamental types of bosonic strings: closed strings, with boundary conditions

$$X^{\mu}(\sigma^0, \sigma^1 + 2\pi) = X^{\mu}(\sigma^0, \sigma^1)\,, \tag{I.2.9}$$

and open strings, which have endpoints that must satisfy a condition ensuring no momentum flows off:

$$n^{\alpha}\partial_{\alpha} X^{\mu}\delta X_{\mu}(\sigma^0, \sigma^1 = 0, \pi) = 0\,, \tag{I.2.10}$$

where n^{α} denotes the normal vector at the boundary.

This thesis will focus primarily on closed strings. With the boundary conditions (I.2.9), the closed string has an oscillator expansion:

$$\begin{aligned} X^{\mu}_{\mathrm{L}}(\sigma^{+}) &= \frac{1}{2}x^{\mu} + \frac{\alpha'}{2}p^{\mu}\sigma^{+} + i\sqrt{\frac{\alpha'}{2}}\sum_{n\neq 0}\frac{\alpha^{\mu}_n}{n}e^{-in\sigma^{+}}, \\ X^{\mu}_{\mathrm{R}}(\sigma^{-}) &= \frac{1}{2}x^{\mu} + \frac{\alpha'}{2}p^{\mu}\sigma^{-} + i\sqrt{\frac{\alpha'}{2}}\sum_{n\neq 0}\frac{\tilde{\alpha}^{\mu}_n}{n}e^{-in\sigma^{-}}. \end{aligned} \tag{I.2.11}$$

where x^{μ} represents the center-of-mass position of the string, and the total momentum p^{μ} is its generator.

Analogous to the quantization of point particles in QFT, the classical string can be quantized using either canonical quantization or path integral quantization. We will begin with the former. In canonical quantization, the Fourier modes of X^{μ}_{L} and X^{μ}_{R} have commutation relations

$$[x^{\mu}, p^{\nu}] = i\eta^{\mu\nu}\,, \quad [\alpha^{\mu}_m, \alpha^{\nu}_n] = [\tilde{\alpha}^{\mu}_m, \tilde{\alpha}^{\nu}_n] = m\delta_{m+n}\eta^{\mu\nu}\,, \quad [\alpha^{\mu}_m, \tilde{\alpha}^{\nu}_n] = 0\,. \tag{I.2.12}$$

Here $\alpha^\mu_{n<0}$ and $\tilde{\alpha}^\mu_{n<0}$ are creation operators, and $\alpha^\mu_{n>0}$ and $\tilde{\alpha}^\mu_{n>0}$ are annihilation operators. The Virasoro generators can be expressed in terms of these oscillators as

$$L_n = \frac{1}{2}\sum_{m\in\mathbb{Z}} :\alpha_{n-m}\cdot\alpha_m:\,, \qquad \widetilde{L}_n = \frac{1}{2}\sum_{m\in\mathbb{Z}} :\tilde{\alpha}_{n-m}\cdot\tilde{\alpha}_m:\,, \tag{I.2.13}$$

with $\alpha^\mu_0 = \sqrt{\frac{\alpha'}{2}}p^\mu$. And in particular,

$$L_0 = \frac{1}{2}\alpha' p^\mu p_\mu + N\,, \qquad \widetilde{L}_0 = \frac{1}{2}\alpha'\tilde{p}^\mu\tilde{p}_\mu + \widetilde{N}\,. \tag{I.2.14}$$

Here

$$N = \sum_{n=1}^{\infty}\alpha_{-n}\cdot\alpha_n\,, \qquad \widetilde{N} = \sum_{n=1}^{\infty}\tilde{\alpha}_{-n}\cdot\tilde{\alpha}_n \tag{I.2.15}$$

are number operators, which count the excitation level of the left- and right-moving modes.

The spectrum of closed strings is generated by the creation operators α^μ_{-n} and $\tilde{\alpha}^\mu_{-n}$, $n>0$. Note that in the conformal gauge, the equation of motion gives $T_{++} = T_{--} = 0$ on-shell. It translates into the Virasoro constraints, that the Fourier modes annihilate physical states in the spectrum:

$$L_n\,|\text{phys}\rangle = \widetilde{L}_n\,|\text{phys}\rangle = 0\,, \quad (L_0 - a)\,|\text{phys}\rangle = \left(\widetilde{L}_0 - a\right)|\text{phys}\rangle = 0\,, \tag{I.2.16}$$

where a is the normal ordering constant as an ambiguity arising from quantization. Combining with (I.2.14), the mass of a physical state is given by

$$m^2 = m_{\text{L}}^2 + m_{\text{R}}^2 = \frac{2}{\alpha'}\left(N + \widetilde{N} - 2a\right)\,. \tag{I.2.17}$$

Furthermore, the periodicity of the closed string requires the vanishing of the worldsheet momentum $P = L_0 - \widetilde{L}_0 = 0$, which is called the level-matching condition, giving $m^2_{\text{L}} = m^2_{\text{R}}$ and here $N = \widetilde{N}$.

By computing expectation values of the Virasoro algebra (I.2.8) and comparing with (I.2.12), it can be found that each bosonic field X^μ in 2D CFT has one central charge $c_{\text{b}} = 1$, and the dimension of spacetime $D = \sum c_b$ is the central charge in a pure Polyakov theory. Here comes a central question: In bosonic string theory, what is the number of spacetime dimensions? It can be determined from two aspects. Firstly, according to the commutation relations between X^μ and their dual momenta in the light-cone covariant quantization of bosonic string theory, spacetime Lorentz invariance is preserved only when the number of dimensions $D = 26$ and the normal ordering constant $a = 1$; secondly, the worldsheet Weyl symmetry keeps the energy-momentum tensor trace $\langle T^\alpha{}_\alpha\rangle = 0$ classically. But at the quantum level, the trace is generally non-zero and proportional to the renormalization group beta function. It can be computed that, the trace $\langle T^\alpha{}_\alpha\rangle = -\frac{1}{12}c_{\text{tot}}R^{(2)}$, where $R^{(2)}$ is the worldsheet Ricci scalar. Hence, to cancel this Weyl

anomaly, the total central charge must be zero. The BRST quantization on the worldsheet involves (b, c)-ghosts which have $c_{\rm gh} = -26$, such that in total

$$c_{\rm tot} = c_{\rm gh} + 26c_{\rm b} = 0\,, \tag{I.2.18}$$

if there are 26 spacetime dimensions.

For bosonic strings, $N = \widetilde{N}$ acts on a basis physical state $|\text{phys}\rangle$ giving a natural number. We can find that the ground state has

$$N = \widetilde{N} = 0, \qquad m^2 = -\frac{4}{\alpha'}\,. \tag{I.2.19}$$

The ground state is a tachyon which has a negative mass square. It corresponds to a local maximum of the potential such that a vacuum with tachyons is unstable. Meanwhile, the propagator of the tachyon violates unitarity and the one-loop amplitude of tachyons is IR-divergent. This indicates the inconsistency of bosonic strings, which can be solved by imposing supersymmetry and GSO projection. We will describe them in the next subsection.

The massless spectrum of closed bosonic strings is the first excitation states $\alpha^\mu_{-1}\tilde{\alpha}^\nu_{-1}$, with $N = \widetilde{N} = 1$. They are in $\mathbf{24} \otimes \mathbf{24}$ representation of SO(24), the compact subgroup of the little group. Such that, they can be decomposed as $G_{\mu\nu}$, $B_{\mu\nu}$ and Φ, which are spacetime metric, the Kalb–Ramond field, and the dilaton, respectively. The massless fields can be interpreted as background fields in which the string propagates. When their expectation values are non-zero, they modify the string's dynamics. The Polyakov action (I.2.1) is then replaced by the non-linear σ-model (NLSM):

$$S_\sigma = \frac{1}{4\pi\alpha'}\int_\Sigma \mathrm{d}^2\sigma\sqrt{-h}\left(G_{\mu\nu}(X)\partial^\alpha X^\mu\partial_\alpha X^\nu + i\epsilon^{\alpha\beta}B_{\mu\nu}(X)\partial_\alpha X^\mu\partial_\beta X^\nu + \alpha' R^{(2)}\Phi\right). \tag{I.2.20}$$

To maintain the worldsheet conformal invariance, the Weyl anomaly $T^\alpha{}_\alpha$ must vanish. As we mentioned, this trace is proportional to the beta functions of background fields $G_{\mu\nu}$, $B_{\mu\nu}$ and Φ as coupling constants. The beta functions are respectively expressed as

$$\begin{aligned}
\beta_{\mu\nu}(G) &= \alpha'\left(R_{\mu\nu} + 2\nabla_\mu\nabla_\nu\Phi - \frac{1}{4}H_{\mu\lambda\kappa}H_\nu^{\lambda\kappa}\right) + \mathcal{O}\left((\alpha')^2\right),\\
\beta_{\mu\nu}(B) &= \alpha'\left(-\frac{1}{2}\nabla^\lambda H_{\lambda\mu\nu} + \left(\nabla^\lambda\Phi\right)H_{\lambda\mu\nu}\right) + \mathcal{O}\left((\alpha')^2\right),\\
\beta(\Phi) &= \frac{D-26}{6} - \alpha'\left(\frac{1}{2}\nabla^2\Phi + \nabla_\mu\Phi\nabla^\mu\Phi - \frac{1}{24}H_{\mu\nu\lambda}H^{\mu\nu\lambda}\right) + \mathcal{O}\left((\alpha')^2\right),
\end{aligned} \tag{I.2.21}$$

with $H = \mathrm{d}B$ as the field strength of the Kalb–Ramond field. The vanishing of beta functions at the $\mathcal{O}(\alpha')$ one-loop level are the equations of motion of background fields, which is equivalent to being derived from the spacetime action

$$S = \frac{1}{2\kappa}\int \mathrm{d}^{26}x\sqrt{-\widetilde{G}}\left(\widetilde{R} - \frac{1}{12}e^{-\frac{\Phi-\langle\Phi\rangle}{3}}H_{\mu\nu\rho}\widetilde{H}^{\mu\nu\rho} - \frac{1}{6}\partial_\mu\Phi\tilde{\partial}^\mu\Phi\right), \tag{I.2.22}$$

where we use the critical dimension $D = 26$, and transform the string frame to Einstein frame via spacetime Weyl transformation $\widetilde{G}_{\mu\nu} = \exp\left[\frac{4(\Phi-\langle\Phi\rangle)}{D-2}\right] G_{\mu\nu}$ and $\kappa = \kappa_0 e^{\langle\Phi\rangle}$. $\langle\Phi\rangle$ is the expectation value of the dilaton.

Note that, string theory with the NLSM action is governed by two fundamental coupling constants. Besides α' which determines the string length and action with specific worldsheet topology, there is the string coupling constant $g_s \equiv e^{\langle\Phi\rangle}$, governing the strength of string interactions. The string coupling characterizes the number of loops of the string amplitude. The Feynman diagram of a string amplitude is a Riemann Surface. As an example, the diagram of the 1-loop amplitude is shown in Figure I.1, which has genus 1 and is equivalent to a torus. Similarly, the tree-level amplitude is topologically equivalent to a sphere. The string amplitude can be expanded by loops as $\mathcal{A} = \sum_{g\geq 0} g_s^{2g-2}\mathcal{A}_g$. This is because the g-loop contribution to the string amplitude is proportional to e^{S_Φ}, with

$$S_\Phi = \frac{1}{4\pi}\int_\Sigma \mathrm{d}^2\sigma\, R^{(2)}\,\langle\Phi\rangle = \chi\,\langle\Phi\rangle = (2g-2)\,\langle\Phi\rangle\ . \tag{I.2.23}$$

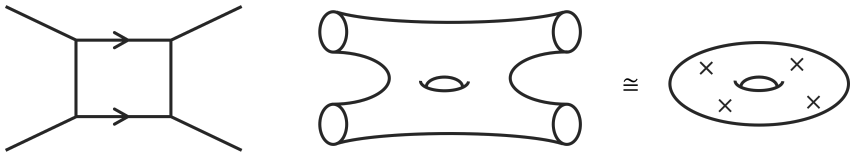

Figure I.1: One-loop 4-point interaction diagrams. The left picture is the diagram of point particles, which is drawn by worldlines. Generalizing to the worldsheet, the middle diagram is the 2-to-2 closed string interaction at the one-loop level, which is a Riemann surface with genus 1. It is topologically equivalent to a torus with four vertex operators over it.

The information of string amplitudes is indicated in the partition function. The sphere (tree-level) partition function can be absorbed into the string coupling constant and set to 1. Hence people are mainly interested in the torus (one-loop) partition function. Denote the complex structure modulus of the torus as τ, which evolves as the parameter of the worldsheet with ends identified. The torus amplitude for closed bosonic strings is

$$\mathscr{T} = \int_{\mathcal{F}} \frac{\mathrm{d}^2\tau}{4\tau_2^2} Z(\tau)\,, \tag{I.2.24}$$

where the one-loop partition function can be written as

$$Z(\tau) = \mathrm{Tr}\left(e^{2\pi i\tau_1 P - 2\pi\tau_2 H}\right) = (q\bar{q})^{-\frac{c}{24}}\,\mathrm{Tr}\left(q^{L_0}\bar{q}^{\widetilde{L}_0}\right), \quad q = e^{2\pi i\tau}\,, \tag{I.2.25}$$

where

$$P = L_0 - \widetilde{L}_0, \qquad H = L_0 + \widetilde{L}_0 - \frac{c}{12} \tag{I.2.26}$$

are the worldsheet momentum and Hamiltonian. By regularization, the partition function of closed strings with D worldsheet bosons can be written as

$$Z(\tau) = \frac{iV_D}{4\pi\alpha'} Z_X(\tau)^{D-2}, \quad Z_X(\tau) = \frac{1}{\sqrt{4\pi\alpha'\tau_2}} \frac{1}{|\eta(\tau)|^2}, \quad \eta(\tau) = q^{\frac{1}{24}} \prod_{n=1}^{\infty} (1-q^n) \,, \tag{I.2.27}$$

where V_D is the spacetime volume. Hence for the closed bosonic string theory with $D = 26$, the partition function is

$$Z(\tau) = \frac{iV_{26}}{(4\pi\alpha')^{13}} \frac{1}{\tau_2^{12}} \frac{1}{|\eta(\tau)|^{48}} \,. \tag{I.2.28}$$

This partition function is modular invariant, which means that it is invariant under the $\mathrm{SL}(2,\mathbb{Z})$ transformation of τ, as a consequence of the worldsheet conformal symmetry. Hence, the inequivalent values of τ are on $\mathcal{F} \cong \mathbb{H}/\mathrm{SL}(2,\mathbb{Z})$, the fundamental domain of $\mathrm{SL}(2,\mathbb{Z})$, which is drawn in Figure I.2.

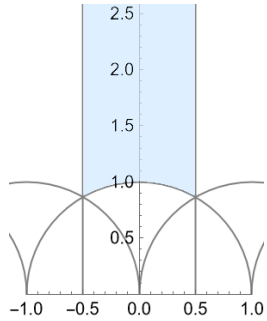

Figure I.2: The fundamental domain of $\mathrm{SL}(2,\mathbb{Z})$, which is the blue shaded region on the complex hyperbolic upper half-plane $\mathbb{H}$ (the Teichmüller space of T^2).

We have briefly introduced the closed bosonic string theory. For the open string, many analyses are similar. Roughly speaking, the closed string spectrum is the double copy of the open string spectrum, and the string coupling of open strings is $\sqrt{g_s}$. The open string worldsheet can have boundaries and crosscaps, which contribute to the Euler characteristic χ of string amplitude diagrams, such that $\chi = 2 - 2g - b - c$, with b the number of boundaries, and c the number of crosscaps. Note that the open string boundary condition (I.2.10) can be classified into two cases:

$$\begin{aligned} \text{Neumann boundary conditions:} \quad & \partial_{\sigma^1} X^\mu(\sigma^1 = 0, \pi) = 0 \,, \\ \text{Dirichlet boundary conditions:} \quad & \delta X^\mu(\sigma^1 = 0, \pi) = 0 \,. \end{aligned} \tag{I.2.29}$$

An endpoint of the open string with $(D-p)$ Dirichlet directions ends at a $(p+1)$-dimensional hyperplane. This hyperplane has its dynamics and is called a Dp-brane, with the brane tension

$$T_p = \frac{1}{(2\pi)^p (\alpha')^{(p+1)/2} g_s} \tag{I.2.30}$$

in the string frame. In the Einstein frame, $T_p^{(\mathrm{E})} = g_s^{(p+1)/4} T_p$. D$p$-branes take an important role in constructing the spectrum in string compactifications, curving the target space background, and reflecting string dualities. A detailed discussion of open strings and D-branes is beyond the scope of this work, but excellent treatments can be found in standard textbooks [15–22].

As we have established, the bosonic string theory is ultimately inconsistent due to the existence of tachyons and the absence of space-time fermions, which can never describe our real world. To cure these problems and construct a phenomenologically viable theory, one must introduce supersymmetry on the worldsheet. We turn to this topic in the next subsection.

I.2.2 Superstring theory

In this subsection, we impose supersymmetry on the string theory. There are two principal formalisms for achieving this: the Ramond–Neveu–Schwarz (RNS) formalism, which introduces worldsheet supersymmetry without guaranteeing spacetime supersymmetry; and the Green–Schwarz (GS) formalism, which ensures spacetime supersymmetry but lacks manifest worldsheet supersymmetry. We focus on the RNS formalism and briefly review how worldsheet supersymmetry modifies the string spectrum and partition function.

As the superpartner of each worldsheet boson X^μ, a worldsheet fermion Ψ^μ can be defined as a Majorana spinor satisfying $\Psi^{\mu *} = \Psi^\mu$. Just as X^μ decomposes into left- and right-moving modes, $X^\mu = X^\mu_{\mathrm{L}} + X^\mu_{\mathrm{R}}$, the fermion can be written as $\Psi^\mu = (\psi^\mu_+, \psi^\mu_-)^T$, where the Majorana–Weyl spinors ψ^μ_+ and ψ^μ_- represent the left- and right-moving components, respectively.

In the superconformal gauge and light-cone coordinates, the worldsheet action becomes the supersymmetric extension of the Polyakov action (I.2.1):

$$\begin{aligned} S &= \frac{1}{2\pi} \int_\Sigma \mathrm{d}^2\sigma \left(\frac{2}{\alpha'} \eta^{\alpha\beta} \partial_\alpha X^\mu \partial_\beta X_\mu + 2i \bar{\Psi}^\mu \gamma^\alpha \partial_\alpha \Psi_\mu \right) \\ &= \frac{1}{2\pi} \int_\Sigma \mathrm{d}^2\sigma \left(\frac{2}{\alpha'} \partial_+ X^\mu \partial_- X_\mu + i(\psi^\mu_+ \partial_- \psi_{+\mu} + \psi^\mu_- \partial_+ \psi_{-\mu}) \right) . \end{aligned} \tag{I.2.31}$$

This action possesses superconformal symmetry. Supersymmetry implies that each target-space dimension corresponds to a boson X^μ and a fermion Ψ^μ. The worldsheet fermions contribute central charge $\frac{1}{2}$ per dimension, giving a total fermionic contribution of $\frac{3}{2}D$. The superghost system (β, γ) contributes central charge 11, so the total ghost central charge is $c_{\mathrm{gh}} = -26 + 11 = -15$. The vanishing of the Weyl anomaly then requires $D = 10$ spacetime dimensions. In the next section, we discuss compactification mechanisms that reduce a higher-dimensional theory to an effective lower-dimensional one by compactifying certain spatial directions. Compared to bosonic string theory, which requires compactification of $26 - 4 = 22$ dimensions, superstring theory only necessitates compactifying 6 dimensions, making the construction of a realistic 4-dimensional spacetime background more tractable.

Let us now analyze the closed string spectrum of superstring theory. In each moving sector of the closed superstring, there are two possible boundary conditions for the worldsheet fermions: periodic boundary conditions $\psi_\pm^\mu(\sigma^1 + 2\pi) = \psi_\pm^\mu(\sigma^1)$, which are referred to as Ramond (R) boundary conditions; and anti-periodic boundary conditions $\psi_\pm^\mu(\sigma^1 + 2\pi) = -\psi_\pm^\mu(\sigma^1)$, which are called Neveu–Schwarz (NS) boundary conditions. The mode expansion of $\psi_\pm^\mu$ in the R-sector is

$$\psi_-^\mu(\sigma^-) = \sum_{r\in\mathbb{Z}} b_r^\mu e^{-ir\sigma^-}\,, \quad \psi_+^\mu(\sigma^+) = \sum_{r\in\mathbb{Z}} \tilde{b}_r^\mu e^{-ir\sigma^+}\,, \tag{I.2.32}$$

and the mode expansion of $\psi_\pm^\mu$ in the NS-sector is

$$\psi_-^\mu(\sigma^-) = \sum_{r\in\mathbb{Z}+\frac{1}{2}} b_r^\mu e^{-ir\sigma^-}\,, \quad \psi_+^\mu(\sigma^+) = \sum_{r\in\mathbb{Z}+\frac{1}{2}} \tilde{b}_r^\mu e^{-ir\sigma^+}\,. \tag{I.2.33}$$

The canonical quantization of fermions gives the commutation relations of the fermionic modes:

$$\{b_r^\mu, b_s^\nu\} = \{\tilde{b}_r^\mu, \tilde{b}_s^\nu\} = \eta^{\mu\nu}\delta_{r,-s}\,. \tag{I.2.34}$$

Combining with worldsheet bosons, we have two conserved quantities: the energy-momentum tensor $T_{\alpha\beta}$, which in light-cone coordinates has components

$$T_{\pm\pm} = -\frac{1}{\alpha'}\partial_\pm X^\mu \partial_\pm X_\mu - \frac{i}{2}\psi_\pm^\mu \partial_\pm \psi_{\pm\mu}\,, \quad \text{and} \quad T_{-+} = T_{+-} = 0\,. \tag{I.2.35}$$

and the conserved supercurrent

$$T_\pm^F = -\frac{1}{\sqrt{2\alpha'}}\psi_\pm^\mu \partial_\pm X_\mu\,, \tag{I.2.36}$$

which satisfies $\partial_- T_+^F = 0 = \partial_+ T_-^F$. Similar to the bosonic string, we again denote L_n and $\widetilde{L}_n$ as the Fourier coefficients of T_{++} and T_{--}, and the Fourier expansion of the supercurrent T^F is

$$T_+^F = \frac{1}{2}\sum_{r\in\mathbb{Z}+p} G_r e^{-in\sigma_+}\,, \quad T_-^F = \frac{1}{2}\sum_{r\in\mathbb{Z}+p} \widetilde{G}_r e^{-in\sigma_-}\,. \tag{I.2.37}$$

Straightforwardly, these Fourier components have identities

$$\begin{aligned} L_n &= L_n^{(\alpha)} + L_n^{(b)} = \frac{1}{2}\sum_{m\in\mathbb{Z}} :\alpha_{-m}\cdot\alpha_{m+n}: + \frac{1}{2}\sum_{r\in\mathbb{Z}+p}\left(r+\frac{n}{2}\right):b_{-r}\cdot b_{r+n}:\,, \\ G_r &= \sum_{m\in\mathbb{Z}} \alpha_{-m}\cdot b_{m+r}\,. \end{aligned} \tag{I.2.38}$$

and the right-moving sector is the same as it. The conserved generators obey the super-Virasoro algebra

$$\begin{aligned}
[L_m, L_n] &= (m-n)L_{m+n} + \frac{c}{12} m(m^2-2p)\delta_{m,-n}\,, \\
[L_m, G_r] &= \left(\frac{m}{2} - r\right) G_{m+r}\,, \\
\{G_r, G_s\} &= 2L_{r+s} + \frac{c}{12}(4r^2-2p)\delta_{r,-s}\,,
\end{aligned} \tag{I.2.39}$$

where $r, s \in \mathbb{Z} + p$; p is 0 for R-sector and $\frac{1}{2}$ for NS-sector, and $c = \frac{3}{2}D$. The right-moving $\widetilde{L}_n$, $\widetilde{G}_r$ have the same property as L_n, G_r. These super-Virasoro algebra generators define physical states. The generators eliminate the physical states as

$$\begin{aligned}
&\text{R-sector: } \widetilde{L}_n \left|\text{phys}\right\rangle = 0,\ n>0\,, \quad \left(\widetilde{L}_0 - a_{\text{R}}\right)\left|\text{phys}\right\rangle = 0\,; \quad \widetilde{G}_r \left|\text{phys}\right\rangle = 0,\ r \geq 0\,; \\
&\text{NS-sector: } \widetilde{L}_n \left|\text{phys}\right\rangle = 0,\ n>0\,, \quad \left(\widetilde{L}_0 - a_{\text{NS}}\right)\left|\text{phys}\right\rangle = 0\,; \quad \widetilde{G}_r \left|\text{phys}\right\rangle = 0,\ r > 0\,.
\end{aligned} \tag{I.2.40}$$

To characterize these physical states, define the left-moving number operator N from $L_0 = \frac{1}{2}\alpha' p^\mu p_\mu + N$, with expansion

$$N = N^{(\alpha)} + N^{(b)} = \sum_{n=1}^{\infty} \alpha_{-n}\cdot\alpha_n + \sum_{r=p}^{\infty} r\ b_{-r}\cdot b_r\,. \tag{I.2.41}$$

The definition formula of the right-moving number operator $\widetilde{N}$ is the same. Here $a_{\text{R}} = 0$ and $a_{\text{NS}} = \frac{1}{2}$ in (I.2.40) are required to ensure unitarity. Hence, there is no tachyon mode in the R-sector. The ground state in the R-sector is massless with $N = 0$, and is generated by the anti-commuting linear combinations of b_0^μ. Such states are denoted as

$$\left|0; \boldsymbol{s}\right\rangle_{\text{R}} = \left|0; s_0, s_1, s_2, s_3, s_4\right\rangle_{\text{R}}\,, \quad s_i = \pm\frac{1}{2}\,. \tag{I.2.42}$$

It is a Weyl spinor as a $\mathbf{8_s}\oplus\mathbf{8_c}$ representation of SO(8), the little group of SO(1, 9). The $\mathbf{8_s}$ representation has positive chirality and an odd number of $s_i = \frac{1}{2}$; the $\mathbf{8_c}$ representation has negative chirality and an even number of $s_i = \frac{1}{2}$.

However, the ground state $\left|0\right\rangle_{\text{NS}}$ with $N = 0$ in the NS-spectrum is a tachyon in the $\mathbf{8_{tach}}$ representation of the little group SO(1, 7). The massless states are at the first fermionic excitation level: $\left|\phi\right\rangle_{\text{NS}} = \xi_\mu b^\mu_{-\frac{1}{2}}\left|0\right\rangle_{\text{NS}}$. They compose a vector representation of SO(8), which we denote as $\mathbf{8_v}$.

With the ground or massless states of both periodicity conditions, we can determine the massless spectrum of the superstring theory by level matching. The left- and right-moving spectra contain both the NS-sector and the R-sector, such that the closed superstring can have four combinations of sectors: NSNS, NSR, RNS, RR. Such a theory with supersymmetry in both left- and right-moving sectors is called a type II superstring theory. However, due to the tachyonic ground

state of the NS-sector, the level-matching in the NSR and RNS sectors is not satisfied. Meanwhile, the worldsheet modular invariance is broken. To solve these problems, the Gliozzi–Scherk–Olive (GSO) projection must be applied. The GSO projection states that, a half of the worldsheet states in both sectors need to be removed to have a consistent type II superstring theory. In the NS-sector, we can naturally project out the tachyon $\mathbf{8_{tach}}$ state; and in the R-sector, we can project out either the $\mathbf{8_s}$ state or the $\mathbf{8_c}$ state. The GSO projection therefore gives two consistent type II theories: the chiral theory, with $\mathbf{8_s}$ in the left-moving R-sector and $\mathbf{8_c}$ in the right-moving R-sector, denoted as type IIA superstring theory; and the non-chiral theory, with $\mathbf{8_s}$ (or equivalently $\mathbf{8_c}$) in both left-moving and right-moving R-sectors, denoted as type IIB superstring theory. The massless spectra of 10D type IIB and type IIA superstring theories are given as:

$$
\begin{aligned}
\text{IIB:}\quad \text{NSNS:}&\quad \mathbf{8_v}\otimes\mathbf{8_v}=\mathbf{1}\oplus\mathbf{28}\oplus\mathbf{35}\\
\text{RR:}&\quad \mathbf{8_s}\otimes\mathbf{8_s}=\mathbf{1}\oplus\mathbf{28_s}\oplus\mathbf{35_s}\\
\text{NSR:}&\quad \mathbf{8_v}\otimes\mathbf{8_s}=\mathbf{8_c}\oplus\mathbf{56_c}\\
\text{RNS:}&\quad \mathbf{8_s}\otimes\mathbf{8_v}=\mathbf{8_c}\oplus\mathbf{56_c}
\end{aligned}
\qquad
\begin{aligned}
\text{IIA:}\quad \text{NSNS:}&\quad \mathbf{8_v}\otimes\mathbf{8_v}=\mathbf{1}\oplus\mathbf{28}\oplus\mathbf{35}\\
\text{RR:}&\quad \mathbf{8_s}\otimes\mathbf{8_c}=\mathbf{8_v}\oplus\mathbf{56_v}\\
\text{NSR:}&\quad \mathbf{8_v}\otimes\mathbf{8_c}=\mathbf{8_s}\oplus\mathbf{56_s}\\
\text{RNS:}&\quad \mathbf{8_s}\otimes\mathbf{8_v}=\mathbf{8_c}\oplus\mathbf{56_c}
\end{aligned}
$$

It is notable that the NSNS and RR spectra are bosons, and NSR and RNS spectra are fermions, and naturally the numbers of bosons and fermions are equal. The NSNS massless spectrum $\mathbf{1}\oplus\mathbf{28}\oplus\mathbf{35}$ is indeed the metric background fields Φ, $B_{\mu\nu}$ and $G_{\mu\nu}$. The RR bosons are electric or magnetic charge fields of D-branes. For example, the representation $\mathbf{28_s}$ is a 2-form, which is the electric field on D1-branes and the magnetic field on D5-branes. Note that the type IIB theory has RR 0-, 2-, and 4-forms, which charge D(-1)-, D1-, D3-, D5-, and D7-branes; and the type IIA theory has RR 1- and 3-forms which charge D0-, D2-, D4- and D6-branes.

The spectrum and interaction are indicated in the superstring worldsheet partition function. The worldsheet Hamiltonian of fermionic modes is

$$
H_{\mathrm{R}}=\sum_{i=2}^{9}\sum_{r=1}^{\infty} r b^i_{-r}b^i_r+\frac{1}{3}\,,\qquad H_{\mathrm{NS}}=\sum_{i=2}^{9}\sum_{r=\frac{1}{2}}^{\infty} r b^i_{-r}b^i_r-\frac{1}{6}\,. \tag{I.2.43}
$$

Such that the torus partition function contribution from left-moving fermions is

$$
\begin{aligned}
Z_{\mathrm{f,\,L}}(\tau)&=\mathrm{Tr}\left[e^{2\pi i\tau H_{\mathrm{NS}}}\frac{1}{2}\left(1-(-1)^F\right)\right]-\mathrm{Tr}\left[e^{2\pi i\tau H_{\mathrm{R}}}\frac{1}{2}\left(1\pm(-1)^F\right)\right]\\
&=\frac{1}{2\eta^4(\tau)}\left(\vartheta_3^4(\tau)-\vartheta_4^4(\tau)-\vartheta_2^4(\tau)\mp\vartheta_1^4(\tau)\right)\,,
\end{aligned} \tag{I.2.44}
$$

where F is the worldsheet fermion number, and $1-(-1)^F$ and $1\pm(-1)^F$ implement the GSO projections in the NS- and R-sectors, respectively. The ϑ-functions are

defined as

$$\begin{aligned}&\vartheta\begin{bmatrix}\alpha\\ \beta\end{bmatrix}(\tau)=\sum_{n=-\infty}^{\infty}e^{\pi i(n+\alpha)^2\tau+2\pi i(n+\alpha)\beta}\,,\\ &\vartheta_1\equiv\vartheta\begin{bmatrix}1/2\\ 1/2\end{bmatrix},\ \vartheta_2\equiv\vartheta\begin{bmatrix}1/2\\ 0\end{bmatrix},\ \vartheta_3\equiv\vartheta\begin{bmatrix}0\\ 0\end{bmatrix},\ \vartheta_4\equiv\vartheta\begin{bmatrix}0\\ 1/2\end{bmatrix},\end{aligned}\tag{I.2.45}$$

and $\vartheta_1(\tau)=0$ due to its definition. Combining with the bosonic contribution (I.2.27), the partition function of the 10-dimensional type II superstring theory is

$$Z(\tau)=Z_{\rm b}Z_{\rm f,\,L}Z_{\rm f,\,R}=\frac{iV_{10}}{(4\pi\alpha')^5}\frac{1}{4\tau_2^4}\frac{1}{|\eta(\tau)|^{24}}\left|\vartheta_3^4(\tau)-\vartheta_4^4(\tau)-\vartheta_2^4(\tau)\right|^2\,.\tag{I.2.46}$$

For convenience, in the later context we may ignore the infinite dimensionless volume $\frac{iV_{10}}{(4\pi\alpha')^5}$. Note that, there is the Riemann identity: $\vartheta_3^4(\tau)-\vartheta_4^4(\tau)-\vartheta_2^4(\tau)=0$, such that the type II superstring partition function vanishes. This is the hallmark of spacetime supersymmetry: the contributions from spacetime bosons and fermions cancel with each other.

The 10D target space of type II string theories has $\mathcal{N}=2$ supersymmetry with 32 supercharges. String theories with $\mathcal{N}=1$ spacetime supersymmetry with 16 supercharges can also be constructed in 10 dimensions. There are two approaches to do it. One approach is to combine the left-moving supersymmetric string and the right-moving bosonic string. There are 10 worldsheet bosons $X^\mu=X^\mu_{\rm L}+X^\mu_{\rm R}$ and 10 left-moving fermions ψ^μ_+. To match $c=\tilde{c}=0$, additional right-moving fields with $\tilde{c}=16$ are required, which can be 32 right-moving Majorana–Weyl spinors or 16 right-moving chiral bosons. Depending on the boundary conditions of these fields, they can only transform under either SO(32) or $\mathrm{E}_8\times\mathrm{E}_8$. These determine two superstring theories: SO(32) heterotic string theory and $\mathrm{E}_8\times\mathrm{E}_8$ heterotic string theory. Note that the type II superstring theories have $N=(1,1)$ worldsheet supersymmetry, while the heterotic string theories have $N=(1,0)$ worldsheet supersymmetry.

Another approach to construct superstring theory in critical 10 dimensions is using the orientifold projection. Note that the spectrum of type IIB superstring theory is symmetric under worldsheet parity transformation $\Omega:(\sigma^0,\sigma^1)\to(\sigma^0,2\pi-\sigma^1)$, which exchanges the left- and right-moving sectors. The NSR and RNS sectors are identical, such that under this Ω parity projection, a half of the fermionic spectrum is projected out. Hence this theory has only one gravitino and one dilatino, giving $\mathcal{N}=1$ supergravity. This construction is called type I superstring theory.

I.3 String compactifications

As discussed in the previous subsection, the consistent superstring theories that preserve Lorentz symmetry and super-Weyl invariance are formulated in ten spacetime dimensions. By contrast, our observable universe is four-dimensional.

To reconcile this apparent contradiction, it is necessary to assume that six of the ten dimensions are compactified into a small-volume internal space, rendering them unobservable at currently accessible energy scales.

I.3.1 Type II toroidal compactifications

The most elementary example of string compactification is to compactify each of the extra dimensions on a circle, such that the resulting internal space is a six-dimensional torus, T^6. In this subsection, we analyze the spectrum and partition function of type II string theory compactified on a torus. As a preliminary step, let us review Kaluza–Klein (KK) compactification from $(d+1)$ dimensions to d dimensions on a circle S^1, subject to the periodicity condition $X^d \sim X^d + 2\pi wR$, where $w \in \mathbb{Z}$.

The requirement of single-valuedness for the wave function $\exp(ix^d p^d)$ restricts the allowed internal momentum to discrete values $p^d = n/R$, with $n \in \mathbb{Z}$. This periodicity modifies the mode expansion of the X^d direction to

$$\begin{aligned} X^d_{\mathrm{L}}(\sigma^+) &= x^d_{\mathrm{L}} + \frac{\alpha'}{2}\left(\frac{n}{R} + \frac{wR}{\alpha'}\right)\sigma^+ + i\sqrt{\frac{\alpha'}{2}}\sum_{n\neq 0}\frac{\alpha^d_n}{n}e^{-in\sigma^+}, \\ X^d_{\mathrm{R}}(\sigma^-) &= x^d_{\mathrm{R}} + \frac{\alpha'}{2}\left(\frac{n}{R} - \frac{wR}{\alpha'}\right)\sigma^- + i\sqrt{\frac{\alpha'}{2}}\sum_{n\neq 0}\frac{\tilde{\alpha}^d_n}{n}e^{-in\sigma^-}. \end{aligned} \tag{I.3.1}$$

Accordingly, the mass formula receives contributions from both quantized momentum and winding modes:

$$\begin{aligned} \frac{1}{2}\alpha' m^2_{\mathrm{L}} &= -\frac{\alpha'}{2}p^\mu p_\mu = \frac{\alpha'}{4}\left(\frac{n}{R} + \frac{wR}{\alpha'}\right)^2 + N - 1\,, \\ \frac{1}{2}\alpha' m^2_{\mathrm{R}} &= -\frac{\alpha'}{2}\tilde{p}^\mu \tilde{p}_\mu = \frac{\alpha'}{4}\left(\frac{n}{R} - \frac{wR}{\alpha'}\right)^2 + \widetilde{N} - 1\,, \end{aligned} \tag{I.3.2}$$

where the index $\mu = 0, 1, \cdots, d-1$. Summing the left- and right-moving contributions yields the total mass formula in the Kaluza–Klein compactification:

$$m^2 = m^2_{\mathrm{L}} + m^2_{\mathrm{R}} = \frac{n^2}{R^2} + \frac{w^2R^2}{\alpha'^2} + \frac{2}{\alpha'}\left(N + \widetilde{N} - 2\right). \tag{I.3.3}$$

And the level-matching condition $m^2_{\mathrm{L}} = m^2_{\mathrm{R}}$ becomes

$$\widetilde{N} - N = nw\,. \tag{I.3.4}$$

It is instructive to note that there exist two massless vector states $\alpha^\mu_{-1}\tilde{\alpha}^d_{-1}\,|0\rangle$ and $\alpha^d_{-1}\tilde{\alpha}^\mu_{-1}\,|0\rangle$, and one scalar $\alpha^d_{-1}\tilde{\alpha}^d_{-1}\,|0\rangle$. The vacuum expectation value of this scalar $\langle\phi\rangle$ determines the radius

$$\varrho = Re^{\beta\langle\phi\rangle}\,, \quad \beta = \sqrt{\frac{d-2}{2(d-1)}}\,. \tag{I.3.5}$$

Moreover, due to the additional terms in the mass formula (I.3.3) and the level matching condition (I.3.4), there are generically massive states when n and/or w are non-zero. Some massive states can become massless for special values of the radius. For example, recall that the previous two vectors are graviphotons of $\mathrm{U}(1)_{\mathrm{L}} \times \mathrm{U}(1)_{\mathrm{R}}$ gauge group; when $\widetilde{N} - N = nw = \pm 1$, there appear four massless vector states in total if $R = \sqrt{\alpha'}$. At this self-dual radius, the gauge group is enhanced to $\mathrm{SU}(2)_{\mathrm{L}} \times \mathrm{SU}(2)_{\mathrm{R}}$. In addition, eight massless scalar states arise, with non-trivial momentum and winding, which together with $\alpha^d_{-1}\tilde{\alpha}^d_{-1}\,|0\rangle$ form the $(\mathbf{3},\mathbf{3})$ representation of $\mathrm{SU}(2)_{\mathrm{L}} \times \mathrm{SU}(2)_{\mathrm{R}}$.

From the spacetime perspective, in the Einstein frame, the periodicity becomes $X^d_{(\mathrm{E})} \sim X^d_{(\mathrm{E})} + w$, such that the target space metric becomes

$$\mathrm{d}s^2 = G_{\mu\nu}\mathrm{d}X^\mu \mathrm{d}X^\nu + G_{dd}\left(\mathrm{d}X^d + A_\mu \mathrm{d}X^\mu\right)^2 . \tag{I.3.6}$$

Here A_μ is the U(1) graviphoton, and the radion ϕ is defined by $G_{dd} = e^{2\beta\phi}$. The $(d+1)$-dimensional Einstein–Hilbert effective action is reduced to

$$\begin{aligned} S_{\mathrm{EH}} &= \int \mathrm{d}^{d+1}X \sqrt{-G^{(d+1)}} R^{(d+1)} \\ &= \int \mathrm{d}^d X \sqrt{G^{(d)}} \left(R^{(d)} - \frac{1}{2}\partial_\mu\phi\partial^\mu\phi - \frac{1}{4} e^{\sqrt{2(d-1)/(d-2)}\phi} F_{\mu\nu}F^{\mu\nu} \right) , \end{aligned} \tag{I.3.7}$$

with $F_{\mu\nu} = \partial_\mu A_\nu - \partial_\nu A_\mu$. A matter field $\hat{\psi}$ with equation of motion $\Box\psi = 0$ in $(d+1)$ dimensions can be expanded as

$$\hat{\psi}(X^\mu, X^d) = \sum_{n\in\mathbb{Z}} \psi_n(X^\mu) e^{2\pi i n X^d} , \tag{I.3.8}$$

where the d-dimensional fields ψ_n satisfy equations of motion

$$\partial^\mu\partial_\mu\psi_n - 4\pi^2 n^2 \psi_n = 0 . \tag{I.3.9}$$

Comparison with the mass formula (I.3.3) confirms that n indeed labels the quantized momentum number as defined in the string frame. Note that, the boundary condition of matter fields in KK reduction (I.3.8) reflects a U(1) action. This can be generalized to a compact Lie group G, resulting in fields with twisted boundary conditions. Such compactifications are known as *Scherk–Schwarz reductions*, which can spontaneously break spacetime supersymmetry. Scherk–Schwarz reductions are closely related to freely acting orbifolds and non-geometric compactifications [23], and will be elaborated in Section III.3.

The above discussion of circular KK compactification generalizes straightforwardly to type II superstring compactification on an n-dimensional torus T^n, reducing from $(d+n)$ dimensions to d dimensions. The n-torus is the quotient of Euclidean space by a lattice: $T^n = \mathbb{R}^n/\Lambda_n$. Denote the indices of the compact directions as $I = d, d+1, \ldots, d+n-1$, and impose periodicity

$$X^I \sim X^I + 2\pi L^I , \quad L^I = w^i e^I_i , \quad w^i \in \mathbb{Z} , \quad i = 1, 2, \cdots, n . \tag{I.3.10}$$

L^I is the component of the lattice vector $\boldsymbol{L} \in \Lambda_n$. And e_i^I is the frame component defining the torus metric: $g_{ij} = e_i^I e_j^J \delta_{IJ}$. Analogous to the S^1 compactification, the lattice vector and internal momentum $\boldsymbol{p}$ satisfy $L^I p_I \in \mathbb{Z}$. Hence the internal momentum is a vector of dual lattice Λ_n^*, with components $p_I = n_i e^{*i}_I$, $n_i \in \mathbb{Z}$. The mode expansion for X^I is then

$$\begin{aligned} X^I_{\mathrm{L}} &= x^I_{\mathrm{L}} + \frac{\alpha'}{2}\left(p^I + \frac{1}{\alpha'}L^I\right)\sigma^+ + i\sqrt{\frac{\alpha'}{2}}\sum_{n\neq 0}\frac{\alpha^I_n}{n}e^{-in\sigma^+}\,, \\ X^I_{\mathrm{R}} &= x^I_{\mathrm{R}} + \frac{\alpha'}{2}\left(p^I - \frac{1}{\alpha'}L^I\right)\sigma^- + i\sqrt{\frac{\alpha'}{2}}\sum_{n\neq 0}\frac{\tilde{\alpha}^I_n}{n}e^{-in\sigma^-}\,, \end{aligned} \tag{I.3.11}$$

We can further define dimensionless momenta

$$p^I_{\mathrm{L}} = \frac{1}{\sqrt{2}}\left(\sqrt{\alpha'}p^I + \frac{1}{\sqrt{\alpha'}}L^I\right)\,, \quad p^I_{\mathrm{R}} = \frac{1}{\sqrt{2}}\left(\sqrt{\alpha'}p^I - \frac{1}{\sqrt{\alpha'}}L^I\right)\,, \tag{I.3.12}$$

such that $\left[x^I_{\mathrm{L/R}}, p^J_{\mathrm{L/R}}\right] = i\sqrt{\alpha'/2}\;\delta^{IJ}$. If the lattice Λ_n is the root lattice of a Lie algebra, $\boldsymbol{p}_{\mathrm{L}}$ and $\boldsymbol{p}_{\mathrm{R}}$ are vectors in the corresponding weight lattice. The mass formula can then be expressed as

$$\alpha' m^2_{\mathrm{L}} = \boldsymbol{p}^2_{\mathrm{L}} + 2(N-1)\,, \qquad \alpha' m^2_{\mathrm{R}} = \boldsymbol{p}^2_{\mathrm{R}} + 2\left(\widetilde{N} - 1\right)\,, \tag{I.3.13}$$

and

$$\begin{aligned} \alpha' m^2 = \alpha'\left(m^2_{\mathrm{L}} + m^2_{\mathrm{R}}\right) &= \alpha' p^I p_I + \frac{1}{\alpha'}L^I L_I + 2\left(N + \widetilde{N} - 2\right) \\ &= \alpha' n^i n_i + \frac{1}{\alpha'}w^i w_i + 2\left(N + \widetilde{N} - 2\right)\,. \end{aligned} \tag{I.3.14}$$

Meanwhile, the level-matching condition becomes

$$\widetilde{N} - N = L^I p_I = w^i n_i\,. \tag{I.3.15}$$

The left- and right-moving momentum vector defined in (I.3.12) can be assembled into a $2n$-dimensional vector, $\boldsymbol{P} = (\boldsymbol{p}_{\mathrm{L}}, \boldsymbol{p}_{\mathrm{R}})^T$. These vectors form an even, self-dual lattice $\Gamma_{n,n}$, with a Lorentzian signature $((+1)^n, (-1)^n)$ and norm $\boldsymbol{P}^2 = 2w^i n_i \in 2\mathbb{Z}$. This lattice is called a *Lorentzian lattice* or a *Narain Lattice*, encoding both momenta and winding modes.

Similar to the Kaluza–Klein compactification on S^1, the creation operators with compact direction indices generate additional fields in the d-dimensional theory. For the bosonic fields, there are $2n$ vectors $\alpha^\mu_{-1}\tilde{\alpha}^I_{-1}$ and $\alpha^I_{-1}\tilde{\alpha}^\mu_{-1}$, and n^2 scalars $\alpha^I_{-1}\tilde{\alpha}^J_{-1}$. The vectors are graviphotons associated with the gauge group $\mathrm{U}(1)^n_{\mathrm{L}} \times \mathrm{U}(1)^n_{\mathrm{R}}$.[3] The symmetric scalar components correspond to the metric

[3] As in S^1 compactification, for special background values, there can be additional massless states and the gauge group may be enhanced. For example, when $g_{ij} = \alpha'\delta_{ij}$, $b_{ij} = 0$, the gauge group is enhanced to $\mathrm{SU}(2)^n_{\mathrm{L}} \times \mathrm{SU}(2)^n_{\mathrm{R}}$.

of the torus, G_{IJ}, while the antisymmetric components correspond to the torus Kalb–Ramond field, B_{IJ}. Defining $g_{ij} = e_i^I G_{IJ} e_j^J$ and $b_{ij} = e_i^I B_{IJ} e_j^J$ as the torus metric and B-field in the momenta and winding coordinates, the dimensionless momenta can be expressed as

$$(p_{\mathrm{L/R}})_I = e^{*i}{}_I \left(\sqrt{\frac{\alpha'}{2}} n_i - \frac{1}{\sqrt{2\alpha'}} (\pm g_{ij} + b_{ij}) w^j \right) . \tag{I.3.16}$$

The torus partition function of type II toroidal compactification takes the form

$$Z(\tau) = Z_{\mathbb{R}^{1,9-n}} Z_{T^n} Z_{\mathrm{f}} \,, \tag{I.3.17}$$

where the three factors are the bosonic parts of non-compact and compact directions, and the fermionic contribution, respectively, with

$$\begin{aligned} Z_{\mathbb{R}^{1,9-n}} &= \frac{iV_{10-n}}{(4\pi\alpha')^{(10-n)/2}} \frac{1}{4\tau_2^{(8-n)/2}} \frac{1}{|\eta(\tau)|^{16-2n}} \,, \\ Z_{T^n} &= \frac{1}{|\eta(\tau)|^{2n}} \sum_{(\boldsymbol{p}_{\mathrm{L}}, \boldsymbol{p}_{\mathrm{R}}) \in \Gamma_{n,n}} q^{\frac{1}{2}\boldsymbol{p}_{\mathrm{L}}^2} \bar{q}^{\frac{1}{2}\boldsymbol{p}_{\mathrm{R}}^2} \,, \\ Z_{\mathrm{f}} &= \frac{1}{|\eta(\tau)|^8} \left| \vartheta_3^4(\tau) - \vartheta_4^4(\tau) - \vartheta_2^4(\tau) \right|^2 . \end{aligned} \tag{I.3.18}$$

It can be shown that this partition function $Z(\tau)$ is modular invariant if $\Gamma_{n,n}$ is even and self-dual. The compact sector partition function can be further evaluated; for instance, in the case of type II compactification on a circle, the partition function for S^1 is

$$\begin{aligned} Z_{S^1} &= \frac{1}{|\eta(\tau)|^2} \sum_{n,w \in \mathbb{Z}} q^{\frac{1}{4}\left(\frac{\sqrt{\alpha'}n}{R} + \frac{wR}{\sqrt{\alpha'}}\right)^2} \bar{q}^{\frac{1}{4}\left(\frac{\sqrt{\alpha'}n}{R} - \frac{wR}{\sqrt{\alpha'}}\right)^2} \\ &= \frac{R}{\sqrt{\alpha'\tau_2}} \frac{1}{|\eta(\tau)|^2} \sum_{n,w \in \mathbb{Z}} e^{-\frac{\pi R^2}{\alpha'\tau_2}|n - w\tau|^2} . \end{aligned} \tag{I.3.19}$$

The second line is obtained from the first by Poisson resummation over n. Note that in the decompactification limit $R \to \infty$, (I.3.19) reduces to the partition function of a non-compact worldsheet boson.

In ten-dimensional spacetime, type II string theory possesses 32 supercharges. Toroidal compactification preserves supersymmetry, such that upon reduction to four dimensions, the theory exhibits $\mathcal{N} = 8$ supersymmetry, which is non-chiral. By contrast, the Standard Model is both non-supersymmetric and chiral, with a significantly smaller spectrum. To achieve a phenomenologically viable model, alternative compactification schemes must be employed. One approach involves compactification on curved or deformed internal spaces, such as Calabi–Yau manifolds, which have SU(3) holonomy and break $\frac{3}{4}$ of supersymmetries, reducing $\mathcal{N} = 8$ to $\mathcal{N} = 2$. Another method is to consider orbifold or orientifold

projections on the internal space, which can eliminate or make massive some of the gravitini to break supersymmetry. At the same time, orbifold or orientifold identifications can reduce the spectrum and introduce new states, such as chiral fermions and novel gauge groups. These aspects of string compactification will be discussed further in Section I.3.

I.3.2 Moduli spaces

In string compactifications, there typically appear massless scalar fields whose vacuum expectation values represent the free parameters of the effective theory. These fields are known as *moduli*, and the *moduli space* of a string compactification is the space of all inequivalent vacuum solutions of moduli. The metric of the moduli space $G_{ab}(\phi^a)$ is determined by the kinetic term of massless scalar fields

$$S_{\text{kin}} = -\int \mathrm{d}^d X \; G_{ab}(\phi^a)\partial^\mu \phi^a(X)\partial_\mu \phi^b(X)\,. \tag{I.3.20}$$

In the closed string spectrum of type II theories, moduli can originate from either the NS-NS or R-R sector. The NS-NS sector moduli (excluding the dilaton) determine the size, shape, and Kalb–Ramond field configuration of the internal space. For example, in bosonic string compactification on T^n, the Narain lattice $\Gamma_{n,n}$ is specified by n^2 background moduli. All such lattices $\Gamma_{n,n}$ can be generated via $\mathrm{O}(n,n)$ transformations acting on a reference lattice $\Gamma_{(0)}$, which can be chosen as $g_{ij} = \alpha' \delta_{ij}$, $b_{ij} = 0$. Meanwhile, $\boldsymbol{p}_{\text{L}}^2$ and $\boldsymbol{p}_{\text{R}}^2$, i.e. the mass spectrum (I.3.13), are invariant under $\mathrm{O}(n) \times \mathrm{O}(n)$ rotations of $\boldsymbol{p}_{\text{L}}$ and $\boldsymbol{p}_{\text{R}}$. Hence, inequivalent geometric structures are parametrized by the coset manifold $\mathrm{O}(n,n)/(\mathrm{O}(n) \times \mathrm{O}(n))$, up to discrete identifications. Moreover, both the mass spectrum and the reference lattice $\Gamma_{(0)}$ are invariant under discrete transformations in $\mathrm{O}(n,n;\mathbb{Z})$. This discrete group is known as the *T-duality group*, which identifies string backgrounds differing by internal geometry parameters but corresponding to the same physical vacuum. Consequently, the moduli space of the n-torus geometry in bosonic string theory is

$$\mathrm{O}(n,n;\mathbb{Z})\backslash \mathrm{O}(n,n)/(\mathrm{O}(n) \times \mathrm{O}(n))\,. \tag{I.3.21}$$

The moduli space before being quotiented by the duality group can be called the marked moduli space or classical moduli space. For type II superstring theory, there is a $\mathbb{Z}_2$ element in $\mathrm{O}(n,n)$, which has determinant -1 and exchanges type IIA and type IIB theories. Hence, for the type IIA(B) superstring theory, the NS-NS moduli space is

$$\mathrm{SO}(n,n;\mathbb{Z})\backslash \mathrm{SO}(n,n)/(\mathrm{SO}(n) \times \mathrm{SO}(n))\,. \tag{I.3.22}$$

For compactifications on complex manifolds such as T^{2n}, the NS-NS moduli naturally split into two classes: Kähler moduli, controlling the sizes of cycles and complexified Kähler forms, and complex structure moduli, determining the complex deformation of the manifold. For example, compactification on T^2 yields one complexified Kähler modulus T and one complex structure modulus U. On a

2-torus, there is the metric g and the B-field b, and the moduli can be expressed as

$$T = T_1 + iT_2 = b_{12} + i\sqrt{\det g}\,, \quad U = U_1 + iU_2 = \frac{g_{12}}{g_{22}} + i\frac{\sqrt{\det g}}{g_{22}}\,. \tag{I.3.23}$$

The kinetic terms and admissible values of T and U imply that their marked moduli space is the product of two upper half-planes, $\mathbb{H} \cong \mathrm{SL}(2,\mathbb{R})/\mathrm{U}(1)$. This is consistent with (I.3.22), as

$$\frac{\mathrm{SL}(2,\mathbb{R})}{\mathrm{U}(1)} \times \frac{\mathrm{SL}(2,\mathbb{R})}{\mathrm{U}(1)} \cong \frac{\mathrm{SO}(2,2)}{\mathrm{SO}(2)\times\mathrm{SO}(2)}\,. \tag{I.3.24}$$

The moduli spaces of T and U are indeed the fundamental domains of $\mathrm{SL}(2,\mathbb{Z})$, as demonstrated in Figure I.2.

Besides geometric moduli, there are Ramond-Ramond moduli from R-R p-forms wrapping p-cycles, as well as the d-dimensional dilaton

$$\phi_d = \frac{\sqrt{\det g}}{(2\pi\alpha')^{(10-d)/2}}\Phi\,. \tag{I.3.25}$$

For example, in the type IIB string theories, there is an axio-dilaton $\sigma = C_0 + ie^{-\Phi}$, where C_0 is the axion (the R-R 0-form) and $g_s = e^{\Phi}$ is the string coupling. Compactifying on T^2, the full moduli space is

$$\frac{\mathrm{SL}(2,\mathbb{R})}{\mathrm{SL}(2,\mathbb{Z})\times\mathrm{U}(1)} \times \frac{\mathrm{SL}(3,\mathbb{R})}{\mathrm{SL}(3,\mathbb{Z})\times\mathrm{SO}(3)}\,, \tag{I.3.26}$$

which includes the NS-NS moduli, the axio-dilaton σ and the modulus from the R-R 2-form wrapping T^2. The discrete group $\mathrm{SL}(3,\mathbb{Z})\times\mathrm{SL}(2,\mathbb{Z})$ is the *U-duality group*. We summarize the T-duality and U-duality groups of type II toroidal compactifications in Table I.1 [24]. In the context of toroidal compactifications, the U-duality group is typically a discrete subgroup of an exceptional Lie group.

Other compactification setups yield different moduli spaces. In the case of toroidal compactifications of the SO(32) or $\mathrm{E}_8\times\mathrm{E}8$ heterotic string theories, the left-moving supersymmetry sector is compactified on T^n, while the right-moving bosonic sector is on T^{n+16}, such that the resulting Narain lattice is $\Gamma_{n,n+16}$, and the geometric moduli space is

$$\mathrm{SO}(n,n+16;\mathbb{Z})\backslash\mathrm{SO}(n,n+16)/(\mathrm{SO}(n)\times\mathrm{SO}(n+16))\,. \tag{I.3.27}$$

Besides the n^2 background moduli, there are $16n$ Wilson lines associated with the internal gauge bundle. It is noteworthy that type IIA(B) string theory compactified on $\mathrm{K3}\times T^{n-4}$ shares the same geometric moduli space [25]. K3 is a complex 2-dimensional Calabi–Yau manifold with SU(2) holonomy group, which breaks half of the supersymmetries.

Compactification	T-duality group	U-duality group
$\mathbb{R}^{1,9}$	1	$\mathrm{SL}(2,\mathbb{Z})$
$\mathbb{R}^{1,8} \times S^1$	$\mathbb{Z}_2$	$\mathrm{SL}(2,\mathbb{Z}) \times \mathbb{Z}_2$
$\mathbb{R}^{1,7} \times T^2$	$\mathrm{O}(2,2;\mathbb{Z})$	$\mathrm{SL}(3,\mathbb{Z}) \times \mathrm{SL}(2,\mathbb{Z})$
$\mathbb{R}^{1,6} \times T^3$	$\mathrm{O}(3,3;\mathbb{Z})$	$\mathrm{SL}(5,\mathbb{Z})$
$\mathbb{R}^{1,5} \times T^4$	$\mathrm{O}(4,4;\mathbb{Z})$	$\mathrm{O}(5,5;\mathbb{Z})$
$\mathbb{R}^{1,4} \times T^5$	$\mathrm{O}(5,5;\mathbb{Z})$	$\mathrm{E}_{6(6)}(\mathbb{Z})$
$\mathbb{R}^{1,3} \times T^6$	$\mathrm{O}(6,6;\mathbb{Z})$	$\mathrm{E}_{7(7)}(\mathbb{Z})$

Table I.1: T-duality groups and U-duality groups of type II (both IIA and IIB) toroidal compactifications.

Another important class of examples arises from compactifying type II strings on Calabi–Yau threefolds, characterized by Hodge numbers $h^{1,1}$ and $h^{1,2}$, resulting in four-dimensional $\mathcal{N} = 2$ supersymmetry. In 4D $\mathcal{N} = 2$ supergravity, the massless scalar fields are organized into vector multiplets and hypermultiplets. For type IIA compactifications, there are $h^{1,1}$ vector multiplets and $h^{1,2}+1$ hypermultiplets; for type IIB, there are $h^{1,2}$ vector multiplets and $h^{1,1}+1$ hypermultiplets. Altogether, these $2h^{1,1} + 4(h^{1,2} + 1)$ moduli in type IIA, or $2h^{1,2} + 4(h^{1,1} + 1)$ moduli in type IIB, constitute the moduli spaces of Calabi–Yau compactifications.

It should be noted that further types of moduli can arise in more general string compactifications. For instance, on D-branes, there exist *open string moduli* associated with the positions and Wilson lines of the D-branes. If the internal manifold is non-Kähler, *torsion moduli* may also appear, related to the torsion classes of the manifold. However, such moduli are beyond the scope of this thesis.

In an effective field theory, the vacuum expectation values of the moduli determine particle masses and coupling constants, making the study of moduli spaces central to string phenomenology. However, the parameters relevant to real-world particle physics are nearly fixed, implying that a scalar potential is needed to stabilize the moduli. In string theory, one can introduce fluxes and non-perturbative quantum effects to generate such potentials in the effective theory. The interplay between moduli dynamics and their potentials is crucial not only for particle physics, but also for cosmology, as it influences dark energy and may help explain inflation and the observed accelerated expansion of the universe. It is therefore essential to investigate the generic properties of moduli spaces. Several Swampland conjectures have been formulated concerning their structure. For example, the Swampland Distance Conjecture, to be discussed in Subsection I.5.1, posits that in the asymptotic regions of moduli space, an infinite tower of states appears

whose masses decrease exponentially. The geometry and asymptotic behavior of moduli spaces will thus be a central focus of this thesis.

I.3.3 String dualities

In the last subsection, we described T-duality groups and U-duality groups, which relate string theories with identical string geometry structure but different moduli expectation values. Beyond these, there exist additional dualities connecting different types of string theories whose partition functions, mass spectra, and moduli spaces nevertheless coincide. In this subsection, we illustrate these dualities through several representative examples.

T-duality

T-duality, short for target space duality, equates effective theories arising from distinct internal string geometries. The simplest instance of T-duality occurs in Kaluza–Klein compactification on a circle. Specifically, if we invert the radius and exchange momentum and winding numbers,

$$R \leftrightarrow \frac{\alpha'}{R}\,, \qquad n \leftrightarrow w\,, \tag{I.3.28}$$

the resulting string theory describes a circle of reciprocal radius. Meanwhile, on the closed string worldsheet, the oscillation expansion of scalar fields (I.3.1) transforms as $\left(p_{\mathrm{L}}^d, p_{\mathrm{R}}^d\right) \to \left(p_{\mathrm{L}}^d, -p_{\mathrm{R}}^d\right)$. To define a consistent symmetry, T-duality acts on the S^1 worldsheet fields as

$$\left(X_{\mathrm{L}}^d, X_{\mathrm{R}}^d\right) \to \left(X_{\mathrm{L}}^d, -X_{\mathrm{R}}^d\right), \qquad \left(\psi_+^d, \psi_-^d\right) \to \left(\psi_+^d, -\psi_-^d\right). \tag{I.3.29}$$

Recall that the GSO projection on the R-sectors is $1 \pm (-1)^F$, with the right-moving fermionic number $(-1)^F = 16\prod_{i=2}^d b_0^i$, which is 1 for type IIB and -1 for type IIA. The sign reversal of ψ_-^d under T-duality changes the sign of b_0^d, so that a type IIA (IIB) string theory is mapped to type IIB (IIA) under this transformation. Despite this change, both the mass formula (I.3.2) and the torus partition function (I.3.19) remain invariant, ensuring that the effective theory is unchanged. Moreover, T-duality is preserved at every order in string perturbation theory, such that higher-genus partition functions are also invariant.

For open strings, this T-duality exchanges Neumann and Dirichlet boundary conditions along the X^d-direction. Consequently, Dp-branes—defined as hypersurfaces where open string endpoints reside—are mapped to D$(p+1)$-branes when imposing the Dirichlet boundary condition for X^d, or to D$(p-1)$-branes for the Neumann X^d-boundary condition.

This duality generalizes naturally to higher-dimensional tori. In type IIA or IIB compactifications on T^n, this $\mathbb{Z}_2$ symmetry combined with the T-duality group $\mathrm{SO}(2,2;\mathbb{Z})$ constitutes $\mathrm{O}(2,2;\mathbb{Z})$, which is the full T-duality symmetry group of the type II partition function. The transformation rules for background fields in the non-linear σ-model are more intricate. For T-duality along the X^d circle in

an internal space with metric G_{IJ} and B-field B_{IJ}, the Buscher rules provide the dual background:

$$\begin{aligned}
\widetilde{G}_{dd} &= \frac{\alpha'^2}{G_{dd}}, \quad \widetilde{G}_{Id} = \pm\frac{\alpha' B_{Id}}{G_{dd}}, \quad \widetilde{G}_{IJ} = G_{IJ} - \frac{G_{Id}G_{Jd} - B_{Id}B_{Jd}}{G_{dd}}, \\
\widetilde{B}_{Id} &= \pm\frac{\alpha' G_{Id}}{G_{dd}}, \quad \widetilde{B}_{IJ} = B_{IJ} - \frac{B_{Id}G_{Jd} - G_{Id}B_{Jd}}{G_{dd}}, \\
\widetilde{\Phi} &= \Phi - \frac{1}{2}\log\frac{G_{dd}}{\alpha'}\,,
\end{aligned} \tag{I.3.30}$$

where $I, J \neq d$ are internal space coordinate indices.

Similar to the relation between type IIA and type IIB string theories, the $\mathrm{E}_8 \times \mathrm{E}_8$ heterotic string compactification on a circle with radius R, is T-dual to the SO(32) heterotic string compactification on a circle with radius α'/R, and vice versa [26–28]. For further details and more examples of T-dualities, see the review [29]. In the context of Calabi–Yau compactifications, T-duality generalizes to mirror symmetry between Calabi–Yau threefolds [30]. For a Calabi–Yau threefold X with Hodge numbers $(h^{1,1}, h^{1,2})$, there exists a mirror manifold $\widetilde{X}$ with Hodge numbers $(h^{1,2}, h^{1,1})$. Compactifying type IIA (IIB) theory on X yields the same effective theory as compactifying type IIB (IIA) theory on $\widetilde{X}$.

S-duality

S-duality, short for strong/weak-coupling duality, originally arose from the Montonen–Olive duality in $\mathcal{N} = 4$ super Yang–Mills theory, which exchanges electric and magnetic sectors and inverts the gauge coupling $g_{\mathrm{YM}} \leftrightarrow 1/g_{\mathrm{YM}}$. Analogously, S-duality in string theory relates theories at strong and weak string coupling g_s.

The most prominent example of S-duality is in ten-dimensional type IIB superstring theory, which possesses an $\mathrm{SL}(2,\mathbb{Z})$ S-duality group [31]. This S-duality acts on the axio-dilaton $\sigma = C_0 + ie^{-\Phi}$, where C_0 is the axion (an R-R 0-form), and Φ is the 10-dimensional dilaton with string coupling $g_s = e^{\Phi}$.[4] In particular, the transformation $\mathcal{S}\colon \sigma \to -1/\sigma$ exchanges the strong- and weak-coupling regimes. Notably, this S-duality is a self-string-string duality [32], exchanging fundamental strings (F-strings) and D1-branes (D-strings). Recall that the tension of an F-string is $1/2\pi\alpha'$ in the string frame, and the tension of a D-string is $1/2\pi\alpha' g_s$. Under S-duality, p F-strings and q D-strings are mixed to form a (p,q)-string with tension

$$T = \frac{1}{2\pi\alpha'}\,|p - \tau q|\,. \tag{I.3.31}$$

The fundamental string has a magnetic dual, the *NS5-brane*, and a similar S-duality action acts on D5-branes and NS5-branes as well.[5]

[4] In 10D type IIB supergravity the S-duality is extended to $\mathrm{SL}(2,\mathbb{R})$. In F-theory, σ is interpreted as the complex structure of the auxiliary elliptic curve that varies over the compact space.

[5] The NS5-brane is also T-dual to the KK monopole; see [33, 34].

Another important example is the S-duality between type I string theory and the SO(32) heterotic string theory in ten dimensions [35]. Identifying the background fields of these two string theories requires the dilatons to satisfy $\Phi^{\mathrm{I}} = -\Phi^{\mathrm{Het}}$, so that $g_s^{\mathrm{I}} = 1/g_s^{\mathrm{Het}}$. Thus, type I theory at strong coupling is dual to the heterotic theory at weak coupling. Moreover, under this duality, the heterotic 2-form B_2 is exchanged with the R-R 2-form C_2 in type I theory, implying a string-string duality between the fundamental SO(32) heterotic string and the type I D-string.

Since type IIB string theory enjoys self S-duality, it is natural to seek a similar S-duality for type IIA string theory. In this context, D0-branes can be interpreted as Kaluza–Klein modes arising from compactification of eleven-dimensional supergravity, with KK radius $R_{11} = g_s\sqrt{\alpha'}$. This indicates that the $g_s \gg 1$ limit of type IIA string theory corresponds to 11-dimensional $\mathcal{N} = 1$ supergravity (with 32 supercharges). The gravitational coupling and Planck scale of 11D supergravity have identities $\kappa_{11}^2 = \frac{1}{2}(2\pi)^8 g_s^3 \alpha'^{\frac{9}{2}}$ and $\ell_{\mathrm{P},11} = g_s^{1/3}\sqrt{\alpha'}$. The complete quantum gravity theory that interpolates between type IIA in the $g_s \ll 1$ limit and eleven-dimensional supergravity in the $g_s \gg 1$ limit is known as *M-theory* [36]. The fundamental string and extended branes of type IIA arise as reductions of the M2- and M5-branes of M-theory. There is also an S-duality relation between M-theory and the $\mathrm{E}_8 \times \mathrm{E}_8$ heterotic string theory, realized via orbifold compactification on $S^1/\mathbb{Z}_2$ [35].

U-duality

U-duality, short for unified or ultimate duality [24], is the full non-perturbative duality group including both T-duality and S-duality. It acts on all moduli (both NS-NS and R-R) in type II string theories. The U-duality groups for type II toroidal compactifications have been summarized in Table I.1. Here we provide further examples of U-duality.

One example is the duality between the heterotic string theory compactified on T^2 and type IIA superstring theory compactified on a K3 surface, mentioned in the previous subsection. Both theories preserve the same supersymmetry and share the same moduli space. Their spectra can be matched by identifying [24, 25]

$$\Phi^{\mathrm{Het}} = -\Phi^{\mathrm{IIA}}, \qquad G_{\mu\nu}^{\mathrm{Het}} = e^{2\Phi^{\mathrm{Het}}} G_{\mu\nu}^{\mathrm{IIA}} \,. \tag{I.3.32}$$

This is a combination of strong/weak-coupling duality and target space duality, and thus serves as an example of U-duality.

Another notable example of U-duality is the Sen–Vafa duality [37] between two string theories compactified on freely acting orbifolds. Consider a string theory with U-duality group G and T-duality group H. There exist duality elements $h, h' \in H \cap \mathbb{Z}_p$, $g \in G \setminus H$, such that $h' = ghg^{-1}$. The moduli space then contains two subspaces $\mathcal{M}$ and $\mathcal{M}'$, which are left invariant under h and h' respectively. For a theory $M \in \mathcal{M}$, there exists a dual theory $M' = gM$. Furthermore, by compactifying M (M') on $S^1/\mathbb{Z}_p$ and modding out by a simultaneous action of h

(h')—where $\mathbb{Z}_p$ is a shift (i.e. a translation) by $1/p$ along the circle—one obtains two Sen–Vafa dual theories. For example, consider type IIA string compactification on T^4. According to Table I.1, there are U-duality group $G = \mathrm{SO}(5,5;\mathbb{Z})$ and T-duality group $H = \mathrm{SO}(4,4;\mathbb{Z})$. Choosing a duality g that acts as

$$\Phi \;\to\; -\Phi, \qquad H \;\to\; e^{-2\Phi}\,(*H)\,, \tag{I.3.33}$$

where $H = \mathrm{d}B$, we see this mirrors the string-string dualities discussed above. With h arbitrary in $\mathrm{SO}(4,4;\mathbb{Z})$, one can define corresponding theories M and M'. Taking further $T^2/\mathbb{Z}_p$ freely acting orbifold compactifications of M (M'), together with modding out by h (h'), yields two four-dimensional dual theories. In the orbifolded theory from M, the Kähler modulus T and the complex structure modulus U parametrize T^2. There is also the axio-dilaton $S = a + e^{-\phi_4}$, where a is dual to the Kalb–Ramond B-field and ϕ_4 is the four-dimensional dilaton that controls the string coupling. The dual orbifolded theory from M' has the same spectrum, denoted T', U', and S'. Owing to the g-action in (I.3.33), the S and T moduli are exchanged: $S' = T$, $T' = S$.

I.3.4 Orbifold compactifications

In Subsection I.3.1, we demonstrated type II string compactifications on tori. We saw that toroidal compactifications produce a rich spectrum, preserving 32 supercharges of supersymmetry. However, to connect with real-world physics, the spectrum must be much smaller, and spacetime supersymmetry must be broken or at least reduced. As mentioned previously, this can be achieved by considering more intricate internal spaces, which lead to reduced supersymmetry and smaller moduli spaces. There are many possible constructions, such as Calabi–Yau manifolds and orbifolds. Covering all such scenarios is beyond the scope of this thesis. In this section, as a preliminary to later chapters, we focus on two important classes of string compactifications: toroidal orbifold compactifications [38, 39] and non-geometric compactifications. We begin by introducing the former.

Consider a Riemannian manifold $\mathscr{M}$ and a discrete group $G \subset \mathrm{ISO}(\mathscr{M})$. An *orbifold* $\mathscr{O} = \mathscr{M}/G$ is defined as the quotient of $\mathscr{M}$ by the action of G, such that for any $g \in G$ and $x \in \mathscr{M}$, the points x and gx are identified under the quotient. Hence, a point $Gx \in \mathscr{O}$ is an orbit of G on $\mathscr{M}$, motivating the term "orbifold".

Let G be an Abelian point group. The partition function of such an orbifold compactification is

$$\begin{aligned} Z(\tau) &= \sum_{g,h\in G} \epsilon(h,g) Z[h,g](\tau) \\ &= \sum_{h\in G} \left[\frac{1}{|G|} \sum_{g\in G} \epsilon(h,g)\, \mathrm{Tr}_h \left(g P_{\mathrm{GSO}}\, q^{L_0(h)-\frac{c}{24}} \bar{q}^{\bar{L}_0(h)-\frac{c}{24}} \right) \right]. \end{aligned} \tag{I.3.34}$$

Here $\epsilon(h,g)$ is called discrete torsion, a phase for maintaining modular invariance. Note that this partition function includes the original partition function on $\mathscr{M}$,

which is $Z[\mathbf{1},\mathbf{1}](\tau)$ and is referred to as the untwisted sector. In the untwisted sector, only states invariant under the orbifold projection survive. The other $Z[h,g](\tau)$ correspond to partition functions of twisted sectors, as the fields have twisted boundary conditions

$$X\left(\sigma^0,\sigma^1+2\pi\right) = hX\left(\sigma^0,\sigma^1\right)h^{-1}\,, \tag{I.3.35}$$

$$X\left(\sigma^0+2\pi\tau_2,\sigma^1+2\pi\tau_1\right) = gX\left(\sigma^0,\sigma^1\right)g^{-1}\,. \tag{I.3.36}$$

The twisted sectors contribute additional states to the spectrum and are necessary for modular invariance.

We point out that there are two kinds of orbifolds: freely acting orbifolds and non-freely acting orbifolds. To distinguish them, consider orbifold actions on a circle as an example, which has the isometry group $\mathrm{ISO}(S^1)=\mathrm{O}(2)$. A shift action $X(\sigma)\to X(\sigma)+2\pi R/p$, with R the radius of the circle, defines an $S^1/\mathbb{Z}_p$ orbifold which is a smooth manifold without fixed points. Hence, the action is free,[6] and $\mathbb{Z}_p\subset\mathrm{SO}(2)\subset\mathrm{O}(2)$. In contrast, a reflection $X(\sigma)\to -X(\sigma)$ gives an $S^1/\mathbb{Z}_2$ orbifold with $\mathbb{Z}_2=\mathrm{O}(2)/\mathrm{SO}(2)$. There is a fixed point $X=0$, such that it is non-freely acting. Thus, non-freely acting orbifolds involve rotations and/or reflections on $\mathscr{M}$, resulting in fixed points or fixed loci, which are metric singularities.

The twisted sectors of non-freely acting orbifolds contain localized twisted states, which have no zero-mode momenta along action directions and are localized at singular fixed points (or loci). In addition, superpartners (such as gravitini) in the untwisted sector are projected out by the non-free orbifold action, leading to explicit supersymmetry breaking. If the orbifold twist introduces non-trivial holonomy in the internal space, the number of covariantly constant spinors is reduced, and supersymmetry can be partly broken. In this case, the localized moduli fields resolve (or blow up) the orbifold singularities, and the resulting space may become isomorphic to a Calabi–Yau manifold.

In freely acting orbifolds, the string zero-modes are shifted. For example, an $S^1/\mathbb{Z}_p$ orbifold action shifts momentum or winding in (I.3.1) by a $1/p$-fractional number. As a consequence, states in the twisted sectors are not localized and are generally massive due to fractional momenta and windings. Meanwhile, some massless states in the untwisted sector are not projected out, but instead acquire masses due to the shift. In particular, superpartners in the untwisted sector, such as some gravitini, become massive by running around the compact dimensions with twisted boundary conditions. The masses of these untwisted and twisted states thus depend on the geometric moduli. In the $S^1/\mathbb{Z}_p$ example, these masses are inversely proportional to the radius. Consequently, in certain decompactification limits, supersymmetry may be restored; we will discuss this in Chapter IV. In the effective field theory, the gravitino eats a Goldstino and becomes massive, so supersymmetry is broken spontaneously. Therefore, a freely acting orbifold that breaks supersymmetry is also called a *Scherk–Schwarz orbifold*.

[6] For more general orbifolds, the free orbifold action can involve both shifts and rotations. Fixed points from rotations can be removed by shifts.

In this section, we focus on orbifolds of the form $\mathscr{O} = T^n/\mathbb{Z}_p$, defined as the quotient of a torus[7] by a discrete $\mathbb{Z}_p$ symmetry. For the partition function of a $\mathbb{Z}_p$ orbifold, all sectors mix under modular transformations and all phases can be chosen as $\epsilon(h,g) = 1$. Here we analyze the partition function of $T^n/\mathbb{Z}_p$ orbifold compactification with even n, where $\mathbb{Z}_p$ acts non-freely on the torus. The derivation for freely acting orbifolds is analogous. A non-freely acting $\mathbb{Z}p$ is generated by a single element θ satisfying $\theta^p = 1$. The action of θ is an $\mathrm{SO}(2)^{n/2} \subset \mathrm{SO}(n)$ rotation, with eigenvalues $\exp(\pm 2\pi i v_i)$, where $v_i = a_i/p$, $a_i \in \mathbb{Z}$, and $i = 1, 2, \ldots, n/2$. To make this explicit, we define torus coordinates in a complex basis:

$$W^i = \frac{1}{\sqrt{2}}\left(X^{2i-1} + iX^{2i}\right), \quad W^{i^*} = \frac{1}{\sqrt{2}}\left(X^{2i-1} - iX^{2i}\right), \quad i = 1, 2, \ldots, \frac{n}{2}, \tag{I.3.37}$$

such that under the θ action,

$$W^i \;\to\; e^{2\pi i v_i} W^i, \qquad W^{i^*} \;\to\; e^{-2\pi i v_i} W^{i^*}. \tag{I.3.38}$$

To ensure the orbifold is crystallographic, the vectors should lie on the lattice after θ-rotation. This restricts the possible values of p. For example, in $n = 2$ dimensions, p can only be $2, 3, 4, 6$. Note that θ acts on the lattice as a matrix of integers. Hence, by the Lefschetz fixed point theorem, the number of fixed points of θ is

$$\chi(\theta) = \det(1 - \theta) = \prod_{i=1}^{n/2} 4\sin^2(\pi v_i). \tag{I.3.39}$$

According to (I.3.34), the partition function of a toroidal orbifold can be expressed as

$$Z_{T^n/\mathbb{Z}_p}(\tau) = \frac{1}{p}\sum_{k,l=0}^{p-1} Z[k,l] = \frac{1}{p}\sum_{k,l=0}^{p-1} Z_{\mathrm{b}}[k,l] Z_{\mathrm{f}}[k,l], \tag{I.3.40}$$

where $Z[k,l]$ is the partition function of the (θ^k, θ^l) twisted sector, with boundary conditions

$$W^i\left(\sigma^0, \sigma^1 + 2\pi\right) = e^{2\pi i k v_i} W^i\left(\sigma^0, \sigma^1\right), \tag{I.3.41}$$

$$W^i\left(\sigma^0 + 2\pi\tau_2, \sigma^1 + 2\pi\tau_1\right) = e^{2\pi i l v_i} W^i\left(\sigma^0, \sigma^1\right). \tag{I.3.42}$$

Especially, the untwisted sector partition function is

$$Z[0,0] = \frac{1}{|\eta(\tau)|^{2n}} \sum_{\boldsymbol{p}\in\Lambda^*} \sum_{\boldsymbol{w}\in\Lambda^*} q^{\frac{1}{2}\left(\boldsymbol{p}+\frac{1}{2}\boldsymbol{w}\right)^2} \bar{q}^{\frac{1}{2}\left(\boldsymbol{p}-\frac{1}{2}\boldsymbol{w}\right)^2}. \tag{I.3.43}$$

[7] A torus $T^n = \mathbb{R}^n/\Lambda$ can also be regarded as an $\mathbb{R}^n$-orbifold quotiented by a lattice action Λ.

While the general partition function of a twisted sector is

$$Z\left[k,l\right]=\chi(\theta^k,\theta^l)\left|\prod_{j=1}^{D/2}\frac{\eta(\tau)}{\vartheta\begin{bmatrix}1/2+kv_j\\1/2-lv_j\end{bmatrix}}\right|^2\,, \tag{I.3.44}$$

where $\chi(\theta^k,\theta^l)$ is the number of simultaneous fixed points of θ^k and θ^l, and the ϑ-functions are defined in (I.2.45).

In Chapter IV we will discuss a freely acting $(T^4\times T^2)/\mathbb{Z}_p$ orbifold, where $\mathbb{Z}_p$ acts as a rotation (non-freely) on T^4 and as a shift on T^2. However, in that construction the T^4 orbifold is *asymmetric*, meaning that $\mathbb{Z}_p$ acts differently on the left- and right-moving sectors. This provides an example of a non-geometric compactification. A detailed computation of the mass spectrum and moduli space in orbifold compactifications will be presented there.

I.3.5 Non-geometric compactifications

One of the main topics of this thesis is non-geometric compactifications [40]. *Non-geometric* refers to internal spaces that lack a globally well-defined Riemannian metric. For example, the internal space may be a fiber bundle whose transition function is beyond the diffeomorphism group. As discussed earlier, string theory admits additional symmetries for internal spaces—the duality groups. By extending the transition functions of the internal space to include both diffeomorphisms and duality transformations, one obtains a non-geometric background, which cannot be globally described by a Riemannian metric. For instance, if the transition function involves both a diffeomorphism and a T-duality transformation, the background is called a *T-fold* [41]. In analogy, one can define S-folds, U-folds, and mirror-folds. Fluxes can also deform the geometry of a manifold, enabling the construction of non-geometric backgrounds by turning on appropriate fluxes in compact spaces [42]. Certain fluxes can obstruct even the local definition of a metric, rendering the internal space locally non-geometric. We will provide explicit examples later. Importantly, these fluxes, especially non-geometric fluxes, are restricted by Bianchi identities [43] and cannot take arbitrary values.

As the most well-studied example, we introduce non-geometric backgrounds arising from T-duality transformations on tori. Consider a flat three-torus T^3 with background $G_{ij}=\mathrm{diag}(R_1^2,R_2^2,R_3^2)$, and constant Kalb–Ramond field strength

$$H=\mathrm{d}B=\frac{\alpha' h}{2\pi}\mathrm{d}X^1\wedge\mathrm{d}X^2\wedge\mathrm{d}X^3\,,\quad h\in\mathbb{Z}\,. \tag{I.3.45}$$

This background carries an H-flux number h. Introducing the vielbein basis e^i, with $e^i=R_i\mathrm{d}X^i$ for $i=1,2,3$, the H-flux can be expressed as

$$H=h_{123}\;e^1\wedge e^2\wedge e^3\,,\quad h_{123}=\frac{\alpha'}{2\pi}\frac{h}{R_1R_2R_3}\,. \tag{I.3.46}$$

Then, we can perform a T-duality transformation along the X^1 direction. The Buscher rules (I.3.30) change the background to be

$$\widetilde{G} = \frac{\alpha'^2}{R_1^2}\xi^2 + R_2^2(\mathrm{d}X^2)^2 + R_3^2(\mathrm{d}X^3)^2\,, \quad \widetilde{H} = 0\,, \quad \widetilde{\Phi} = -\log\frac{R_1}{\sqrt{\alpha'}}\,, \tag{I.3.47}$$

with $\mathrm{d}\xi = \frac{h}{2\pi}\mathrm{d}X^2 \wedge \mathrm{d}X^3$ and veilbein $\tilde{e}^1 = \frac{\alpha'}{R_1}\xi$. Under this T-duality, the H-flux is mapped to a twisting of the torus, and the H-flux itself vanishes. The resulting *twisted torus*, which is a nilmanifold, has a spin connection with structure constants $f^i{}_{jk}$, defined by $\mathrm{d}e^i = \frac{1}{2}f^i{}_{jk}\, e^j \wedge e^k$. From the above construction, the non-trivial structure constant is

$$f^1{}_{23} = \frac{\alpha'}{2\pi}\frac{h}{R_1R_2R_3}\,, \tag{I.3.48}$$

which is exactly the H-flux before the T-duality transformation. We refer to $f^i{}_{jk}$ as the *geometric flux* or f-flux.

Performing a further T-duality along the X^2 direction on this twisted torus with f-flux yields a more involved background. In particular, the dual metric acquires an inconsistent boundary condition: $\mathcal{R}(X^3 = 0) \neq \mathcal{R}(X^3 = 2\pi)$, with $\mathcal{R}$ the Ricci scalar. This signals that the Ricci scalar is not invariant under diffeomorphisms, and the background becomes a T-fold whose transition functions include T-duality. Such a T-fold is globally non-geometric but locally geometric, in the sense that while a local metric exists, there is no globally well-defined metric. The geometric f-flux vanishes and is replaced by the *non-geometric Q-flux*, with

$$Q^{12}{}_3 = \frac{\alpha'}{2\pi}\frac{h}{R_1R_2R_3}\,, \tag{I.3.49}$$

A further T-duality along the X^3 direction transforms the T-fold into an *R-space*. The R-space is locally non-geometric, which means the background fields cannot be defined consistently even locally. The aforementioned Q-flux vanishes and is replaced by the *non-geometric R-flux*, with $R^{123} = \frac{\alpha'}{2\pi}\frac{h}{R_1R_2R_3}$.

In summary, one obtains a chain of fluxes related by successive T-duality transformations [43, 44]:

$$H_{ijk} \xrightarrow{\mathrm{T}_i} f^i{}_{jk} \xrightarrow{\mathrm{T}_j} Q^{ij}{}_k \xrightarrow{\mathrm{T}_k} R^{ijk}\,. \tag{I.3.50}$$

In Chapter III, we will investigate the phenomenology of T-fold compactifications with the turning on of H-, f-, and Q-fluxes. For comprehensive reviews of non-geometric compactifications, see [45, 46].

A particularly useful and well-defined class of non-geometric spaces is provided by *asymmetric orbifolds* [47], in which the orbifold group acts differently on the left- and right-moving sectors. The partition functions of asymmetric orbifolds are often subtle, but consistent models satisfying modular invariance in worldsheet CFTs have been constructed [48].

Many asymmetric orbifolds can be constructed from non-geometric fluxes [49, 50]. For concreteness, we focus on T^n toroidal compactifications with T-duality twists. Recall that in the T^n toroidal compactification, there are $2n$ U(1) photons from the reduction of metric G and B. These gauge symmetries become non-Abelian in the presence of a T-duality twist. Consider an asymmetric orbifold $\left(T^{n-1}\times S^1\right)/\mathbb{Z}_p$ with coordinates $X^1,\cdots,X^{n-1},Y$, with a freely-acting orbifold element $e^{2\pi(F_\mathrm{L}+F_\mathrm{R})}\delta_{a,b}\in \mathrm{O}(n,n;\mathbb{Z})$. $F_{\mathrm{L,R}}$ are the generators of the orbifold rotation on T^{n-1}, and $\delta_{a,b}$ is an order-p shift along the base S^1, acting on its coordinate Y as

$$Y_\mathrm{L}\ \to\ Y_\mathrm{L}+\frac{a\pi R}{p}+\frac{b\pi}{pR}\,,\qquad Y_\mathrm{R}\ \to\ Y_\mathrm{R}+\frac{a\pi R}{p}-\frac{b\pi}{pR}\,. \tag{I.3.51}$$

The case $(a,b)=(1,0)$ corresponds a momentum shift and yields a Scherk–Schwarz compactification [51]. In this situation, the structure constants of the gauge algebra coincide with those in a T-fold compactification with nonzero Q-flux [49]. Similarly, asymmetric $(a,b)=(0,1)$ shift gives rise to nonzero R-flux.

The effective theory of a non-geometric compactification on T^n with a T-duality twist can be formulated as a *double field theory* (DFT), which corresponds to a geometric compactification on a $2n$-dimensional internal space, twisted from a Lorentzian torus $T^{n,n}$ [41]. This $2n$-dimensional twisted torus is equipped with a generalized metric, which can be expressed (for vanishing R-flux) as

$$\mathcal{H}=\begin{pmatrix}\frac{1}{\alpha'}\left(G-BG^{-1}B\right) & BG^{-1}\\ -G^{-1}B & \alpha' G^{-1}\end{pmatrix}\in \mathrm{O}(n,n)\,. \tag{I.3.52}$$

The twisted torus is a group manifold $\mathcal{G}/\Gamma$, where $\mathcal{G}$ is a subgroup of $\mathrm{O}(n,n)$ with structure constants $\mathcal{F}_{ABC}$. The components $\mathcal{F}ABC$ encode the generalized geometric flux on $T^{n,n}$ and relate to H-, f-, Q-, and R-fluxes via

$$\mathcal{F}_{ijk}=H_{ijk}\,,\quad \mathcal{F}^{i}{}_{jk}=f^{i}{}_{jk}\,,\quad \mathcal{F}^{ij}{}_{k}=Q^{ij}{}_{k}\,,\quad \mathcal{F}^{ijk}=R^{ijk}\,. \tag{I.3.53}$$

For a pedagogical review of double field theory, see [52].

Analogous to DFT, non-geometric compactifications with U-duality twists are effectively described by *exceptional field theories* [53], which provide a unified framework for 11D supergravity incorporating U-duality symmetries. We will not discuss these theories in detail, as they lie beyond the scope of this thesis.

I.4 String cosmology

The intersection of string theory and cosmology represents a crucial frontier in theoretical physics. Although modern cosmology has achieved significant success in explaining observations, the microscopic origins of many phenomena remain unclear, and string theory provides a unique and indispensable framework for their study. The application of string theory to cosmology can be organized into two main aspects. The first concerns early-universe cosmology and the dynamics

of cosmic evolution, including the origin of inflation and subsequent transitions through various epochs. Distinct phases such as moduli domination, kination, and curvature domination can be motivated by string theory. The second aspect pertains to late-time cosmology, aiming to explain late-time (present-day) cosmology, seeking to explain contemporary observational data and phenomena, including the cosmic microwave background (CMB), gravitational waves, dark matter, dark radiation, and especially dark energy. For a recent review of string cosmology, see [54].

Of particular interest is the current accelerated expansion of the universe, i.e., dark energy. There are numerous models of dark energy, and scalar fields play a central role in many of them. As discussed earlier, string compactifications naturally generate a large number of scalar fields, including moduli, which can be relevant for cosmological model building. In this section, we discuss the realization of dark energy in string compactifications and examine the challenges inherent to these constructions.

I.4.1 Cosmic acceleration

The large-scale structure of our Universe is homogeneous and isotropic. Therefore, its geometry can be described by the four-dimensional Friedmann–Lemaître–Robertson–Walker (FLRW) metric

$$\mathrm{d}\Delta^2 = -\mathrm{d}t^2 + a(t)^2 \left(\frac{\mathrm{d}r^2}{1-kr^2} + r^2 \left(\mathrm{d}\theta^2 + \sin^2\theta \mathrm{d}\varphi^2 \right) \right) , \tag{I.4.1}$$

where $a(t)$ is the scale factor encoding the relative space scale of the universe, and k represents the curvature of the space, with $k = 1, 0, -1$ corresponding to a closed, flat, and open universe, respectively.

When the scale factor satisfies $\dot{a} > 0$ and $\ddot{a} > 0$, where the dot denotes a derivative with respect to t, the universe undergoes accelerated expansion. This phase is known as *cosmic acceleration*. It is widely believed that our Universe has experienced two epochs of accelerated expansion: the early inflationary epoch and the present dark energy-dominated epoch. Observations from type Ia Supernovae [55–57], cosmic microwave background (CMB) [58, 59] and baryon acoustic oscillations (BAO) [60] have established the existence of late-time cosmic acceleration, finding that approximately 68% of the current energy density of the Universe is due to an unknown component termed *dark energy*.

Dark energy is often modeled by scalar fields. Consider the action for a scalar field ϕ with potential $V(\phi)$ in the presence of matter fields:

$$S = \int \mathrm{d}^4x \frac{\sqrt{-g}}{2} \left(\frac{\mathcal{R}}{8\pi G_\mathrm{N}} - g^{\mu\nu}\partial_\mu\phi\partial_\nu\phi - V(\phi) \right) + S_M , \tag{I.4.2}$$

where the metric g is the FLRW metric (I.4.1), and S_M is the action of matter fields, including dust (ordinary matter and dark matter) and radiation. Define the Hubble parameter as $H(t) \equiv \dot{a}(t)/a(t)$. Due to the spatial homogeneity, the

scalar field depends only on time, $\phi = \phi(t)$, and the equation of motion of the scalar field is

$$\ddot{\phi} + 3H\dot{\phi} + \partial_\phi V = 0\,. \tag{I.4.3}$$

On cosmological scales, the components of the Universe can be treated as a perfect fluid, with energy-momentum tensor $T_{\mu\nu} = \text{diag}\,(-\rho, p, p, p)$, where $\rho(t)$ and $p(t)$ are the total energy density and the total pressure, including contributions from both the scalar field and matter. The equation of state parameter is defined as $w = p/\rho$. For various components, we have: $w_m = 0$ for dust, $w_r = 1/3$ for radiation, and

$$w_\phi = \frac{p_\phi}{\rho_\phi} = \frac{\frac{1}{2}\dot{\phi}^2 - V(\phi)}{\frac{1}{2}\dot{\phi}^2 + V(\phi)} \tag{I.4.4}$$

for the scalar field. The total equation of state parameter is $w = \Omega_m w_m + \Omega_r w_r + \Omega_\phi w_\phi$, where Ω_i is the density fraction for each component. Similarly, the matter equation of state is $w_M = \Omega_m w_m + \Omega_r w_r$.

Furthermore, applying the Einstein field equation $G_{\mu\nu} = 8\pi G_\text{N} T_{\mu\nu}$ to the FLRW metric yields the Friedmann equations, governing the evolution of $a(t)$. The first Friedmann equation reads:

$$H^2 = \frac{\dot{a}^2}{a^2} = \frac{8\pi G_\text{N}}{3}\rho - \frac{k}{a^2}\,. \tag{I.4.5}$$

Observational data favor $k = 0$, which we assume henceforth. The second Friedmann equation is

$$\frac{\ddot{a}}{a} = -\frac{4\pi G_\text{N}}{3}(\rho + 3p) = -\frac{4\pi G_\text{N}}{3}\rho(1 + 3w)\,. \tag{I.4.6}$$

It means that an accelerating universe has

$$\ddot{a} > 0 \quad \Leftrightarrow \quad w < -\tfrac{1}{3} \tag{I.4.7}$$

for a positive ρ. Note that $w_M \geq 0$ while $-1 < w_\phi < 1$, so accelerated expansion can only occur during a scalar-dominated epoch, with $V(\phi) > \frac{1}{2}\dot{\phi}^2$.

Another useful parameter is the *acceleration parameter*, or called *slow-roll parameter*, defined as

$$\epsilon \equiv -\frac{\dot{H}}{H^2}\,. \tag{I.4.8}$$

Cosmic acceleration requires $0 \leq \epsilon < 1$. In the scalar-dominated regime, with $\rho \simeq \rho_\phi$, the acceleration parameter satisfies

$$\epsilon \simeq \frac{\dot{\phi}^2}{2H^2} = \frac{3}{2}(1 + w_\phi)\,. \tag{I.4.9}$$

An alternative definition is the *potential show-roll parameter* ϵ_V, which is

$$\epsilon_V \equiv \frac{M_\text{P}^2}{2}\left(\frac{\partial_\phi V}{V}\right)^2\,. \tag{I.4.10}$$

If there is only one scalar field and no matter, then $\epsilon_V = \epsilon$.

There are two main scenarios for realizing cosmic acceleration. The first is when the scalar field is static, i.e., stabilized at the minimum of its potential. From the first Friedmann equation (I.4.5) and $\rho_\phi \equiv \frac{1}{2}\dot{\phi}^2 + V = V$, cosmic expansion requires $V(\phi) > 0$. In this case, $w_\phi = -1$; the scalar potential acts as a *cosmological constant* $\Lambda = 8\pi G_{\rm N} V$, corresponding to a positive, uniform energy density. The resulting cosmological background is de Sitter space. Observational data show that our late-time Universe is well described by the ΛCDM model, consisting of a cosmological constant Λ, cold dark matter, and Standard Model fields.

Instead, another scenario assumes that dark energy is dynamical. These are called *quintessence* or dynamical dark energy models. In this context, it is convenient to define

$$x \equiv \frac{\dot{\phi}}{\sqrt{6} M_{\rm P} H}, \qquad y \equiv \frac{\sqrt{V(\phi)}}{\sqrt{3} M_{\rm P} H}. \tag{I.4.11}$$

The evolution of the universe's dynamical system toward the fixed points, where

$$\begin{aligned} \frac{{\rm d}x}{{\rm d}N} &= -3x + \frac{\sqrt{6}}{2}\lambda y^2 + \frac{3}{2}x\left[(1-w_M)\,x^2 + (1+w_M)\left(1-y^2\right)\right] = 0\,, \\ \frac{{\rm d}y}{{\rm d}N} &= -\frac{\sqrt{6}}{2}\lambda x y + \frac{3}{2}y\left[(1-w_M)\,x^2 + (1+w_M)\left(1-y^2\right)\right] = 0\,, \end{aligned} \tag{I.4.12}$$

with $N \equiv \ln a$ is the e-folding number, characterizing the evolution time. And $\lambda \equiv -M_{\rm P}\frac{\partial_\phi V}{V}$ corresponds to the slope of the potential. Consider a model with a constant λ, then the potential takes the exponential form

$$V(\phi) = V_0 e^{-\lambda\phi/M_{\rm P}}\,, \quad \lambda > 0\,. \tag{I.4.13}$$

This system exhibits four fixed points:

- $(x, y) = (0, 0)$: There is $\Omega_\phi = 0$ and $w = w_M \geq 0$; this corresponds to a matter-dominated phase with no acceleration.
- $(x, y) = (1, 0)$: This point is unstable for $\lambda < \sqrt{6}$ and a saddle for $\lambda > \sqrt{6}$. Here, $\Omega_\phi = 1$ and $w = 1$, describing a *kination* phase, dominated by the kinetic energy of the scalar field, again with no acceleration.
- $(x, y) = \left(\frac{\lambda}{\sqrt{6}}, \sqrt{1 - \frac{\lambda^2}{6}}\right)$: At this fixed point, $\Omega_\phi = 1$, and $w = \frac{\lambda^2}{3} - 1$. It is a cosmic acceleration phase if $0 \leq \lambda < \sqrt{2}$. This point is stable for $\lambda < \sqrt{2}$ and a saddle for $\sqrt{2} < \lambda < \sqrt{6}$.
- $(x, y) = \left(\sqrt{\frac{3}{2}}\frac{1+w_M}{\lambda}, \sqrt{\frac{3(1-w_M^2)}{2\lambda^2}}\right)$: There is $\Omega_\phi = \frac{3(1+w_M)}{\lambda^2}$. This case is called the scaling solution, where $\Omega_\phi/\Omega_M =$ constant. We will not focus on this solution since our Universe transitioned from matter domination to scalar domination.

From the above discussion, the Universe exhibits accelerated expansion if $\lambda < \sqrt{2}$, approaching the fixed point $(x, y) = \left(\frac{\lambda}{\sqrt{6}}, \sqrt{1 - \frac{\lambda^2}{6}}\right)$. Thus, in the single-field exponential potential model (I.4.13), eternal acceleration requires $\lambda < \sqrt{2}$. Ref. [61] shows that transient acceleration can be achieved if $\lambda < \sqrt{3} + \mathcal{O}(0.01)$. There also exist quintessence models with non-constant λ (non-exponential potentials), which we do not discuss here. For a review of these quintessence models, see [62].

In Subsection II.3.3 and Appendix III.B, we will discuss the cosmic acceleration driven by multiple scalar fields, whose dynamics tend to follow the $-\nabla V$ direction in field space. Such multi-field models are more natural in string theory, as we will elaborate.

It is important to remark that both the ΛCDM and quintessence models face significant challenges in describing our Universe. In the ΛCDM model, the energy density of the cosmological constant is extremely small, $\Lambda \sim 10^{-122} M_{\rm P}^4$, which is highly unnatural. Furthermore, it is notoriously difficult to derive a small, nonzero cosmological constant from quantum gravity, as we will see in the next subsection. Another puzzle is the so-called "coincidence problem": why the dark energy density is comparable to the matter density ρ_M today. Quintessence models also face this coincidence problem, but do not have the same degree of fine-tuning for the vacuum energy. However, they come with additional challenges: (1) There may still be a residual cosmological constant, if the potential is asymptotically nonzero; (2) The quintessence field must be extremely light, $m \lesssim H_0 \simeq 10^{-33}, \text{eV}$, and is highly sensitive to quantum corrections; (3) The quintessence field could mediate a fifth force, in conflict with experimental constraints, though this issue can be avoided if the field is an axion or resides in a hidden sector [54, 63].

As previously noted, earlier observations have provided strong support for the ΛCDM model with a small, positive cosmological constant. However, low-redshift observations have shown tensions with the ΛCDM model, and prefer dynamical dark energy [4, 64]. Especially, in the past two years, results from the DESI experiment [6, 7], when combined with other observational datasets, suggest evidence for dynamical dark energy at more than 3σ confidence. With further data collection and improved analysis, it may soon become possible to discern whether dark energy is truly a cosmological constant or instead has a dynamical, quintessence-like origin.

In the following chapters, we will adopt units where the four-dimensional Planck mass and gravitational constant are set to unity, $M_{\rm P} = 8\pi G_{\rm N} = 1$.

I.4.2 String realizations of dark energy

In Subsection I.3.2 we discussed the moduli in string theory. Moduli play a central role in determining the parameters of particle physics, which are observed to be almost fixed in our Universe. Therefore, the moduli must be stabilized at their minima or evolve extremely slowly under the influence of the scalar potential. In the same way, dark energy can be sourced by these stabilized or slowly rolling

moduli fields, realizing either a cosmological constant or a dynamical quintessence scenario. This mechanism is known as *moduli stabilization*.

String theory offers a variety of mechanisms for generating scalar potentials and stabilizing moduli. For instance, consider the overall radius of the internal compactification space, denoted r. In string theory, p-form fluxes can thread p-cycles of the internal manifold, leading to quantized flux numbers via the Dirac quantization condition. The presence of such background fluxes induces a scalar potential $V \propto r^{-6-2p}$ for the radius modulus. Extended objects, such as Dp-branes, also contribute to the scalar potential: space-filling Dp-branes generate $V \propto T_p, r^{p-15}$, where T_p is the brane tension. Orientifold planes have the same contribution but with negative tension. Other effects, including gaugino condensation, wrapping Euclidean branes, extra-dimensional curvature, and higher loop α' and g_s corrections, also contribute to the scalar potential and play a role in moduli stabilization [54]. We will use some of them to attempt string realizations of dark energy in two main frameworks: de Sitter (dS) minima and runaway quintessence.

De Sitter realizations

We begin by briefly reviewing some string constructions of de Sitter vacua. There exist general no-go theorems [65] ruling out dS vacua if the internal space is static, compact, and nonsingular. As a result, most de Sitter constructions are metastable and based on orientifold compactifications with reduced supersymmetry and internal singularities. The problem of moduli stabilization is best understood in type II string theories, and we focus here on type IIB Calabi–Yau orientifold compactifications, which preserve $\mathcal{N} = 1$ supersymmetry in four dimensions. In these compactifications, there are $h^{1,1}_+$ Kähler moduli

$$T_\alpha = \int_{\Sigma_\alpha} C_4 + \frac{i}{2} \int_{\Sigma_\alpha} J \wedge J \,, \tag{I.4.14}$$

$h^{1,2}_-$ complex structure moduli U_i, and the axio-dilaton $S = C_0 + i g_s^{-1}$, with J the Kähler form. In addition, there are 3-form fluxes from F_3 and H_3, which couple respectively to D-strings and fundamental strings. These can be combined into the imaginary self-dual (ISD) 3-flux $G_3 = F_3 - i g_s^{-1} H_3$, satisfying $iG = *_6 G$.

The effective theory is characterized by the Kähler potential

$$K = -2 \log \mathcal{V} - \log \left(S - \bar{S}\right) - \log \left(-i \int \Omega \wedge \Omega \right) , \tag{I.4.15}$$

and the Gukov–Vafa–Witten superpotential

$$W_{\text{flux}} = \int_X G_3 \wedge \Omega \,, \tag{I.4.16}$$

where Ω is the holomorphic $(3,0)$-form on the Calabi–Yau manifold X. The $\mathcal{N} = 1$ supergravity with Kähler potential K and superpotential W has the F-term scalar

potential

$$V = e^K \left(K^{a\bar{b}} D_a W D_{\bar{b}} W - 3W^2 \right) , \quad \text{with} \quad D_a W = \partial_a W - W \partial_a K . \tag{I.4.17}$$

The F-term of Kähler moduli satisfies the no-scale condition $K^{\alpha\bar{\beta}} \partial_\alpha K \partial_{\bar{\beta}} K = 3$, such that the F-term potential for the complex structure moduli and dilaton is

$$V(U_i, S) = e^K K^{i\bar{j}} D_i W D_{\bar{j}} W . \tag{I.4.18}$$

This potential admits Minkowski minima at $D_i W = 0$, equivalent to the ISD condition on G_3. In this case, the energy contributions from fluxes and negative-tension orientifold planes (O-planes) cancel, yielding a vanishing potential.

At these Minkowski minima, the complex structure moduli and the dilaton are stabilized, but the Kähler moduli remain as flat directions. There are two major scenarios for stabilizing the Kähler moduli, which are the KKLT construction [66] and the Large Volume Scenario (LVS) [67]. Both of which allow for the construction of de Sitter vacua. We illustrate the essential ideas using the KKLT mechanism.

Non-renormalization theorems imply that the only allowed corrections to the superpotential are non-perturbative. In the KKLT framework, such corrections arise from Euclidean D3-brane instantons wrapping supersymmetric 4-cycles, or from gaugino condensation on D7-branes. For simplicity, consider there is only one Kähler modulus T, then the superpotential is

$$W = W_0 + W_{\text{np}} = W_0 + A(U_i, S) e^{-aT} , \tag{I.4.19}$$

where $a = 2\pi$ for ED3-instantons and $a = 2\pi/N$ for gaugino condensation ("fractional instantons"), with N the rank of condensing gauge group $\mathrm{SU}(N)$. Here we assumed the on-shell constant W_0 from (I.4.16) can be added simply. The resulting scalar potential admits a supersymmetric anti-de Sitter (AdS) minimum with $V_{\text{min}} < 0$, which approaches zero as $\mathrm{Im}\, T \to \infty$. The value of V_{min} is controlled by $|W_0|$ and thus by the choice of fluxes. The fluxes from the above non-perturbative effects lead to a long throat characterized by a warped factor e^{A_0}, such that the metric takes the form $\mathrm{d}s_{10}^2 = e^{2A_0} \mathrm{d}s_4^2 + \mathrm{d}s_6^2$.

It is possible to obtain de Sitter vacua by imposing additional effects. In the original KKLT construction [66], anti-D3-branes are placed at the tip of the warped throat, which break supersymmetry and contribute a positive term to the scalar potential:

$$V_{\overline{\text{D3}}} \sim \frac{2 e^{4A_0}}{T - \overline{T}} . \tag{I.4.20}$$

This positive contribution can uplift the AdS minimum to a metastable de Sitter vacuum.

Beyond KKLT and LVS, several other frameworks have been proposed for realizing de Sitter vacua in string theory. One important example is the construction

of de Sitter solutions in non-geometric compactifications. In such scenarios, the ten-dimensional string-frame metric can be written as [68, 69]

$$\mathrm{d}s_{10}^2 = \tau^{-2}\mathrm{d}s_4^2 + \rho\mathrm{d}s_6^2\,, \qquad \tau^2 = e^{-2\phi}\rho^3\,, \tag{I.4.21}$$

in the approximation of smeared localized sources. Here $\rho = (\mathrm{Vol})^{1/3}$ is associated with the internal volume and the Kaluza–Klein scale, and ϕ is the 4D dilaton. With T-duality twists, the H-, f-, Q-, R-fluxes contribute to the potential as

$$V_H \sim \rho^{-3}\tau^{-2}\,, \quad V_f \sim \rho^{-1}\tau^{-2}\,, \quad V_Q \sim \rho\,\tau^{-2}\,, \quad V_R \sim \rho^3\tau^{-2}\,, \tag{I.4.22}$$

respectively [68]. By appropriately tuning these flux-induced potentials and including additional free parameters, it is possible to construct tachyon-free, metastable de Sitter vacua in these non-geometric backgrounds [70–73]. Interestingly, many de Sitter vacua generated via non-perturbative effects are locally equivalent to those arising from non-geometric fluxes [74].

Despite these various proposals, all known string theory constructions of de Sitter vacua remain controversial and subject to intense debate [69, 75]. For instance, many explicit de Sitter constructions are found to harbor at least one tachyonic mode, indicating perturbative instability [76]. Additionally, it is often problematic to rely on an effective four-dimensional supergravity description when the resulting vacua are non-supersymmetric, since light modes may become destabilized beyond the regime of control. In the KKLT scenario, backreaction from the introduction of anti-D3-branes presents further challenges.

Quintessence realizations

In contrast to the challenge of string realizations of a positive cosmological constant, it is generally much more tractable to obtain runaway potentials suitable for dynamical dark energy (quintessence) scenarios. The essential requirement in these models is a sufficiently shallow potential slope to drive cosmic acceleration; for instance, in the single-field exponential potential discussed previously, the parameter λ must satisfy $\lambda < \sqrt{2}$ (or $\lambda \lesssim \sqrt{3}$ for transient acceleration).

Given the abundance of moduli in string compactifications, one must carefully identify viable runaway directions on the moduli space. Notably, the overall volume modulus and the dilaton are disfavored as quintessence candidates: they couple universally to matter, and thus would mediate variations in fundamental couplings and long-range fifth forces, neither of which are observed. In fact, it has been shown that along these directions the potential is generically too steep to support accelerated expansion [77]. On the contrary, axions are arguably the most attractive quintessence candidates. The axion are among the most promising candidates for quintessence. Their approximate shift symmetry constrains their interactions and naturally protects both the axion mass and its potential energy density. Furthermore, the spin-independent fifth force bounds [78] have no restriction on pseudo-scalars.

It should be emphasized, however, that there are powerful no-go theorems against shallow single-field quintessence with cosmic acceleration in string theory.

For instance, [79] shows that in $\mathcal{N} = 1$ supergravity, the scalar potential for a single field must either have a large slow-roll parameter (I.4.10), $\epsilon_V > 1$, or admit $V < \rho_\phi < 0$. As an explicit example, consider a generic $\mathcal{N} = 1$ model with a single flat direction, a bulk modulus Φ. It typically has the Kähler potential and the superpotential

$$K = -p \log(\Phi - \overline{\Phi}) \,, \quad W = A e^{-a\Phi} \,. \tag{I.4.23}$$

This structure yields a scalar potential with a runaway direction along the saxion $\mathrm{Im}\,\Phi$, for which the potential slow-roll parameter behaves as $\epsilon_V \to \frac{4}{p} a^2 (\mathrm{Im}\,\Phi)^2$ as $\mathrm{Im}\,\Phi \to \infty$. It diverges such that the rolling evolution quickly becomes too steep to drive cosmic acceleration.

These difficulties motivate consideration of multi-field quintessence models, which can address several challenges faced by their single-field counterparts. Such models are also natural from the perspective of string theory, where compactifications generically yield large numbers of scalar fields. Even if the overall potential remains steep, cosmic acceleration can arise through dynamics involving non-geodesic field-space trajectories or via alignment in gradient flow directions.

Non-geodesic trajectories in field space can be very gentle, allowing for effective realization of cosmic acceleration even when the underlying potential is steep. Various EFT multi-field models from string theory have been proposed that are compatible with both observational data and Swampland conjectures [54]. However, when requiring a standard cosmological history with a prolonged matter-dominated epoch preceding dark energy domination, it has been shown that none of these models naturally evolve to the currently observed values $(\Omega_\phi, w_\phi) \approx (0.7, -1)$, except in cases where the initial condition is set deep in the regime of kinetic domination [80]. Consequently, it remains an open question whether fully realistic and observationally viable models can be realized in alternative multi-field string theory constructions. In addition, according to our work in Chapter II, the Swampland Distance Conjecture imposes significant restrictions on the allowed asymptotic trajectories in scalar field space. Realizing a quintessence model with cosmic acceleration in the asymptotic region of field space is very hard unless the moduli space exhibits large curvature.

Multi-field quintessence models with trajectories along the gradient flow have also been studied. For example, [81] constructed a potential with two scalars ϕ_1 and ϕ_2, and the potential takes the form

$$V = f^2 \frac{\phi_2}{\phi_1} + h^2 \frac{\phi_1}{\phi_2^3} \,, \tag{I.4.24}$$

where f and h are constants determined by flux choices. This potential admits an asymptotic gradient flow with $\frac{|\nabla V|}{V} = \sqrt{\frac{2}{7}} < \sqrt{2}$, thus satisfying the condition for cosmic acceleration in the single-field exponential case. Such constructions demonstrate that, with appropriate alignment and dynamics, multi-field models can in principle realize slow-roll quintessence compatible with both theory and observation, though explicit models satisfying all real-world constraints remain elusive.

I.5 Swampland program

The various compactifications in string theory, with their vast array of choices for fluxes, branes, and other setups, give rise to a multitude of (but finite) distinct string vacua. Such viable low-energy effective field theories (EFTs) derived from quantum gravity theory are said to populate the Landscape. In contrast, one can construct many other EFTs that appear consistent at low energies but cannot be consistently coupled to a quantum theory of gravity. Such theories are said to lie in the Swampland.[8] The Swampland program aims to identify the universal properties of theories within the Landscape, proposing conjectured criteria, which are often called Swampland conjectures, to distinguish them from those in the Swampland.

A foundational example of such a criterion is the No Global Symmetry Conjecture. It states that when coupled to gravity, any global symmetry in a consistent theory must be either broken or gauged. A primary motivation for this conjecture comes from heuristic arguments of black holes, that a black hole could destroy global charges by swallowing a charged object and then evaporating via Hawking radiation. According to this conjecture, any EFT coupled to gravity that possesses an exact, ungauged global symmetry is inconsistent and lies in the Swampland.

Below, we summarize several Swampland conjectures that have deep implications and motivate the investigations of later chapters in this thesis.

I.5.1 Swampland Distance Conjecture

One of the most influential conjectures in the Swampland program is the *Swampland Distance Conjecture* (SDC) [83]. Its statement is as follows:

Swampland Distance Conjecture

Consider a theory coupled to gravity with a moduli space $\mathcal{M}$. A point in $\mathcal{M}$ specifies the expectation values of all moduli and can be denoted as $\boldsymbol{\Phi} = (\Phi^1, \Phi^2, \ldots)$. Then starting from any point $\boldsymbol{\Phi}_0 \in \mathcal{M}$, there exists another point $\boldsymbol{\Phi}_1$, such that the geodesic distance between them is infinite, i.e., $\Delta\Phi \equiv |\boldsymbol{\Phi}_1 - \boldsymbol{\Phi}_0| \to \infty$. Meanwhile, when $\Delta\Phi \to \infty$, there must exist an infinite mass tower of states, with associated mass scale m, such that

$$m(\boldsymbol{\Phi}_1) = m(\boldsymbol{\Phi}_0) e^{-\lambda \Delta\Phi}\,, \tag{I.5.1}$$

where λ is a positive $\mathcal{O}(1)$ constant.

The exponent λ is subject to a lower bound. A sharpened version of the SDC asserts that $\lambda \geq 1/\sqrt{d-2}$, where d denotes the number of spacetime dimensions

[8] In much of the contemporary literature, the quantum gravity in the Swampland context is just the string theory. The String Lamppost Principle [82] proposes that all consistent EFTs that can be coupled to quantum gravity are derivable from string theory.

[84]. The SDC can also be generalized to field spaces in the presence of scalar potentials, as proposed in [85].

This conjecture is closely related to string duality. To illustrate this, consider the simple case of circular compactification, where the radion ϕ parameterizes the circle radius $\varrho = Re^{\beta\phi}$ (see (I.3.5)). In the Einstein frame, there exists a KK tower with a mass scale

$$m_{\mathrm{KK}}^{(\mathrm{E})} = \frac{n}{R} e^{\alpha\phi}, \qquad \alpha = -\frac{1}{\sqrt{2(d-1)(d-2)}}\,, \tag{I.5.2}$$

which decreases exponentially as $\phi \to +\infty$. Conversely, a winding tower arises with mass scale $m_w = wRe^{-\alpha\phi}$, which decreases exponentially in the opposite limit $\phi \to -\infty$. Since T-duality relates these two limits of the moduli space, the existence of an SDC-tower in one direction implies the presence of a corresponding tower in the dual direction. We explicitly verify this idea in Appendix IV.A for a more intricate non-geometric model.

Emergent String Conjecture

The Emergent String Conjecture (ESC) [86] provides a strengthened formulation of the SDC. It further proposes that, for every infinite distance limit in moduli space, there exists a lightest infinite tower of states, which takes one of the following forms:

- A decompactification limit, in which an infinite tower of Kaluza–Klein modes becomes massless;
- A limit where a string becomes tensionless, so that an infinite tower of string oscillator modes becomes massless. This string is either fundamental or dual to a fundamental string, with the tension vanishing due to $g_s \to 0$, corresponding to a theory with vanishing interactions.

A simple illustration is provided by ten-dimensional type II string theories. The dilaton Φ controls the string coupling, $g_s = e^{\Phi}$, and admits two asymptotic regimes $\Phi \to \pm\infty$. For type IIA theory, the limit $\Phi \to +\infty$ corresponds to decompactification to eleven-dimensional M-theory, while the $\Phi \to -\infty$ limit yields a tensionless fundamental string, originating from an M2-brane wrapped on a shrinking circle $R_{11} \to 0$. In type IIB theory, it is more direct: the dilaton Φ has an S-duality exchanging the D-string and the F-string. In the Einstein frame, the tensions of strings scale as

$$T_{\mathrm{F1}}^{(\mathrm{E})} \sim g_s^{1/2}\,, \qquad T_{\mathrm{D1}}^{(\mathrm{E})} \sim g_s^{-1/2}\,. \tag{I.5.3}$$

Hence, in the $\Phi \to -\infty$ limit the fundamental string becomes massless, while in the $\Phi \to +\infty$ limit the D1-brane becomes massless, realizing the ESC in both directions.

I.5.2 De Sitter Conjecture

As we mentioned in Subsection I.4.2, there are significant challenges and drawbacks in realizing a positive cosmological constant within string theory. In light of these difficulties, the de Sitter Conjecture (dSC) was proposed [87, 88]:

De Sitter Conjecture

In any consistent effective field theory, the scalar potential must satisfy

$$|\nabla V| \geq \frac{c}{M_{\rm P}}\, V\,, \tag{I.5.4}$$

where c is a positive $\mathcal{O}(1)$ constant.

This condition is always satisfied for $V \leq 0$, but for positive V it becomes highly nontrivial. In fact, it is in tension with observations, which suggest $c \lesssim 0.6$. The conjecture also rules out all de Sitter minima and restricts quintessence models to be sufficiently steep. A stronger version of the de Sitter Conjecture even requires $c > \sqrt{2}$, thereby excluding single-field quintessence entirely. By combining with the SDC, a refined de Sitter Conjecture was formulated [89], which asserts that the scalar potential should satisfy

$$\text{either} \quad |\nabla V| \geq \frac{c}{M_{\rm P}}\, V \qquad \text{or} \quad \min(\nabla_i \nabla_j V) \leq -\frac{c'}{M_{\rm P}^2}\, V\,, \tag{I.5.5}$$

with c, c' two positive $\mathcal{O}(1)$ constants. Clearly, the former imposes a lower bound on the potential slow-roll parameter ϵ_V defined in (I.4.10), while the latter constrains the second potential slow-roll parameter

$$\eta_V \equiv M_{\rm P}^2 \frac{\nabla^2 V}{V}\,. \tag{I.5.6}$$

A much weaker and more phenomenologically viable version is the asymptotic de Sitter Conjecture, which posits that these constraints need only be satisfied near asymptotic regions of field space. This is consistent with the de Sitter constructions discussed in Subsection I.4.2, where de Sitter vacua are metastable and the potential vanishes asymptotically.

AdS Distance Conjecture

The AdS Distance Conjecture is inspired by both the Swampland Distance Conjecture and the de Sitter Conjecture [90]. Consider quantum gravity on an AdS spacetime with cosmological constant Λ. The conjecture posits that, as one approaches an infinite distance limit in scalar field space, an infinite tower of states emerges with mass scale m, while the cosmological constant Λ tends to zero. Specifically, the mass scale behaves as $m \sim |\Lambda|^{\alpha}$, where α is a positive constant of order one.

The Dark Dimension Scenario [91] is proposed based on the dS version of the AdS Distance Conjecture. We will introduce this scenario and explore its realization through non-geometric string compactifications in Chapter III.

I.5.3 Other Swampland conjectures

To complete this introduction to the Swampland program, we briefly mention several additional Swampland conjectures that, while not central to the topics of this thesis, remain important and intriguing in the broader context of physics research. There has been a surge of research on the Swampland program in recent years, with many deep and fascinating developments. For overviews, see the reviews [92–95].[9]

Weak Gravity Conjecture

The Weak Gravity Conjecture (WGC) [96] is one of the central conjectures in the Swampland program, which consists of two parts:

- The electric Weak Gravity Conjecture: Consider a d-dimensional effective field theory coupled to gravity with U(1) gauge symmetry. There exists a particle, called the *WGC particle*, of mass $m < M_{\rm P}^d$ and charge q satisfying the inequality
$$m \leq \sqrt{\frac{d-2}{d-3}} g q \left(M_{\rm P}^d\right)^{\frac{d-2}{2}} \ ; \tag{I.5.7}$$
- The magnetic Weak Gravity Conjecture: The cutoff scale $\Lambda_{\rm cutoff}$ of this effective theory is bounded above by the U(1) gauge coupling g,
$$\Lambda_{\rm cutoff} \lesssim g \left(M_{\rm P}^d\right)^{\frac{d-2}{2}} \ . \tag{I.5.8}$$

Cobordism Conjecture

The Cobordism Conjecture [97] is generalized from the No Global Symmetry Conjecture. Cobordism is an equivalence relation between two manifolds: two manifolds are called to be cobordant if their disjoint union forms the boundary of another manifold of one higher dimension. The conjecture states that, in a consistent theory of gravity, all cobordism classes must be trivial.

Finiteness and the Tameness Conjecture

Finiteness is a fundamental property of the string Landscape. The Tameness Conjecture [98, 99] states that, all effective theories that can be consistently coupled to quantum gravity can be defined using "tame geometry". Explicitly, an EFT valid below a fixed cut-off scale is labeled by a *definable* parameter space and must have scalar field spaces and coupling functions that are definable in an *o-minimal*

[9] The author began exploring this field by reading [93].

structure. In addition, the corresponding o-minimal structure is $\mathbb{R}_{\text{an,exp}}$. This conjecture is supported in the finiteness of the number of flux vacua for F-theory Calabi–Yau fourfold [12, 13, 100–102], where the locus of self-dual flux vacua is definable in $\mathbb{R}_{\text{an,exp}}$ [103].

The moduli space of EFTs under a fixed cut-off scale Λ_{cutoff} also exhibits finiteness [104]. Its volume remains finite due to duality symmetries and the requirement of finite quantum gravity amplitudes [105]. For example, although the axio-dilaton takes values in the upper half-plane $\mathbb{H}$, the presence of an $\mathrm{SL}(2,\mathbb{Z})$ duality restricts the moduli space to a fundamental domain with volume $\mathrm{Vol}(\mathcal{F}) = \pi/3$. A further manifestation of finiteness arises in the context of complexity: it has been proposed that the aforementioned moduli space should admit an isometric embedding into $\mathbb{R}^n$ with finite complexity, as a consequence of its volume finiteness [106].

Trans-Planckian Censorship Conjecture

During the inflation epoch, microscopic quantum fluctuations blow up and may become macroscopic and observable at present. The Trans-Planckian Censorship Conjecture (TCC) [107] states that, if the fluctuation is smaller than the Planck scale at the beginning of inflation, after expansion it should never be stretched to a cosmological size, specifically a size larger than the Hubble horizon. This requirement imposes an upper bound on the number of e-folds of inflation:

$$e^N = \frac{a_{\text{final}}}{a_{\text{initial}}} \lesssim \frac{M_{\text{P}}}{H_{\text{initial}}} \,. \tag{I.5.9}$$

I.6 Content of the thesis

This thesis comprises three research projects conducted during the author's doctoral program, which are presented individually in the following chapters.

In Chapter II, we demonstrate that field trajectories leading to cosmic acceleration and exhibiting rapid turns near the boundary of the moduli space lie within the Swampland. Specifically, our analysis assumes the validity of the Swampland Distance Conjecture in the presence of a scalar potential and focuses on hyperbolic spaces, as prototypical geometries characterizing infinite distance limits in Calabi–Yau compactifications. We find that, in a quasi-de Sitter space with Hubble rate H and acceleration parameter ϵ, the turning rate Ω is subject to an upper bound, $\Omega/H \lesssim \mathcal{O}(\sqrt{\epsilon})$. Therefore, field trajectories consistent with the SDC can only have a negligible deviation from geodesics. This places strong constraints on the viability and consistency of multi-field quintessence scenarios in string theory. Within this framework, we further show that for a universe with asymptotic accelerated expansion, the asymptotic de Sitter conjecture is generically violated.

Chapter III investigates the feasibility of a classical realization of the Dark

Dimension Scenario through T-fold compactifications on $T^5 \times S^1$. The Dark Dimension Scenario posits the existence of a single extra dimension in our Universe, which is mesoscopically large and may be accessible to near-future experimental probes. By utilizing Scherk–Schwarz reduction from 5D to 4D and incorporating duality twists via T-fold fluxes associated with T^5, we achieve stabilization of the T^5 volume modulus as well as several other geometric moduli. This construction generates a scalar potential exhibiting two runaway directions, one of which is aligned with the Scherk–Schwarz radion corresponding to the S^1. Upon further stabilization, we find that this S^1 naturally realizes the mesoscopic extra dimension required by the Dark Dimension Scenario, as the resulting effective potential scales as $V \sim m_{\mathrm{KK}}^4$, in agreement with the expectations of the scenario.

In Chapter IV, we employ freely acting asymmetric orbifolds of type IIB string theory to construct a class of four-dimensional theories with eight supercharges. The resulting low-energy effective theories are analogous to *STU* models, but with a key distinction: the free orbifold action reduces the duality group to a congruence subgroup of the parent toroidal compactification. This reduction enlarges the moduli space, introducing both singular loci at finite distance and additional infinite distance limits. We verify that the Swampland Distance Conjecture and the Emergent String Conjecture are satisfied in the non-geometric compactifications of string theory considered here. In particular, we identify infinite distance points in the moduli space at which the theory decompactifies to distinct higher-dimensional compactifications.

References

[1] ATLAS collaboration, G. Aad et al., *Observation of a new particle in the search for the Standard Model Higgs boson with the ATLAS detector at the LHC*, *Phys. Lett. B* **716** (2012) 1–29, [1207.7214].

[2] CMS collaboration, S. Chatrchyan et al., *Observation of a New Boson at a Mass of 125 GeV with the CMS Experiment at the LHC*, *Phys. Lett. B* **716** (2012) 30–61, [1207.7235].

[3] Planck collaboration, P. A. R. Ade et al., *Planck 2013 results. I. Overview of products and scientific results*, *Astron. Astrophys.* **571** (2014) A1, [1303.5062].

[4] G.-B. Zhao et al., *Dynamical dark energy in light of the latest observations*, *Nature Astron.* **1** (2017) 627–632, [1701.08165].

[5] DES collaboration, T. M. C. Abbott et al., *The Dark Energy Survey: Cosmology Results with ∼1500 New High-redshift Type Ia Supernovae Using the Full 5 yr Data Set*, *Astrophys. J. Lett.* **973** (2024) L14, [2401.02929].

[6] DESI collaboration, A. G. Adame et al., *DESI 2024 VI: Cosmological Constraints from the Measurements of Baryon Acoustic Oscillations*, 2404.03002.

[7] DESI collaboration, A. G. Adame et al., *DESI 2024 VII: Cosmological Constraints from the Full-Shape Modeling of Clustering Measurements*, 2411.12022.

[8] Planck collaboration, P. A. R. Ade et al., *Planck 2013 results. XXIII. Isotropy and statistics of the CMB*, *Astron. Astrophys.* **571** (2014) A23, [1303.5083].

[9] Planck collaboration, P. A. R. Ade et al., *Planck 2015 results. XVI. Isotropy and statistics of the CMB*, *Astron. Astrophys.* **594** (2016) A16, [1506.07135].

[10] Planck collaboration, Y. Akrami et al., *Planck 2018 results. VII. Isotropy and Statistics of the CMB*, *Astron. Astrophys.* **641** (2020) A7, [1906.02552].

[11] F. Denef and M. R. Douglas, *Distributions of flux vacua*, *JHEP* **05** (2004) 072, [hep-th/0404116].

[12] M. R. Douglas and S. Kachru, *Flux compactification*, *Rev. Mod. Phys.* **79** (2007) 733–796, [hep-th/0610102].

[13] W. Taylor and Y.-N. Wang, *The F-theory geometry with most flux vacua*, *JHEP* **12** (2015) 164, [1511.03209].

[14] C. Vafa, *The String landscape and the swampland*, hep-th/0509212.

[15] R. Blumenhagen, D. Lüst and S. Theisen, *Basic concepts of string theory*. Theoretical and Mathematical Physics. Springer, Heidelberg, Germany, 2013, 10.1007/978-3-642-29497-6.

[16] E. Kiritsis, *String Theory in a Nutshell: Second Edition*. Princeton University Press, USA, 4, 2019.

[17] J. Polchinski, *String theory. Vol. 1: An introduction to the bosonic string*. Cambridge Monographs on Mathematical Physics. Cambridge University Press, 12, 2007, 10.1017/CBO9780511816079.

[18] D. Tong, *String Theory*, 0908.0333.

[19] K. Becker, M. Becker and J. H. Schwarz, *String theory and M-theory: A modern introduction*. Cambridge University Press, 12, 2006, 10.1017/CBO9780511816086.

[20] M. B. Green, J. H. Schwarz and E. Witten, *Superstring Theory Vol. 1: 25th Anniversary Edition*. Cambridge Monographs on Mathematical Physics. Cambridge University Press, 11, 2012, 10.1017/CBO9781139248563.

[21] B. Zwiebach, *A first course in string theory*. Cambridge University Press, 7, 2006.

[22] L. E. Ibanez and A. M. Uranga, *String theory and particle physics: An introduction to string phenomenology*. Cambridge University Press, 2, 2012.

[23] A. Dabholkar and C. Hull, *Duality twists, orbifolds, and fluxes*, *JHEP* **09** (2003) 054, [hep-th/0210209].

[24] C. M. Hull and P. K. Townsend, *Unity of superstring dualities*, *Nucl. Phys. B* **438** (1995) 109–137, [hep-th/9410167].

[25] P. S. Aspinwall, *K3 surfaces and string duality*, in *Theoretical Advanced Study Institute in Elementary Particle Physics (TASI 96): Fields, Strings, and Duality*, pp. 421–540, 11, 1996. hep-th/9611137.

[26] K. S. Narain, *New Heterotic String Theories in Uncompactified Dimensions < 10*, *Phys. Lett. B* **169** (1986) 41–46.

[27] K. S. Narain, M. H. Sarmadi and E. Witten, *A Note on Toroidal Compactification of Heterotic String Theory*, *Nucl. Phys. B* **279** (1987) 369–379.

[28] P. H. Ginsparg, *Comment on Toroidal Compactification of Heterotic Superstrings*, *Phys. Rev. D* **35** (1987) 648.

[29] A. Giveon, M. Porrati and E. Rabinovici, *Target space duality in string theory*, *Phys. Rept.* **244** (1994) 77–202, [hep-th/9401139].

[30] A. Strominger, S.-T. Yau and E. Zaslow, *Mirror symmetry is T duality*, *Nucl. Phys. B* **479** (1996) 243–259, [hep-th/9606040].

[31] J. H. Schwarz and A. Sen, *Duality symmetries of 4-D heterotic strings*, *Phys. Lett. B* **312** (1993) 105–114, [hep-th/9305185].

[32] M. J. Duff and R. R. Khuri, *Four-dimensional string / string duality*, *Nucl. Phys. B* **411** (1994) 473–486, [hep-th/9305142].

[33] E. Eyras, B. Janssen and Y. Lozano, *Five-branes, K K monopoles and T duality*, *Nucl. Phys. B* **531** (1998) 275–301, [hep-th/9806169].

[34] D. Tong, *NS5-branes, T duality and world sheet instantons*, *JHEP* **07** (2002) 013, [hep-th/0204186].

[35] P. Horava and E. Witten, *Heterotic and Type I string dynamics from eleven dimensions*, *Nucl. Phys. B* **460** (1996) 506–524, [hep-th/9510209].

[36] E. Witten, *String theory dynamics in various dimensions*, *Nucl. Phys. B* **443** (1995) 85–126, [hep-th/9503124].

[37] A. Sen and C. Vafa, *Dual pairs of type II string compactification*, *Nucl. Phys. B* **455** (1995) 165–187, [hep-th/9508064].

[38] L. J. Dixon, J. A. Harvey, C. Vafa and E. Witten, *Strings on Orbifolds*, *Nucl. Phys. B* **261** (1985) 678–686.

[39] L. J. Dixon, J. A. Harvey, C. Vafa and E. Witten, *Strings on Orbifolds. 2.*, *Nucl. Phys. B* **274** (1986) 285–314.

[40] A. Flournoy, B. Wecht and B. Williams, *Constructing nongeometric vacua in string theory*, *Nucl. Phys. B* **706** (2005) 127–149, [hep-th/0404217].

[41] C. M. Hull, *A Geometry for non-geometric string backgrounds*, *JHEP* **10** (2005) 065, [hep-th/0406102].

[42] A. Font, A. Guarino and J. M. Moreno, *Algebras and non-geometric flux vacua*, *JHEP* **12** (2008) 050, [0809.3748].

[43] J. Shelton, W. Taylor and B. Wecht, *Nongeometric flux compactifications*, *JHEP* **10** (2005) 085, [hep-th/0508133].

[44] S. Kachru, M. B. Schulz, P. K. Tripathy and S. P. Trivedi, *New supersymmetric string compactifications*, *JHEP* **03** (2003) 061, [hep-th/0211182].

[45] B. Wecht, *Lectures on Nongeometric Flux Compactifications*, *Class. Quant. Grav.* **24** (2007) S773–S794, [0708.3984].

[46] E. Plauschinn, *Non-geometric backgrounds in string theory*, *Phys. Rept.* **798** (2019) 1–122, [1811.11203].

[47] K. S. Narain, M. H. Sarmadi and C. Vafa, *Asymmetric Orbifolds*, *Nucl. Phys. B* **288** (1987) 551.

[48] K. Aoki, E. D'Hoker and D. H. Phong, *On the construction of asymmetric orbifold models*, *Nucl. Phys. B* **695** (2004) 132–168, [hep-th/0402134].

[49] C. Condeescu, I. Florakis, C. Kounnas and D. Lüst, *Gauged supergravities and non-geometric Q/R-fluxes from asymmetric orbifold CFT's*, *JHEP* **10** (2013) 057, [1307.0999].

[50] C. Condeescu, I. Florakis and D. Lust, *Asymmetric Orbifolds, Non-Geometric Fluxes and Non-Commutativity in Closed String Theory*, *JHEP* **04** (2012) 121, [1202.6366].

[51] C. A. Scrucca and M. Serone, *On string models with Scherk-Schwarz supersymmetry breaking*, *JHEP* **10** (2001) 017, [hep-th/0107159].

[52] G. Aldazabal, D. Marques and C. Nunez, *Double Field Theory: A Pedagogical Review*, *Class. Quant. Grav.* **30** (2013) 163001, [1305.1907].

[53] O. Hohm and H. Samtleben, *Exceptional Form of D=11 Supergravity*, *Phys. Rev. Lett.* **111** (2013) 231601, [1308.1673].

[54] M. Cicoli, J. P. Conlon, A. Maharana, S. Parameswaran, F. Quevedo and I. Zavala, *String cosmology: From the early universe to today*, *Phys. Rept.* **1059** (2024) 1–155, [2303.04819].

[55] A. G. Riess, A. V. Filippenko, P. Challis, A. Clocchiatti, A. Diercks, P. M. Garnavich et al., *Observational evidence from supernovae for an accelerating universe and a cosmological constant*, *The Astronomical Journal* **116** (sep, 1998) 1009.

[56] S. Perlmutter, G. Aldering, G. Goldhaber, R. A. Knop, P. Nugent, P. G. Castro et al., *Measurements of ω and λ from 42 high-redshift supernovae*, *The Astrophysical Journal* **517** (jun, 1999) 565.

[57] A. G. Riess et al., *A Comprehensive Measurement of the Local Value of the Hubble Constant with 1 km/s/Mpc Uncertainty from the Hubble Space Telescope and the SH0ES Team*, *Astrophys. J. Lett.* **934** (2022) L7, [2112.04510].

[58] WMAP collaboration, D. N. Spergel et al., *First year Wilkinson Microwave Anisotropy Probe (WMAP) observations: Determination of cosmological parameters*, *Astrophys. J. Suppl.* **148** (2003) 175–194, [astro-ph/0302209].

[59] Planck collaboration, P. A. R. Ade et al., *Planck 2013 results. XVI. Cosmological parameters*, *Astron. Astrophys.* **571** (2014) A16, [1303.5076].

[60] SDSS collaboration, D. J. Eisenstein et al., *Detection of the Baryon Acoustic Peak in the Large-Scale Correlation Function of SDSS Luminous Red Galaxies*, *Astrophys. J.* **633** (2005) 560–574, [astro-ph/0501171].

[61] D. Andriot, S. Parameswaran, D. Tsimpis, T. Wrase and I. Zavala, *Exponential quintessence: curved, steep and stringy?*, *JHEP* **08** (2024) 117, [2405.09323].

[62] S. Tsujikawa, *Quintessence: A Review*, *Class. Quant. Grav.* **30** (2013) 214003, [1304.1961].

[63] M. Cicoli, S. De Alwis, A. Maharana, F. Muia and F. Quevedo, *De Sitter vs Quintessence in String Theory*, *Fortsch. Phys.* **67** (2019) 1800079, [1808.08967].

[64] E. G. M. Ferreira, J. Quintin, A. A. Costa, E. Abdalla and B. Wang, *Evidence for interacting dark energy from BOSS*, *Phys. Rev. D* **95** (2017) 043520, [1412.2777].

[65] J. M. Maldacena and C. Nunez, *Supergravity description of field theories on curved manifolds and a no go theorem*, *Int. J. Mod. Phys. A* **16** (2001) 822–855, [hep-th/0007018].

[66] S. Kachru, R. Kallosh, A. D. Linde and S. P. Trivedi, *De Sitter vacua in string theory*, *Phys. Rev. D* **68** (2003) 046005, [hep-th/0301240].

[67] V. Balasubramanian, P. Berglund, J. P. Conlon and F. Quevedo, *Systematics of moduli stabilisation in Calabi-Yau flux compactifications*, *JHEP* **03** (2005) 007, [hep-th/0502058].

[68] M. P. Hertzberg, S. Kachru, W. Taylor and M. Tegmark, *Inflationary Constraints on Type IIA String Theory*, *JHEP* **12** (2007) 095, [0711.2512].

[69] U. H. Danielsson and T. Van Riet, *What if string theory has no de Sitter vacua?*, *Int. J. Mod. Phys. D* **27** (2018) 1830007, [1804.01120].

[70] E. Silverstein, *Simple de Sitter Solutions*, *Phys. Rev. D* **77** (2008) 106006, [0712.1196].

[71] S. S. Haque, G. Shiu, B. Underwood and T. Van Riet, *Minimal simple de Sitter solutions*, *Phys. Rev. D* **79** (2009) 086005, [0810.5328].

[72] B. de Carlos, A. Guarino and J. M. Moreno, *Flux moduli stabilisation, Supergravity algebras and no-go theorems*, *JHEP* **01** (2010) 012, [0907.5580].

[73] B. de Carlos, A. Guarino and J. M. Moreno, *Complete classification of Minkowski vacua in generalised flux models*, *JHEP* **02** (2010) 076, [0911.2876].

[74] J. Blåbäck, U. H. Danielsson, G. Dibitetto and S. C. Vargas, *Universal dS vacua in STU-models*, *JHEP* **10** (2015) 069, [1505.04283].

[75] I. Bena, M. Graña and T. Van Riet, *Trustworthy de Sitter compactifications of string theory: a comprehensive review*, 2303.17680.

[76] U. H. Danielsson, S. S. Haque, P. Koerber, G. Shiu, T. Van Riet and T. Wrase, *De Sitter hunting in a classical landscape*, *Fortsch. Phys.* **59** (2011) 897–933, [1103.4858].

[77] M. Cicoli, F. Cunillera, A. Padilla and F. G. Pedro, *Quintessence and the Swampland: The Parametrically Controlled Regime of Moduli Space*, *Fortsch. Phys.* **70** (2022) 2200009, [2112.10779].

[78] L. Cong et al., *Spin-dependent exotic interactions*, *Rev. Mod. Phys.* **97** (2025) 025005, [2408.15691].

[79] B. Valeixo Bento, D. Chakraborty, S. L. Parameswaran and I. Zavala, *Dark Energy in String Theory*, *PoS* **CORFU2019** (2020) 123, [2005.10168].

[80] M. Brinkmann, M. Cicoli, G. Dibitetto and F. G. Pedro, *Stringy multifield quintessence and the Swampland*, *JHEP* **11** (2022) 044, [2206.10649].

[81] J. Calderón-Infante, I. Ruiz and I. Valenzuela, *Asymptotic accelerated expansion in string theory and the Swampland*, *JHEP* **06** (2023) 129, [2209.11821].

[82] H.-C. Kim, H.-C. Tarazi and C. Vafa, *Four-dimensional $\mathcal{N} = 4$ SYM theory and the swampland*, *Phys. Rev. D* **102** (2020) 026003, [1912.06144].

[83] H. Ooguri and C. Vafa, *On the Geometry of the String Landscape and the Swampland*, *Nucl. Phys. B* **766** (2007) 21–33, [hep-th/0605264].

[84] M. Etheredge, B. Heidenreich, S. Kaya, Y. Qiu and T. Rudelius, *Sharpening the Distance Conjecture in diverse dimensions*, *JHEP* **12** (2022) 114, [2206.04063].

[85] J. Calderón-Infante, A. M. Uranga and I. Valenzuela, *The Convex Hull Swampland Distance Conjecture and Bounds on Non-geodesics*, *JHEP* **03** (2021) 299, [2012.00034].

[86] S.-J. Lee, W. Lerche and T. Weigand, *Emergent strings from infinite distance limits*, *JHEP* **02** (2022) 190, [1910.01135].

[87] G. Obied, H. Ooguri, L. Spodyneiko and C. Vafa, *De Sitter Space and the Swampland*, 1806.08362.

[88] S. K. Garg and C. Krishnan, *Bounds on Slow Roll and the de Sitter Swampland*, *JHEP* **11** (2019) 075, [1807.05193].

[89] H. Ooguri, E. Palti, G. Shiu and C. Vafa, *Distance and de Sitter Conjectures on the Swampland*, *Phys. Lett. B* **788** (2019) 180–184, [1810.05506].

[90] E. Gonzalo, L. E. Ibáñez and I. Valenzuela, *AdS swampland conjectures and light fermions*, *Phys. Lett. B* **822** (2021) 136691, [2104.06415].

[91] M. Montero, C. Vafa and I. Valenzuela, *The dark dimension and the Swampland*, *JHEP* **02** (2023) 022, [2205.12293].

[92] T. D. Brennan, F. Carta and C. Vafa, *The String Landscape, the Swampland, and the Missing Corner*, *PoS* **TASI2017** (2017) 015, [1711.00864].

[93] E. Palti, *The Swampland: Introduction and Review*, *Fortsch. Phys.* **67** (2019) 1900037, [1903.06239].

[94] M. van Beest, J. Calderón-Infante, D. Mirfendereski and I. Valenzuela, *Lectures on the Swampland Program in String Compactifications*, *Phys. Rept.* **989** (2022) 1–50, [2102.01111].

[95] N. B. Agmon, A. Bedroya, M. J. Kang and C. Vafa, *Lectures on the string landscape and the Swampland*, 2212.06187.

[96] N. Arkani-Hamed, L. Motl, A. Nicolis and C. Vafa, *The String landscape, black holes and gravity as the weakest force*, *JHEP* **06** (2007) 060, [hep-th/0601001].

[97] J. McNamara and C. Vafa, *Cobordism Classes and the Swampland*, 1909.10355.

[98] T. W. Grimm, *Taming the landscape of effective theories*, *JHEP* **11** (2022) 003, [2112.08383].

[99] T. W. Grimm, S. Lanza and C. Li, *Tameness, Strings, and the Distance Conjecture*, *JHEP* **09** (2022) 149, [2206.00697].

[100] T. Eguchi and Y. Tachikawa, *Distribution of flux vacua around singular points in Calabi-Yau moduli space*, *JHEP* **01** (2006) 100, [hep-th/0510061].

[101] M. Douglas and Z. Lu, *On the geometry of moduli space of polarized Calabi-Yau manifolds*, math/0603414.

[102] B. S. Acharya and M. R. Douglas, *A Finite landscape?*, hep-th/0606212.

[103] B. Bakker, T. W. Grimm, C. Schnell and J. Tsimerman, *Finiteness for self-dual classes in integral variations of Hodge structure*, 2112.06995.

[104] M. Delgado, D. van de Heisteeg, S. Raman, E. Torres, C. Vafa and K. Xu, *Finiteness and the Emergence of Dualities*, 2412.03640.

[105] Y. Hamada, M. Montero, C. Vafa and I. Valenzuela, *Finiteness and the swampland*, *J. Phys. A* **55** (2022) 224005, [2111.00015].

[106] T. W. Grimm, D. Prieto and M. van Vliet, *Tame Embeddings, Volume Growth, and Complexity of Moduli Spaces*, 2503.15601.

[107] A. Bedroya and C. Vafa, *Trans-Planckian Censorship and the Swampland*, *JHEP* **09** (2020) 123, [1909.11063].

Chapter II

Cosmic Acceleration and Turns in the Swampland

Section II.1−Appendix II.B of this chapter is based on the work arXiv:2306.17217, JCAP 11 (2023) 080, *collaborating with Julian Freigang, Dieter Lüst and Marco Scalisi.*

II.1 Introduction

Cosmic acceleration plays a fundamental role in the current understanding of our Universe (see Subsection I.4.1). While we have a good understanding of how this phase can be realized in terms of an effective scalar field theory, we still struggle to agree on a full-fledged embedding of it in string theory. The presence of several light scalar fields, active during the acceleration phase,[1] is a natural expectation for such an embedding. String theory comes with many moduli, often spanning non-trivial field geometries, and giving them a mass is definitely a complex task. As we discussed in Subsection I.4.2, multi-field models typically feature non-geodesic trajectories in field space.[2] Deviations from geodesics can be sourced by a non-zero scalar potential and they are usually quantified by the so-called *turning rate* Ω. Strong non-geodesic motion, characterized by rapid turns in field space with $\Omega \gg 1$ (in Hubble units), can lead to intriguing and rich phenomenology. Examples have been provided in the context of inflation (see, e.g., [1–14]) and also for quintessence models (see, e.g., [15–22]). These can be modifications of the inflationary power spectrum [4, 6], production of primordial black holes [23–25], possibility to inflate on a steep potential [9, 17, 19] (namely with large potential gradient) and also enhanced growth of large-scale structure [17]. Despite the great attention this topic gained in the research community, the results are mainly model-dependent and so we lack a general principle of what a consistent quantum gravity embedding allows for (see [12] for some work in this direction in the context of supergravity).

An alternative route to (string) model building is given by the Swampland program [26–29], which suggests that one can employ a bottom-up approach to restrict the set of effective field theories (EFTs) consistent with quantum gravity. This is based on a number of universal consistency constraints, which act already at energies typically lower than the Planck mass $M_{\rm P}$, thus making them meaningful for phenomenology. One property that consistent EFTs appear to possess is a finite range of validity in field space. This is indeed one of the powerful implications of the Swampland Distance Conjecture (see Subsection I.5.1), which states that infinite scalar field variations are always accompanied by (at least) one infinite tower of states with exponentially decreasing mass scale. In this limit, the quantum gravity cut-off, which we identify with the species scale $\Lambda_{\rm s}$ [30–34], decays exponentially in field space, thus leading to a breakdown of the effective theory.[3] Field displacements of order $M_{\rm P}$ are enough to observe this behaviour [43, 44] and to extract consequences relevant for phenomenology (see also [45]). Implications of the SDC for cosmic inflation were first studied in [46]

[1] In this chapter, we consider only time-dependent acceleration phase, such as inflation or quintessence, with certain displacements in field space.

[2] It should be noted that the most common strategy to construct an effective (supergravity) model is to stabilize all fields except one, which drives the acceleration phase. However, despite its simplicity, this approach may not be the most natural and often demands precise control over the effective theory.

[3] It has also been pointed out that the limits of small (AdS) cosmological constant [35], small gravitino mass [36–38] and small/large entropy [39–42] lead to analogous conclusions.

(see also [47, 48]), where a universal upper bound on the inflaton range was found (see also [49, 50] for some variations of it with fixed decay rate).

The SDC finds a natural test around the *boundary of moduli space*. These asymptotic regions are located at an infinite distance from any other point, hence referred to as "infinite-distance singularities". Around these regions, the geometry exhibits negative curvature and non-compactness[4], while maintaining a finite volume [27]. The effective theory becomes simple and can be expressed as a perturbative expansion on a certain parameter. Additionally, there is evidence suggesting that the scalar potential approaches zero in this limit [57, 58]. These factors have led to serious consideration of the boundary of moduli space as a promising framework for embedding models of cosmic acceleration [21, 22, 59–64], often referred to as "asymptotic acceleration".

In this chapter, we study the implications of the SDC for multi-field models of cosmic acceleration at the boundary of moduli space. As the main result, we find that the ratio between the turning rate Ω and the Hubble parameter H is constrained by

$$\frac{\Omega}{H} < c\,\sqrt{\epsilon}\,, \tag{II.1.1}$$

with the acceleration parameter ϵ defined in (I.4.8) and c a $\mathcal{O}(1)$ quantity, depending on the curvature of the moduli space and on the decay rate of the tower mass scale. Since $\epsilon < 1$ by definition, this result implies that asymptotic acceleration is incompatible with rapid turns or any strong non-geodesic motion. At the boundary of moduli space, quantum gravity imposes predominantly geodesic motion. We argue that this result should be valid also in the more conservative case of super-Planckian excursions, for which one can consistently apply the SDC.

One direct implication of (II.1.1) is a clear tension between asymptotic acceleration and the de Sitter conjecture (cf. Subsection I.5.2). In fact, a distinctive characteristic of multi-field models is that the acceleration phase is not solely determined by the gradient of the scalar potential, but rather by the interplay of this and the turning rate, as given by the following formula[5]:

$$\epsilon = \frac{1}{2}\frac{|\nabla V|^2}{V^2}\left(1+\frac{\Omega^2}{9H^2}\right)^{-1}\,. \tag{II.1.2}$$

It has been previously highlighted in the literature [9] that, when $\Omega \gg H$, this formula allows for the fulfillment of the de Sitter conjecture (i.e., $|\nabla V| > \mathcal{O}(1)V$) while also enabling an acceleration phase with $\epsilon \ll 1$. However, our result (II.1.1) significantly limits this possibility within the context of asymptotic acceleration,

[4] In the context of inflationary cosmology, it has been shown [51–56] that non-compact symmetries and negative curvature of the field space are key features for an excellent fit to the observational data. The relation between the SDC and such a cosmological scenario has in fact been investigated in [46].

[5] Let us remark that (II.1.2) relies on a slow-roll approximation, which assumes that the second derivative of the fields is sub-dominant compared to the friction term in the equations of motion. The full formula, as discussed in Subsection II.3.4, reveals that relaxing this condition can potentially aid in satisfying the de Sitter conjecture in an accelerating background.

since it implies that the second term in the bracket of (II.1.2) is sub-leading. Given the current observational bounds, we conclude that models of early/late-time acceleration, near the boundary of moduli space, typically exhibit tension with the de Sitter conjecture.

This chapter is organized as follows. In Section II.2, we introduce the SDC and show how the tower mass decay rate can strictly depend on the deviations from geodesic trajectories in field space. In Section II.3, we provide a pedagogical discussion of the multi-field framework and introduce the turning rate. In Section II.4, we investigate the case of infinite-distance trajectories with constant geodesic deviation and obtain our main result (II.1.1). We focus on hyperbolic field geometries, as prototype manifolds of the moduli space boundary for Calabi–Yau compactifications. In Section II.5, we extend our result to the case of infinite-distance trajectories with a time-dependent deviation angle from geodesics. In Section II.6, we provide our conclusions. Throughout the text, we work in reduced Planck mass units ($M_{\rm P} = 1$).

II.2 SDC, mass decay rate and non-geodesics

We briefly introduced the Swampland Distance Conjecture in Subsection I.5.1. For ease of reference, we restate it here: The SDC implies the existence of at least one infinite tower of states with mass scale exponentially decreasing in field space, in the infinite distance limit, namely

$$m = m_0 \exp(-\lambda \Delta) \qquad \text{as} \qquad \Delta \to \infty \,, \tag{II.2.1}$$

where m_0 is the typical mass scale of the tower before any displacement, Δ is the traversed distance in moduli space and λ is the *decay rate*, namely the parameter regulating how fast the mass of the tower decreases in field space. It has been argued that λ is order one [44], in reduced Planck mass units, and lower bounds have also been pointed out in different contexts [37, 49, 65–67]. The existence of a lower bound is very important as it defines the validity of the EFT. Namely, it indicates how fast/slow one can approach the infinite distance singularity in field space, and therefore how much field distance can be traversed, before the EFT completely breaks down, due to genuine quantum gravity effects. It happens, in fact, that the quantum gravity cut-off $\Lambda_{\rm s}$, namely the species scale [30–34], decreases exponentially in field space, together with the mass scale of the tower. While a finite small number of light states can always be integrated in, such to define a new EFT, the presence of an *infinite* number of light states necessarily drives the cut-off to zero with exponential rate γ, which is in general different from the rate λ of the tower. In the case of states equally spaced, such as Kaluza–Klein modes, one can show that $\Lambda_{\rm s} = m^{1/3}$ (assuming $M_{\rm P} = 1$), thus yielding $\gamma = \lambda/3$ [36, 46, 58, 68]. This is consistent with the fact that, in the infinite distance limit, the quantum gravity cut-off lies still above the typical mass scale of the tower. While traversing a distance in field space, some states of the tower

can enter the EFT and produce observational effects, while the quantum gravity cut-off remains still above the typical energy scale of the EFT.

The exponential rate of the tower λ can in general depend on the *path* followed in moduli space to approach the infinite-distance point. A first example of this situation was given in [46] for the hyperbolic half-plane, where it was shown that trajectories, with the axion and saxion linear to each other[6], yield an effective reduction of the decay rate. This translates also into the possibility of engineering a larger field excursion. A more general analysis is given in [73]. In fact, one can reverse (II.2.1) and express the *mass decay rate* of the tower as

$$\lambda(\Delta) = -\frac{\mathrm{d}\log m}{\mathrm{d}\Delta} = -T^i \partial_i \log m \,, \tag{II.2.2}$$

that is the scalar product between the normalized tangent vector T^i, along the trajectory that we follow to reach the point at infinity, and the gradient of the (logarithm of the) mass of the tower. In the most general case, the gradient of the mass can be aligned along any direction in moduli space [73]. However, in most of the string theory examples, $\partial_i \log m$ is aligned along geodesics. This implies that λ becomes a measure to quantify the *non-geodicity* of the trajectory. In this case, we can write

$$\lambda = -|\boldsymbol{\partial} \log m| \cos\theta = \lambda_{\mathrm{g}} \cos\theta \,, \tag{II.2.3}$$

where θ is the angle between the trajectory we are following in field space and the geodesic. Both paths will reach the infinite-distance singularity but with different angles. The parameter λ_{g} represents the highest value of λ and it corresponds in fact to the decay rate for a geodesic trajectory. Moving along a non-geodesic trajectory can be the result of introducing a scalar potential for the moduli (see Section II.3).

The expression (II.2.3) seems to suggest that λ could even become zero, if one moves along a trajectory, which is orthogonal to a geodesic (i.e. $\theta = \pi/2$). This would mean that arbitrary distances could be traversed without the mass scale of a tower dropping-off. The EFT would be valid for arbitrary long distances, and one could easily avoid the drastic implication of the SDC.[7] However, as mentioned above, we have clear indications that string theory sets a lowest possible value for such a decay rate [37, 49, 65–67]. If we generically indicate the existence of such a lower bound with $\lambda \geq \lambda_0$, then we can translate this into a maximum deviation angle θ_0 from the geodesic trajectory allowed by the SDC, namely

$$\cos\theta \geq \cos\theta_0 = -\frac{\lambda_0}{|\boldsymbol{\partial} \log m|} = \frac{\lambda_0}{\lambda_{\mathrm{g}}} \,. \tag{II.2.4}$$

[6] Situations where the axion has a typical linear backreaction with the saxion, for large field displacements, have been observed in string theory models such as in [43, 69–72].

[7] Models with highly curved trajectories and large field ranges have in fact been proposed in literature [6, 9–11, 16, 17, 74]. Whether these effective scenarios could be realized in a consistent string theory embedding is still unclear. Recent work [12] seems in fact to restrict such a possibility.

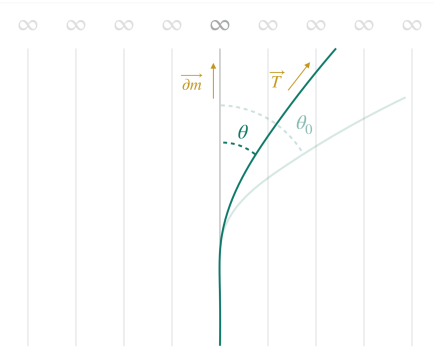

Figure II.1: Cartoon picture of a non-geodesic trajectory with tangent vector $\boldsymbol{T}$ deviating from the geodesic by an angle θ. The set of infinite-distance geodesics is represented as parallel gray lines. The gradient of the tower mass $\boldsymbol{\partial m}$ aligns with the geodesic. Both the geodesic and the non-geodesic trajectories approach the infinite distance region. The angle θ_0 represents the maximum deviation, which is constrained by the lower bound on the decay rate of the SDC tower mass.

A bound on the angle θ means that not all the trajectories in moduli space are allowed by the SDC and can deviate by a maximum angle from the geodesic (see Figure II.1). In the next section, we recall how the introduction of a scalar potential can lead to a departure from a moduli space geodesic equation.

At this juncture, it is important to emphasize that our focus will now be solely on *infinite-distance trajectories* in the subsequent discussion. These trajectories are characterized by distances that can extend infinitely, providing a robust framework to apply the SDC. Specifically, we will first examine deviations from geodesics with a constant angle[8] $\theta = \text{const}$ (Section II.4) and then trajectories with a time-dependent deviation angle $\theta = \theta(t)$ (Section II.5). Let us emphasize that, given the expression (II.2.3), the latter case corresponds to a time-dependent, or rather Δ-dependent, decay rate of the tower mass $\lambda = \lambda(\Delta)$. This will effectively induce field-dependent corrections such that the mass formula (II.2.1) will deviate from its the exponential form when moving away from the moduli space boundary (which is placed at $\Delta \to \infty$). Therefore, a time-dependent decay rate can serve as a convenient means to parameterize a departure from the boundary.

[8]The situation of trajectories with constant deviation angle from a geodesic has been named 'critical case' in [73]. In a 2-dimensional hyperbolic space, it corresponds to a linear backreaction between the saxion and the axion, as discussed in [46] and in Subsection II.4.1.

II.3 Multi-scalar field setup and trajectories in moduli space

String theory comes naturally with many moduli, namely massless scalar fields. The internal field geometry, defined by their kinetic terms, is generically non-flat, as the result of the compactification process, and characterized by a set of geodesics. However, the introduction of a scalar potential (e.g. by means of fluxes) can lead to a deviation from the original geodesic trajectories and a consequent change of dynamics.[9]

In this section, we present a pedagogical introduction to a convenient framework for studying multi-scalar field systems [9]. This is based on projecting the equations of motion along the tangent and normal directions of the trajectory along which the system evolves. By employing this approach, we demonstrate how the system can be described using an equation resembling the equation of motion for a single scalar field, as well as another equation involving the turning rate Ω. We emphasize the relationship between the equations of motion and the trajectories (geodesic or non-geodesic) in field space. The presentation includes increasing levels of complexity. We begin by considering the case of free massless scalar fields in a flat Minkowski background in Subsection II.3.1. Next, we introduce a scalar potential and demonstrate how it leads to deviations from geodesic motion in Subsection II.3.2. Subsequently, we incorporate gravity and investigate the effects of a Friedmann–Lemaître–Robertson–Walker (FLRW) background in Subsection II.3.3. Finally, in Subsection II.3.4, we describe the equations governing a multi-field system that gives rise to cosmic acceleration.

II.3.1 Scalar fields in Minkowski spacetime

Let us consider the Lagrangian of n free massless homogeneous scalar fields $\Phi^a = \Phi^a(t)$, thus depending just on the time variable t:

$$\mathcal{L} = -\frac{1}{2}\eta^{\mu\nu} G_{ab}\, \partial_\mu \Phi^a \partial_\nu \Phi^b \,, \tag{II.3.1}$$

where $\eta^{\mu\nu}$ is the Minkowski spacetime metric, $G_{ab} = G_{ab}(\mathbf{\Phi})$ is the internal field space metric, and Latin indices a, b run from 1 to n. The equations of motion then take the form

$$\ddot{\Phi}^a + \Gamma^a_{bc} \dot{\Phi}^b \dot{\Phi}^c = 0 \,, \tag{II.3.2}$$

where the dot $\dot{}$ is indicating a time derivative, and

$$\Gamma^a_{bc} = \frac{1}{2} G^{ad} \left(\frac{\partial G_{bd}}{\partial \Phi^c} + \frac{\partial G_{cd}}{\partial \Phi^b} - \frac{\partial G_{bc}}{\partial \Phi^d} \right) \tag{II.3.3}$$

[9] There are instead situations where the dynamics remains quite insensitive to a great variety of scalar potentials and is instead mainly determined by the geometric properties of the internal manifold. In the context of inflationary cosmology, the α-attractor scenario [51, 52, 55, 75] is a primary example of such a circumstance.

are the Christoffel symbols of the moduli space. Note that (II.3.2) has precisely the form of a *geodesic equation*. It describes in fact the set of (geodesic) trajectories along which the scalar fields Φ^a evolve in time. Notice that the time t is not a preferred parameter for the geodesic and we can shift and rescale it as the result of the shift-symmetry of the Lagrangian (II.3.1) and scale-symmetry of the equations of motion (II.3.2).

Let us introduce the covariant derivative D_t, which is defined as

$$D_t A^a \equiv \dot{A}^a + \Gamma^a_{bc} A^b \dot{\Phi}^c \,, \tag{II.3.4}$$

for a given vector A^a. Having $D_t A^a = 0$ means that the vector A^a is parallel transported along the trajectory Φ^a, i.e. A^a always 'points at the same direction' along Φ^a. Moreover, D_t acting on a field scalar reduces to an ordinary time derivative. With this definition, the above set of equations (II.3.2) reduces to

$$D_t \dot{\Phi}^a = 0 \,, \tag{II.3.5}$$

which is consistent with the fact that the equations of motion are just geodesic equations and a geodesic is a trajectory which is autoparallel transported along itself.

We now introduce the tangent and the normal vector to the trajectory Φ^a, respectively, as

$$T^a = \frac{\dot{\Phi}^a}{\dot{\Phi}}, \qquad N^a = -\frac{1}{|D_t T|} D_t T^a \,, \tag{II.3.6}$$

where $\dot{\Phi}$ is the speed along the trajectory, defined as

$$\dot{\Phi} = \sqrt{G_{ab} \dot{\Phi}^a \dot{\Phi}^b} \,. \tag{II.3.7}$$

Both vectors T^a and N^a are normalised and orthogonal to each other, namely $G_{ab} T^a T^b = G_{ab} N^a N^b = 1$ and $G_{ab} T^a N^b = 0$. Now we can project the equations of motion along the tangent and normal vectors. This just means contracting the equations of motion with T^a and N^a. The tangential projection yields

$$\ddot{\Phi} = 0 \,, \tag{II.3.8}$$

where we have used the product rule for D_t and the orthogonality property of T^a and N^a. Instead, the normal projection gives

$$\Omega \dot{\Phi} = 0 \,, \tag{II.3.9}$$

where we have introduced the *turning rate* as

$$\Omega = |D_t T| \,, \tag{II.3.10}$$

and used again orthogonality of the two vectors together with the fact that

$$D_t \dot{\Phi}^a = \dot{\Phi} D_t T^a + \ddot{\Phi} T^a \,. \tag{II.3.11}$$

Excluding the trivial case $\dot{\Phi} = 0$, (II.3.9) implies that we need $\Omega = 0$ in order to fulfill the geodesic equation. That is the reason why Ω is also called non-geodesity factor. Furthermore, let us note that if T^a gets parallel transported along Φ^a, i.e. $D_t T^a = 0$, we immediately get $\Omega = 0$ and the equation of motion just reduces to the equation $\ddot{\Phi} = 0$. Since we are dealing with positive definite Riemannian field manifolds, the statement $\Omega = 0$ is equivalent to $D_t T^a = 0$. Geometrically, Ω measures the failure of T^a being parallel transported along Φ^a.

II.3.2 Scalar fields with potential in Minkowski spacetime

As next step, we now introduce a potential $V(\Phi^a)$ for the scalar fields. We still consider still flat Minkowski background such that the Lagrangian $\mathcal{L}$ becomes

$$\mathcal{L} = -\frac{1}{2}\eta^{\mu\nu} G_{ab} \partial_\mu \Phi^a \partial_\nu \Phi^b - V(\Phi^a)\,. \tag{II.3.12}$$

The equations of motion hence read

$$D_t \dot{\Phi}^a + G^{ab} V_b = 0\,, \tag{II.3.13}$$

where we define $V_b \equiv \partial V / \partial \Phi^b$. Projecting again the set of equations in the tangential and normal direction we get

$$\ddot{\Phi} + V_T = 0\,, \tag{II.3.14}$$

$$\Omega \dot{\Phi} = V_N\,, \tag{II.3.15}$$

where we have introduced $V_T \equiv T^a V_a$ and $V_N \equiv N^a V_a$, i.e., the corresponding projections of the gradient of the potential V. It is interesting to understand what happens in the case $D_t T^a = 0$, which is, as explained earlier, equivalent to $\Omega = 0$. Rearranging the relation (II.3.11), we get

$$D_t T^a = \frac{1}{\dot{\Phi}} \left(D_t \dot{\Phi}^a - T^a \ddot{\Phi} \right)\,. \tag{II.3.16}$$

In the case of zero potential, as seen before, both terms in the bracket of the last equation vanish, thus automatically leading to the turning rate $\Omega = 0$. Instead, in the presence of a non-zero potential, the situation is slightly more involved. The two terms can in fact cancel each other, so that the trajectory will follow a geodesic path in field space. However, the acceleration along the trajectory will be still determined by the tangential projection of V, as expressed in (II.3.14). We can get more insight about this situation by using the equations of motion (II.3.13) and (II.3.14) and rewriting (II.3.16) as

$$D_t T^a = -\frac{1}{\dot{\Phi}} \left(G^{ab} V_b - T^a V_T \right)\,. \tag{II.3.17}$$

In order to have $\Omega = 0$, we immediately see that the gradient of the potential V_a and the tangent vector T_a have to be aligned. This means that geodesic trajectories are always characterized by a zero normal component of the scalar potential,

namely $V_N = 0$. Intuitively, the trajectory corresponds to a valley of the scalar potential. If there is no normal force, the tangent vector gets parallel transported along the trajectory. This is an approach used very often in string/supergravity model building as it hugely simplifies the analysis of the system. In a typical axion-saxion system, it corresponds to stabilizing one of the two fields and leave the other very light to drive the acceleration phase. On the other hand, the multi-field framework allows, in principle, also for very sharp turns, $\Omega \gg 1$, which means a great misalignment between the potential gradient flow and the tangent vector T^a.

II.3.3 Scalar fields with potential in FLRW spacetime

We further generalise our setup by taking the 4d spacetime to be an FLRW metric $g_{\mu\nu}$ with line element of the form

$$\mathrm{d}s^2 = -\mathrm{d}t^2 + a^2(t)\mathrm{d}\boldsymbol{x}^2\,. \tag{II.3.18}$$

Then, given the action

$$S = \int \mathrm{d}^4x\sqrt{-g}\left(\frac{1}{2}R - \frac{1}{2}g^{\mu\nu}G_{ab}\partial_\mu\Phi^a\partial_\nu\Phi^b - V(\Phi^a)\right)\,, \tag{II.3.19}$$

with g being the determinant of $g_{\mu\nu}$ and R the Ricci scalar, we get the following equations

$$D_t\dot{\Phi}^a + 3H\dot{\Phi}^a + G^{ab}V_b = 0\,. \tag{II.3.20}$$

These contain an additional friction term, proportional to the Hubble expansion rate $H = \dot{a}/a$. The projections work completely analogous to the previous cases, namely we get

$$\ddot{\Phi} + 3H\dot{\Phi} + V_T = 0\,, \tag{II.3.21}$$

$$\Omega\dot{\Phi} = V_N\,. \tag{II.3.22}$$

We note that the set of equations (II.3.20) just reduces to two simple equations. The first, (II.3.21) has the form of the equation for a single scalar field in a FLRW spacetime. The second, (II.3.22), involves the turning rate Ω and it is not affected by the friction term. Since only the first equation is altered, we can draw the same conclusions about the case $D_tT^a = 0$, as discussed in the previous sub-section. In Appendix II.A, we show that the friction term can be nevertheless eliminated by an appropriate affine reparametrisation.

II.3.4 Multi-field cosmic acceleration

As the final step, we consider the coupled system and include the backreaction of the scalar dynamics on the FLRW background. We will explicitly state the conditions required to achieve cosmic acceleration. The action we consider is as

before in (II.3.19). Therefore, the background dynamics of the full system is given by

$$3H^2 - \frac{1}{2}\dot{\Phi}^2 - V = 0\,, \tag{II.3.23}$$

$$\ddot{\Phi} + 3H\dot{\Phi} + V_T = 0\,, \tag{II.3.24}$$

$$\Omega\dot{\Phi} = V_N\,. \tag{II.3.25}$$

where the first equation is the Friedmann equation associated to the FLRW metric while the last two equations refer to the dynamics of the scalar fields and are already in projected form, as introduced before.

Cosmic acceleration happens when $\ddot{a} > 0$. One can show that this is equivalent to requiring

$$\epsilon < 1\,, \tag{II.3.26}$$

with ϵ equal to

$$\epsilon \equiv -\frac{\dot{H}}{H^2} = \frac{\dot{\Phi}^2}{2H^2}\,. \tag{II.3.27}$$

To require that the acceleration phase lasts for a sufficient number of Hubble times[10], one can require

$$\eta \equiv \frac{\dot{\epsilon}}{H\epsilon} = 2\epsilon + 2\frac{\ddot{\Phi}}{H\dot{\Phi}} < 1\,. \tag{II.3.28}$$

Note that the latter expressions are exact and do not assume any slow-roll condition. They can be obtained simply by differentiating (II.3.23) with respect to the cosmic time t and combining this with (II.3.24), once we observe that $V_T\ \dot{\Phi} = T^a V_a \dot{\Phi} = \dot{\Phi}^a V_a = \dot{V}$.

Using these definitions, one can rewrite the Friedmann equation (II.3.23) simply as

$$H^2 = \frac{V}{3-\epsilon}\,. \tag{II.3.29}$$

Finally, one can derive an expression, which relates the fractional gradient of V and the acceleration parameter ϵ in a multi-field setup. Let us note that

$$\frac{|\nabla V|^2}{V^2} = \frac{V_T^2 + V_N^2}{V^2}\,, \tag{II.3.30}$$

where we have used that $V^a = T^a V_T + N^a V_N$. We can obtain an expression for the tangential derivative of V as

$$V_T^2 = \frac{1}{2}\epsilon\left(6 - (2\epsilon - \eta)\right)^2 H^4\,, \tag{II.3.31}$$

[10]This condition is particularly relevant in the case of cosmic inflation to solve the horizon problem. In this case, it is necessary for ϵ to remain small for a minimum of around 60 e-foldings. In the case of quintessence dark energy, this condition can be relaxed.

by combining (II.3.24), (II.3.27) and the expression for η given in (II.3.28). Similarly, we can obtain an expression for the normal derivative of V, namely

$$V_N^2 = 2\Omega^2 H^2 \epsilon \,. \tag{II.3.32}$$

By combining the last four numbered equations, one finally obtains

$$\frac{|\nabla V|^2}{V^2} = 2\epsilon \left[\left(1 + \frac{\eta}{2(3-\epsilon)} \right)^2 + \frac{\Omega^2}{H^2 (3-\epsilon)^2} \right] . \tag{II.3.33}$$

If we demand a phase of cosmic acceleration, namely $\epsilon < 1$, then one has

$$\frac{|\nabla V|^2}{V^2} \simeq 2\epsilon \left[\left(1 + \frac{\eta}{6} \right)^2 + \frac{\Omega^2}{9H^2} \right] . \tag{II.3.34}$$

The latter expression shows that one may full-fill the de Sitter conjecture [76], in an accelerating background, either by having a large turning rate Ω (namely, a misalignment between the tangent vector and the gradient flow of V) or a large η parameter (see [77] for a recent analysis of this regime in the context of single field inflation). If one instead insists on $\eta \ll 1$, then one effectively requires a slow roll condition, namely $\ddot{\Phi} \ll H\dot{\Phi}$. In this regime, one obtains

$$\frac{|\nabla V|^2}{V^2} \simeq 2\epsilon \left(1 + \frac{\Omega^2}{9H^2} \right) , \tag{II.3.35}$$

which was already displayed in the introduction section of this chapter as (II.1.2).

II.4 Asymptotic acceleration and bound on the turning rate

The boundary of the moduli space provides an ideal testing ground to examine the predictions of the SDC. It allows for trajectories that extend infinitely, enabling the identification of a tower of states with exponentially decreasing mass along such paths.[11] Around these asymptotic regions, effective field theories exhibit significant simplifications and possess distinct features. Recent investigations [21, 22, 61] have therefore focused on studying cosmic acceleration in these limits.

In this section, we examine the implications of the SDC on a multi-field system that leads to 'asymptotic acceleration', referring to cosmic acceleration occurring at the boundary of moduli space. We focus on *infinite-distance trajectories*, namely paths in field space that can approach such asymptotic regions. These trajectories can either follow geodesics or deviate from them by a certain angle

[11] The Emergence String Conjecture [78] implies that the tower can be represented by either Kaluza-Klein modes or tensionless strings. However, for the purposes of our discussion, the specific nature is not relevant.

θ, as already discussed in Section II.2. The SDC imposes a strict constraint on this deviation angle, requiring it to approach a constant value in the full infinite-distance limit [73]. In this section, we specifically consider trajectories with a constant deviation angle from a geodesic throughout the duration of the acceleration.[12] Moreover, we focus on *hyperbolic spaces*, as prototype geometries of infinite distance limits of Calabi–Yau compactifications.

As a key result, we find that the turning rate of such infinite-distance trajectories is negligible, during the acceleration phase. It takes, in fact, the following general form:

$$\frac{\Omega}{H} = F(\theta, R)\ \sqrt{\epsilon}\,, \tag{II.4.1}$$

with F being a function of the deviation angle θ and proportional to the (sectional) curvature of the field manifold. We also show that this function F is upper bounded by an order one quantity such as

$$F(\theta, R) < F(\theta_0, R) = \mathcal{O}(1)\,, \tag{II.4.2}$$

where θ_0 is the maximum allowed deviation angle, which is related to the lowest allowed value λ_0 of the tower mass decay rate (as shown in (II.2.4)). The precise form of the function F depends on the specific case and dimensionality of the hyperbolic space and the class of trajectories being followed. It is worth noting that going beyond (II.4.2) and allowing for larger turning rates would require either a very high curvature of the internal space (see also [12]) or considering a product of an unnaturally large number of hyperbolic spaces (see Subsection II.4.3). However, we argue that this is not a typical situation in generic string effective theories.

We will proceed as follows. First, in Subsection II.4.1, we begin by considering the simplest case of a single hyperbolic plane, which corresponds to a typical axion-saxion system. Next, in Subsection II.4.2, we move on to a more complex scenario by considering a product of two hyperbolic planes. We will explore the diverse trajectory possibilities that arise in this setup. Finally, in Subsection II.4.3, we extend our analysis to the case of N hyperbolic planes and generalize our derived formulas.

II.4.1 One hyperbolic plane

Let us begin with a system of two real scalar fields $\Phi^a = (s, \phi)$, namely the saxion s and the axion ϕ. Their kinetic term is such that it defines an internal field space with hyperbolic geometry. The metric of a single hyperbolic upper half-plane is given by

$$\mathrm{d}\Delta^2 = G_{ab}\ \mathrm{d}\Phi^a \mathrm{d}\Phi^b = \frac{n^2}{s^2}\left(\mathrm{d}s^2 + \mathrm{d}\phi^2\right)\,, \tag{II.4.3}$$

with $n > 0$ controlling the curvature of the field manifold, which reads $R = -2/n^2$.

[12] Moving away from the boundary allows to have more freedom, such as path-dependent deviations from geodesic trajectories. We will consider this case in the following section.

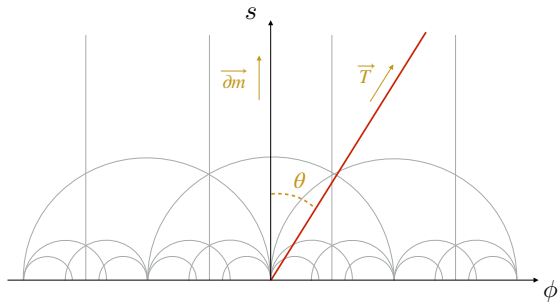

Figure II.2: Geodesics of one hyperbolic plane. Just the set of geodesics with constant ϕ can approach the infinite distant region. The red line represents a trajectory with a constant deviation angle θ from the infinite-distance geodesic.

Infinite-distance geodesics of this field space are those characterised by constant value of the axion ϕ and extend to infinity in the s-direction. Along these geodesics, we assume that the mass of an infinite tower of states decreases as $m_s \sim s^{-a}$ for some positive constant a. Other geodesics are semicircles but, in fact, they explore just finite regions of the moduli space and, therefore, will not be considered for our purposes. To test the SDC, we are interested just in the region of large s.[13]

We now consider a family of trajectories deviating by a constant angle θ from the infinite-distance geodesics (parallel to the s-axis) and then apply what we have learned in Section II.3 to calculate the turning rate (see Figure II.2). These paths have a non-zero velocity in both axionic and saxionic directions. For our convenience, we define the ratio of these velocities as

$$\beta \equiv \frac{\dot{\phi}}{\dot{s}} = \frac{\mathrm{d}\phi}{\mathrm{d}s}\,, \tag{II.4.4}$$

and we will show that this is constant for this class of trajectories. Constant deviations from geodesics are characterized by

$$G_{ab}\; T_g^a T^b = \cos\theta = \text{const.}\,, \tag{II.4.5}$$

where T_g^a is the unit vector tangent to the geodesic trajectory and T^a is the unit vector tangent to the trajectory followed in field space. The components of T_g^a read

$$T_g^s = \frac{1}{\dot{\Phi}_g}\dot{s}\,, \qquad T_g^\phi = 0\,, \qquad \text{with} \qquad \dot{\Phi}_g = n\frac{\dot{s}}{s}\,, \tag{II.4.6}$$

[13] As it was already pointed out in [46, 73], the duality of the system under $s \to 1/s$ is just an artifact of this simple model. In realistic string frameworks, this duality is in fact broken once we move away from the boundary and include corrections.

while the components of T^a read

$$T^s = \frac{1}{\dot\Phi}\dot s\,, \qquad T^\phi = \frac{1}{\dot\Phi}\dot\phi = \frac{1}{\dot\Phi}\beta\dot s\,, \tag{II.4.7}$$

with the speed along the trajectory given by

$$\dot\Phi = \frac{n}{s}\sqrt{\dot s^2+\dot\phi^2} = n\frac{\dot s}{s}\sqrt{1+\beta^2}\,. \tag{II.4.8}$$

Given the above equations, one obtains that

$$\cos\theta = \frac{1}{\sqrt{1+\beta^2}}\,, \tag{II.4.9}$$

which means that trajectories, with a constant deviation angle θ from a geodesic, have also a constant ratio between the velocities $\dot\phi$ and $\dot s$ such that

$$\beta = \frac{\mathrm{d}\phi}{\mathrm{d}s} = \tan\theta = \text{const}\,. \tag{II.4.10}$$

We can now calculate the turning rate in this setup. This is given by

$$\Omega = \frac{n}{s}\sqrt{(D_tT^s)^2+(D_tT^\phi)^2}\,, \tag{II.4.11}$$

with

$$D_tT^s = \dot T^s + \Gamma^s_{bc}T^b\dot\Phi^c = \dot T^s - \frac{1}{s}T^s\dot s + \frac{1}{s}T^\phi\dot\phi\,, \tag{II.4.12}$$

$$D_tT^\phi = \dot T^\phi + \Gamma^\phi_{bc}T^b\dot\Phi^c = \dot T^\phi - \frac{1}{s}T^s\dot\phi - \frac{1}{s}T^\phi\dot s\,, \tag{II.4.13}$$

where we have used the fact that, for the single hyperbolic plane, the only non-vanishing Christoffel symbols are $\Gamma^s_{ss} = \Gamma^\phi_{s\phi} = -1/s$ and $\Gamma^s_{\phi\phi} = 1/s$. For trajectories with a constant deviation angle, as defined by (II.4.4), we get

$$D_tT^s = \frac{1}{\dot\Phi}\left(\ddot s - \frac{\dot s}{\dot\Phi}\ddot\Phi - \frac{\dot s^2}{s}(1-\beta^2)\right)\,, \tag{II.4.14}$$

$$D_tT^\phi = \frac{1}{\dot\Phi}\beta\left(\ddot s - \frac{\dot s}{\dot\Phi}\ddot\Phi - 2\frac{\dot s^2}{s}\right)\,. \tag{II.4.15}$$

Using the relation $\dot s\ddot\Phi/\dot\Phi = \ddot s - \dot s^2/s$, the above equations become

$$D_tT^s = \frac{\beta^2}{\dot\Phi}\frac{\dot s^2}{s} = \frac{\beta^2}{n\sqrt{1+\beta^2}}\dot s\,, \tag{II.4.16}$$

$$D_tT^\phi = -\frac{\beta}{\dot\Phi}\frac{\dot s^2}{s} = -\frac{\beta}{n\sqrt{1+\beta^2}}\dot s\,. \tag{II.4.17}$$

The turning rate then finally reads

$$\Omega = \beta \frac{\dot{s}}{s} = \frac{\beta}{n\sqrt{1+\beta^2}} \dot{\Phi} \,, \tag{II.4.18}$$

namely, the trajectory defined by (II.4.4) is not a geodesic of this field space. As already said, geodesics in the hyperbolic plane are well-known to be just vertical lines and semicircles. More about that can also be found in Appendix II.B. The non-geodesic nature of the trajectory implies that in order to move in a non-vertical straight line on a hyperbolic plane, a normal force V_N needs to be applied. This is indeed an unintuitive property of hyperbolic spaces and one of their unusual characteristics. The presence of the normal force is required to counteract the curvature of the space and allow for straight-line motion.

Finally, we express the speed along the trajectory and the turning rate in terms of the deviation angle as

$$\dot{\Phi} = \frac{n}{\cos\theta} \frac{\dot{s}}{s} \,, \tag{II.4.19}$$

$$\Omega = \frac{|\sin\theta|}{n} \dot{\Phi} \,. \tag{II.4.20}$$

Assuming cosmic acceleration along this non-geodesic trajectory, we can use (II.3.27), which relates the speed along the path to the acceleration parameter, and finally obtain

$$\frac{\Omega}{H} = \frac{|\sin\theta|}{n} \sqrt{2\epsilon} \,. \tag{II.4.21}$$

Recalling that the field space curvature is given by $R = -2/n^2$, the above equation can be written in the form as given in the introduction of this section, namely

$$\frac{\Omega}{H} = F(\theta, R)\sqrt{\epsilon} \,, \qquad \text{with} \qquad F(\theta, R) = |\sin\theta|\sqrt{-R} \,. \tag{II.4.22}$$

The function F is upper bounded as $F < |\sin\theta_0|\sqrt{-R}$, with θ_0 being the maximum possible value allowed by the SDC, as described in Section II.2. This upper bound is typically an order one quantity. Just unnaturally big curvatures would allow to obtain large turning rates in this framework (a similar conclusion was reached by [12]). Using (II.2.4), we can express the bound in terms of the decay rate of the tower mass. We then obtain that the turning rate is directly bounded by

$$\frac{\Omega}{H} < \frac{\sqrt{\lambda_0^2 - \lambda_g^2}}{\lambda_g} \sqrt{R\,\epsilon} \,, \tag{II.4.23}$$

where we recall that λ_g is the decay rate along the geodesic path, while we use λ_0 to generically mean a lower bound as imposed by string theory (see [37, 49, 65–67] for some works in this direction).

The result derived in equation (II.4.21) indicates that the turning rate of the trajectory is severely constrained, being proportional to the small parameter

$\sqrt{\epsilon}$. This implies that asymptotic acceleration is predominantly geodesic, with deviations from the geodesic path being highly suppressed. We have obtained this result within the framework of a single hyperbolic plane. In the next section, we will further investigate more complex setups to explore the behavior of trajectories in those cases.

II.4.2 Two hyperbolic planes

As soon as we include a second hyperbolic plane, the situation becomes more intricate. In a product of two hyperbolic planes, we have four real scalar fields $\Phi^a = (s, \phi, u, \psi)$, namely 2 saxions s, u and 2 axions ϕ, ψ. In this case, the metric takes the following form:

$$\mathrm{d}\Delta^2 = G_{ab}\ \mathrm{d}\Phi^a \mathrm{d}\Phi^b = \frac{n^2}{s^2}\left(\mathrm{d}s^2 + \mathrm{d}\phi^2\right) + \frac{m^2}{u^2}\left(\mathrm{d}u^2 + \mathrm{d}\psi^2\right)\,. \tag{II.4.24}$$

We associate a tower of states with each saxionic direction such that the respective masses decrease as $m_s \sim s^{-a}$ and $m_u \sim u^{-b}$, with a and b some positive constants. Beside the purely saxionic directions, we now have a wider range of possibilities for infinite-distance trajectories. A trivial choice is to keep u and ψ fixed (or s and ϕ fixed). In this case, we immediately recover results analogous to the single hyperbolic plane. In the following, instead, we consider other possible non-trivial cases.

Saxion-axion trajectories

As a first non-trivial case, we consider trajectories with u and ϕ fixed ($u = u_0$ and $\phi = \phi_0$). Namely, we consider the saxion s, from the first hyperbolic plane, evolving together with the axion ψ, from the second hyperbolic plane. In particular, analogously to Subsection II.4.1, we consider paths deviating by a constant angle from the infinite-distance geodesics (namely trajectories for which just the saxion s evolves). This, again, corresponds to the case of constant ratio of velocities along the two directions, namely

$$\gamma \equiv s\frac{\dot{\psi}}{\dot{s}} = \text{const}\,. \tag{II.4.25}$$

Notice that, unlike in the previous section, the formula above contains a factor of s. This arises because the field u, which multiplies the kinetic term of ψ, has been set to a constant value, while the saxion s retains its non-canonical kinetic term. In section II.4.1, both the fields s and ϕ had kinetic terms with a multiplying factor of $1/s$, which canceled out in the ratio given by (II.4.4). One can now calculate the deviation angle from the geodesic trajectory and obtain

$$\cos\theta = G_{ab}\ T_g^a T^b = \left(1 + \frac{m^2\gamma^2}{u_0^2 n^2}\right)^{-\frac{1}{2}}\,, \tag{II.4.26}$$

which gives the identification

$$\tan\theta = \frac{m\gamma}{u_0 n}\,. \tag{II.4.27}$$

From the equations above, we can deduce that the constant ratio of velocities γ corresponds in fact to the constant deviation angle θ from a geodesic trajectory.

We can now calculate the turning rate in this setup. This is given by

$$\Omega^2 = \frac{n^2}{s^2}\left((D_t T^s)^2 + (D_t T^\phi)^2\right) + \frac{m^2}{u^2}\left((D_t T^u)^2 + (D_t T^\psi)^2\right)\,. \tag{II.4.28}$$

After some algebra, the covariant derivatives turn out to be

$$D_t T^u = \frac{1}{u_0}\frac{1}{\dot\Phi}\dot\psi^2 = \frac{1}{u_0}\frac{1}{\dot\Phi}\gamma^2\frac{\dot s^2}{s^2}\,, \qquad D_t T^s = D_t T^\phi = D_t T^\psi = 0\,, \tag{II.4.29}$$

with the speed along the trajectory given by

$$\dot\Phi^2 = \frac{n^2}{s^2}\dot s^2 + \frac{m^2}{u_0^2}\dot\psi^2 = n^2\frac{\dot s^2}{s^2}\left(1 + \frac{m^2\gamma^2}{u_0^2 n^2}\right)\,. \tag{II.4.30}$$

(II.4.29) shows that, despite the fact that the saxion u is taken to be constant, the only non-zero contribution to the turning rate is given by the projection of the covariant derivative in the u-direction. Namely, for this class of trajectories, the tangent vector fails to be parallel transported along the u-direction. We can then express the turning rate as

$$\Omega^2 = \frac{m^2\gamma^4}{u_0^4}\frac{1}{\dot\Phi^2}\left(\frac{\dot s^2}{s^2}\right)^2 = \frac{\frac{m^2\gamma^4}{u_0^4 n^4}}{\left(1 + \frac{m^2\gamma^2}{u_0^2 n^2}\right)^2}\dot\Phi^2\,, \tag{II.4.31}$$

where we immediately recognise the same quadratic dependence of the speed $\dot\Phi$ as in (II.4.20). The speed and the turning rate can be now given in terms of the deviation angle as

$$\dot\Phi = \frac{n}{\cos\theta}\frac{\dot s}{s}\,, \tag{II.4.32}$$

$$\Omega = \frac{\sin^2\theta}{m}\dot\Phi\,. \tag{II.4.33}$$

The speed $\dot\Phi$ has formally the same expression as for the single hyperbolic plane. However, the turning rate Ω has instead a different power of the sine, when compared to (II.4.20). Moreover, the curvature parameter appearing in Ω is the one of the second hyperbolic plane, reflecting the fact that the tangent vector turns with respect to the saxion u.

Finally, assuming cosmic acceleration along this non-geodesic trajectory, and using (II.3.27) to relate the speed to the acceleration parameter, we obtain

$$\frac{\Omega}{H} = \frac{\sin^2\theta}{m}\sqrt{2\epsilon}. \tag{II.4.34}$$

One can draw conclusions analogous to those presented for the case of a single hyperbolic plane. At the boundary of this moduli space, asymptotic acceleration is mainly geodesic. The presence of a non-geodesic trajectory introduces deviations from geodesic behavior, but the turning rate remains small compared to the Hubble parameter, indicating that geodesic motion dominates the dynamics.

Saxion-saxion trajectories

Here we consider another two-field infinite-distance trajectory where we keep the two axions ϕ and ψ fixed and allow the two saxions s and u to evolve together. Again, this class of trajectories is characterized by a constant ratio of the velocities along the two directions, namely

$$\delta \equiv \frac{\dot{u}}{\dot{s}}\frac{s}{u} = \text{const}\,, \tag{II.4.35}$$

where we have considered that both saxions have non-canonical kinetic terms. With this definition, the speed along the trajectory becomes

$$\dot{\Phi}^2 = \frac{n^2}{s^2}\dot{s}^2 + \frac{m^2}{u^2}\dot{u}^2 = n^2\frac{\dot{s}^2}{s^2}\left(1 + \frac{m^2}{n^2}\delta^2\right)\,, \tag{II.4.36}$$

while the tangent vector components read

$$T^s = \frac{1}{\dot{\Phi}}\dot{s}\,, \qquad T^u = \frac{1}{\dot{\Phi}}\dot{u} = \frac{u}{\dot{\Phi}}\delta\frac{\dot{s}}{s}\,, \qquad T^\phi = T^\psi = 0\,. \tag{II.4.37}$$

After some algebra, one can prove that

$$D_t T^s = D_t T^\phi = D_t T^u = D_t T^\psi = 0\,, \tag{II.4.38}$$

which directly implies

$$\Omega = 0\,. \tag{II.4.39}$$

Hence, a trajectory involving only two saxions is always geodesic for any δ. More about this can be found in Appendix II.B.

Saxion-axion-axion trajectories

Here we consider one final combination where only the second saxion u is constant, i.e. $u = u_0$. This is the first trajectory involving the evolution of three fields, which brings another new feature with it. We consider trajectories where the velocities along the three directions satisfy

$$\left(\frac{\dot{\phi}}{\dot{s}}\right)^2 + \frac{m^2}{n^2 u_0^2}\left(\frac{\dot{\psi}}{\frac{\dot{s}}{s}}\right)^2 = \text{const}\,. \tag{II.4.40}$$

However, we do not study this case in full generality, rather we assume that both terms are separately constant, namely

$$\beta \equiv \frac{\dot{\phi}}{\dot{s}} = \text{const}\,, \qquad \gamma \equiv s\frac{\dot{\psi}}{\dot{s}} = \text{const}\,. \tag{II.4.41}$$

With these definitions, the speed along the trajectory is then given by

$$\dot{\Phi}^2 = \frac{n^2}{s^2}(\dot{s}^2 + \dot{\phi}^2) + \frac{m^2}{u_0^2}\dot{\psi}^2 = n^2\frac{\dot{s}^2}{s^2}\left(1 + \beta^2 + \frac{m^2\gamma^2}{u_0^2 n^2}\right) \tag{II.4.42}$$

while the tangent vector components are

$$T^s = \frac{1}{\dot{\Phi}}\dot{s}\,, \qquad T^\phi = \frac{1}{\dot{\Phi}}\dot{\phi} = \frac{1}{\dot{\Phi}}\beta\dot{s}\,, \qquad T^u = 0\,, \qquad T^\psi = \frac{1}{\dot{\Phi}}\dot{\psi} = \frac{1}{\dot{\Phi}}\gamma\frac{\dot{s}}{s}\,. \tag{II.4.43}$$

After some algebra, one obtains that the covariant derivative components are given by

$$D_t T^s = \frac{\beta^2}{\dot{\Phi}}\frac{\dot{s}^2}{s}\,, \qquad D_t T^\phi = -\frac{\beta}{\dot{\Phi}}\frac{\dot{s}^2}{s}\,, \qquad D_t T^u = \frac{1}{u_0}\frac{1}{\dot{\Phi}}\gamma^2\frac{\dot{s}^2}{s^2}\,, \qquad D_t T^\psi = 0\,, \tag{II.4.44}$$

which implies that the turning rate is

$$\Omega^2 = \frac{\dot{\Phi}^2}{\left(1 + \beta^2 + \frac{m^2\gamma^2}{u_0^2 n^2}\right)^2}\left(\frac{\beta^2}{n^2}(1+\beta^2) + \frac{m^2\gamma^4}{u_0^4 n^4}\right). \tag{II.4.45}$$

Setting either $\beta = 0$ or $\gamma = 0$ yields the previous cases, which serves as a nice consistency check. Importantly, we observe that the turning rate Ω still scales with $\dot{\Phi}$, despite the different expressions for the speed $\dot{\Phi}$ in each case, considered so far. This emerges as a universal feature and it proves to be a crucial property when relating the results to cosmic acceleration.

We can again calculate the angle between the tangent vector to the geodesic (any line parallel to the s-axis) and the tangent vector to the trajectory. Thus, we have

$$\cos\theta = G_{ab}\, T_g^a T^b = \left(1 + \beta^2 + \frac{m^2\gamma^2}{u_0^2 n^2}\right)^{-\frac{1}{2}}\,, \tag{II.4.46}$$

such that

$$\tan\theta = \sqrt{\beta^2 + \frac{m^2\gamma^2}{u_0^2 n^2}}\,. \tag{II.4.47}$$

Furthermore, we can define the angle θ_ϕ in the s-ϕ-plane by setting $\gamma = 0$ in T^a and analogously the angle θ_ψ in the s-ψ-plane by setting $\beta = 0$. We then have

$$\tan\theta_\phi = \beta\,, \qquad \tan\theta_\psi = \frac{m\gamma}{n u_0}\,. \tag{II.4.48}$$

This enables us to express the speed $\dot{\Phi}$ and the turning rate Ω in terms of these angles as

$$\dot{\Phi}^2 = \frac{n^2}{\cos^2\theta}\frac{\dot{s}^2}{s^2}\,, \tag{II.4.49}$$

$$\Omega^2 = \cos^4\theta\left(\frac{1}{n^2}\frac{\tan^2\theta_\phi}{\cos^2\theta_\phi} + \frac{1}{m^2}\tan^4\theta_\psi\right)\dot{\Phi}^2\,. \tag{II.4.50}$$

In this formulation, the connection to the previous results becomes even more apparent. If we set $\gamma = 0$, we get $\theta = \theta_\phi$ and $\theta_\psi = 0$ thereby recovering the result of the single hyperbolic plane. Of course, the same logic works for setting $\beta = 0$. Finally, if we assume that cosmic acceleration occurs along this trajectory, then we obtain

$$\frac{\Omega^2}{H^2} = 2\epsilon \cos^4\theta \left(\frac{1}{n^2} \frac{\tan^2\theta_\phi}{\cos^2\theta_\phi} + \frac{1}{m^2} \tan^4\theta_\psi \right) , \tag{II.4.51}$$

where the trigonometric function is bounded to be $\max\{m^{-2}, n^{-2}\}$, namely, an order one factor. This result indicates once more that trajectories leading to asymptotic acceleration must have a negligible turning rate.

II.4.3 N hyperbolic planes

In this section, we extend our computations to an arbitrary number N of hyperbolic planes. The generalization to N hyperbolic planes follows the same principles discussed for the cases of one and two hyperbolic planes. Each additional hyperbolic plane introduces more components and equations, but they can be categorized into the two base cases: saxion with an axion from the same hyperbolic plane, and saxion with an axion from another hyperbolic plane. We do not discuss the case of several saxions since we have already seen that it leads to zero contribution to the turning rate Ω.

We consider the product of N hyperbolic planes with N saxions s_i and N axions ϕ_i, making a total of $2N$ real scalar fields $\Phi^a = (s_1, \phi_1, ..., s_N, \phi_N)$. The metric of this field space is

$$\mathrm{d}\Delta^2 = G_{ab}\, \mathrm{d}\Phi^a \mathrm{d}\Phi^b = \sum_{i=1}^{N} \frac{n_i^2}{s_i^2} \left(\mathrm{d}s_i^2 + \mathrm{d}\phi_i^2 \right) . \tag{II.4.52}$$

with n_i being the curvature parameter of each i-th hyperbolic plane. Also in this case, we assume that along each saxionic direction a tower of states will have decreasing mass as $m_{s_i} \sim s^{-a_i}$, for some constants $a_i > 0$.

From now on, we fix a saxionic direction, without loss of generality. We choose s_1 and drop the index 1 from all quantities of the first hyperbolic plane, i.e. $s_1 \equiv s$, $\phi_1 \equiv \phi$ and $n_1 \equiv n$. Next, we fix the trajectory as the one which involves displacement of the saxion s and of all axions ϕ and ϕ_i. The other saxions are taken to be constant, that is $s_i = \text{const}$ for $i \neq 1$. To simplify the notation, we drop the label 0 here, so we write s_i instead of s_{0i}. By analogy with the previous subsection, these trajectories satisfy

$$\left(\frac{\dot\phi}{\dot s} \right)^2 + \sum_{i=2}^{N} \frac{n_i^2}{n^2 s_i^2} \left(\frac{\dot\phi_i}{\frac{\dot s}{s}} \right)^2 = \text{const} . \tag{II.4.53}$$

Again, we simplify the situation by assuming that all terms are individually constant, such as

$$\beta \equiv \frac{\dot\phi}{\dot s} = \text{const} , \qquad \beta_i \equiv s \frac{\dot\phi_i}{\dot s} = \text{const} , \qquad \text{for } i \geq 2 . \tag{II.4.54}$$

With these definitions, we can write the expression of the speed along the trajectory as

$$\dot{\Phi}^2 = \frac{n^2}{s^2}(\dot{s}^2 + \dot{\phi}^2) + \sum_{i=2}^{N} \frac{n_i^2}{s_i^2} \dot{\phi_i}^2 = n^2 \frac{\dot{s}^2}{s^2} \left(1 + \beta^2 + \sum_{i=2}^{N} \frac{n_i^2 \beta_i^2}{s_i^2 n^2} \right) . \tag{II.4.55}$$

The turning rate thus becomes

$$\Omega^2 = \frac{\dot{\Phi}^2}{\left(1 + \beta^2 + \sum_{i=2}^{N} \frac{n_i^2 \beta_i^2}{s_i^2 n^2} \right)^2} \left(\frac{\beta^2}{n^2}(1+\beta^2) + \sum_{i=2}^{N} \frac{n_i^2 \beta_i^4}{s_i^4 n^4} \right) , \tag{II.4.56}$$

where, once more, we confirm the relation such as $\Omega \sim \dot{\Phi}$.

As in the previous cases, it is again possible to define the angle between the geodesic tangent vector T_g^a, which corresponds to setting $\beta = \beta_i = 0$, and the tangent vector to the trajectory T^a. This deviation angle is given by

$$\cos\theta = G_{ab}\, T_g^a T^b = \left(1 + \beta^2 + \sum_{i=2}^{N} \frac{n_i^2 \beta_i^2}{s_i^2 n^2} \right)^{-\frac{1}{2}} . \tag{II.4.57}$$

Furthermore, we can define the angle θ_ϕ in the s-ϕ-plane by setting $\beta_i = 0$ for $i \geq 2$ and the angle θ_{ϕ_i} in the s-ϕ_i-plane by setting $\beta = \beta_j = 0$ for $j \neq i$. We then have

$$\tan\theta_\phi = \beta\,, \qquad \tan\theta_{\phi_i} = \frac{n_i \beta_i}{n s_i}\,, \tag{II.4.58}$$

This allows us to express the speed $\dot{\Phi}$ and the turning rate Ω in terms of these angles, namely

$$\dot{\Phi}^2 = \frac{n^2}{\cos^2\theta} \frac{\dot{s}^2}{s^2} \tag{II.4.59}$$

$$\Omega^2 = \cos^4\theta \left(\frac{1}{n^2} \frac{\tan^2\theta_\phi}{\cos^2\theta_\phi} + \sum_{i=2}^{N} \frac{1}{n_i^2} \tan^4\theta_{\phi_i} \right) \dot{\Phi}^2 . \tag{II.4.60}$$

This is perfectly consistent with the results of the previous subsections. Finally, if we assume that cosmic acceleration occurs along this path, then one has

$$\frac{\Omega^2}{H^2} = 2\epsilon \cos^4\theta \left(\frac{1}{n^2} \frac{\tan^2\theta_\phi}{\cos^2\theta_\phi} + \sum_{i=2}^{N} \frac{1}{n_i^2} \tan^4\theta_{\phi_i} \right) , \tag{II.4.61}$$

where the trigonometric function is upper-bounded by $\max\{n^{-2}, n_1^{-2}, \ldots, n_{N-1}^{-2}\}$. This nicely generalizes all previous results.

II.5 Moving away from the boundary of moduli space

In the previous section, we have demonstrated that the boundary of moduli space highly restricts the possibility of realizing large turning rates in a multi-field setup that leads to cosmic acceleration. We have found this result by focusing on hyperbolic spaces and on trajectories, which have a constant deviation angle from geodesics, namely $\theta = \text{const}$. The SDC, in fact, does not allow for any other non-geodesic behaviour in the full infinite distance limit, as already pointed out in [73].

However, the constraints relax when moving away from the boundary, thus allowing trajectories with time-dependent deviations from a geodesic. A time-dependent deviation angle $\theta = \theta(t)$ corresponds to a path-dependent decay rate $\lambda = \lambda(\Delta)$ of the tower, following (II.2.3). Specifically, one expects a structure like $\lambda = \lambda_\infty + \delta\lambda(\Delta)$, with a leading constant term λ_∞ and some corrections $\delta\lambda$ that vanish at the boundary. This leads to corrections to the SDC exponential formula of the tower mass, such as

$$m = m_0 \exp(-\lambda\Delta) + \delta m(\Delta) \tag{II.5.1}$$

with $\delta m \to 0$ in the limit $\Delta \to \infty$, namely at the boundary.

In this section, we examine the case of a time-dependent deviation angle and explore its implications for the turning rate. We find that achieving a large turning rate Ω requires non-generic conditions for the trajectory. After providing the general formulas in Subsection II.5.1, we present a specific example of θ as a Taylor expansion in negative powers of the saxion s in Subsection II.5.2. For the sake of simplicity, we focus on the framework of a single hyperbolic plane.

II.5.1 Non-constant deviation angle

In the framework of a single hyperbolic plane, considering a non-constant deviation angle corresponds to a time-dependent ratio of the velocities along the saxionic and axionic directions:

$$\frac{\mathrm{d}\phi}{\mathrm{d}s} = \beta(t) = \tan\theta(t)\,. \tag{II.5.2}$$

The trajectory (see Figure II.3) is now defined by following tangent vector and speed

$$T^s = \frac{1}{\dot\Phi}\dot s\,, \qquad T^\phi = \frac{1}{\dot\Phi}\beta(t)\dot s\,, \qquad \dot\Phi^2 = n^2\frac{\dot s^2}{s^2}\left(1+\beta(t)^2\right)\,. \tag{II.5.3}$$

Then, we observe all the second derivative terms, which implicitly involve $\beta(t)$, get extra contributions, namely

$$\frac{\dot{s}}{\dot{\Phi}}\ddot{\Phi} = \ddot{s} - \frac{\dot{s}^2}{s} + \frac{\dot{s}}{1+\beta^2}\beta\dot{\beta}\,, \tag{II.5.4}$$

$$\ddot{\phi} = \ddot{s}\beta + \dot{s}\dot{\beta}\,, \tag{II.5.5}$$

$$\frac{\dot{\phi}}{\dot{\Phi}}\ddot{\Phi} = \beta\left(\ddot{s} - \frac{\dot{s}^2}{s}\right) + \frac{\beta^2}{1+\beta^2}\dot{s}\dot{\beta}\,. \tag{II.5.6}$$

We can plug the above expressions into (II.4.14) and (II.4.15) and obtain

$$D_t T^s = \frac{\beta^2}{n\sqrt{1+\beta^2}}\dot{s} - \frac{s\beta}{n\,(1+\beta^2)^{\frac{3}{2}}}\dot{\beta}\,, \tag{II.5.7}$$

$$D_t T^\phi = -\frac{\beta}{n\sqrt{1+\beta^2}}\dot{s} + \frac{s}{n\,(1+\beta^2)^{\frac{3}{2}}}\dot{\beta}\,, \tag{II.5.8}$$

which is of course consistent with previous findings upon setting $\dot{\beta} = 0$. Switching to the formulation in terms of the deviation angle θ, we obtain

$$D_t T^s = \frac{1}{n}\tan^2\theta\cos\theta\ \dot{s} - \frac{s}{n}\sin\theta\ \dot{\theta}\,, \tag{II.5.9}$$

$$D_t T^\phi = -\frac{1}{n}\sin\theta\ \dot{s} + \frac{s}{n}\cos\theta\ \dot{\theta}\,, \tag{II.5.10}$$

where we used $\dot{\beta} = \dot{\theta}/\cos^2\theta$. Plugging this into the expression of the turning rate (II.4.11), we get

$$\Omega^2 = \left(\tan\theta\ \frac{\dot{s}}{s} - \dot{\theta}\right)^2\,. \tag{II.5.11}$$

Furthermore, using (II.4.19) for the speed $\dot{\Phi}$ in terms of the angle θ, we arrive at the final result

$$\Omega = \left|\frac{\sin\theta}{n}\dot{\Phi} - \dot{\theta}\right|\,. \tag{II.5.12}$$

This is still fully consistent with (II.4.20), which was obtained in the case of $\dot{\theta} = 0$. In an accelerating background, the first term of the above equation is small, being proportional to $\sqrt{\epsilon}$. This implies that a large turning rate Ω can be achieved just in the case of large $\dot{\theta}$. We argue that this is not a generic situation for trajectories, which eventually approach the boundary of moduli space. We give an example in the next subsection.

II.5.2 Asymptotic expansion of θ

Approaching the boundary of moduli space, in the framework of a single hyperbolic space, translates into moving towards large values of s. A natural choice of

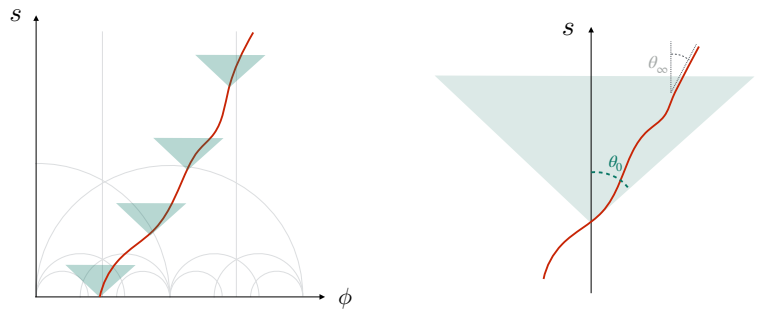

Figure II.3: Trajectory with a non-constant deviation angle in a hyperbolic plane. The trajectory, at any point, remains inside the cone $|\theta(s)| \leq \theta_0$, related to the lower bound on the mass decay rate of the tower of states. θ_∞ represents the deviation angle at the boundary ($s \to \infty$).

non-constant deviation angle, to parameterize the departure from the boundary, is a Taylor expansion in negative powers of the saxion s. Therefore, we consider[14]

$$\theta(s) = \theta_\infty + \sum_{n>0} \frac{c_n}{s^n} \,, \tag{II.5.13}$$

where θ_∞ is the value of theta at the boundary ($s = \infty$). Note that we still require that

$$\theta(s) \leq \theta_0 \,, \tag{II.5.14}$$

at any point in field space, with θ_0 being the maximum possible value of the angle (see Figure II.3). This is to be consistent with the existence of a universal lower bound on the decay rate of the SDC tower mass as, for example, claimed in [37, 49, 65–67]. Let us consider just the constant and the first leading of the above expansion

$$\theta(s) \simeq \theta_\infty + \frac{c_k}{s^k} \,, \tag{II.5.15}$$

where k must not be necessarily equal to 1. Using (II.5.14), we then find

$$\frac{c_k}{s^k} \leq \theta_0 - \theta_\infty \leq 2\theta_0 \,, \tag{II.5.16}$$

because θ_∞ could at most be equal to $-\theta_0$. We can now calculate the angular velocity, that is

$$\dot{\theta}(s) \approx -k \frac{c_k}{s^k} \frac{\dot{s}}{s} \,. \tag{II.5.17}$$

[14] Another option would be to consider an expansion of $\beta(s) = \tan\theta(s)$ in negative powers of the saxion s (this possibility was already suggested in [46]).

We note that, for this type of trajectories, also $\dot{\theta}$ vanishes in the limit $s \to \infty$. More importantly, using (II.4.19) and (II.5.17), we can get an upper bound for the absolute value of the angular velocity

$$\left|\dot{\theta}(s)\right| \leq \frac{2k}{n}\theta_0 \cos\theta(s)\ \dot{\Phi}\,. \tag{II.5.18}$$

If cosmic acceleration occurs along this non-geodesic trajectory, then one can use (II.3.27) and express the speed $\dot{\Phi}$ in terms of the Hubble parameter H and the acceleration parameter ϵ. The bound on the angular velocity thus becomes

$$\left|\frac{\dot{\theta}(s)}{H}\right| \leq 2\sqrt{2}\ \frac{k}{n}\ \theta_0\ \sqrt{\epsilon}\,, \tag{II.5.19}$$

namely, also the angular velocity (in Hubble units) is constrained by the parameter ϵ, which is less than unity during acceleration. This result, combined with the more general formula (II.5.12) on the turning rate, again implies

$$\frac{\Omega}{H} \simeq \sqrt{\epsilon}. \tag{II.5.20}$$

The significance of this last equation is that, even when moving away from the boundary, the SDC imposes strict constraints on the turning rate of non-geodesic trajectories in an accelerating background.

II.6 Conclusions

In this chapter, we have studied the constraints imposed by SDC on multi-field acceleration scenarios at the boundary of moduli space. This is a natural framework for string effective models, which typically involve a rich spectrum of massless and/or light scalar fields. Furthermore, the EFTs offer simplified perturbative descriptions in these asymptotic regions of the moduli space, making the boundary an ideal setting to extract robust predictions.

As a key result of this investigation, we have found that, in accelerating backgrounds, field trajectories that extend infinitely and satisfy the SDC must exhibit a negligible turning rate. Specifically, we have established that the turning rate Ω (measured in Hubble units) must be proportional to $\sqrt{\epsilon}$, where ϵ denotes the acceleration parameter. Since $\epsilon < 1$ in a quasi-de Sitter space, this proportionality implies that Ω is indeed small. Furthermore, we have shown that the turning rate Ω is bounded above by a function of the minimal value allowed for the mass decay rate of the SDC tower within string theory [37, 49, 65–67]. A specific expression for this bound can be found in (II.4.23). We have obtained this result in the context of hyperbolic spaces of different dimensionality (namely, with an arbitrary number of fields), as systematically described in Section II.4. Furthermore, we have tested this result both for trajectories with a constant deviation from a geodesic (Section II.4) and with a time-dependent deviation from the geodesics (Section II.5).

The latter case becomes a convenient way to parameterize departures from the boundary.

This finding aligns perfectly with the well-established understanding that the physics at the boundary of the moduli space is subject to stringent constraints. Several properties characterize this limit. For instance, the species scale Λ_s tends to zero (see e.g. [42, 79]), while corrections to the Kähler- and super-potential of the EFT vanish. The scalar potential and the gravitino mass approach zero value [36, 37, 57, 58], while the entropy instead increases (see e.g. [42]). Our work adds to this list of properties by showing that asymptotic acceleration is primarily geodesic.

The implications of this result are manifold:

- Fulfilling the de Sitter conjecture [57, 76], in an accelerating background and at the boundary of moduli space, becomes challenging, given our result. Despite the fact that we are in a multi-field setup, the gradient of the scalar potential is predominantly determined by the acceleration parameter ϵ (see (II.3.35)), giving results analogous to the single-field case . As pointed out in Section II.3, an alternative interesting way to obtain large values of $|\nabla V|/V$, and satisfy the de Sitter conjecture, is to assume cosmological phases with large parameter η (see [77] for a recent analysis of this situation in single-field inflation). In this case, a slow-roll condition is violated, namely, the second derivatives of the fields are not smaller than the friction Hubble term in the equations of motion.

- Models engineering cosmic acceleration with rapid turns face significant constraints at the boundary of the moduli space, making it more favorable to explore such scenarios in the *bulk* of the moduli space, consistent with the results of [64, 80]. In the bulk, both perturbative and non-perturbative corrections are expected to play a fundamental role in shaping the dynamics of the system. These corrections can potentially provide additional degrees of freedom and interactions that allow for more flexible and diverse trajectories, facilitating the realization of desired acceleration patterns.

- The total field displacement Δ is subject to a universal upper bound $\Delta \lesssim -\log H$, as established in [46]. In the context of multi-field inflation, our findings suggest that the total field displacement remains bounded by the tensor-to-scalar ratio measured at CMB scales, denoted as $\Delta \lesssim -\log r$. Although the original derivation of this bound in [46] was focused on single-field scenarios, it is applicable to the case of multi-field inflation due to the fact that trajectories must be (quasi-)geodesic.

- Our result on the turning rate, in the context of inflation, implies also that the speed of sound c_s of primordial perturbations must be close to unity, as in the single-field case. The expression of the speed of sound in multi-field models is indeed $c_s = \left(1 + 4\Omega^2/M^2\right)^{-1/2}$, with M being the mass of the fluctuations orthogonal to the trajectory and typically assumed larger

than the Hubble scale H. This seems to be consistent with the results of [81], which found a stringent lower bound on c_s in the context of $\mathcal{N} = 1$ supergravity.

As a caveat, our bound on the turning rate can be relaxed in the case of very large curvatures of the field space (see also [12]). However, we have argued this is not a generic situation in string effective models and considered instead this contribution of order one. For example, the parameter n of the metric of the hyperbolic spaces is typically very constrained by Calabi–Yau compactifications and takes very specific $\mathcal{O}(1)$ values. Furthermore, our results should not be regarded as strictly valid only *at* the exact boundary of moduli space or *slightly away* from it (as discussed in Section II.5). They can be applied more generally whenever the geometry of the moduli space can be approximated as hyperbolic and to any scenario of cosmic acceleration characterized by *large field excursions*, as long as the SDC is satisfied.

Finally, we acknowledge that our investigation has focused on a minimal setup and has not taken into account other details that can arise in realistic cosmological descriptions of inflation or dark energy. One important aspect that we have not considered is the presence of other sources of energy density. One such example is provided by scalar-gauge field interactions, which lead to additional friction terms in the equations of motion. In the context of inflation, this has been studied in the seminal paper [82]. In the context of (quintessence) dark energy, it has been recently investigated in [83]. Furthermore, we have studied just the homogeneous case with the scalar fields depending just on the time variable. The case of inhomogeneous fields, i.e. $\mathbf{\Phi} = \mathbf{\Phi}(t, \boldsymbol{x})$, can be understood as introducing extra forces in moduli space, thus again leading to deviation from geodesic trajectories. See [84] for one specific study of spatial-dependent fields and its relation to the SDC. We leave these and other exciting directions for future work.

II.A Non-affine geodesic equation

Here we show that a non-affine geodesic equation can always be brought to the form of an affine geodesic equation.

This reparametrization is unique (for a given non-affine geodesic equation) up to an affine transformation (which is just a linear reparametrization, i.e. $t \to mt + n$).

Let us start with a non-affine geodesic equation. This equation has an additional term which is proportional to the first derivative, namely

$$\frac{\mathrm{d}^2 x^a}{\mathrm{d}t^2} + \Gamma^a_{bc} \frac{\mathrm{d}x^b}{\mathrm{d}t} \frac{\mathrm{d}x^c}{\mathrm{d}t} = \alpha \frac{\mathrm{d}x^a}{\mathrm{d}t} \,. \tag{II.A.1}$$

Such a first order derivative term is usually referred to as a friction term (depending on the sign). Now we can introduce a new parameter $s(t)$ so that

$$\frac{\mathrm{d}}{\mathrm{d}t} = \frac{\mathrm{d}s}{\mathrm{d}t} \frac{\mathrm{d}}{\mathrm{d}s} \,. \tag{II.A.2}$$

Then we get

$$\frac{\mathrm{d}}{\mathrm{d}t}\frac{\mathrm{d}x^a}{\mathrm{d}t} = \frac{\mathrm{d}}{\mathrm{d}t}\left(\frac{\mathrm{d}s}{\mathrm{d}t}\frac{\mathrm{d}x^a}{\mathrm{d}s}\right) \tag{II.A.3}$$

$$= \left(\frac{\mathrm{d}s}{\mathrm{d}t}\right)^2\frac{\mathrm{d}^2x^a}{\mathrm{d}s^2} + \frac{\mathrm{d}x^a}{\mathrm{d}s}\frac{\mathrm{d}}{\mathrm{d}t}\left(\frac{\mathrm{d}s}{\mathrm{d}t}\right). \tag{II.A.4}$$

This allows us the rewrite the geodesic equation (II.A.1) as

$$\left(\frac{\mathrm{d}s}{\mathrm{d}t}\right)^2\frac{\mathrm{d}^2x^a}{\mathrm{d}s^2} + \left(\frac{\mathrm{d}s}{\mathrm{d}t}\right)^2\Gamma^a_{bc}\frac{\mathrm{d}x^b}{\mathrm{d}s}\frac{\mathrm{d}x^c}{\mathrm{d}s} = \frac{\mathrm{d}x^a}{\mathrm{d}s}\left(\alpha\frac{\mathrm{d}s}{\mathrm{d}t} - \frac{\mathrm{d}}{\mathrm{d}t}\left(\frac{\mathrm{d}s}{\mathrm{d}t}\right)\right). \tag{II.A.5}$$

Therefore, if we want the right-hand side to vanish, we need to solve the following equation (setting $\lambda \equiv \mathrm{d}s/\mathrm{d}t$)

$$\alpha\lambda = \frac{\mathrm{d}\lambda}{\mathrm{d}t}, \tag{II.A.6}$$

which can be integrated and one gets

$$\lambda = \lambda_0 e^{\int \alpha\,\mathrm{d}t}. \tag{II.A.7}$$

Hence, the geodesic equation (II.A.1) becomes affine in the s-parametrization, that is

$$\frac{\mathrm{d}^2x^a}{\mathrm{d}s^2} + \Gamma^a_{bc}\frac{\mathrm{d}x^b}{\mathrm{d}s}\frac{\mathrm{d}x^c}{\mathrm{d}s} = 0, \tag{II.A.8}$$

which is the standard geodesic equation form and the equation defining the parallel transport of a tangent vector along itself.

We can now apply this strategy to the setup defined by (II.3.20), where we have

$$\frac{\mathrm{d}^2\Phi^a}{\mathrm{d}t^2} + \Gamma^a_{bc}\frac{\mathrm{d}\Phi^b}{\mathrm{d}t}\frac{\mathrm{d}\Phi^c}{\mathrm{d}t} + 3H\frac{\mathrm{d}\Phi^a}{\mathrm{d}t} + G^{ab}V_b = 0. \tag{II.A.9}$$

We now introduce the parameter $s(t)$. The potential term stays unchanged since it does not involve any derivative with respect to the parameter along the curve. The above equation then becomes

$$\frac{\mathrm{d}^2\Phi^a}{\mathrm{d}s^2} + \Gamma^a_{bc}\frac{\mathrm{d}\Phi^b}{\mathrm{d}s}\frac{\mathrm{d}\Phi^c}{\mathrm{d}s} + g^{ab}V_b = 0, \tag{II.A.10}$$

provided we have

$$\frac{\mathrm{d}s}{\mathrm{d}t} = \lambda = \lambda_0 e^{3Ht}, \tag{II.A.11}$$

with H approximately constant. So, we have seen that a simple reparametrization can eliminate the friction term of the equation of motion. This will have an impact on the velocity along the curve, which depends on the specific parameter.

II.B Geodesics of hyperbolic planes

This appendix provides a complementary perspective to the results obtained in Section II.4. We show here that, if $\Omega = 0$ for a trajectory, then this trajectory fulfills the standard geodesic equation. We begin by examining the single hyperbolic plane which we recall here again

$$\mathrm{d}\Delta^2 = \frac{n^2}{s^2}\left(\mathrm{d}s^2 + \mathrm{d}\phi^2\right) . \tag{II.B.1}$$

This parameterizes the upper half of the hyperbolic plane, i.e. $s > 0$. The non-vanishing Christoffel symbols are

$$\Gamma^s_{ss} = -\frac{1}{s} = \Gamma^\phi_{s\phi}, \quad \Gamma^s_{\phi\phi} = \frac{1}{s}, \tag{II.B.2}$$

such that the geodesic equation (II.3.2) or (II.3.5) becomes

$$\ddot{s} - \frac{1}{s}\dot{s}^2 + \frac{1}{s}\dot{\phi}^2 = 0\,, \tag{II.B.3}$$

$$\ddot{\phi} - \frac{2}{s}\dot{s}\dot{\phi} = 0\,. \tag{II.B.4}$$

There are two types of geodesics which solve these equations: semi-circles with centers in $s = 0$ and vertical lines with $\phi = \phi_0 = \text{const}$. We are interested in the region of large s, so we focus on the vertical lines. For this case, the second geodesic equation becomes trivial (0=0) whereas the first reads

$$\ddot{s} - \frac{1}{s}\dot{s}^2 = 0\,. \tag{II.B.5}$$

After some simple algebra, we get the solution

$$s(t) = C\, e^{at}\,, \tag{II.B.6}$$

with a and C some integration constants. We now explore what happens when we assume a constant deviation angle from a geodesic, namely, a constant velocity ratio, such as $\beta = \dot{\phi}/\dot{s} = \text{const}$. We can immediately understand that this cannot be a geodesic unless $\beta = 0$, because we just learned that a (infinite-distance) geodesic must have $\dot{\phi} = 0$. In this case, the set of two geodesic equations becomes

$$\ddot{s} - \frac{1}{s}\dot{s}^2(1-\beta^2) = 0\,, \tag{II.B.7}$$

$$\beta\left(\ddot{s} - \frac{2}{s}\dot{s}^2\right) = 0\,. \tag{II.B.8}$$

It turns out this can only be consistently solved only for $\beta = 0$. That explains what happens at the level of the geodesic equation and is in perfect agreement with the result for the turning rate (II.4.18). This is also consistent with the findings in [73].

Next, we turn to the product of two hyperbolic planes. Here the metric reads

$$\mathrm{d}\Delta^2 = \frac{n^2}{s^2}\left(\mathrm{d}s^2 + \mathrm{d}\phi^2\right) + \frac{m^2}{u^2}\left(\mathrm{d}u^2 + \mathrm{d}\psi^2\right) . \tag{II.B.9}$$

The non-vanishing Christoffel symbols are

$$\Gamma^s_{ss} = -\frac{1}{s} = \Gamma^\phi_{s\phi}\,, \qquad \Gamma^s_{\phi\phi} = \frac{1}{s}\,, \qquad \Gamma^u_{uu} = -\frac{1}{u} = \Gamma^\psi_{s\psi}\,, \qquad \Gamma^u_{\psi\psi} = \frac{1}{u}\,. \tag{II.B.10}$$

Therefore, we arrive at the following geodesic equation

$$\ddot{s} - \frac{1}{s}\dot{s}^2 + \frac{1}{s}\dot{\phi}^2 = 0\,, \tag{II.B.11}$$

$$\ddot{\phi} - \frac{2}{s}\dot{s}\dot{\phi} = 0\,, \tag{II.B.12}$$

$$\ddot{u} - \frac{1}{u}\dot{u}^2 + \frac{1}{u}\dot{\psi}^2 = 0\,, \tag{II.B.13}$$

$$\ddot{\psi} - \frac{2}{u}\dot{u}\dot{\psi} = 0\,. \tag{II.B.14}$$

It is pretty evident from these equations that a geodesic for the product of two hyperbolic planes consists of two geodesics of the single hyperbolic plane combined in one vector. Due to the same reasons as above we reject all the semi-circle solutions and just focus on the case with constant axions, namely $\phi = \phi_0 = \text{const}$ and $\psi = \psi_0 = \text{const}$. Hence, the axion equations become again trivial and we get two copies the same saxion equation which is precisely the same as above.

$$\ddot{s} - \frac{1}{s}\dot{s}^2 = 0\,, \tag{II.B.15}$$

$$\ddot{u} - \frac{1}{u}\dot{u}^2 = 0\,. \tag{II.B.16}$$

The solutions to these equations also works out to be

$$s(t) = Ce^{at}\,, \tag{II.B.17}$$

$$u(t) = De^{bt}\,, \tag{II.B.18}$$

where a, b, C, D are positive numbers. Now it is interesting to see what happens in the case of constant deviation between the two geodesic trajectories. This correspond to a constant ratio of velocities, namely, $\dot{u}/u = \delta\dot{s}/s$ for some $\delta = \text{const}$. We then get

$$\ddot{s} - \frac{1}{s}\dot{s}^2 = 0\,, \tag{II.B.19}$$

$$\delta\left(\ddot{s} - \frac{1}{s}\dot{s}^2\right) = 0\,. \tag{II.B.20}$$

Unlike above, these two equations are of course compatible. The solution of this equation is precisely as given above in (II.B.18). Now we can integrate the condition on the velocities

$$\ln u = \delta \ln s + k \tag{II.B.21}$$

where k is an integration constant. Plugging the solution for s into that, we arrive at

$$\ln u = \delta \ln s + k = (\delta a)\ t + (\delta C + k) \tag{II.B.22}$$

which is obviously also a solution to the geodesic equation for constant axions. Therefore, in a product of two hyperbolic spaces, any linear combination of saxionic trajectories is a geodesic, which is in agreement with the result $\Omega = 0$ of Equation II.4.2.

Let us now explore what happens in the case of trajectories involving displacements of the saxion and the axion of two different hyperbolic planes, as discussed in Equation II.4.2. So we consider $\phi = \phi_0 = \text{const}$ and $u = u_0 = \text{const}$. This makes the equation associated with ϕ trivial again. However, the equation for the other constant coordinate u is not trivial and this makes a crucial difference with the previous case. Omitting the equation for the field ϕ, we get

$$\ddot{s} - \frac{1}{s}\dot{s}^2 = 0\,, \tag{II.B.23}$$

$$\frac{1}{u_0}\dot{\psi}^2 = 0\,, \tag{II.B.24}$$

$$\ddot{\psi} = 0\,. \tag{II.B.25}$$

We can already read off some implications from this set of equations, namely ψ has to be constant. But let us employ condition for which the trajectory is characterized by a constant ratio of the velocities, namely $\dot{\psi} = \gamma \dot{s}/s$. So the above equations turn into

$$\ddot{s} - \frac{1}{s}\dot{s}^2 = 0 \tag{II.B.26}$$

$$\frac{1}{u_0}\gamma^2 \left(\frac{\dot{s}}{s}\right)^2 = 0 \tag{II.B.27}$$

$$\gamma\left(\ddot{s} - \frac{1}{s}\dot{s}^2\right) = 0. \tag{II.B.28}$$

Without the second equation we would be in the same situation as in the previous case, which had implied $\Omega = 0$. However, precisely this second equation spoils the situation since it forces upon us the uninteresting case $s = \text{const}$. Instead, we have required our trajectory to approach $s = \infty$. So there is no solution to the geodesic equation in this case. In agreement with the findings of Section II.4, we conclude that $\Omega \neq 0$ and that we have to include all the coordinates in order to get a proper result.

II.C Geodesics of universal hypermultiplet moduli space

As an example of a moduli space in string theory closely related to the Poincaré hyperbolic plane, here we introduce the geometry of the universal hypermulti-

plet moduli space and classify its geodesics. The universal hypermultiplet arises in $\mathcal{N}=2$ supergravity from various string compactifications. In particular, as discussed in the first chapter, Calabi–Yau compactifications from 10D to 4D always yield at least one hypermultiplet, the universal hypermultiplet. There exist special cases of $\mathcal{N}=2$ compactifications in which the spectrum contains no hypermultiplet [85, 86].

Classical universal hypermultiplet moduli space

The universal hypermultiplet comprises four real scalar moduli. Classically, its moduli space is $\mathrm{SU}(2,1)/\mathrm{U}(2)$, which is quaternion-Kähler and endowed with the metric

$$\mathrm{d}\Delta^2 = \mathrm{d}\phi^2 + e^{-\phi}\left(\mathrm{d}\chi^2+\mathrm{d}\varphi^2\right) + e^{-2\phi}\left(\mathrm{d}\sigma+\chi\mathrm{d}\varphi\right)^2 , \tag{II.C.1}$$

where ϕ is a dilaton, and χ,σ,φ are 3 axionic fields. Introducing $s=e^{\phi}$, the metric becomes

$$\mathrm{d}\Delta^2 = \frac{1}{s^2}\mathrm{d}s^2 + \frac{1}{s}\left(\mathrm{d}\chi^2+\mathrm{d}\varphi^2\right) + \frac{1}{s^2}\left(\mathrm{d}\sigma+\chi\mathrm{d}\varphi\right)^2 . \tag{II.C.2}$$

The geodesic equations are

$$\ddot{s} - \frac{\dot{s}^2}{s} + \frac{\dot{\chi}^2}{2} + \frac{\dot{\sigma}^2}{s} + \frac{2\chi}{s}\dot{\sigma}\dot{\varphi} + \left(\frac{1}{2}+\frac{\chi^2}{s}\right)\dot{\varphi}^2 = 0 , \tag{II.C.3}$$

$$\ddot{\chi} - \frac{\dot{s}\dot{\chi}}{s} - \frac{\dot{\sigma}\dot{\varphi}}{s} - \frac{\chi}{s}\dot{\varphi}^2 = 0 , \tag{II.C.4}$$

$$\ddot{\sigma} - \frac{2}{s}\dot{s}\dot{\sigma} - \frac{\chi}{s}\dot{s}\dot{\varphi} - \frac{\chi}{s}\dot{\chi}\dot{\sigma} + \left(1-\frac{\chi^2}{s}\right)\dot{\chi}\dot{\varphi} = 0 , \tag{II.C.5}$$

$$\ddot{\varphi} - \frac{\dot{s}\dot{\varphi}}{s} + \frac{\dot{\chi}\dot{\sigma}}{s} + \frac{\chi}{s}\dot{\chi}\dot{\varphi} = 0 . \tag{II.C.6}$$

Different classes of geodesics arise depending on the initial conditions of the above equations. As in the case of the hyperbolic half-plane in Section II.B, we distinguish two nontrivial types: the first type is the initial conditions satisfying $\dot{s}(0)\neq 0$ and $\dot{\chi}(0)=\dot{\sigma}(0)=\dot{\varphi}(0)=0$. Then the geodesics are straight rays with $s(t\to-\infty)=0$ to $s(t\to+\infty)=+\infty$; the second type is that initially at least one of $\dot{\chi}(0),\dot{\sigma}(0),\dot{\varphi}(0)$ is non-zero. Then the geodesics are curves with end-points on $s=0$ hyperplane, $s(t\to-\infty)=s(t\to+\infty)=0$. Generically, these curves are not semicircles as in the Poincaré half-plane. Note that given two endpoints, there exists a unique geodesic connecting them. This uniqueness follows from the homogeneity and negative Ricci curvature ($R=-6$) of the universal hypermultiplet moduli space.

Meanwhile, it is worth noting that there exist three 2D subspaces within the universal hypermultiplet moduli space, each admitting simplified geodesic equations. The first subspace is for initial values $\dot{\chi}=0,\dot{\varphi}=0$, the geodesic equations

are exactly the same as (II.B.3) and (II.B.4):

$$\ddot{s} - \frac{\dot{s}^2}{s} + \frac{\dot{\sigma}^2}{s} = 0\,, \tag{II.C.7}$$

$$\ddot{\sigma} - \frac{2}{s}\dot{s}\dot{\sigma} = 0\,. \tag{II.C.8}$$

The geodesics only lie on the 2D subspace with coordinates $\{s, \sigma\}$, and this subspace is exactly a Poincaré halfplane. Another two subspaces are from initial values $\dot{\sigma} = 0, \dot{\varphi} = 0$, and $\chi = 0, \dot{\chi} = 0, \dot{\sigma} = 0$. Their geodesic equations are

$$\ddot{s} - \frac{\dot{s}^2}{s} + \frac{\dot{\chi}^2}{2} = 0\,, \tag{II.C.9}$$

$$\ddot{\chi} - \frac{\dot{s}\dot{\chi}}{s} = 0\,, \tag{II.C.10}$$

and

$$\ddot{s} - \frac{\dot{s}^2}{s} + \frac{\dot{\varphi}^2}{2} = 0\,, \tag{II.C.11}$$

$$\ddot{\varphi} - \frac{\dot{s}\dot{\varphi}}{s} = 0\,, \tag{II.C.12}$$

separately. Both of these latter cases describe the same geometry, up to relabeling. In each case, geodesics in these subspaces are either rays along the s-direction, or curves that begin and end on the $s = 0$ line.

One-loop corrected universal hypermultiplet moduli space

The perturbative correction to the moduli space of the universal hypermultiplet arises only at one-loop from R^4 terms in the effective action [87–89]. The resulting metric for the one-loop corrected moduli space takes the form

$$\mathrm{d}L^2 = \frac{f}{s^2}\mathrm{d}s^2 + \frac{1}{s}\left(1 + \frac{2\Delta}{s}\right)\left(\mathrm{d}\chi^2 + \mathrm{d}\varphi^2\right) + \frac{1}{fs^2}\left(\mathrm{d}\sigma - \chi\mathrm{d}\varphi\right)^2\,, \tag{II.C.13}$$

where $\Delta < 0$ corresponds to the 1-loop contribution, proportional to the Euler characteristic of the underlying Calabi–Yau manifold, and

$$f \equiv \frac{1 + 2\Delta/s}{1 + \Delta/s}\,. \tag{II.C.14}$$

This corrected moduli space retains a constant Ricci scalar $R = -6$. With this corrected metric, the geodesic equations for the four moduli fields are given by

$$\begin{aligned}\ddot{s} - \frac{2s^2 + 7\Delta s + 4\Delta^2}{2s(s+\Delta)(s+2\Delta)}\dot{s}^2 + (s+\Delta)\Bigg[\frac{s+4\Delta}{2s(s+2\Delta)}\dot{\chi}^2 + \frac{2s^2 + 5\Delta s + 4\Delta^2}{2s(s+2\Delta)^3}\dot{\sigma}^2 \\ - \frac{\chi\left(2s^2 + 5\Delta s + 4\Delta^2\right)}{s(s+2\Delta)^3}\dot{\sigma}\dot{\varphi} + \frac{s^3 + \left(\chi^2 + 4\Delta\right)\left(2s^2 + 5\Delta s + 4\Delta^2\right)}{2s(s+2\Delta)^3}\dot{\varphi}^2\Bigg] = 0\,,\end{aligned} \tag{II.C.15}$$

$$\ddot{\sigma} - \frac{2s^2+5\Delta s+4\Delta^2}{s(s+\Delta)(s+2\Delta)}\dot{s}\dot{\sigma} + \frac{s\chi}{(s+\Delta)(s+2\Delta)}\dot{s}\dot{\varphi} - \frac{\chi(s+\Delta)}{(s+2\Delta)^2}\dot{\chi}\dot{\sigma} + \frac{(s+\Delta)\left(\chi^2-4\Delta\right)-s^2}{(s+2\Delta)^2}\dot{\chi}\dot{\varphi} = 0\,, \tag{II.C.16}$$

$$\ddot{\chi} - \frac{s+4\Delta}{s(s+2\Delta)}\dot{s}\dot{\chi} + \frac{s+\Delta}{(s+2\Delta)^2}\dot{\sigma}\dot{\varphi} - \frac{\chi(s+\Delta)}{(s+2\Delta)^2}\dot{\varphi}^2 = 0\,, \tag{II.C.17}$$

$$\ddot{\varphi} - \frac{s+4\Delta}{s(s+2\Delta)}\dot{s}\dot{\varphi} - \frac{s+\Delta}{(s+2\Delta)^2}\dot{\chi}\dot{\sigma} + \frac{\chi(s+\Delta)}{(s+2\Delta)^2}\dot{\chi}\dot{\varphi} = 0\,. \tag{II.C.18}$$

Examining the geodesic equations above, we observe that there are two positive singularities along the s-direction, located at $s=-\Delta$ and $s=-2\Delta$. These singularities partition the moduli space into three disconnected regions: $0<s<-\Delta$, $-\Delta<s<-2\Delta$, and $s>-2\Delta$. Each geodesic is confined to a single region and cannot cross into the others, effectively imposing boundaries in the moduli space. These domains can be naturally interpreted as the strong-coupling region, the intermediate-coupling region, and the weak-coupling region, respectively. In the following, we primarily focus on classifying the geodesics in the region $0<s<-\Delta$, noting that analogous behaviors are found in the other two regions based on numerical verifications. We can classify the geodesics based on their embedding in subspaces:

- The first case is to choose the initial condition $\dot{\chi}=\dot{\sigma}=\dot{\varphi}=0$. In this case, the geodesic is only along the s-axis, which is a one-dimensional subspace. For initial $\dot{s}>0$, the trajectory reaches the singularity at $s=-\Delta$, turns around, and then asymptotically approaches $s=0$ as $t\to\pm\infty$.

- The second class corresponds to the motion inside a two-dimensional subspace of the moduli space, which means two out of $\dot{\chi}$, $\dot{\sigma}$, $\dot{\varphi}$ are initially zeros. Depending on the specific initial values, periodic geodesics can occur. An example is illustrated in Figure II.4.

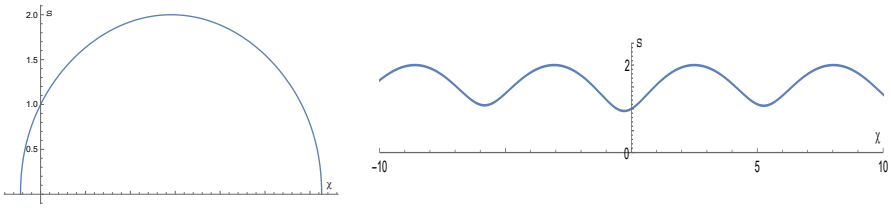

Figure II.4: Geodesics on the (s,χ)-plane with $\Delta=-2$. The left panel corresponds to initial values $s=1,\chi=0,\dot{s}=\frac{1}{3},\dot{\chi}=\frac{1}{6}$. The right figure has initial values $s=1,\chi=0,\dot{s}=\frac{1}{3},\dot{\chi}=1$, displaying nearly linear asymptotic behavior, and $\chi(t\to\infty)\to\infty$.

- The third class of geodesics is for the generic initial values, i.e. the initial values not covered in the first two classes. In this case, asymptotically $\sigma(t \to \infty) \to \infty$, and the geodesic projected onto the (χ, φ)-plane forms a circle, reflecting the exchange symmetry between χ and φ. See Figure II.5 for an explicit example.

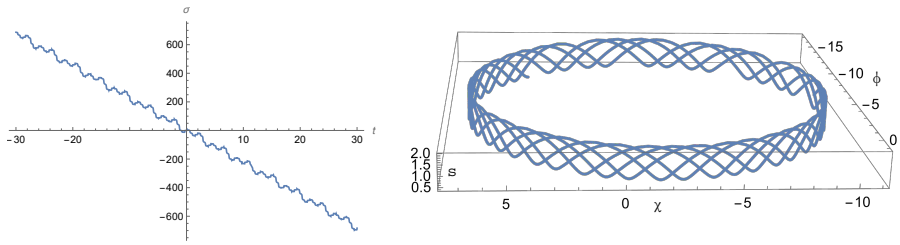

Figure II.5: Time evolution of the σ-coordinate, and the geodesic projection on the (s, χ, φ)-subspace, with randomly chosen $\Delta = -2$ and initial values $s = \frac{1}{2}, \chi = 1, \sigma = 0, \varphi = 0, \dot{s} = 2, \dot{\chi} = 3, \dot{\sigma} = 2, \dot{\varphi} = -1$.

There are also non-perturbative instanton corrections to the universal hypermultiplet moduli space [90], which is more involved and will not be discussed here.

References

[1] D. Chakraborty, R. Chiovoloni, O. Loaiza-Brito, G. Niz and I. Zavala, *Fat inflatons, large turns and the η-problem*, *JCAP* **01** (2020) 020, [1908.09797].

[2] S. Dimopoulos, S. Kachru, J. McGreevy and J. G. Wacker, *N-flation*, *JCAP* **08** (2008) 003, [hep-th/0507205].

[3] D. Wands, *Multiple field inflation*, *Lect. Notes Phys.* **738** (2008) 275–304, [astro-ph/0702187].

[4] S. Cremonini, Z. Lalak and K. Turzynski, *Strongly Coupled Perturbations in Two-Field Inflationary Models*, *JCAP* **03** (2011) 016, [1010.3021].

[5] I.-S. Yang, *The Strong Multifield Slowroll Condition and Spiral Inflation*, *Phys. Rev. D* **85** (2012) 123532, [1202.3388].

[6] A. R. Brown, *Hyperbolic Inflation*, *Phys. Rev. Lett.* **121** (2018) 251601, [1705.03023].

[7] P. Christodoulidis, D. Roest and E. I. Sfakianakis, *Angular inflation in multi-field α-attractors*, *JCAP* **11** (2019) 002, [1803.09841].

[8] M. Dias, J. Frazer, A. Retolaza, M. Scalisi and A. Westphal, *Pole N-flation*, *JHEP* **02** (2019) 120, [1805.02659].

[9] A. Achúcarro and G. A. Palma, *The string swampland constraints require multi-field inflation*, *JCAP* **02** (2019) 041, [1807.04390].

[10] V. Aragam, S. Paban and R. Rosati, *Multi-field Inflation in High-Slope Potentials*, *JCAP* **04** (2020) 022, [1905.07495].

[11] V. Aragam, S. Paban and R. Rosati, *The Multi-Field, Rapid-Turn Inflationary Solution*, *JHEP* **03** (2021) 009, [2010.15933].

[12] V. Aragam, R. Chiovoloni, S. Paban, R. Rosati and I. Zavala, *Rapid-turn inflation in supergravity is rare and tachyonic*, *JCAP* **03** (2022) 002, [2110.05516].

[13] S. Renaux-Petel, *Inflation with strongly non-geodesic motion: theoretical motivations and observational imprints*, *PoS* **EPS-HEP2021** (2022) 128, [2111.00989].

[14] S. Bhattacharya and I. Zavala, *Sharp turns in axion monodromy: primordial black holes and gravitational waves*, *JCAP* **04** (2023) 065, [2205.06065].

[15] M. Cicoli, G. Dibitetto and F. G. Pedro, *New accelerating solutions in late-time cosmology*, *Phys. Rev. D* **101** (2020) 103524, [2002.02695].

[16] M. Cicoli, G. Dibitetto and F. G. Pedro, *Out of the Swampland with Multifield Quintessence?*, *JHEP* **10** (2020) 035, [2007.11011].

[17] Y. Akrami, M. Sasaki, A. R. Solomon and V. Vardanyan, *Multi-field dark energy: Cosmic acceleration on a steep potential*, *Phys. Lett. B* **819** (2021) 136427, [2008.13660].

[18] L. Anguelova, J. Dumancic, R. Gass and L. C. R. Wijewardhana, *Dark energy from inspiraling in field space*, *JCAP* **03** (2022) 018, [2111.12136].

[19] J. R. Eskilt, Y. Akrami, A. R. Solomon and V. Vardanyan, *Cosmological dynamics of multifield dark energy*, *Phys. Rev. D* **106** (2022) 023512, [2201.08841].

[20] M. Brinkmann, M. Cicoli, G. Dibitetto and F. G. Pedro, *Stringy multifield quintessence and the Swampland*, *JHEP* **11** (2022) 044, [2206.10649].

[21] G. Shiu, F. Tonioni and H. V. Tran, *Accelerating universe at the end of time*, 2303.03418.

[22] G. Shiu, F. Tonioni and H. V. Tran, *Late-time attractors and cosmic acceleration*, 2306.07327.

[23] G. A. Palma, S. Sypsas and C. Zenteno, *Seeding primordial black holes in multifield inflation*, *Phys. Rev. Lett.* **125** (2020) 121301, [2004.06106].

[24] J. Fumagalli, S. Renaux-Petel, J. W. Ronayne and L. T. Witkowski, *Turning in the landscape: A new mechanism for generating primordial black holes*, *Phys. Lett. B* **841** (2023) 137921, [2004.08369].

[25] L. Anguelova, *On Primordial Black Holes from Rapid Turns in Two-field Models*, *JCAP* **06** (2021) 004, [2012.03705].

[26] C. Vafa, *The String landscape and the swampland*, hep-th/0509212.

[27] H. Ooguri and C. Vafa, *On the Geometry of the String Landscape and the Swampland*, *Nucl. Phys. B* **766** (2007) 21–33, [hep-th/0605264].

[28] E. Palti, *The Swampland: Introduction and Review*, *Fortsch. Phys.* **67** (2019) 1900037, [1903.06239].

[29] M. van Beest, J. Calderón-Infante, D. Mirfendereski and I. Valenzuela, *Lectures on the Swampland Program in String Compactifications*, *Phys. Rept.* **989** (2022) 1–50, [2102.01111].

[30] G. Dvali, *Black Holes and Large N Species Solution to the Hierarchy Problem*, *Fortsch. Phys.* **58** (2010) 528–536, [0706.2050].

[31] G. Dvali and M. Redi, *Black Hole Bound on the Number of Species and Quantum Gravity at LHC*, *Phys. Rev. D* **77** (2008) 045027, [0710.4344].

[32] G. Dvali and D. Lüst, *Evaporation of Microscopic Black Holes in String Theory and the Bound on Species*, *Fortsch. Phys.* **58** (2010) 505–527, [0912.3167].

[33] G. Dvali and C. Gomez, *Species and Strings*, 1004.3744.

[34] G. Dvali, C. Gomez and D. Lüst, *Black Hole Quantum Mechanics in the Presence of Species*, *Fortsch. Phys.* **61** (2013) 768–778, [1206.2365].

[35] D. Lüst, E. Palti and C. Vafa, *AdS and the Swampland*, *Phys. Lett. B* **797** (2019) 134867, [1906.05225].

[36] N. Cribiori, D. Lüst and M. Scalisi, *The gravitino and the swampland*, *JHEP* **06** (2021) 071, [2104.08288].

[37] A. Castellano, A. Font, A. Herraez and L. E. Ibáñez, *A gravitino distance conjecture*, *JHEP* **08** (2021) 092, [2104.10181].

[38] L. A. Anchordoqui, I. Antoniadis, N. Cribiori, D. Lüst and M. Scalisi, *The Scale of Supersymmetry Breaking and the Dark Dimension*, *JHEP* **05** (2023) 060, [2301.07719].

[39] Q. Bonnefoy, L. Ciambelli, D. Lüst and S. Lüst, *Infinite Black Hole Entropies at Infinite Distances and Tower of States*, *Nucl. Phys. B* **958** (2020) 115112, [1912.07453].

[40] N. Cribiori, M. Dierigl, A. Gnecchi, D. Lüst and M. Scalisi, *Large and small non-extremal black holes, thermodynamic dualities, and the Swampland*, *JHEP* **10** (2022) 093, [2202.04657].

[41] M. Delgado, M. Montero and C. Vafa, *Black holes as probes of moduli space geometry*, *JHEP* **04** (2023) 045, [2212.08676].

[42] N. Cribiori, D. Lüst and C. Montella, *Species Entropy and Thermodynamics*, 2305.10489.

[43] F. Baume and E. Palti, *Backreacted Axion Field Ranges in String Theory*, *JHEP* **08** (2016) 043, [1602.06517].

[44] D. Klaewer and E. Palti, *Super-Planckian Spatial Field Variations and Quantum Gravity*, *JHEP* **01** (2017) 088, [1610.00010].

[45] T. Rudelius, *Revisiting the Refined Distance Conjecture*, 2303.12103.

[46] M. Scalisi and I. Valenzuela, *Swampland distance conjecture, inflation and α-attractors*, *JHEP* **08** (2019) 160, [1812.07558].

[47] M. Scalisi, *Inflation, Higher Spins and the Swampland*, *Phys. Lett. B* **808** (2020) 135683, [1912.04283].

[48] R. Bravo, G. A. Palma and S. Riquelme, *A Tip for Landscape Riders: Multi-Field Inflation Can Fulfill the Swampland Distance Conjecture*, *JCAP* **02** (2020) 004, [1906.05772].

[49] M. Etheredge, B. Heidenreich, S. Kaya, Y. Qiu and T. Rudelius, *Sharpening the Distance Conjecture in diverse dimensions*, *JHEP* **12** (2022) 114, [2206.04063].

[50] D. van de Heisteeg, C. Vafa, M. Wiesner and D. H. Wu, *Bounds on Field Range for Slowly Varying Positive Potentials*, 2305.07701.

[51] D. Roest, M. Scalisi and I. Zavala, *Kähler potentials for Planck inflation*, *JCAP* **11** (2013) 007, [1307.4343].

[52] R. Kallosh, A. Linde and D. Roest, *Superconformal Inflationary α-Attractors*, *JHEP* **11** (2013) 198, [1311.0472].

[53] C. P. Burgess, M. Cicoli, F. Quevedo and M. Williams, *Inflating with Large Effective Fields*, *JCAP* **11** (2014) 045, [1404.6236].

[54] C. Burgess and D. Roest, *Inflation by Alignment*, *JCAP* **06** (2015) 012, [1412.1614].

[55] D. Roest and M. Scalisi, *Cosmological attractors from α-scale supergravity*, *Phys. Rev. D* **92** (2015) 043525, [1503.07909].

[56] C. P. Burgess, M. Cicoli, D. Ciupke, S. Krippendorf and F. Quevedo, *UV Shadows in EFTs: Accidental Symmetries, Robustness and No-Scale Supergravity*, *Fortsch. Phys.* **68** (2020) 2000076, [2006.06694].

[57] H. Ooguri, E. Palti, G. Shiu and C. Vafa, *Distance and de Sitter Conjectures on the Swampland*, *Phys. Lett. B* **788** (2019) 180–184, [1810.05506].

[58] A. Hebecker and T. Wrase, *The Asymptotic dS Swampland Conjecture - a Simplified Derivation and a Potential Loophole*, *Fortsch. Phys.* **67** (2019) 1800097, [1810.08182].

[59] T. Rudelius, *Asymptotic observables and the swampland*, *Phys. Rev. D* **104** (2021) 126023, [2106.09026].

[60] T. Rudelius, *Asymptotic scalar field cosmology in string theory*, *JHEP* **10** (2022) 018, [2208.08989].

[61] J. Calderón-Infante, I. Ruiz and I. Valenzuela, *Asymptotic Accelerated Expansion in String Theory and the Swampland*, 2209.11821.

[62] P. Marconnet and D. Tsimpis, *Universal accelerating cosmologies from 10d supergravity*, *JHEP* **01** (2023) 033, [2210.10813].

[63] F. Apers, J. P. Conlon, M. Mosny and F. Revello, *Kination, Meet Kasner: On The Asymptotic Cosmology of String Compactifications*, 2212.10293.

[64] S. Cremonini, E. Gonzalo, M. Rajaguru, Y. Tang and T. Wrase, *On Asymptotic Dark Energy in String Theory*, 2306.15714.

[65] D. Andriot, N. Cribiori and D. Erkinger, *The web of swampland conjectures and the TCC bound*, *JHEP* **07** (2020) 162, [2004.00030].

[66] N. Gendler and I. Valenzuela, *Merging the weak gravity and distance conjectures using BPS extremal black holes*, *JHEP* **01** (2021) 176, [2004.10768].

[67] S. Lanza, F. Marchesano, L. Martucci and I. Valenzuela, *The EFT stringy viewpoint on large distances*, *JHEP* **09** (2021) 197, [2104.05726].

[68] T. W. Grimm, E. Palti and I. Valenzuela, *Infinite Distances in Field Space and Massless Towers of States*, *JHEP* **08** (2018) 143, [1802.08264].

[69] R. Blumenhagen, A. Font, M. Fuchs, D. Herschmann and E. Plauschinn, *Towards Axionic Starobinsky-like Inflation in String Theory*, *Phys. Lett. B* **746** (2015) 217–222, [1503.01607].

[70] I. Valenzuela, *Backreaction Issues in Axion Monodromy and Minkowski 4-forms*, *JHEP* **06** (2017) 098, [1611.00394].

[71] R. Blumenhagen, *Large Field Inflation/Quintessence and the Refined Swampland Distance Conjecture*, *PoS* **CORFU2017** (2018) 175, [1804.10504].

[72] T. W. Grimm and C. Li, *Universal axion backreaction in flux compactifications*, *JHEP* **06** (2021) 067, [2012.08272].

[73] J. Calderón-Infante, A. M. Uranga and I. Valenzuela, *The Convex Hull Swampland Distance Conjecture and Bounds on Non-geodesics*, *JHEP* **03** (2021) 299, [2012.00034].

[74] T. Bjorkmo and M. C. D. Marsh, *Hyperinflation generalised: from its attractor mechanism to its tension with the 'swampland conditions'*, *JHEP* **04** (2019) 172, [1901.08603].

[75] M. Scalisi, *Cosmological α-attractors and de Sitter landscape*, *JHEP* **12** (2015) 134, [1506.01368].

[76] G. Obied, H. Ooguri, L. Spodyneiko and C. Vafa, *De Sitter Space and the Swampland*, 1806.08362.

[77] G. Tasinato, *A large $|\eta|$ approach to single field inflation*, 2305.11568.

[78] S.-J. Lee, W. Lerche and T. Weigand, *Emergent strings from infinite distance limits*, *JHEP* **02** (2022) 190, [1910.01135].

[79] D. van de Heisteeg, C. Vafa and M. Wiesner, *Bounds on Species Scale and the Distance Conjecture*, 2303.13580.

[80] M. Cicoli, F. Cunillera, A. Padilla and F. G. Pedro, *Quintessence and the Swampland: The Parametrically Controlled Regime of Moduli Space*, *Fortsch. Phys.* **70** (2022) 2200009, [2112.10779].

[81] A. Hetz and G. A. Palma, *Sound Speed of Primordial Fluctuations in Supergravity Inflation*, *Phys. Rev. Lett.* **117** (2016) 101301, [1601.05457].

[82] M. M. Anber and L. Sorbo, *Naturally inflating on steep potentials through electromagnetic dissipation*, *Phys. Rev. D* **81** (2010) 043534, [0908.4089].

[83] G. Dall'Agata, S. González-Martín, A. Papageorgiou and M. Peloso, *Warm dark energy*, *JCAP* **08** (2020) 032, [1912.09950].

[84] G. Buratti, J. Calderón and A. M. Uranga, *Transplanckian axion monodromy!?*, *JHEP* **05** (2019) 176, [1812.05016].

[85] Z. K. Baykara, Y. Hamada, H.-C. Tarazi and C. Vafa, *On the string landscape without hypermultiplets*, *JHEP* **04** (2024) 121, [2309.15152].

[86] G. Gkountoumis, C. Hull and S. Vandoren, *Exact moduli spaces for $\mathcal{N} = 2$, $D = 5$ freely acting orbifolds*, *JHEP* **07** (2024) 126, [2403.05650].

[87] L. Anguelova, M. Rocek and S. Vandoren, *Quantum corrections to the universal hypermultiplet and superspace*, *Phys. Rev. D* **70** (2004) 066001, [hep-th/0402132].

[88] A. Strominger, *Loop corrections to the universal hypermultiplet*, *Phys. Lett. B* **421** (1998) 139–148, [hep-th/9706195].

[89] I. Antoniadis, R. Minasian, S. Theisen and P. Vanhove, *String loop corrections to the universal hypermultiplet*, *Class. Quant. Grav.* **20** (2003) 5079–5102, [hep-th/0307268].

[90] M. Davidse, M. de Vroome, U. Theis and S. Vandoren, *Instanton solutions for the universal hypermultiplet*, *Fortsch. Phys.* **52** (2004) 696–701, [hep-th/0309220].

Chapter III

Towards a String Realization of the Dark Dimension via T-folds

This chapter is based on the work arXiv:2411.19216, JHEP 08 (2025) 106, *collaborating with Stefan Vandoren.*

III.1 Introduction

There is a longstanding history of connecting string theory with cosmology, particularly in constructing an effective theory that accounts for the small and positive dark energy observed in our Universe. As we demonstrated in Subsection I.4.2, there are two main approaches, both of which are challenging: one involves realizing a metastable de Sitter vacuum, and the other involves constructing a cosmological model with dynamical dark energy. In the latter case, the dark energy is characterized by a decreasing scalar potential. Recent observations by DESI [1, 2] suggest that the dark energy in our Universe might be time-dependent, lending support to the second approach, though previous astronomical observations prefer a cosmological constant.

Meanwhile, the effective theories consistent with quantum gravity satisfy some universal criteria. These criteria are called Swampland conjectures, and distinguish the effective cosmological models and particle physics in the Landscape or the Swampland. By relating Swampland conjectures to certain observational data of our Universe, a particular corner of the string Landscape, known as the Dark Dimension Scenario [3], emerges. This scenario connects the neutrino mass scale and the dark energy scale, with the smallness of both corresponding to an asymptotic region of the field space. The Dark Dimension Scenario requires the existence of exactly one mesoscopic extra dimension, referred to as the Dark Dimension, and the scalar potential behaves as $V \propto m_{\rm KK}^4$, where $m_{\rm KK}$ is the Kaluza–Klein mass scale of this Dark Dimension. We will provide a concise introduction to the Dark Dimension in Section III.2. The scenario also predicts the sterile neutrino scale and the strong gravity scale, which are beyond the scope of this chapter and will not be discussed. There have been attempts to find specific models satisfying the Dark Dimension Scenario, such as in [4–9]. For instance, [4] tries to realize this scenario near a warped throat, but it is challenging to obtain the mass of the Kaluza–Klein tower along the Dark Dimension. In [7], the Dark Dimension potential behavior is realized using an STU model under Scherk–Schwarz reduction from $\mathcal{N} = 1$ supergravity. And [9] determines the Dark Dimension potential from the Casimir energy of the worldsheet torus partition function in infinite-distance limits.

In addition, in Subsection I.3.5 we briefly introduced non-geometric compactifications, which form a significant subset of string compactifications and have been studied for over two decades. In non-geometric compactifications, the internal space is a fiber bundle whose transition functions combine diffeomorphisms with duality transformations. A key example is the T-fold, which we will discuss in this work, where the duality involved is T-duality. The effective field theory of these compactifications is obtained via the Scherk–Schwarz mechanism, and T-duality introduces twists in the periodicity conditions of fields. Depending on the twist from the duality group, the internal space is altered, corresponding to the generation of fluxes over the non-geometric space. These fluxes can be understood as arising from T-duality transformations of the H-fluxes.

Previous investigations into non-geometric string realizations of de Sitter vacua

have shown that such string theories are inconsistent with several no-go theorems established [10, 11]. In this work, we focus instead on non-geometric string compactifications with dynamical dark energy and attempt to realize the Dark Dimension Scenario.

The chapter is organized as follows. In Section III.2, we provide an introduction to the Dark Dimension Scenario, focusing particularly on the behavior of dynamical dark energy. In Section III.3, we introduce the Scherk–Schwarz reduction and derive its potential. We consider nine-dimensional type IIB supergravity as an example of Scherk–Schwarz stringy uplift, which has the $\mathrm{SL}(2,\mathbb{Z})$ S-duality group as the twist group. In Section III.4, we present a toy model as a precursor to the string realization of the Dark Dimension. This model involves the pure gravity theory of a type II T-fold string compactification from 10D to 7D, with T^2 T-duality $\mathrm{O}(2,2;\mathbb{Z})$ as the twist group. In Section III.5, we realize the scalar potential behavior required by the Dark Dimension Scenario in four dimensions, via $T^5 \times S^1$ T-fold compactification with T^5 T-duality as the twist group.

Throughout this chapter, we set the four-dimensional Planck mass $M_{\rm Pl} = 1$.

III.2 Dark Dimension Scenario

In this section, we provide a brief overview of the Dark Dimension Scenario proposed in [3]. This scenario offers a compelling framework that connects string phenomenology with observable cosmological parameters.

The theoretical foundation of the scenario is built upon two key Swampland criteria. The first criterion is the (A)dS Distance Conjecture (cf. Subsection I.5.2 and [12]). This conjecture posits that, when approaching the infinity of the field space, the distance over the field space scales proportionally to $\log\left(1/|\Lambda|\right)$, where Λ is the cosmological "constant". Meanwhile, according to the Swampland Distance Conjecture in Subsection I.5.1, in the context of string compactifications, there exists a tower of states with the smallest mass scale near the infinity of the field space, and he mass scale of the tower decreases exponentially with the geodesic distance [13]. Consequently, when $\Lambda \to 0$, the mass scale m of the tower of states adheres to the following relation

$$m = \lambda^{-1}|\Lambda|^{\alpha}, \quad \alpha \sim \mathcal{O}(1)\,. \tag{III.2.1}$$

For $\Lambda > 0$, the Higuchi bound [14] imposes an upper limit on the exponent α, specifically $\alpha \leq \frac{1}{2}$. This bound ensures that the classical contribution to the potential does not exceed $V \sim m^2$. Additionally, there exists a lower bound on α, given by $\alpha \geq \frac{1}{d}$, where d denotes the number of external dimensions. This lower bound arises from the 1-loop Casimir energy contribution to the potential, $V_{\rm Casimir} \sim m^d$, in scenarios where there are more massless fermions than massless bosons. When α attains its lower bound, the parameter λ in equation (III.2.1) is expected to satisfy the relation $m^{1/2} \lesssim \lambda^4 \lesssim 1$. This implies that the cosmological constant Λ must lie within the range $m^{9/2} \lesssim \Lambda \lesssim m^4$ in four dimensions. Furthermore, if the potential is predominantly influenced by the Casimir corrections

asymptotically, the parameter λ should approach its upper bound. The values of the parameters α and λ are crucial for aligning the theoretical predictions with realistic observational data.

The second essential Swampland conjecture is the Emergent String Conjecture (ESC) [15] we mentioned in Subsection I.5.1, and we repeat it here. Based on the SDC, the ESC further states that, approaching the asymptotic limits of the field space, there are only two possible types of towers of states that can emerge. These towers must consist of either:

- A tower of string excited states, or
- a Kaluza–Klein tower associated with decompactification.

To determine which of these cases corresponds to the mass scale described in equation (III.2.1), it is necessary to consider observational and experimental data from our universe. In the first case, the mass scale corresponds to the string scale, at which the local EFT ceases to be valid; in the second case, the presence of decompactifying extra dimensions influences gravity propagation. Experimental constraints from torsion balance experiments, which measure deviations in Newton's gravitational force, are particularly relevant for detecting the smallest possible mass scales. The most recent findings [16] impose that

$$m^{-1} \lesssim 30\ \mu\text{m}, \quad \text{i.e.} \quad m \gtrsim 6.6\ \text{meV}\,. \tag{III.2.2}$$

Interestingly, this mass scale coincides with the neutrino scale. In addition, the observed value of the cosmological constant is $\Lambda \sim 10^{-122}$, which is too small and implies $\Lambda^{1/4} = 2.31\ \text{meV} \lesssim m$. Therefore, within the framework of (III.2.1), we anticipate the parameters to satisfy:

$$\alpha = \frac{1}{4}, \quad \text{and} \quad \lambda \sim 10^{-1}\,. \tag{III.2.3}$$

If this minimal tower with mass scale (III.2.2) corresponds to the first case of the ESC, there would be no valid EFT beyond m, contradicting our current understanding of the universe. Hence, it is more plausible that the mass scale m in (III.2.1) represents a Kaluza–Klein decompactification scale, with neutrinos acting as Kaluza–Klein spinors.

Further constraints on the Kaluza–Klein scale arise from observations of KK gravitons in the neutron star surrounding cloud [17, 18]. Specifically, if there is only one relatively large extra dimension and the other extra dimensions are negligible, the upper bound on the KK scale is $m_{\text{KK}}^{-1} < 44\ \mu$m; if there are two relatively large extra dimensions, the upper bound becomes $m_{\text{KK}}^{-1} < 1.6\times10^{-4}\ \mu$m; the bound becomes even smaller for more large extra dimensions. Only the first scenario, involving a single large extra dimension, is consistent with the constraint in equation (III.2.2). This single large extra dimension is referred to as the Dark Dimension in [3]. In this context, the scalar potential is given by:

$$V = \Lambda \propto m_{\text{KK}}^4\,, \tag{III.2.4}$$

where m_{KK} denotes the Kaluza–Klein scale associated with the Dark Dimension. The seminal paper [3] emphasizes the potential with $V \sim m^4$ interpreted as a 1-loop Casimir correction. The computation of the Casimir correction requires a worldsheet torus partition function, which is only known for some familiar models. In our work, we explore a model in which the Scherk–Schwarz potential exhibits the necessary behavior to align with the Dark Dimension Scenario.

III.3 Scherk–Schwarz reduction

We begin by considering a Scherk–Schwarz reduction [19, 20] from $d+1$ to d dimensions, with coordinates $x^{\hat{\mu}} = \{x^\mu, y\}$, $\mu = 0, 1, \cdots, d-1$. The d-th dimension compactifies to a circle, with periodicity condition $y \sim y + 2\pi R$. The radius of the circle ϱ is modulated by the radion field ϕ, such that

$$\varrho = Re^{\beta\phi}\,, \tag{III.3.1}$$

where β is a real constant to be determined later.

Assuming the theory inherits a global symmetry G from higher dimensions, a field $\hat{\psi}$ in the fundamental representation transforms under the Scherk–Schwarz reduction can be ansated as

$$\hat{\psi}\left(x^\mu,\, y\right) = \exp\left(\frac{My}{2\pi R}\right)\psi\left(x^\mu\right), \quad M \in \mathfrak{g}\,. \tag{III.3.2}$$

In many cases, the scalar fields parametrize a coset space G/H with H the maximal compact subgroup of G, and can be arranged into a matrix field $\hat{\mathcal{H}}$, which transforms as the adjoint representation of G and expands as

$$\hat{\mathcal{H}}\left(x^\mu,\, y\right) = \exp\left(\frac{My}{2\pi R}\right)\mathcal{H}\left(x^\mu\right)\exp\left(\frac{M^T y}{2\pi R}\right). \tag{III.3.3}$$

The $d+1$-dimensional bosonic action involving a G-matrix scalar field in the Einstein frame is

$$S = \int \mathrm{d}^{d+1}x\sqrt{-\hat{g}_{(d+1)}}\,\frac{1}{2\kappa^2_{(d+1)}}\left[R_{(d+1)} + \mathrm{Tr}\left(\hat{g}^{\hat{\mu}\hat{\nu}}\partial_{\hat{\mu}}\hat{\mathcal{H}}^{-1}\partial_{\hat{\nu}}\hat{\mathcal{H}}\right)\right]. \tag{III.3.4}$$

Upon reduction to d dimensions, the metric $\hat{g}_{\hat{\mu}\hat{\nu}}$ in $d+1$ dimensions transforms as:

$$\hat{g}_{\hat{\mu}\hat{\nu}} = \begin{pmatrix} e^{2\alpha\phi}g_{\mu\nu} & \\ & e^{2\beta\phi} \end{pmatrix}, \tag{III.3.5}$$

where $g_{\mu\nu}$ is the d-dimensional metric, and $\phi(x^\mu)$ denotes the radion field. We only focus on the scalar potential and ignore graviphoton contributions for this analysis. To decouple the radion and the curvature, and normalize the kinetic term of the radion, it is derived that

$$\alpha = -\sqrt{\frac{1}{2(d-1)(d-2)}}\,, \quad \beta = -(d-2)\alpha\,. \tag{III.3.6}$$

Especially for $d = 4$, the coefficients simplify to

$$\alpha = -\frac{1}{2\sqrt{3}}\,, \quad \beta = \frac{1}{\sqrt{3}}\,. \tag{III.3.7}$$

Following the reduction to d dimensions, the relevant dimensional equations and transformations are

$$\int \mathrm{d}^{d+1}x = 2\pi R \int \mathrm{d}^d x\,, \tag{III.3.8}$$

$$\sqrt{-g_{(d+1)}} = \sqrt{-g_{(d)}} e^{(d\alpha+\beta)\phi} = \sqrt{-g_{(d)}} e^{2\alpha\phi}\,, \tag{III.3.9}$$

$$\frac{1}{2\kappa^2_{(d+1)}} = \frac{1}{2\kappa^2_{(d)} 2\pi R}\,, \tag{III.3.10}$$

$$R_{(d+1)} = e^{-2\alpha\phi} R_{(d)} - \frac{1}{2} e^{-2\alpha\phi} g^{\mu\nu}\partial_\mu\phi\partial_\nu\phi + \text{bdr.}\,, \tag{III.3.11}$$

$$\begin{aligned}\mathrm{Tr}\left(\hat{g}^{\hat{\mu}\hat{\nu}}\partial_{\hat{\mu}}\hat{\mathcal{H}}^{-1}\partial_{\hat{\nu}}\hat{\mathcal{H}}\right) &= e^{-2\alpha\phi}\,\mathrm{Tr}\left(g^{\mu\nu}\partial_\mu\mathcal{H}^{-1}\partial_\nu\mathcal{H}\right) \\ &\quad -2e^{-2\beta\phi}\,\mathrm{Tr}\left(\frac{M^2}{(2\pi R)^2} + \frac{M^T}{2\pi R}\mathcal{H}^{-1}\frac{M}{2\pi R}\mathcal{H}\right).\end{aligned} \tag{III.3.12}$$

Thus, the d-dimensional action within the Einstein frame is formulated as

$$S = \int \mathrm{d}^d x \sqrt{-g_{(d)}} \frac{1}{2\kappa^2_{(d)}} \left[R_{(d)} - \frac{1}{2} g^{\mu\nu}\partial_\mu\phi\partial_\nu\phi + \mathrm{Tr}\left(g^{\mu\nu}\partial_\mu\mathcal{H}^{-1}\partial_\nu\mathcal{H}\right) - V\right], \tag{III.3.13}$$

where the potential V is

$$V = 2e^{2(\alpha-\beta)\phi}\,\mathrm{Tr}\left(\frac{M^2}{(2\pi R)^2} + \frac{M^T}{2\pi R}\mathcal{H}^{-1}\frac{M}{2\pi R}\mathcal{H}\right). \tag{III.3.14}$$

Note that $\mathcal{H} \in G/H$ and for M a real matrix, this potential is non-negative definite. The potential becomes zero specifically when M conjugates to a rotation generator, i.e. there is a constant matrix $S \in G$, such that $\widetilde{M} = SMS^{-1}$ and $\widetilde{M} = -\widetilde{M}^T$. In this case, there can be a Minkowski vacuum. For example, the elliptic conjugacy classes of $G = \mathrm{SL}(2,\mathbb{R})$ give a classical Minkowski vacuum at $\tau = i$ (see e.g. [21]), which will be further discussed in the next subsection.

In string theory, duality groups provide a natural candidate for the non-Abelian global symmetries utilized in Scherk–Schwarz reductions. When the global symmetry group G is a duality group, the corresponding group element $\mathcal{M} = e^M \in G$ is known as a duality twist, and fields like those in (III.3.2) and (III.3.3) acquire twisted boundary conditions characterized by a monodromy matrix $M \in \mathfrak{g}$. Such a twist effectively deforms the geometry of the internal space, an effect that is equivalent to introducing background fluxes. In Section III.4, we demonstrate this principle by deducing the NS-NS fluxes from T-duality twists and subsequently parametrizing the potential (III.3.14) in terms of the resulting flux numbers.

We aim to align this potential with the required potential proportional to the Kaluza–Klein scale in the Dark Dimension Scenario. The Kaluza–Klein scale in string frame is known as

$$m_{\mathrm{KK}}^{(\mathrm{S})} = \frac{1}{\varrho} = \frac{1}{R} e^{-\beta\phi} \,. \tag{III.3.15}$$

To convert to the Einstein frame, the square of the mass scale should be multiplied by the metric factor $e^{2\alpha\phi}$, such that

$$m_{\mathrm{KK}}^2 = \frac{1}{R^2} e^{2(\alpha-\beta)\phi} \,. \tag{III.3.16}$$

Notably, m_{KK}^2 is proportional to the part outside the trace parentheses of (III.3.14). However, as highlighted previously, the Dark Dimension Scenario necessitates that $V \propto m_{\mathrm{KK}}^4$. This suggests that the contributions inside the trace parentheses to the potential should influence the radion's exponent at least equally as the outside. In the next sections, we will demonstrate how it is naturally realized in our model, via a specific parabolic duality twist of T-fold constructions. Without loss of generality, from now on we take $2\pi R = 1$ for convenience.

III.3.1 Potential with $\mathrm{SL}(2,\mathbb{R})$ and $\mathrm{SL}(2,\mathbb{Z})$ monodromy

The stringy uplift of the Scherk–Schwarz mechanism typically incorporates a duality twist within a duality group $G(\mathbb{Z})$. A straightforward example of this is provided by compactifying type IIB supergravity on a circle to yield a nine-dimensional theory, with S-duality group $\mathrm{SL}(2,\mathbb{Z})$ acting as the twist group. This group operates on the axio-dilaton field $\tau = \tau_1 + i\tau_2$, which in the adjoint representation is expressed as

$$\mathcal{H}(\tau) = \frac{1}{\tau_2} \begin{pmatrix} |\tau|^2 & \tau_1 \\ \tau_1 & 1 \end{pmatrix} . \tag{III.3.17}$$

The Scherk–Schwarz potential (III.3.14) is intrinsically characterized by the conjugacy classes of the twist group. To start with, we first examine the conjugacy classes of the classical S-duality group $G = \mathrm{SL}(2,\mathbb{R})$ which corresponds to the truncated theory with only massless states. This group comprises three kinds of conjugacy classes, which are called: parabolic, if $|\operatorname{Tr}\mathcal{M}| = 2$; elliptic, if $|\operatorname{Tr}\mathcal{M}| < 2$; and hyperbolic, if $|\operatorname{Tr}\mathcal{M}| > 2$. Corresponding to these classes, the monodromy matrices can be represented as [21, 22]

$$\mathcal{M}_p = \begin{pmatrix} 1 & m \\ 0 & 1 \end{pmatrix}, \quad \mathcal{M}_e = \begin{pmatrix} \cos m & \sin m \\ -\sin m & \cos m \end{pmatrix}, \quad \mathcal{M}_h = \begin{pmatrix} e^m & 0 \\ 0 & e^{-m} \end{pmatrix}, \tag{III.3.18}$$

where m is called the mass parameter. These matrices correspond to shift, rotation, and boost transformations for the parabolic, elliptic, and hyperbolic conjugacy classes, respectively. The generators M associated with these transformations are given by:

$$M_p = \begin{pmatrix} 0 & m \\ 0 & 0 \end{pmatrix}, \quad M_e = \begin{pmatrix} 0 & m \\ -m & 0 \end{pmatrix}, \quad M_h = \begin{pmatrix} m & 0 \\ 0 & -m \end{pmatrix}. \tag{III.3.19}$$

Utilizing equation (III.3.17) and the generator matrices in (III.3.19), we can compute the Scherk–Schwarz potential (III.3.14) corresponding to monodromies in different conjugacy classes as follows:

- Parabolic monodromy: The potential becomes

$$V_p = 2m^2 e^{-a\phi} \frac{1}{\tau_2^2}\,, \quad a \equiv 2(\beta - \alpha)\,. \tag{III.3.20}$$

  This form of the potential indicates that τ_1 remains a flat direction, while both ϕ and τ_2 tend to run away towards $+\infty$.

- Elliptic monodromy: For the elliptic monodromy $\mathcal{M}_e$ of $\mathrm{SL}(2,\mathbb{R})$, the potential is given by

$$V_e = 2m^2 e^{-a\phi} \left(\frac{|\tau|^4 + 2\tau_1^2 + 1}{\tau_2^2} - 2 \right). \tag{III.3.21}$$

  This potential is non-negative and possesses a minimum at $\tau = i$, corresponding to a Minkowski vacuum.

- Hyperbolic monodromy: The potential is

$$V_h = 8m^2 e^{-a\phi} \left(\frac{\tau_1^2}{\tau_2^2} + 1 \right). \tag{III.3.22}$$

  In this case, τ_1 is stabilized at $\tau_1 = 0$ and τ_2 is a flat direction, such that at $\tau_1 = 0$, the potential simplifies to

$$V_{h,\,\mathrm{stab.}} = 8m^2 e^{-a\phi}\,. \tag{III.3.23}$$

The rationale for introducing potentials with monodromies corresponding to the conjugacy classes of $\mathrm{SL}(2,\mathbb{R})$ lies in the fact that $\mathrm{SL}(2,\mathbb{Z})$ monodromies are conjugate to these classes. When incorporating massive states into the theory, the monodromy matrices $\mathcal{M}$ must belong to $\mathrm{SL}(2,\mathbb{Z})$. In this context, the parabolic conjugacy classes retain the same form as in $\mathrm{SL}(2,\mathbb{R})$, with the mass parameter $m \in \mathbb{Z}$; the elliptic and hyperbolic classes correspond to integer conjugations of $\mathcal{M}_e$ and $\mathcal{M}_h$ respectively. Notably, there exist four rotational $\mathrm{SL}(2,\mathbb{Z})$ conjugacy classes with representatives [21, 23]

$$\begin{aligned} \mathcal{M}_2 &= \begin{pmatrix} -1 & 0 \\ 0 & -1 \end{pmatrix}, & \mathcal{M}_3 &= \begin{pmatrix} 0 & 1 \\ -1 & -1 \end{pmatrix}, \\ \mathcal{M}_4 &= \begin{pmatrix} 0 & 1 \\ -1 & 0 \end{pmatrix}, & \mathcal{M}_6 &= \begin{pmatrix} 1 & 1 \\ -1 & 0 \end{pmatrix}, \end{aligned} \tag{III.3.24}$$

with corresponding generators

$$\begin{aligned} M_2 &= \pi \begin{pmatrix} 0 & 1 \\ -1 & 0 \end{pmatrix}, & M_3 &= \frac{2\pi}{3\sqrt{3}} \begin{pmatrix} 1 & 2 \\ -2 & 1 \end{pmatrix}, \\ M_4 &= \frac{\pi}{2} \begin{pmatrix} 0 & 1 \\ -1 & 0 \end{pmatrix}, & M_6 &= \frac{\pi}{3\sqrt{3}} \begin{pmatrix} 1 & 2 \\ -2 & 1 \end{pmatrix}. \end{aligned} \tag{III.3.25}$$

These matrices correspond to the $\mathbb{Z}_2$, $\mathbb{Z}_3$, $\mathbb{Z}_4$, $\mathbb{Z}_6$ subgroups of $\mathrm{SL}(2,\mathbb{Z})$ respectively. $\mathcal{M}_3$, $\mathcal{M}_4$, $\mathcal{M}_6$ are elliptic, while $\mathcal{M}_2$ represents the $m \to \pi$ limit of $\mathcal{M}_e$ in $\mathrm{SL}(2,\mathbb{R})$. Furthermore, $\mathcal{M}_3$ and $\mathcal{M}_6$ are $\mathrm{SL}(2,\mathbb{R})$-conjugate to $\mathbb{Z}_3$ and $\mathbb{Z}_6$ elements of $\mathcal{M}_e$. For example,

$$\mathcal{M}_6 = \begin{pmatrix} \sqrt{\frac{2}{\sqrt{3}}} & 0 \\ -\sqrt{\frac{1}{2\sqrt{3}}} & \sqrt{\frac{\sqrt{3}}{2}} \end{pmatrix} \mathcal{M}_e\left(\frac{\pi}{3}\right) \begin{pmatrix} \sqrt{\frac{2}{\sqrt{3}}} & 0 \\ -\sqrt{\frac{1}{2\sqrt{3}}} & \sqrt{\frac{\sqrt{3}}{2}} \end{pmatrix}^{-1} . \tag{III.3.26}$$

Incorporating these conjugacy class representatives into the potential expression (III.3.14) allows us to derive the corresponding potentials. It is straightforward to verify that, for $\mathcal{M}_2$, $\mathcal{M}_4$ the potential exhibits the same minimum as in equation (III.3.21). For $\mathcal{M}_3$ and $\mathcal{M}_6$, the potentials are equivalent to (III.3.21) up to conjugations, with shifted locations for the minima. It can be calculated that the Minkowski minimum is at $\tau = \exp\frac{2\pi i}{3}$.

The hyperbolic conjugacy classes of $\mathrm{SL}(2,\mathbb{Z})$ are a bit complicated. In the following section, we will explore hyperbolic conjugacy classes in greater detail in terms of T-fold fluxes. Nevertheless, as indicated in equation (III.3.23), hyperbolic conjugacy classes contribute trivially to the potential, thereby precluding the derivation of the Dark Dimension ratio from these classes.

III.4 $T^2 \times S^1$ T-fold as a toy model

This section discusses the feasibility of realizing the Dark Dimension Scenario through potentials derived from T-fold compactifications, where the twist group is the T-duality group. To facilitate comprehension of our construction, we begin by presenting a toy model. We consider the compactification of 10-dimensional type II superstring theory down to 8 dimensions via a T^2 reduction, focusing exclusively on the pure gravity spectrum. Subsequently, we perform a Scherk–Schwarz reduction over an additional S^1, utilizing a twist matrix $\mathcal{M} = e^M$ that belongs to the T-duality group associated with T^2.

Denote the coordinates of T^2 as $\{z_1, z_2\}$, and the S^1-coordinate as y. The compactification over T^2 introduces one complexified Kähler modulus ρ and one complex structure modulus τ, defined as[1]

$$\tau = \tau_1 + i\tau_2 = \frac{g_{12}}{g_{22}} + i\frac{\sqrt{\det g}}{g_{22}}\,, \quad \rho = \rho_1 + i\rho_2 = \frac{1}{\alpha'}\left(b_{12} + i\sqrt{\det g}\right), \tag{III.4.1}$$

which parameterize the moduli space

$$\mathrm{O}(2,2;\mathbb{Z})\backslash\mathrm{O}(2,2;\mathbb{R})/(U(1)\times U(1))\,. \tag{III.4.2}$$

[1] In Chapter I and Chapter IV, we define the Kähler modulus as T and the complex structure modulus as U, to avoid the confusion with the complex structure of the closed-string worldsheet torus.

The corresponding T-duality group is given by (cf. Table I.1)

$$G(\mathbb{Z}) = \mathrm{O}(2,2;\mathbb{Z}) \cong \mathrm{SL}(2,\mathbb{Z}) \times \mathrm{SL}(2,\mathbb{Z}) \times \mathbb{Z}_2 \ltimes \mathbb{Z}_2 \,. \tag{III.4.3}$$

As discussed in the previous subsection, we considered $\mathrm{SL}(2,\mathbb{R})$ and certain $\mathrm{SL}(2,\mathbb{Z})$ monodromies. From (III.4.3) it is evident that each $\mathrm{SL}(2,\mathbb{Z})$ corresponds to one of the two moduli, representing half of the T-duality group. Analogous to (III.3.17), these two moduli can be expressed in the representations of $\mathrm{SL}(2,\mathbb{R})$ as

$$\mathcal{H}_\tau = \frac{1}{\tau_2}\begin{pmatrix} |\tau|^2 & \tau_1 \\ \tau_1 & 1 \end{pmatrix}, \quad \mathcal{H}_\rho = \frac{1}{\rho_2}\begin{pmatrix} |\rho|^2 & \rho_1 \\ \rho_1 & 1 \end{pmatrix}. \tag{III.4.4}$$

Besides these geometric moduli, the T^2 compactification yields two Ramond-Ramond real scalars, which transform as spinors under T-duality [24, 25], and one lower-dimensional dilaton, which is invariant under T-duality. In our analysis, we concentrate on T-fold constructions, which cannot generate potentials involving these additional fields. Hence we truncate these fields to ensure that the remaining scalar fields parameterize the quotient group G/H. The truncated fields, together with the Kähler modulus, transform under the adjoint representation of $\mathrm{SL}(3,\mathbb{R})$, corresponding to a part of the U-duality group. A detailed discussion of such a U-fold compactification is provided in Appendix III.A.

III.4.1 Monodromy classification in terms of fluxes

In this subsection, we examine the classification of monodromies in terms of fluxes within the framework of T-fold compactifications. Specifically, we explore how fluxes arise from duality twists in the T-duality group and their implications for the Dark Dimension Scenario.

Generically, the NS-NS moduli of a torus T^n excluding the dilaton can be represented as the generalized metric in (I.3.52):

$$\mathcal{H} = \begin{pmatrix} \frac{1}{\alpha'}\left(g - bg^{-1}b\right) & bg^{-1} \\ -g^{-1}b & \alpha' g^{-1} \end{pmatrix} \in \mathrm{O}(n,n)\,, \tag{III.4.5}$$

where g is the metric and b is the Kalb–Ramond two-form field. For a two-dimensional torus T^2, comparing with (III.4.1), the moduli matrix under this representation becomes

$$\mathcal{H} = \frac{1}{\rho_2\tau_2}\begin{pmatrix} |\rho|^2|\tau|^2 & |\rho|^2\tau_1 & -\rho_1\tau_1 & \rho_1|\tau|^2 \\ |\rho|^2\tau_1 & |\rho|^2 & -\rho_1 & \rho_1\tau_1 \\ -\rho_1\tau_1 & -\rho_1 & 1 & -\tau_1 \\ \rho_1|\tau|^2 & \rho_1\tau_1 & -\tau_1 & |\tau|^2 \end{pmatrix}. \tag{III.4.6}$$

The element $\mathcal{M}$ of the T-duality group $\mathrm{O}(n,n;\mathbb{Z})$ of torus T^n acts on $\mathcal{H}$ as

$$\mathcal{H} \to \mathcal{M}^{-T}\mathcal{H}\mathcal{M}^{-1}\,. \tag{III.4.7}$$

For the representation (III.4.4) of moduli τ and ρ, the generic monodromy matrices can be parametrized as

$$\mathcal{M}_\tau = \begin{pmatrix} a & b \\ c & d \end{pmatrix}, \quad \mathcal{M}_\rho = \begin{pmatrix} a' & b' \\ c' & d' \end{pmatrix}, \tag{III.4.8}$$

with $ad - bc = 1$ and $a'd' - b'c' = 1$. Under the same representation as (III.4.6), the combined monodromy matrix is then constructed as

$$\mathcal{M} = \begin{pmatrix} aa' & ba' & -bb' & ab' \\ ca' & da' & -db' & cb' \\ -cc' & -dc' & dd' & -cd' \\ ac' & bc' & -bd' & ad' \end{pmatrix} \in \mathrm{O}(2,2;\mathbb{Z})\,. \tag{III.4.9}$$

The twist group $\mathrm{O}(n,n;\mathbb{Z})$ is generated by three fundamental types of global transformations [26–28]:

- Diffeomorphism duality $\mathcal{M}_A$:

$$\mathcal{M}_A = \begin{pmatrix} A^{-1} & 0 \\ 0 & A^T \end{pmatrix}, \quad A \in \mathrm{GL}(n,\mathbb{Z})\,, \tag{III.4.10}$$

  acting on the background geometry as a diffeomorphism $g+b \to A^T(g+b)A$;

- B-field transformation $\mathcal{M}_B$:

$$\mathcal{M}_B = \begin{pmatrix} \mathbb{1} & 0 \\ B & \mathbb{1} \end{pmatrix}, \quad \text{with } B \text{ anti-symmetric}, \tag{III.4.11}$$

  corresponding to a shift of the Kalb–Ramond field: $g \to g$, $b \to b + \alpha' B$;

- Factorized dualities $\mathcal{M}_{\pm i}$:

$$\mathcal{M}_{\pm i} = \begin{pmatrix} \mathbb{1} - E_i & \pm E_i \\ \pm E_i & \mathbb{1} - E_i \end{pmatrix}, \tag{III.4.12}$$

  where $E_i = \mathrm{diag}(0, \cdots, 1, \cdots, 0)$, with the 1 in the i-th position. This transformation corresponds to performing a duality along the z^i-circle.

Combining $\mathcal{M}_B$ with factorized dualities yields another useful transformation, which is called β-transformation:

$$\mathcal{M}_\beta = \left(\prod_{i=1}^{n} \mathcal{M}_{\pm i}\right) \mathcal{M}_{B(\beta)} \left(\prod_{i=1}^{n} \mathcal{M}_{\pm i}\right) = \begin{pmatrix} \mathbb{1} & \beta \\ 0 & \mathbb{1} \end{pmatrix}, \quad \text{with } \beta \text{ anti-symmetric}. \tag{III.4.13}$$

Back to our specific $T^2 \times S^1$ model, we can select duality twists from the aforementioned transformations. These twists deform the geometry of the internal space and modify the periodicity conditions of the fields, thereby generating

various generalized fluxes, including both geometric and non-geometric fluxes. Consider a twist $\mathcal{M}_{B(h)}$ defined as

$$\mathcal{M}_{B(h)} = \begin{pmatrix} \mathbb{1} & 0 \\ B(h) & \mathbb{1} \end{pmatrix}, \quad \text{with } B(h) = \begin{pmatrix} 0 & h \\ -h & 0 \end{pmatrix}, \quad h \in \mathbb{Z}\,. \tag{III.4.14}$$

This transformation is equivalent to introducing a constant H-flux, $H = \frac{\alpha' h}{2\pi}\, \mathrm{d}z_1 \wedge \mathrm{d}z_2 \wedge \mathrm{d}y$. The corresponding Kalb–Ramond field can be represented as

$$b = \begin{pmatrix} 0 & \frac{\alpha' h y}{2\pi} & 0 \\ -\frac{\alpha' h y}{2\pi} & 0 & 0 \\ 0 & 0 & 0 \end{pmatrix}. \tag{III.4.15}$$

Under this twist, the periodicity condition of the generalized metric becomes

$$\mathcal{H}(x + 2\pi) = \mathcal{M}_{B(h)}^{-T} \mathcal{H}(x) \mathcal{M}_{B(h)}^{-1}\,. \tag{III.4.16}$$

As we described in Subsection I.3.5, performing a T-duality transformation $\mathcal{M}_{+1}$ along z_1-direction, the B-field gets trivial and the geometric f-flux is generated. Performing an additional T-duality transformation $\mathcal{M}_{+2}$ along z_2-direction, the f-flux is converted to Q-flux [29]. The resulting internal space with non-trivial Q-flux forms a T-fold, which is locally geometric but globally non-geometric, because the transition function is the combination of diffeomorphism and T-duality [30].

Now consider that over the internal space there is a duality twist

$$\mathcal{M} = \mathcal{M}_{B(h)} \mathcal{M}_{A(f)} \mathcal{M}_{\beta(q)}\,, \tag{III.4.17}$$

with

$$A(f) = \begin{pmatrix} 1 & -f \\ 0 & 1 \end{pmatrix}, \quad \beta(q) = \begin{pmatrix} 0 & q \\ -q & 0 \end{pmatrix}. \tag{III.4.18}$$

Such a twist corresponds to a T-fold background with H-, f-, and Q-fluxes turned on, with flux numbers h, f, $q \in \mathbb{Z}$ respectively. Combining (III.4.17) with the generic expression (III.4.9), we observe that the decomposed monodromy matrices for the two moduli are given by

$$\mathcal{M}_\tau = \begin{pmatrix} 1 & f \\ 0 & 1 \end{pmatrix}, \quad \mathcal{M}_\rho = \begin{pmatrix} 1 & q \\ -h & 1 - hq \end{pmatrix}. \tag{III.4.19}$$

The monodromy of the complex structure modulus τ naturally falls into the parabolic conjugacy class, whereas the ρ-monodromy can belong to either a parabolic, elliptic, or hyperbolic conjugacy class. Depending on the values of h and q, $\mathrm{Tr}\, M_\rho^2$ takes different values and the ρ-monodromy can be classified as follows:

- if one of h and $q = 0$, the monodromy is a shift on ρ and is parabolic, similar as $\mathcal{M}_\tau$;
- if $hq = 1$, it is a $\mathbb{Z}_6$ elliptic monodromy. For $h = q = 1$ it is indeed $\mathcal{M}_6$ in (III.3.25);

- if $hq = 2$, it is a $\mathbb{Z}_4$ elliptic monodromy, which is conjugate to $\mathcal{M}_4$ in (III.3.25) by $\mathrm{SL}(2,\mathbb{Z})$-conjugation, but the Minkowski minimum situation is different. For example, for $h = 2$, $q = 1$,

$$\mathcal{M}_\rho = \begin{pmatrix} 1 & 1 \\ -2 & -1 \end{pmatrix} = \begin{pmatrix} 1 & 0 \\ -1 & 1 \end{pmatrix} \mathcal{M}_4 \begin{pmatrix} 1 & 0 \\ -1 & 1 \end{pmatrix}^{-1}, \tag{III.4.20}$$

  and the minimum is at $\rho = \frac{-1+i}{2}$;

- if $hq = 3$, it is a $\mathbb{Z}_3$ elliptic monodromy conjugate to $\mathcal{M}_3$;

- if $hq < 0$, the monodromy is hyperbolic and conjugate to $\mathcal{M}_h$;

- if $hq \geq 4$, the monodromy M_ρ becomes imaginary, corresponding to complexified generators of the duality group. For $hq > 4$, the monodromy is hyperbolic and the mass matrix M_ρ is

$$\begin{pmatrix} \sqrt{\frac{hq}{hq-4}} \arctan(-A) & 2\sqrt{\frac{q}{h(hq-4)}} \arctan(-A) \\ 2\sqrt{\frac{h}{q(hq-4)}} \arctan A & \sqrt{\frac{hq}{hq-4}} \arctan A \end{pmatrix} + i\pi \begin{pmatrix} 1 & \\ & 1 \end{pmatrix}. \tag{III.4.21}$$

  where $A = \sqrt{1 - \frac{4}{(hq-2)^2}}$. This gives a minimal orbit at $h|\rho|^2 + hq\rho_1 + q = 0$, with $\rho_{2,\max} = \sqrt{\frac{q}{h}} \frac{\sqrt{hq-4}}{2}$. At the orbit the potential picks the minimal value, with

$$v^\rho_{\min} \equiv 4 \left(\log \frac{hq - 2 - \sqrt{hq(hq-4)}}{2} \right)^2 - 4\pi^2, \tag{III.4.22}$$

  contributing to the potential

$$V \equiv 2e^{2(\alpha-\beta)\phi} (v^\tau + v^\rho). \tag{III.4.23}$$

  Such a minimum is negative for $hq \leq 25$ ($\mathrm{Tr}\, M_\rho^2 < 0$) and positive for $hq > 25$ ($\mathrm{Tr}\, M_\rho^2 > 0$).

  For $hq = 4$, it is parabolic. As an example, for $h = q = 2$,

$$M_\rho = \begin{pmatrix} -2 + i\pi & -2 \\ 2 & 2 + i\pi \end{pmatrix}. \tag{III.4.24}$$

  There is a minimum at $\rho_1 = -1$, $\rho_2 \to 0$, with value

$$v^\rho_{\min} \equiv \mathrm{Tr} \left(M_\rho^2 + M_\rho^T \mathcal{H}_\rho^{-1} M_\rho \mathcal{H}_\rho \right)_{\min} \to -4\pi^2. \tag{III.4.25}$$

  Conclusively, stabilized ρ with $hq \geq 4$ gives a non-zero constant contribution to the potential and dominates over the runaway τ contribution. For $4 \leq hq \leq 25$, the potential V negatively diverges when it goes towards

$\phi \to -\infty$, where the Scherk–Schwarz radius shrinks to a point and the effective theory breaks down. For $hq > 25$, the modulus ρ is stabilized at the valley of the potential, while the radion remains a runaway direction along which the potential tends to zero. Additional fluxes and non-perturbative effects [31, 32] may stabilize the Scherk–Schwarz radion to create a potential minimum.

In addition, the $\mathbb{Z}_2$ monodromy can be achieved via a further T-duality such that $\mathcal{M}_\rho \to -\mathcal{M}_\rho$.

III.4.2 Dark Dimension realization in the toy model

We now endeavor to realize the Dark Dimension Scenario within the framework of our seven-dimensional toy model. Referring to (III.4.19), we assign a parabolic monodromy for τ and an elliptic monodromy for ρ. For instance, by activating fluxes with $h = 2$, $q = 1$ and f arbitrary, the monodromy generator M is given by

$$M_{p,4} = \begin{pmatrix} \frac{\pi}{2} & f & 0 & \frac{\pi}{2} \\ 0 & \frac{\pi}{2} & -\frac{\pi}{2} & 0 \\ 0 & \pi & -\frac{\pi}{2} & 0 \\ -\pi & 0 & -f & -\frac{\pi}{2} \end{pmatrix} . \tag{III.4.26}$$

Incorporating this monodromy generator with the moduli matrix defined in equation (III.4.6), the scalar potential (III.3.14) becomes

$$V = 2e^{2(\alpha-\beta)\phi} \left(\frac{f^2}{\tau_2^2} + \frac{\pi^2}{4} \frac{4|\rho|^4 + 4\rho_1 \left(2|\rho|^2 + 2\rho_1 + 1\right) + 1}{\rho_2^2} \right) \overset{\rho \text{ stab.}}{=\!=} 2e^{2(\alpha-\beta)\phi} \frac{f^2}{\tau_2^2} . \tag{III.4.27}$$

In this expression, the Kähler scalar ρ of this potential is stabilized at $\rho = \frac{-1+i}{2}$. The real part τ_1 is a flat direction, while the imaginary part τ_2 exhibits runaway behavior, driving the system towards a large complex structure limit. To further analyze the potential, we perform a reparameterization of the scalar fields as follows:

$$e^{a\phi} = x = r\cos\vartheta, \quad \tau_2^2 = y = r\sin\vartheta, \quad a = 2(\beta - \alpha), \tag{III.4.28}$$

with $0 < \vartheta < \frac{\pi}{2}$. Hence, we can express the potential in terms of a trajectory field r and a transverse field ϑ. Substituting these variables into the potential, we obtain:

$$V = \frac{2f^2}{r^2} \frac{1}{\cos\vartheta \sin\vartheta} , \tag{III.4.29}$$

which stabilizes the modulus ϑ at $\vartheta = \frac{\pi}{4}$, corresponding to the opposite direction of the gradient of the potential. Consequently, as the system evolves over time, the potential approaches:

$$V_{\text{stab.}} = \frac{4f^2}{r^2} = 4f^2 e^{-2a\phi} \propto m_{\text{KK}}^4 . \tag{III.4.30}$$

This result indeed satisfies the requirements of the Dark Dimension Scenario, where the Dark Dimension is naturally identified with the Scherk–Schwarz S^1-radius. We will comment on this potential in the next section, where the 4-dimensional result can be similar to (III.4.27) by stabilizing more moduli.

III.5 Dark Dimension realization in 4 dimensions

The method used in the toy model can be naturally extended to 4 dimensions. Consider a type II superstring theory compactified on $T^5 \times S^1$. We perform a Scherk–Schwarz reduction over S^1, with twists taken from the T-duality group $\mathrm{O}(5,5;\mathbb{Z})$ of T^5. We truncate the Ramond-Ramond fields and focus on the NS-NS background moduli $\mathcal{H}$, as given by expression (III.4.5), to fit into the representation of the T-duality group. As in the toy model, we require at least one runaway scalar from $\mathcal{H}$, while the other scalars are either flat or stabilized at Minkowski minima. In the last section, we utilize the parabolic conjugacy class of $\mathrm{SL}(2,\mathbb{Z})$ to generate the required runaway potential, and the elliptic conjugacy class to stabilize the T^2-volume at $V^\rho = 0$. However, the conjugacy structures of larger groups are highly complex; for example, there is still no explicit characterization of the conjugacy classes of $\mathrm{SL}(3,\mathbb{Z})$ [33].

Nevertheless, if we set aside the moduli stabilization problem, the toy model provides a straightforward example of duality twists. The torus T^5 can be decomposed as $T^2_A \times T^2_B \times S^1$, with coordinates $\{z^1, z^2; z^3, z^4; z^5\}$. We can turn on the T-fold fluxes with corresponding monodromy given by (III.4.19) for each T^2 over the base S^1. As an example, for both T^2's we take the monodromy as in (III.4.26). Then the potential (III.3.14) is

$$\begin{aligned} V = 2e^{2(\alpha-\beta)\phi} \Bigg(& \frac{f_A^2}{\left(\tau_2^A\right)^2} + \frac{\pi^2}{4} \frac{4|\rho^A|^4 + 4\rho_1 \left(2|\rho^A|^2 + 2\rho_1^A + 1\right) + 1}{\left(\rho_2^A\right)^2} \\ & + \frac{f_B^2}{\left(\tau_2^B\right)^2} + \frac{\pi^2}{4} \frac{4|\rho^B|^4 + 4\rho_1 \left(2|\rho^B|^2 + 2\rho_1^B + 1\right) + 1}{\left(\rho_2^B\right)^2} \Bigg) , \end{aligned} \tag{III.5.1}$$

where $2(\alpha-\beta) = -\sqrt{3}$. Upon stabilizing ρ^A and ρ^B as in (III.4.26), the potential simplifies to

$$V = 2e^{-\sqrt{3}\phi} \left(\frac{f_A^2}{\left(\tau_2^A\right)^2} + \frac{f_B^2}{\left(\tau_2^B\right)^2} \right) . \tag{III.5.2}$$

Similar to (III.4.29), the potential can be further stabilized by reparametrizing the remaining moduli into spherical coordinates

$$e^{\sqrt{3}\phi} = r\cos\vartheta, \quad \left(\tau_2^A\right)^2 = r\sin\vartheta\cos\varphi, \quad \left(\tau_2^B\right)^2 = r\sin\vartheta\sin\varphi\,, \tag{III.5.3}$$

with $0 < \vartheta, \varphi < \frac{\pi}{2}$. The potential now becomes

$$V = \frac{2}{r^2\cos\vartheta\sin\vartheta} \left(\frac{f_A^2}{\cos\varphi} + \frac{f_B^2}{\sin\varphi} \right) , \tag{III.5.4}$$

which attains a minimum at $\vartheta = \frac{\pi}{4}$, $\tan\varphi = (f_B/f_A)^{\frac{2}{3}}$, where

$$V = \frac{4}{r^2}\left(f_A^{\frac{4}{3}} + f_B^{\frac{4}{3}}\right)^{\frac{3}{2}} = 2e^{-2\sqrt{3}\phi}\left(f_A^{\frac{4}{3}} + f_B^{\frac{4}{3}}\right)^{\frac{3}{2}} \propto m_{\rm KK}^4 \,. \tag{III.5.5}$$

In this model, we indeed obtain the Dark Dimension power relation between the potential and the S^1_y-Kaluza–Klein scale. The complexified volumes of the two subtori are fixed, and two shape scalars run away. However, there remain many flat directions in the field space, especially since the z^5-direction is not stabilized. In the Dark Dimension Scenario, the number of large internal dimensions should be one, and an additional uncontrolled radius could be problematic.

On the other hand, stabilizing all relevant moduli in $\mathcal{H}$ via nontrivial monodromies in $\mathrm{O}(5,5;\mathbb{Z})$ is almost impossible. Here we choose to keep some off-diagonal metric fields and corresponding B-field components flat, and decompose the twist group to $\mathrm{O}(3,3;\mathbb{Z}) \times \mathrm{O}(2,2;\mathbb{Z})$ of $T^3 \times T^2$. For the twist over T^3, we only turn on H- and Q-fluxes.

Denote the coordinates of T^3 to be $\{w^1, w^2, w^3\}$. Note that we can take a monodromy $\mathcal{M}_B$ such that the Kalb–Ramond field over T^3 is

$$b_{ij} = -b_{ji} = \frac{\alpha' h_{ij} y}{2\pi}, \quad i > j,\ i,j = 1,2,3, \tag{III.5.6}$$

where h_{ij} are the H-flux numbers. This configuration yields a constant H-flux over $T^3 \times S^1$. Applying factorized T-duality transformations $\mathcal{M}_{+j}\mathcal{M}_{+i}$ on this background, the twist becomes a β-transformation $\mathcal{M}_\beta$, converting the H-flux components into corresponding Q-fluxes. Now consider a monodromy $\mathcal{M} = \mathcal{M}_{B(h)}\mathcal{M}_{\beta(q)} \in \mathrm{O}(3,3;\mathbb{Z})$, such that the matrix $\mathcal{M}$ is

$$\begin{pmatrix}
1 & 0 & 0 & 0 & q_{12} & q_{13} \\
0 & 1 & 0 & -q_{12} & 0 & q_{23} \\
0 & 0 & 1 & -q_{13} & -q_{23} & 0 \\
0 & h_{12} & h_{13} & 1-h_{12}q_{12}-h_{13}q_{13} & -h_{13}q_{23} & h_{12}q_{23} \\
-h_{12} & 0 & h_{23} & -h_{23}q_{13} & 1-h_{12}q_{12}-h_{23}q_{23} & -h_{12}q_{13} \\
-h_{13} & -h_{23} & 0 & h_{23}q_{12} & -h_{13}q_{12} & 1-h_{13}q_{13}-h_{23}q_{23}
\end{pmatrix}, \tag{III.5.7}$$

with flux numbers $h_{ij}, q_{ij} \in \mathbb{Z}$. The conjugacy classes of $\mathcal{M}$ remain complicated. We require that the volume of T^3 is stabilized at a Minkowski minimum. To achieve that, $\mathcal{M}$ should be conjugated to a rotation. Suppose all flux numbers are nontrivial, then numerical cases indicate that the only possible values might be $h_{12}q_{12} = h_{13}q_{13} = h_{23}q_{23} = 1$. As an example, we choose $h_{12} = q_{12} = h_{13} = q_{13} = 1$, $h_{23} = q_{23} = -1$. This configuration has a minimum $V_{T^3} = 0$ at

$$b_{12} = -b_{13} = b_{23} = -\frac{1}{2}, \quad g_{ij} = \frac{1}{2}\delta_{ij} \,. \tag{III.5.8}$$

For the twist over T^2, we take the monodromy (III.4.17) with generator (III.4.26) as an example, such that its Kähler modulus is stabilized by H- and Q-fluxes, and

the complex structure modulus runs away. Then the potential (III.3.14) becomes

$$V = V_{T^3} + V_{T^2} = V_{T^2} = 2e^{-\sqrt{3}\phi}\left(\frac{f^2}{\tau_2^2} + \frac{\pi^2}{4}\frac{4|\rho|^4 + 4\rho_1\left(2|\rho|^2 + 2\rho_1 + 1\right) + 1}{\rho_2^2}\right), \tag{III.5.9}$$

which is the same as (III.4.27). After evolving for enough time, the potential becomes proportional to m_{KK}^4, aligning with the requirements of the Dark Dimension Scenario.

The flux construction presented here, featuring a duality-twisted T^5 over a Scherk–Schwarz S^1 base, inherently satisfies the Bianchi identities [34]. The NS-NS Bianchi identities, which arise from applying T-duality to the condition $\mathrm{d}H = 0$, impose constraints on the allowed values of the geometric and non-geometric fluxes. In our construction, which is free of R-flux and R-R fluxes, the relevant Bianchi identities for the non-vanishing H-, f-, and Q-fluxes are expressed as:

$$H_{e[ab}F^{e}{}_{cd]} = 0\,, \tag{III.5.10}$$

$$F^{a}{}_{e[b}F^{e}{}_{cd]} + H_{e[bc}Q^{ae}{}_{d]} = 0\,, \tag{III.5.11}$$

$$Q^{ab}{}_{e}F^{e}{}_{cd} - 4F^{[a}{}_{e[c}Q^{c]e}{}_{d]} = 0\,, \tag{III.5.12}$$

$$Q^{[ab}{}_{e}Q^{c]e}{}_{d} = 0\,. \tag{III.5.13}$$

To map these general expressions to our specific flux components, we first denote the T^2 coordinates as $\{w^4, w^5\}$, such that $h \equiv h_{45}$, $f \equiv f_{45}$, $q \equiv q_{45}$. The H-flux components are then identified as $H_{aby} \equiv h_{ab}$, where $a, b = 1, 2, 3, 4, 5$ and y denotes the Scherk–Schwarz S^1 direction. Similarly, the Q-flux components are identified as $Q^{ab}{}_{y} \equiv q_{ab}$, satisfying upper-indices anti-symmetry $Q^{ab}{}_{c} = -Q^{ba}{}_{c}$. Given that the f-flux vanishes on the T^3 subspace, its only non-trivial components are $F^{1}{}_{2y} = -F^{1}{}_{y2} \equiv f$. A direct computation confirms that all Bianchi identities are satisfied, both for components purely on the T^2 and T^3 subspaces and for components involving their intersection. This result holds primarily because the T-duality transformations defining our twist in (III.4.19) and (III.5.7) do not act on the Scherk–Schwarz circle, which ensures the absence of any $F^{y}{}_{ab}$ or $Q^{ya}{}_{b}$ flux components. Furthermore, the first identity, (III.5.10), provides a consistency check that justifies our decomposition $T^5 = T^3 \times T^2$.

Our model yields an effective theory characterized by a constant T^5-volume and an expanding Scherk–Schwarz S^1-radius. The additional runaway scalar is the complex structure of some T^2 subtorus within T^5, and the volume of this T^2 is fixed. Consequently, for a square torus, this dynamic means one direction of the T^2 shrinks while the other expands. Denote the torus radii as R_1 and R_2. The imaginary part of the complex structure modulus is then given by $\tau_2 = R_1/R_2$. The potential (III.4.29) is stabilized at $\vartheta = \pi/4$, while along this runaway direction, the Scherk–Schwarz radius satisifies $\varrho = e^{\sqrt{3}\phi} = \tau_2$. Since the growth of τ_2 is sourced by both an increasing R_1 and a decreasing R_2, it follows that the expansion rate of R_1 is necessarily slower than the growth rate of ϱ. After long-time evolution, this results in a significantly larger Scherk–Schwarz radius, identifying it as the Dark Dimension.

In our model, supersymmetry is completely broken due to the runaway potential, with the supersymmetry-breaking scale at least the scale of the gravitino mass. The gravitini belong to the representation of the R-symmetry group, which is the compact subgroup of the T-duality associated with rotational (elliptic) conjugacy classes. By applying a rotational twist, we simultaneously stabilize the volume and the B-field and impart mass to the gravitini, as elaborated in the seminal work by Scherk and Schwarz [20]. In the string frame, the gravitino mass is inversely proportional to ϱ [35], such that in the Einstein frame,

$$M_{3/2} \sim \varrho^{-\frac{3}{2}} = e^{-\frac{3}{2}\beta\phi} = m_{\mathrm{KK}}\,, \tag{III.5.14}$$

which is much higher than the scale of our potential.

Furthermore, if $f = 0$ such that the monodromy is purely elliptic ($V_{\mathrm{classical}} = 0$), the theory allows for an exact worldsheet description and features an asymmetric orbifold internal space [36, 37], and the 1-loop Casimir potential of 4D Scherk–Schwarz compactifications is known as [32, 38]

$$V_{\mathrm{Casimir}} = \xi \left(N_{\mathrm{f}}^0 - N_{\mathrm{b}}^0\right) m_{\mathrm{KK}}^4\,, \tag{III.5.15}$$

where ξ is an $\mathcal{O}(10^{-3})$ number [38] and $N_{\mathrm{f}}^0 - N_{\mathrm{b}}^0 \sim \mathcal{O}(10)$ [32]. In this case, more massless bosons than massless fermions exist around the Minkowski vacuum from the elliptic monodromy, resulting in a negative one-loop Casimir energy. This energy becomes unstable as $\phi \to -\infty$, corresponding to the zero-volume and strong coupling limit. Stabilization of this potential might be achievable by introducing proper fluxes [32]. However, in our models with non-trivial f-fluxes and lacking a worldsheet description, the 1-loop Casimir correction for a twisted background with a runaway potential remains undetermined, and the mass spectrum is time-dependent. Suppose the quantum corrections in our model mimic the expression in (III.5.15), it follows that the Casimir corrections are strongly suppressed relative to the classical Scherk–Schwarz potential, $V_{\mathrm{Casimir}} \ll V_{\mathrm{classical}}$. This suppression occurs because the coefficient of the classical potential $4f^2 \gtrsim \mathcal{O}(1-10)$ for proper flux numbers values, making it substantially larger than the factor $\xi \left(N_{\mathrm{f}}^0 - N_{\mathrm{b}}^0\right) \sim -\mathcal{O}(10^{-2})$ that governs the magnitude of the Casimir energy.

III.6 Conclusion and Outlook

In this chapter, we presented a novel approach to integrating the concept of the Dark Dimension with non-geometric compactifications. Our investigation demonstrates that the Dark Dimension Scenario can be realized within the framework of type II superstring theory by employing a Scherk–Schwarz reduction mechanism combined with T-folds. This T-fold compactification on $T^5 \times S^1$ utilizes T^5 T-duality $\mathrm{O}(5,5;\mathbb{Z})$ as the twist group, and S^1 serves as the Scherk–Schwarz radius.

To construct a Scherk–Schwarz potential with the required properties, the duality twist over T^5 was determined. We decomposed the T-duality to be the

subgroup $\mathrm{O}(2,2;\mathbb{Z}) \times \mathrm{O}(3,3;\mathbb{Z})$. In the T^2 segment, characterized by T-duality $\mathrm{O}(2,2;\mathbb{Z}) \sim \mathrm{SL}(2,\mathbb{Z})_\tau \times \mathrm{SL}(2,\mathbb{Z})_\rho$, we engineered twists to ensure the complex structure modulus τ experiences a parabolic monodromy, while the Kähler modulus ρ undergoes an elliptic monodromy. This parabolic monodromy of τ is characterized by the f-flux, and the monodromy of τ is characterized by H- and Q-flux. We also provided a comprehensive classification of $\mathrm{SL}(2,\mathbb{Z})$ conjugacy classes in terms of H-, Q-flux numbers in SubSubsection III.4.1, especially noting the imaginary monodromy with $hq \geq 4$. For the remaining T^3 component, we identified elliptic conjugacy classes of $\mathrm{O}(3,3;\mathbb{Z})$ like (III.5.7). The elliptic conjugacy classes stabilize corresponding moduli and contribute $V_e = 0$ to the potential, whereas the parabolic monodromy in our setup results in a runaway potential for τ_2. By stabilizing the turning to another runaway direction ϕ, we aligned these two scalars to produce a potential that towards a desirable direction with $V \propto e^{-2\sqrt{3}\phi} \propto m_{\mathrm{KK}}^4$, as required by the Dark Dimension.

Note that the moduli stabilization remains challenging. With our decomposition of T-duality into $\mathrm{O}(3,3;\mathbb{Z}) \times \mathrm{O}(2,2;\mathbb{Z})$, some off-diagonal scalar fields present flat directions. Further exploration into conjugacy classification could potentially stabilize more moduli. Investigating the tadpole contributions and Bianchi identities may allow for the stabilization of all NS-NS moduli using non-geometric fluxes, as discussed in [10]. Additional moduli might be stabilized by RR fluxes. However, our model necessitates that the Scherk–Schwarz radion is not stabilized and at least one more modulus contributes to a runaway potential. Fully understanding the behaviors of moduli under these conditions requires quantum corrections at various levels, which are complex to compute in a dynamic background. Future research may address these challenges.

We achieved the required exponent by aligning other scalar fields with the radion. Dynamically, the scalars can move along a non-geodesic trajectory before approaching the steepest direction. Suppose that the current universe has the potential proportional behavior in the Dark Dimension Scenario, but is not near the boundary of the field space, then the potential after angular stabilization could run faster than m_{KK}^4. The multi-field quintessence models follow the same idea to acquire the transient cosmic acceleration. However, within our framework, the exponent in the expression $V \propto e^{-2\sqrt{3}\phi}$, indicative of an asymptotic exponential quintessence model, is too large to feasibly achieve the cosmic acceleration. For additional discussion, see Appendix III.B.

III.A $T^2 \times S^1$ U-fold compactification

Consider a compactification of type IIB superstring theory on $T^2 \times S^1$ or an 11D supergravity on $T^3 \times S^1$. We implement a Scherk–Schwarz reduction over the S^1, with the monodromy matrix $\mathcal{M} = e^M$ a component of the U-duality group of T^2. The U-duality group is isomorphic to $\mathrm{SL}(2,\mathbb{Z}) \times \mathrm{SL}(3,\mathbb{Z})$ [39]. Within this setup, the theory comprises a gravity multiplet that includes seven scalars: the Kähler modulus ρ, the complex structure modulus τ, the axio-dilaton $\sigma = c_0 + ie^{-\phi_{10}}$,

and the reduced RR 2-form c_2. The corresponding moduli space is described by

$$\frac{\mathrm{SL}(2,\mathbb{R})}{\mathrm{SL}(2,\mathbb{Z})\times \mathrm{U}(1)} \times \frac{\mathrm{SL}(3,\mathbb{R})}{\mathrm{SL}(3,\mathbb{Z})\times \mathrm{SO}(3)}\,. \tag{III.A.1}$$

We organize the scalar fields into the adjoint representation $\mathcal{H} \in \mathrm{SL}(2,\mathbb{R})_\tau \times \mathrm{SL}(3,\mathbb{R})$. In this structure, the complex structure modulus τ transforms under $\mathrm{SL}(2,\mathbb{R})\tau$, while other fields fall under $\mathrm{SL}(3,\mathbb{R})$. The composition of the fields in $\mathrm{SL}(3,\mathbb{R})$ is given by [40, 41]

$$\mathcal{H}_{\mathrm{SL}(3)} = \frac{e^{\phi_8/3}}{\rho_2}\begin{pmatrix} \rho_2 e^{-\phi_8} + |c_2+\sigma_1\rho|^2 & c_2\rho_1+\sigma_1|\rho|^2 & c_2+\sigma_1\rho_1 \\ c_2\rho_1+\sigma_1|\rho|^2 & |\rho|^2 & \rho_1 \\ c_2+\sigma_1\rho_1 & \rho_1 & 1 \end{pmatrix}. \tag{III.A.2}$$

Despite the complexity of the complete conjugacy classification of $\mathrm{SL}(3,\mathbb{Z})$, stabilizing the scalars requires only a suitable elliptic conjugacy class. Here, we select a $\mathbb{Z}_2$-monodromy

$$\mathcal{M}_{\mathrm{SL}(3)} = e^M = \begin{pmatrix} 0 & 0 & 1 \\ 0 & -1 & 0 \\ 1 & 0 & 0 \end{pmatrix}, \quad \text{with } M = \frac{\pi}{\sqrt{2}}\begin{pmatrix} 0 & 1 & 0 \\ -1 & 0 & 1 \\ 0 & -1 & 0 \end{pmatrix}. \tag{III.A.3}$$

This configuration allows the SL(3) fields to contribute to a Minkowski minimum, effectively stabilizing the moduli at $\rho = i, \sigma = i, c_2 = 0$. For the complex structure modulus τ, we apply the parabolic conjugacy class of $\mathrm{SL}(2,\mathbb{R})_\tau$ as the monodromy. Then we get the same potential as (III.4.27) and so on in our T-fold constructions.

III.B Multi-field quintessence

The runaway potentials discussed in this chapter are characteristic examples of multi-field quintessence models. Consider a single-field quintessence model in a flat space with zero spatial curvature. The potential is given by:

$$V = V_0\, e^{-\lambda\phi}\,, \tag{III.B.1}$$

where to sustain an eternally accelerating universe, the exponent λ must satisfy $\lambda \leq \sqrt{2}$. Asymptotically, quintessence models incorporating multiple fields typically exhibit trajectories with steeper declines. For example, a potential involving two fields might be expressed as

$$V = V_0\, e^{-\lambda(\phi_1+\phi_2)}\,, \tag{III.B.2}$$

with ϕ_1, ϕ_2 canonically normalized. By naively defining a new normalized field $\Phi = \frac{1}{\sqrt{2}}(\phi_1+\phi_2)$, we observe that the stabilized trajectory aligns along Φ, resulting in a potential of the form $V = V_0 e^{-\lambda_{\mathrm{eff}}\Phi}$, with $\lambda_{\mathrm{eff}} = \sqrt{2}\lambda$.

However, depending on initial conditions, λ_{eff} may vary over time. For example, if the initial universe was in a kination epoch before the 5D decompactification as described by (III.5.9) or (III.4.27), it would initially evolve along the ϑ-direction, effectively setting $\lambda_{\text{eff}} = 0$. As the evolution progresses, λ_{eff} increases until it aligns with the steepest descent. Note that in our models, the field space metric for τ is

$$\mathrm{d}s_\tau^2 = \frac{4}{\tau_2^2}\left(\mathrm{d}\tau_1^2 + \mathrm{d}\tau_2^2\right). \tag{III.B.3}$$

This yields a maximal $\lambda_{\text{eff}} > 2\sqrt{3}$, which is unsuitable for supporting the required accelerated expansion phase in our universe. However, with more runaway directions and slowly descending scalar fields we may realize the cosmic accelerated Dark Dimension.

Furthermore, general theories might include couplings between the radion or dilaton ϕ and the kinetic terms of other fields. Consider the theory

$$\mathcal{L}_{\text{scalar}} = -\frac{1}{2}\partial^\mu\phi\partial_\mu\phi - \frac{1}{2}e^{-2k\phi}\partial^\mu\chi\partial_\mu\chi - e^{-\lambda_1\phi-\lambda_2\chi}. \tag{III.B.4}$$

The kinetic term corresponds to an axion-saxion pair. The dynamics of such a theory is also discussed in for example [42]. Notably, for large values of ϕ, the kinetic term of χ becomes exponentially suppressed. The normalization of the effective field Φ in $e^{-\lambda_{\text{eff}}\Phi} = e^{-\lambda_1\phi-\lambda_2\chi}$ is predominantly influenced by ϕ, such that the value of λ_{eff} is slightly elevated above λ_1. As detailed in [43], the universe may experience a transient accelerating expansion if $\lambda < \sqrt{3} + \mathcal{O}(0.01)$ for a flat universe or $\lambda < \sqrt{3} + \mathcal{O}(0.1)$ for an open universe. By setting $\lambda_1 = \sqrt{3}$, as in our Scherk–Schwarz models, λ_{eff} could evolve from zero to a value slightly exceeding $\lambda = \sqrt{3}$, thereby enabling an accelerated expansion history.

References

[1] DESI collaboration, A. G. Adame et al., *DESI 2024 VI: Cosmological Constraints from the Measurements of Baryon Acoustic Oscillations*, 2404.03002.

[2] DESI collaboration, A. G. Adame et al., *DESI 2024 VII: Cosmological Constraints from the Full-Shape Modeling of Clustering Measurements*, 2411.12022.

[3] M. Montero, C. Vafa and I. Valenzuela, *The dark dimension and the Swampland*, *JHEP* **02** (2023) 022, [2205.12293].

[4] R. Blumenhagen, M. Brinkmann and A. Makridou, *The dark dimension in a warped throat*, *Phys. Lett. B* **838** (2023) 137699, [2208.01057].

[5] U. Danielsson, O. Henriksson and D. Panizo, *Stringy realization of a small and positive cosmological constant in dark bubble cosmology*, *Phys. Rev. D* **107** (2023) 026020, [2211.10191].

[6] C. Cui and S. Ning, *Casimir Energy Stabilization of Standard Model Landscape in Dark Dimension*, 2310.19592.

[7] L. A. Anchordoqui, I. Antoniadis, N. Cribiori, D. Lust and M. Scalisi, *The Scale of Supersymmetry Breaking and the Dark Dimension*, *JHEP* **05** (2023) 060, [2301.07719].

[8] J. J. Heckman, C. Vafa, T. Weigand and F. Xu, *Dark dimension and the grand unification of forces*, *Phys. Rev. D* **111** (2025) 046014, [2409.01405].

[9] I. Basile and D. Lust, *Dark dimension with (little) strings attached*, 2409.12231.

[10] E. Plauschinn, *Moduli Stabilization with Non-Geometric Fluxes — Comments on Tadpole Contributions and de-Sitter Vacua*, *Fortsch. Phys.* **69** (2021) 2100003, [2011.08227].

[11] D. Prieto, J. Quirant and P. Shukla, *On the limitations of non-geometric fluxes to realize dS vacua*, *JHEP* **05** (2024) 008, [2402.13899].

[12] D. Lüst, E. Palti and C. Vafa, *Ads and the swampland*, *Physics Letters B* **797** (Oct., 2019) 134867.

[13] H. Ooguri and C. Vafa, *On the Geometry of the String Landscape and the Swampland*, *Nucl. Phys. B* **766** (2007) 21–33, [hep-th/0605264].

[14] A. Higuchi, *Forbidden Mass Range for Spin-2 Field Theory in De Sitter Space-time*, *Nucl. Phys. B* **282** (1987) 397–436.

[15] S.-J. Lee, W. Lerche and T. Weigand, *Emergent strings from infinite distance limits*, *JHEP* **02** (2022) 190, [1910.01135].

[16] J. G. Lee, E. G. Adelberger, T. S. Cook, S. M. Fleischer and B. R. Heckel, *New Test of the Gravitational $1/r^2$ Law at Separations down to 52 μm*, *Phys. Rev. Lett.* **124** (2020) 101101, [2002.11761].

[17] P. D. Group, P. A. Zyla, R. M. Barnett, J. Beringer, O. Dahl, D. A. Dwyer et al., *Review of particle physics*, *Progress of Theoretical and Experimental Physics* **2020** (08, 2020) 083C01.

[18] S. Hannestad and G. G. Raffelt, *Supernova and neutron-star limits on large extra dimensions reexamined*, *Phys. Rev. D* **67** (Jun, 2003) 125008.

[19] J. Scherk and J. H. Schwarz, *Spontaneous Breaking of Supersymmetry Through Dimensional Reduction*, *Phys. Lett. B* **82** (1979) 60–64.

[20] J. Scherk and J. H. Schwarz, *How to Get Masses from Extra Dimensions*, *Nucl. Phys. B* **153** (1979) 61–88.

[21] A. Dabholkar and C. Hull, *Duality twists, orbifolds, and fluxes*, *Journal of High Energy Physics* **2003** (Sept., 2003) 054–054.

[22] C. M. Hull, *Massive string theories from M theory and F theory*, *JHEP* **11** (1998) 027, [hep-th/9811021].

[23] O. DeWolfe, T. Hauer, A. Iqbal and B. Zwiebach, *Uncovering infinite symmetries on [p, q] 7-branes: Kac-Moody algebras and beyond*, *Adv. Theor. Math. Phys.* **3** (1999) 1835–1891, [hep-th/9812209].

[24] E. Bergshoeff, C. M. Hull and T. Ortin, *Duality in the type II superstring effective action*, *Nucl. Phys. B* **451** (1995) 547–578, [hep-th/9504081].

[25] S. Hassan, *transformations of ramond–ramond fields and space–time spinors*, *Nuclear Physics B* **583** (Sept., 2000) 431–453.

[26] A. Giveon, E. Rabinovici and G. Veneziano, *Duality in String Background Space*, *Nucl. Phys. B* **322** (1989) 167–184.

[27] A. D. Shapere and F. Wilczek, *Selfdual Models with Theta Terms*, *Nucl. Phys. B* **320** (1989) 669–695.

[28] E. Plauschinn, *Non-geometric backgrounds in string theory*, *Phys. Rept.* **798** (2019) 1–122, [1811.11203].

[29] S. Kachru, M. B. Schulz, P. K. Tripathy and S. P. Trivedi, *New supersymmetric string compactifications*, *JHEP* **03** (2003) 061, [hep-th/0211182].

[30] C. M. Hull, *A geometry for non-geometric string backgrounds*, *Journal of High Energy Physics* **2005** (oct, 2005) 065.

[31] M. Quiros, *Spontaneous Scherk-Schwarz supersymmetry breaking and radion stabilization*, in *11th International Conference on Supersymmetry and the Unification of Fundamental Interactions*, pp. 315–322, 2, 2004. hep-ph/0402143. DOI.

[32] S. Parameswaran and M. Serra, *On (A)dS solutions from Scherk-Schwarz orbifolds*, *JHEP* **10** (2024) 039, [2407.16781].

[33] I. Achmed-Zade, M. J. D. Hamilton, D. Lüst and S. Massai, *A note on t-folds and t3 fibrations*, *Journal of High Energy Physics* **2018** (Dec., 2018) .

[34] J. Shelton, W. Taylor and B. Wecht, *Nongeometric flux compactifications*, *JHEP* **10** (2005) 085, [hep-th/0508133].

[35] E. Kiritsis, C. Kounnas, P. M. Petropoulos and J. Rizos, *Solving the decompactification problem in string theory*, *Phys. Lett. B* **385** (1996) 87–95, [hep-th/9606087].

[36] C. Condeescu, I. Florakis and D. Lust, *Asymmetric Orbifolds, Non-Geometric Fluxes and Non-Commutativity in Closed String Theory*, *JHEP* **04** (2012) 121, [1202.6366].

[37] G. Gkountoumis, C. Hull, K. Stemerdink and S. Vandoren, *Freely acting orbifolds of type IIB string theory on T^5*, *JHEP* **08** (2023) 089, [2302.09112].

[38] S. Abel, *A dynamical mechanism for large volumes with consistent couplings*, *JHEP* **11** (2016) 085, [1609.01311].

[39] C. M. Hull and P. K. Townsend, *Unity of superstring dualities*, *Nucl. Phys. B* **438** (1995) 109–137, [hep-th/9410167].

[40] J. T. Liu and R. Minasian, *U-branes and t3 fibrations*, *Nuclear Physics B* **510** (Jan., 1998) 538–554.

[41] A. Castellano, A. Herráez and L. E. Ibáñez, *On the Species Scale, Modular Invariance and the Gravitational EFT expansion*, 2310.07708.

[42] M. Cicoli, J. P. Conlon, A. Maharana, S. Parameswaran, F. Quevedo and I. Zavala, *String cosmology: From the early universe to today*, *Phys. Rept.* **1059** (2024) 1–155, [2303.04819].

[43] D. Andriot, S. Parameswaran, D. Tsimpis, T. Wrase and I. Zavala, *Exponential quintessence: curved, steep and stringy?*, *JHEP* **08** (2024) 117, [2405.09323].

Chapter IV

Duality and Infinite Distance Limits in Asymmetric Freely Acting Orbifolds

Section IV.1–Appendix IV.B of this chapter is based on the work arXiv:2506.11699, JHEP 09 (2025) 198, *collaborating with George Gkountoumis, Chris Hull and Stefan Vandoren.*
Appendix IV.C–Appendix IV.D on quantum corrections to the moduli space is based on the continuing work collaborating with George Gkountoumis and Stefan Vandoren.

IV.1 Introduction

Recently, there has been a revival of interest in asymmetric orbifolds [1–10]. In general, toroidal orbifolds provide a way to construct string models with reduced (or no) supersymmetry, and asymmetric orbifolds are particularly interesting because many more moduli can be frozen for these models than can be frozen for symmetric orbifolds. In Subsection I.3.4, we mentioned that if we orbifold by a freely acting symmetry, then all states in the twisted sectors are typically massive at generic points in the moduli space, and hence the number of moduli is reduced even further. If the free action involves a shift on a circle coordinate, the orbifold can also be understood as a string compactification with a duality twist [11]. Asymmetric orbifolds constitute an interesting region in the string Landscape of non-geometric string compactifications, and their corresponding effective supergravity theories provide highly non-trivial examples, in which the various conjectures of the Swampland programme can be tested.

As we break supersymmetry, using toroidal orbifolds, the duality group $G(\mathbb{Z})$ arising from toroidal compactification is broken by the orbifold twist to a subgroup $K(\mathbb{Z}) \subset G(\mathbb{Z})$, which is a symmetry of the untwisted sector. When the orbifold twist is accompanied by a shift on a circle, the duality group of the untwisted sector reduces to an even smaller subgroup $\Gamma(\mathbb{Z}) \subset K(\mathbb{Z})$, which is the group that preserves both the orbifold twist and the shift. This breaking of the toroidal duality group was seen in [12] and we revisit and further discuss it in this chapter. There are interesting and important consequences for the moduli space of such orbifolds, since we need to quotient by $\Gamma(\mathbb{Z})$ to get the space of inequivalent theories. The moduli space then takes the form $\widetilde{\mathcal{M}} = \mathcal{M}/\Gamma(\mathbb{Z})$ and should obey all the Swampland conjectures such as the Distance Conjecture and the finiteness of the volume of $\widetilde{\mathcal{M}}$ (see Section I.5). See also [13, 14] for more on the Distance Conjecture in the context of Calabi–Yau compactifications.

Freely acting orbifolds resemble models with spontaneous supersymmetry breaking (see e.g. [15–18]), as some (or all) gravitini obtain masses instead of being projected out of the orbifold spectrum. In this chapter, we focus on orbifolds breaking supersymmetry spontaneously from $\mathcal{N} = 8$ (32 supersymmetries) to $\mathcal{N} = 2$ (8 supersymmetries) in 4 dimensions. At points of infinite distance in the moduli space, some (or all) gravitini can become massless, indicating supersymmetry enhancement. For the models studied in this work, all such points can be understood as decompactification limits of the original orbifold theory. Remarkably, at points on the real axis of the upper half plane, an asymmetric freely acting orbifold may decompactify to a non-freely acting symmetric orbifold. We will discuss such cases in detail later.

In Section IV.2 we review the general construction of asymmetric freely acting orbifolds of type IIB on T^6, and we discuss the S- and T-duality groups of the orbifold theory, as well as those of the effective supergravity theory. Then in Section IV.3 we construct an STU-like model by using an asymmetric freely acting $\mathbb{Z}_6$ orbifold, preserving 8 supersymmetries in four dimensions, and we analyse

the spectrum of lightest states in the untwisted and twisted orbifold sectors. In Section IV.4 we discuss the classical moduli space of our orbifold model and we carefully determine all special points and lines in the moduli space where generically massive states can become massless. At infinite distance points in the moduli space we find infinite towers of states becoming massless. In the bulk of the moduli space we find only a finite number of states that become massless. We conclude this chapter with a discussion in Section IV.5.

IV.2 Freely acting orbifolds

In this section we first briefly review freely acting asymmetric orbifolds of type IIB string theory on T^6, closely following a similar discussion in [2, 4]. We then discuss the S- and T-duality groups of the orbifold theory, and those of the effective supergravity theory.

The orbifolds we focus on here have target spaces of the form

$$\mathbb{R}^{1,3} \times T^4 \times T^2 \ , \tag{IV.2.1}$$

identified under the action of a $\mathbb{Z}_p$ symmetry. At a point in moduli space where the T^4 CFT has a $\mathbb{Z}_p$ symmetry, we orbifold by this $\mathbb{Z}_p$ acting on the T^4 CFT combined with a shift along one cycle of the T^2 which makes the orbifold freely acting. Freely acting orbifolds have no fixed points and, at generic points in the moduli space, all states coming from the twisted sectors are massive. Supersymmetry is spontaneously broken in these models with some (or all) of the gravitini becoming massive, in contrast to non-freely acting orbifolds in which some (or all) gravitini are projected out and supersymmetry is explicitly broken.

Symmetric orbifolds arise when the $\mathbb{Z}_p$ action on T^4 is a geometric discrete symmetry of T^4, generated by a diffeomorphism on T^4, i.e. by an element in GL(4,$\mathbb{Z}$). These orbifolds preserve $\mathcal{N} = 4$ or 0 supersymmetry in 4D. For asymmetric orbifolds, the $\mathbb{Z}_p$ group acts as a T-duality transformation on the T^4 CFT. The T-duality group for superstrings on T^4 is $\mathrm{Spin}(4,4;\mathbb{Z})$, a discrete subgroup of the double cover $\mathrm{Spin}(4,4)$ of $\mathrm{SO}(4,4)$, as the D-brane states transform as a spinor representation of $\mathrm{Spin}(4,4)$ [19]. The background fields, namely the torus metric G and the two-form B-field, can be combined into a matrix $E = G + B$. T-duality transforms E to a new background E' through a fractional linear transformation[1]. Consistency of the asymmetric orbifold then requires that the $\mathbb{Z}_p$ transformation is a symmetry under which $E' = E$. This can be achieved only for special values of the moduli, which are therefore stabilised in these non-geometric constructions. The class of asymmetric orbifolds we consider preserves $\mathcal{N} = 6, 4, 2$ or 0 supersymmetry in 4D.

[1]For details on how T-duality acts on the background fields we refer to Buscher rules in Subsection I.3.3 and e.g. [20, 21].

IV.2.1 Asymmetric orbifolds

For the construction of asymmetric orbifolds we follow the procedure presented in the original papers [22, 23]. In general, upon compactification of the IIB superstring on T^6 the momentum and winding numbers take values in a Narain lattice $\Gamma^{6,6}$, which is an even, self-dual lattice [24]. For our purposes we decompose $T^6 = T^4 \times T^2$ and correspondingly decompose the lattice as $\Gamma^{4,4}(\mathfrak{g}) \oplus \Gamma^{2,2}$, where $\Gamma^{4,4}(\mathfrak{g})$ is an even, self-dual Lie algebra lattice which has symmetries acting purely on the left-movers and symmetries acting purely on the right-movers. Such a lattice can be realised at special points in the moduli space as

$$\Gamma^{4,4}(\mathfrak{g}) \equiv \{(p_{\rm L}, p_{\rm R}) |\, p_{\rm L} \in \Lambda_W(\mathfrak{g}),\, p_{\rm R} \in \Lambda_W(\mathfrak{g}),\, p_{\rm L} - p_{\rm R} \in \Lambda_R(\mathfrak{g})\}\,. \tag{IV.2.2}$$

Here $\mathfrak{g}$ is a Lie algebra of rank four and $\Lambda_W(\mathfrak{g})$, $\Lambda_R(\mathfrak{g})$ denote the weight and root lattices of $\mathfrak{g}$, respectively. Now, the symmetry we orbifold by acts as an automorphism of $\Gamma^{4,4}(\mathfrak{g})$ and as a shift on $\Gamma^{2,2}$. Here we will only consider automorphisms that act as a rotation on the left-movers and a separate rotation on the right-movers[2], $\mathcal{M}_\theta = (\mathcal{N}_{\rm L}, \mathcal{N}_{\rm R}) \in {\rm SO}(4)_{\rm L} \times {\rm SO}(4)_{\rm R} \subset {\rm SO}(4,4)$, the latter being the T-duality group of T^4. For a $\mathbb{Z}_p$ orbifold, we require that the rotation satisfies $(\mathcal{M}_\theta)^p = 1$. Also, in order to properly define the orbifold action on fermions the rotation matrix $\mathcal{M}_\theta \in {\rm SO}(4,4)$ should be uplifted to a monodromy matrix $\mathcal{M} \in {\rm Spin}(4,4)$; for more details see [2].

Since the orbifold acts as a shift on $\Gamma^{2,2}$, it leaves $\Gamma^{2,2}$ invariant[3]. On the other hand, $\Gamma^{4,4}(\mathfrak{g})$ is not in general invariant under the rotation $\mathcal{M}_\theta$. The sublattice $I \subset \Gamma^{4,4}(\mathfrak{g})$ that is invariant under the orbifold action is given by

$$I \equiv \{p \in \Gamma^{4,4}(\mathfrak{g}) \,|\, \mathcal{M}_\theta \cdot p = p\}\,. \tag{IV.2.3}$$

Then the complete sublattice that is invariant under the orbifold action is

$$\hat{I} = I \oplus \Gamma^{2,2}\,. \tag{IV.2.4}$$

It will be useful to determine the orbifold action on the worldsheet fields. We denote the two real T^2 coordinates by Z_1, Z_2 and the four real T^4 coordinates by $Y^m, m = 1, \ldots 4$, which we combine into two complex coordinates $W^i = \frac{1}{\sqrt{2}}(Y^{2i-1} + iY^{2i})$ with $i = 1, 2$. We parametrize the rotations $(\mathcal{N}_{\rm L}, \mathcal{N}_{\rm R}) \in {\rm SO}(4)_{\rm L} \times {\rm SO}(4)_{\rm R} \subset {\rm SO}(4,4)$ by four mass parameters

$$\mathcal{N}_{\rm L} = \begin{pmatrix} \mathscr{R}(m_1 + m_3) & 0 \\ 0 & \mathscr{R}(m_1 - m_3) \end{pmatrix}, \quad \mathcal{N}_{\rm R} = \begin{pmatrix} \mathscr{R}(m_2 + m_4) & 0 \\ 0 & \mathscr{R}(m_2 - m_4) \end{pmatrix}, \tag{IV.2.5}$$

where we use the notation $\mathscr{R}(x) = \left(\begin{smallmatrix} \cos x & -\sin x \\ \sin x & \cos x \end{smallmatrix}\right)$ for a 2×2 rotation matrix. Then, the orbifold acts on the bosonic torus coordinates through (asymmetric)

[2] A discussion on consistent rotations can be found e.g. in [25], cf. appendix B.

[3] Due to the shift, momentum states pick up a phase in the untwisted sector. In the twisted sectors states become massive.

rotations

$$\begin{aligned} W_{\rm L}^1 &\to e^{i(m_1+m_3)}\, W_{\rm L}^1\,, \quad W_{\rm L}^2 \to e^{i(m_1-m_3)}\, W_{\rm L}^2\,, \\ W_{\rm R}^1 &\to e^{i(m_2+m_4)}\, W_{\rm R}^1\,, \quad W_{\rm R}^2 \to e^{i(m_2-m_4)}\, W_{\rm R}^2\,, \end{aligned} \tag{IV.2.6}$$

and with the same action on their worldsheet superpartners. Symmetric orbifolds arise in the case in which $m_1 = m_2$ and $m_3 = m_4$. The rotations on the torus are accompanied by a shift along one of the T^2 coordinates, which makes the orbifold freely acting. Without loss of generality, we choose

$$Z_1 \to Z_1 + \tfrac{2\pi\mathcal{R}_5}{p}\,, \quad Z_2 \to Z_2\,, \tag{IV.2.7}$$

where $\mathcal{R}_5$ is the radius of the S^1 on which the orbifold acts as a shift, and $\mathcal{R}_5 = pR_5$ where R_5 is the no-shift S^1 radius. Also, we will denote by $\mathcal{R}_4$ the radius of the S^1 which is inert under the orbifold action.

In order for strings to close in our geometry, they need to satisfy the boundary conditions

$$\begin{aligned} X^{\hat\mu}(\sigma^0,\sigma^1+2\pi) &= X^{\hat\mu}(\sigma^0,\sigma^1)\,, \\ Z_1(\sigma^0,\sigma^1+2\pi) &= Z_1(\sigma^0,\sigma^1) + 2\pi\mathcal{R}_5\left(w^1+\tfrac{k}{p}\right)\,, \\ W_{\rm L}^1(\sigma^0,\sigma^1+2\pi) &= e^{ik(m_1+m_3)}\, W_{\rm L}^1(\sigma^0,\sigma^1)\,, \\ W_{\rm R}^1(\sigma^0,\sigma^1+2\pi) &= e^{ik(m_2+m_4)}\, W_{\rm R}^1(\sigma^0,\sigma^1)\,, \\ W_{\rm L}^2(\sigma^0,\sigma^1+2\pi) &= e^{ik(m_1-m_3)}\, W_{\rm L}^2(\sigma^0,\sigma^1)\,, \\ W_{\rm R}^2(\sigma^0,\sigma^1+2\pi) &= e^{ik(m_2-m_4)}\, W_{\rm R}^2(\sigma^0,\sigma^1)\,. \end{aligned} \tag{IV.2.8}$$

Here, $X^{\hat\mu} = \{X^0,\ldots,X^3,Z_2\}$, σ^0 and σ^1 are the Lorentzian coordinates on the worldsheet, and $w^1 \in \mathbb{Z}$ is the winding number along the S^1 on which the orbifold acts with a shift (we omit writing down the winding modes on the rest of the compact directions here for simplicity of the formulae). Such a background is non-geometric and also non-commutative. Also, $k = 0,\ldots,p-1$ is an integer that distinguishes between the various sectors. We have the untwisted sector for $k = 0$, and $p-1$ twisted sectors for the other values of k in which case the string closes up to the action of the $\mathbb{Z}_p$ symmetry.

For each mass parameter that is not zero (mod 2π) a pair of gravitini becomes massive. So, in order to obtain an $\mathcal{N} = 2$ theory only one mass parameter should be set to zero. These mass parameters can be translated to the more familiar language of twist vectors used in the orbifold literature as follows[4]

$$\begin{aligned} \tilde u \equiv (\tilde u_3,\, \tilde u_4) &= \frac{1}{2\pi}\,(m_1+m_3,\, m_1-m_3)\ , \\ u \equiv (u_3,\, u_4) &= \frac{1}{2\pi}\,(m_2+m_4,\, m_2-m_4)\ . \end{aligned} \tag{IV.2.9}$$

[4]In this chapter, the left-moving and right-moving convention is inverse from Chapter I, i.e. the tilde variables (and barred functions in the partition function) in this chapter are in the left-moving sector. In addition, compared with the notation used in [2], we simply omit here the two first trivial entries of the twist vectors. Comparing with [3], we have $\tilde u = \phi_{\rm L}$ and $u = \phi_{\rm R}$.

With these at hand, it is straightforward to see that

$$\mathcal{N}_{\rm L} = \begin{pmatrix} \mathscr{R}(2\pi\tilde{u}_3) & 0 \\ 0 & \mathscr{R}(2\pi\tilde{u}_4) \end{pmatrix}, \qquad \mathcal{N}_{\rm R} = \begin{pmatrix} \mathscr{R}(2\pi u_3) & 0 \\ 0 & \mathscr{R}(2\pi u_4) \end{pmatrix}, \tag{IV.2.10}$$

Also, the shift along the one circle of T^2 (IV.2.7) can be represented by a shift vector

$$v = \begin{pmatrix} \frac{1}{p} \\ 0 \\ 0 \\ 0 \end{pmatrix}. \tag{IV.2.11}$$

This is in the vector representation of $\mathrm{Spin}(2,2)$ and written in the basis of winding (w^i) and momentum (n_i) numbers. Recall that in this basis a vector of the lattice $\Gamma^{2,2}$, associated with T^2, can be written as

$$P = \begin{pmatrix} w^1 \\ w^2 \\ n_1 \\ n_2 \end{pmatrix}. \tag{IV.2.12}$$

Finally, we have to ensure that our models are modular invariant. This requires that the following conditions hold [3, 26]

$$p\sum_{i=3}^{4} \tilde{u}_i \in 2\mathbb{Z} \qquad \text{and} \qquad p\sum_{i=3}^{4} u_i \in 2\mathbb{Z}\,, \tag{IV.2.13}$$

where p is the orbifold rank. Also, if p is even, we need to check the additional condition for the momenta[5] $(p_{\rm L}, p_{\rm R}) \in \Gamma^{4,4}(\mathfrak{g})$

$$p_{\rm L}\mathcal{N}_{\rm L}^{p/2}p_{\rm L} - p_{\rm R}\mathcal{N}_{\rm R}^{p/2}p_{\rm R} \in 2\mathbb{Z}\,. \tag{IV.2.14}$$

IV.2.2 Duality groups of the orbifolded theory

The compactification of type II string theory on T^6 has $\mathcal{N} = 8$ supergravity as its low energy effective field theory. This has 70 massless scalars that parametrise the moduli space

$$\mathcal{M} = \frac{\mathrm{E}_{7(7)}}{\mathrm{SU}(8)/\mathbb{Z}_2}\,. \tag{IV.2.15}$$

The 38 scalars from the NS-NS sector parametrise a subspace, which factorises as

$$\mathcal{M}_{\rm NS} = \frac{\mathrm{SL}(2)}{\mathrm{U}(1)} \times \frac{\mathrm{Spin}(6,6)}{\mathrm{Spin}(6)\times\mathrm{Spin}(6)}\,. \tag{IV.2.16}$$

In type IIB, the first factor is parametrised by the axion and a shifted dilaton (the axion is a scalar dual to the 4D NS-NS two form) and the second factor is parameterised by the 36 moduli for the metric and B-field on T^6.

[5] In some cases it is possible to construct consistent orbifolds even if this condition is not satisfied [27].

The duality group of the effective supergravity theory is $\mathrm{E}_{7(7)}$, which has a maximal subgroup

$$\mathrm{E}_{7(7)} \supset \mathrm{SL}(2) \times \mathrm{Spin}(6,6)\ . \tag{IV.2.17}$$

In the quantum theory the duality group $\mathrm{E}_{7(7)}$ is broken to its discrete U-duality subgroup $\mathrm{E}_{7(7)}(\mathbb{Z})$, so that the $\mathrm{SL}(2) \times \mathrm{Spin}(6,6)$ subgroup is broken to a discrete group $\mathrm{SL}(2,\mathbb{Z}) \times \mathrm{Spin}(6,6;\mathbb{Z})$, forming the S- and T-duality groups of type II string theory on T^6 [19]. We mention that this 4D S-duality, which will be referred to here as $\mathrm{SL}(2)_S$, should not be confused with the $10D$ S-duality of type IIB. Note that the **56** representation of $\mathrm{E}_{7(7)}$ decomposes into $\mathrm{SL}(2) \times \mathrm{Spin}(6,6)$ representations as follows:

$$\mathbf{56} \to (\mathbf{2},\mathbf{12}) + (\mathbf{1},\mathbf{32}). \tag{IV.2.18}$$

The NS-NS charges are in the $(\mathbf{2},\mathbf{12})$ representation, consisting of the 6 momenta and 6 winding numbers, which are the perturbative charges, together with 6 NS5-brane charges and 6 KK monopole charges, which are the non-perturbative charges [19].

Orbifolding this theory breaks the U-duality group $\mathrm{E}_{7(7)}(\mathbb{Z})$ to a subgroup. The orbifold is specified by a twist and a shift, and the U-duality group is broken to the subgroup that preserves both of these, which we will refer to as the orbifold duality group. This is then the subgroup of $\mathrm{E}_{7(7)}(\mathbb{Z})$ that commutes with the twist and preserves the shift vector (up to the addition of a lattice vector and up to a sign; see below).

For the theories we consider in this chapter with decomposition $T^6 = T^4 \times T^2$, the orbifold duality group is in fact a subgroup of $\mathrm{SL}(2,\mathbb{Z}) \times \mathrm{Spin}(6,6;\mathbb{Z})$. The subgroup of $\mathrm{Spin}(6,6)$ acting as T-duality on T^4 is $\mathrm{Spin}(4,4)$ and, for each orbifold, the twist matrix specified by (IV.2.10) is in the compact part of this, $\mathrm{Spin}(4) \times \mathrm{Spin}(4)$. Let $\mathcal{C}$ be the subgroup of $\mathrm{Spin}(4,4)$ that commutes with the twist. For the theories considered here, the twist then breaks $\mathrm{Spin}(6,6)$ to $\mathrm{Spin}(2,2) \times \mathcal{C}$ in the supergravity theory. In the orbifolded string theory, the group $\mathcal{C}$ is broken further to a discrete subgroup $\mathcal{C}(\mathbb{Z})$.

The shift vector (IV.2.11) leads to a further breaking of the symmetry. As in (IV.2.7), this vector v represents an orbifold shift along the circle with radius $\mathcal{R}_5$ by $2\pi\mathcal{R}_5/p$. Adding any integer-valued 4-vector w in the lattice $\mathbb{Z}^4$ to v will give the same orbifold. Furthermore, v and $-v$ specify physically equivalent orbifolds as the sign of v is changed by the reflection $Z_1 \to -Z_1$; such a reflection is an element of the T-duality group $\mathrm{Spin}(6,6,\mathbb{Z})$. Note that changing v to $-v$ has the same effect as replacing the monodromy $\mathcal{M}$ with $\mathcal{M}^{-1}$. If $\mathcal{M}$ is expressed in terms of a mass matrix M by $\mathcal{M} = e^M$, then this amounts to changing the sign of the mass matrix M.

Note that this discussion of duality symmetries applies to the untwisted sector, and we discuss the subgroup of the original duality that is a symmetry of the untwisted sector of the orbifold. However, the orbifold introduces twisted sectors, and there can be new duality symmetries relating the untwisted and twisted sectors that do not directly arise from the duality symmetry of the theory before

the orbifold. For example, consider type IIA string theory compactified on T^4, with U-duality symmetry $\mathrm{Spin}(5,5;\mathbb{Z})$. Consider now the $\mathbb{Z}_2$ orbifold of this which gives a special point in the K3 moduli space. The untwisted sector is invariant under an $\mathrm{SO}(4,4;\mathbb{Z})$ subgroup of the duality group, but the full theory in fact has a duality symmetry $\mathrm{SO}(4,20;\mathbb{Z})$. Note that $\mathrm{SO}(4,20)$ is not a subgroup of $\mathrm{Spin}(5,5)$ and the extra duality symmetries include ones mixing untwisted and twisted sectors. Whether or not there are extra symmetries of this kind depends on the model. We will see below that some of our orbifold examples have this kind of duality enhancement.

Before turning to the subgroup of $\mathrm{Spin}(2,2)$ that is preserved in the orbifold, we discuss an $\mathrm{SL}(2)$ analogue that introduces the relevant groups. Consider, then, the simpler problem of finding the subgroup of $\mathrm{SL}(2,\mathbb{Z})$ that preserves a 2-vector of the form

$$V = \begin{pmatrix} \frac{1}{p} \\ 0 \end{pmatrix} \tag{IV.2.19}$$

up to the addition of a lattice vector $\begin{pmatrix} w \\ n \end{pmatrix} \in \mathbb{Z}^2$. It is easy to check that the result is the group

$$\Gamma_1(p) = \left\{ \begin{pmatrix} a & b \\ c & d \end{pmatrix} \in \mathrm{SL}(2,\mathbb{Z}) : \quad a,d = 1 \bmod p\,, \quad c = 0 \bmod p \right\}. \tag{IV.2.20}$$

The subgroup preserving V up to a sign, i.e. taking V to $\pm V$ plus a lattice vector, is

$$\hat{\Gamma}_1(p) = \left\{ \begin{pmatrix} a & b \\ c & d \end{pmatrix} \in \mathrm{SL}(2,\mathbb{Z}) : \quad a,d = \pm 1 \bmod p\,, \quad c = 0 \bmod p \right\}. \tag{IV.2.21}$$

For $p = 2$, we have that $-1 = 1 \bmod 2$ and so

$$\hat{\Gamma}_1(2) = \Gamma_1(2)\,, \tag{IV.2.22}$$

while for $p > 2$

$$\hat{\Gamma}_1(p) = \Gamma_1(p) \times \mathbb{Z}_2\,, \tag{IV.2.23}$$

with the $\mathbb{Z}_2$ consisting of the 2×2 matrices $\{\mathbf{1}, -\mathbf{1}\}$.

For $\mathrm{SL}(2,\mathbb{R})$, the subgroup preserving V up to a lattice vector is

$$\Delta_1(p) = \left\{ \begin{pmatrix} a & b \\ c & d \end{pmatrix} \in \mathrm{SL}(2,\mathbb{R}) : \quad a = 1 \bmod p\,, \quad c = 0 \bmod p \right\}, \tag{IV.2.24}$$

while the subgroup taking V to $\pm V$ plus a lattice vector is

$$\hat{\Delta}_1(p) = \left\{ \begin{pmatrix} a & b \\ c & d \end{pmatrix} \in \mathrm{SL}(2,\mathbb{R}) : \quad a = \pm 1 \bmod p\,, \quad c = 0 \bmod p \right\}, \tag{IV.2.25}$$

Both of these contain the stability subgroup preserving V, which is the group $\mathbb{R}$ of upper triangular matrices

$$\begin{pmatrix} 1 & b \\ 0 & 1 \end{pmatrix} . \tag{IV.2.26}$$

We now return to the breaking of the T-duality group of T^2, which is

$$\mathrm{Spin}(2,2;\mathbb{Z}) \cong \mathrm{SL}(2,\mathbb{Z})_T \times \mathrm{SL}(2,\mathbb{Z})_U \,, \tag{IV.2.27}$$

where $\mathrm{SL}(2,\mathbb{Z})_T$ acts on the complexified Kähler modulus T of the T^2, while $\mathrm{SL}(2,\mathbb{Z})_U$ acts on the complex structure modulus U. We denote the (dimensionful) metric and antisymmetric Kalb-Ramond B-field on T^2 by g_{ij} and b_{ij}, respectively. Here $i,j = 1,2$, and $b_{ij} = b\,\varepsilon_{ij}$, where b is a constant, and $\varepsilon_{12} = -\varepsilon_{21} = 1$, $\varepsilon_{11} = \varepsilon_{22} = 0$. Given these, we can define the moduli T and U as[6] (see e.g. [28])

$$\begin{aligned} T &= T_1 + iT_2 = \frac{1}{\alpha'}\left(b + i\sqrt{\det g}\right) , \\ U &= U_1 + iU_2 = \frac{g_{12}}{g_{11}} + i\frac{\sqrt{\det g}}{g_{11}} . \end{aligned} \tag{IV.2.28}$$

Then, the T^2 metric can be expressed in terms of these moduli as

$$g_{ij} = \alpha' \frac{T_2}{U_2} \begin{pmatrix} 1 & U_1 \\ U_1 & |U|^2 \end{pmatrix} . \tag{IV.2.29}$$

Note that for a rectangular torus, that is $U_1 = 0$, and a trivial B-field, $T_2 = \mathcal{R}_5\mathcal{R}_4/\alpha'$ and $U_2 = \mathcal{R}_4/\mathcal{R}_5$, where $\mathcal{R}_5$ is the radius of the circle on which the orbifold acts by a shift and $\mathcal{R}_4$ is the radius of the circle that is invariant under the orbifold action.

The T^2 partition function, in the untwisted orbifold sector and without the insertion of the orbifold group element, reads

$$Z_{T^2}[0,0] = \frac{1}{(\eta\bar{\eta})^2} \sum_{\{n_i,w_i\}\in\mathbb{Z}^4} \bar{q}^{\frac{1}{2}p_{\mathrm{L}}^2}\, q^{\frac{1}{2}p_{\mathrm{R}}^2} , \qquad i = 1,2 \,, \tag{IV.2.30}$$

where[7]

$$\begin{aligned} p_{\mathrm{L}}^2 &= \frac{1}{2T_2U_2}\left|n_2 - Un_1 + \overline{T}w_1 + \overline{T}Uw_2\right|^2 , \\ p_{\mathrm{R}}^2 &= \frac{1}{2T_2U_2}\left|n_2 - Un_1 + Tw_1 + TUw_2\right|^2 . \end{aligned} \tag{IV.2.31}$$

Now, the two $\mathrm{SL}(2,\mathbb{Z})$ subgroups of the T-duality group of T^2 act on the moduli T and U as follows:

$$\mathrm{SL}(2,\mathbb{Z})_T : \quad \frac{aT+b}{cT+d} \,, \qquad ad - bc = 1 \,, \tag{IV.2.32}$$

[6] Different from other chapters, due to the shift, we define $U \propto 1/g_{11}$ rather than $1/g_{22}$.

[7] Here and below we label both momentum and winding numbers by a subscript for simplicity of the formulae.

$$\mathrm{SL}(2,\mathbb{Z})_U : \quad \frac{a'U+b'}{c'U+d'}\,, \qquad a'd'-b'c'=1\,. \tag{IV.2.33}$$

The T-duality group also acts on the momentum and winding numbers by $\mathrm{Spin}(2,2;\mathbb{Z})$ transformations, leaving $p^2_{\mathrm{L/R}}$ invariant. The action on the Narain lattice is given by (see e.g. [29])

$$\mathrm{SL}(2,\mathbb{Z})_T : \quad \begin{pmatrix} w_1\\ w_2\\ n_1\\ n_2 \end{pmatrix} \to \begin{pmatrix} d & 0 & 0 & -c\\ 0 & d & c & 0\\ 0 & b & a & 0\\ -b & 0 & 0 & a \end{pmatrix} \begin{pmatrix} w_1\\ w_2\\ n_1\\ n_2 \end{pmatrix}\,, \tag{IV.2.34}$$

$$\mathrm{SL}(2,\mathbb{Z})_U : \quad \begin{pmatrix} w_1\\ w_2\\ n_1\\ n_2 \end{pmatrix} \to \begin{pmatrix} a' & -b' & 0 & 0\\ -c' & d' & 0 & 0\\ 0 & 0 & d' & c'\\ 0 & 0 & b' & a' \end{pmatrix} \begin{pmatrix} w_1\\ w_2\\ n_1\\ n_2 \end{pmatrix}\,, \tag{IV.2.35}$$

Notice that $\mathrm{SL}(2,\mathbb{Z})_U$ does not mix winding and momenta, but $\mathrm{SL}(2,\mathbb{Z})_T$ does. It is easy to check that the two SL(2)'s commute in the basis of winding and momentum numbers. Also, an element $(g_T, g_U) \in \mathrm{SL}(2,\mathbb{Z})_T \times \mathrm{SL}(2,\mathbb{Z})_U$ can be embedded in $\mathrm{SO}^+(2,2;\mathbb{Z})$ as[8]

$$(g_T,g_U) \in \mathrm{SL}(2,\mathbb{Z})_T \times \mathrm{SL}(2,\mathbb{Z})_U \cong \mathrm{SO}^+(2,2;\mathbb{Z}) : \begin{pmatrix} da' & -db' & -cb' & -ca'\\ -dc' & dd' & cd' & cc'\\ -bc' & bd' & ad' & ac'\\ -ba' & bb' & ab' & aa' \end{pmatrix}. \tag{IV.2.36}$$

Consider now the shift vector v given in (IV.2.11). Under $\mathrm{SL}(2,\mathbb{Z})_T \times \mathrm{SL}(2,\mathbb{Z})_U$, it transforms as the $(\mathbf{2},\mathbf{2})$ representation. The vector v represents the orbifold shift along the circle of radius $\mathcal{R}_5$, and induces a shift in the winding number w_1. Then, the "shifted" T^2 partition function will be given by[9]

$$Z_{T^2}[k,l] = \frac{1}{(\eta\bar\eta)^2} \sum_{\{n_i,w_i\}\in\mathbb{Z}^4} e^{\frac{2\pi i l n_1}{p}}\, \bar q^{\frac12 p^2_{\mathrm{L}}(k)}\, q^{\frac12 p^2_{\mathrm{R}}(k)}\,, \qquad i=1,2\,, \tag{IV.2.37}$$

where $k = 0,\dots,p-1$ labels the twisted sectors ($k=0$ corresponds to the untwisted sector) and summation over $l = 0,\dots,p-1$ implements the orbifold projection[10]. Also,

$$\begin{aligned} p^2_{\mathrm{L}}(k) &= \frac{1}{2T_2U_2}\left|n_2 - Un_1 + \overline{T}\left(w_1+\tfrac{k}{p}\right) + \overline{T}Uw_2\right|^2\,,\\ p^2_{\mathrm{R}}(k) &= \frac{1}{2T_2U_2}\left|n_2 - Un_1 + T\left(w_1+\tfrac{k}{p}\right) + TUw_2\right|^2\,. \end{aligned} \tag{IV.2.38}$$

[8] $\mathrm{SO}^+(2,2;\mathbb{Z})$ is the component of $\mathrm{O}(2,2;\mathbb{Z})$ connected to the identity. Also, $\mathrm{SL}(2,\mathbb{Z}) \times \mathrm{SL}(2,\mathbb{Z}) \cong \mathrm{Spin}(2,2;\mathbb{Z})$ is the double cover of $\mathrm{SO}^+(2,2;\mathbb{Z})$.

[9] A more general discussion on shifted lattice sums can be found in e.g. [30].

[10] If we denote the orbifold group element by g, with $g^p = 1$, then the projection operator takes the form $P = \frac{1}{p}(1+g+g^2+\cdots+g^{p-1})$.

Now, a generic $\mathrm{Spin}(2,2;\mathbb{Z})$ T-duality transformation will transform the shift vector v to another shift vector v', which will not leave the partition function invariant. This means that if we start with a model with shift vector v, after a T-duality transformation we will end up with an inequivalent model with shift vector v'. Hence, generic T-duality transformations will not be in the orbifold duality group.

However, as in the SL(2) example discussed before, there exists a subgroup of the T-duality group, $\mathrm{Spin}(2,2;\mathbb{Z})$, that acts on the shift vector in such a way that the partition function remains invariant. This subgroup will be in the orbifold duality group. Firstly, a shift, $v \to v+P$, where P is a lattice vector, corresponds to a shift $1/p \to 1/p+\mathbb{Z}$ in the phase factor in (IV.2.37), and a shift of the momentum and winding numbers in (IV.2.38) by integers. Therefore, this is a symmetry of the partition function. In addition, a reflection, $v \to -v$ simply amounts to $l \to -l$ and $k \to -k$ in (IV.2.37) and (IV.2.38), which is also a symmetry of the partition function. So, in order to determine the orbifold duality group associated with T^2, we need to find the subgroup of $\mathrm{Spin}(2,2;\mathbb{Z})$ that generates these two symmetries (for a similar discussion see also [31], appendix C).

Let us first focus on the transformations that preserve the shift vector v up to lattice translations. By combining (IV.2.11) with (IV.2.34) and (IV.2.35), we find that the duality group $\mathrm{SL}(2,\mathbb{Z})_T$ is broken to $\Gamma^1(p)_T$ and $\mathrm{SL}(2,\mathbb{Z})_U$ is broken to $\Gamma_1(p)_U$, where

$$\Gamma^1(p)_T = \left\{ \begin{pmatrix} a & b \\ c & d \end{pmatrix} \in \mathrm{SL}(2,\mathbb{Z})_T : a,d = 1 \bmod p\,, \quad b = 0 \bmod p \right\}, \tag{IV.2.39}$$

$$\Gamma_1(p)_U = \left\{ \begin{pmatrix} a' & b' \\ c' & d' \end{pmatrix} \in \mathrm{SL}(2,\mathbb{Z})_U : a',d' = 1 \bmod p\,, \quad c' = 0 \bmod p \right\}. \tag{IV.2.40}$$

The groups $\Gamma^1(p)$ and $\Gamma_1(p)$ are isomorphic (the isomorphism is simply given by transposition) but are embedded differently in $\mathrm{SL}(2,\mathbb{Z})$. The appearance of $\Gamma^1(p)_T$ instead of $\Gamma_1(p)_T$ is due to the embedding of $\mathrm{SL}(2,\mathbb{Z})_T$ in $\mathrm{Spin}(2,2,\mathbb{Z})$. It is important to stress that the surviving duality groups depend on the particular shift vector. For instance, a shift along the radius $\mathcal{R}_4$ that shifts w_2 instead of w_1, would lead to two identical $\Gamma^1(p)_T \times \Gamma^1(p)_U$ subgroups (see e.g. [12, 32] or [31] for examples).

Regarding the reflection, $v \to -v$, we can see that it can be realized by the values $a = d = -1, b = c = 0$ in (IV.2.34), and $a' = d' = -1, b' = c' = 0$ in (IV.2.35), which generate another two $\mathbb{Z}_2$ subgroups for $p > 2$. Concluding, we have found that the T-duality group of T^2 is broken, due to the presence of the shift vector, to

$$\hat{\Gamma}^1(p)_T \times \hat{\Gamma}_1(p)_U \subset \mathrm{SL}(2,\mathbb{Z})_T \times \mathrm{SL}(2,\mathbb{Z})_U\,. \tag{IV.2.41}$$

Now, by combining all the above, we conclude that the T-duality group

$\mathrm{Spin}(6,6;\mathbb{Z})$ of T^6 is broken to the orbifold T-duality group

$$\hat{\Gamma}^1(p)_T \times \hat{\Gamma}_1(p)_U \times \mathcal{C}(\mathbb{Z}) \subset \mathrm{SL}(2,\mathbb{Z})_T \times \mathrm{SL}(2,\mathbb{Z})_U \times \mathrm{Spin}(4,4;\mathbb{Z}) \subset \mathrm{Spin}(6,6;\mathbb{Z})\,. \tag{IV.2.42}$$

For the supergravity theory, the shift breaks $\mathrm{SL}(2,\mathbb{R})_T \times \mathrm{SL}(2,\mathbb{R})_U$ to the subgroup of matrices

$$\left\{ \begin{pmatrix} a & b \\ c & d \end{pmatrix} \in \mathrm{SL}(2,\mathbb{R})_T, \quad \begin{pmatrix} a' & b' \\ c' & d' \end{pmatrix} \in \mathrm{SL}(2,\mathbb{R})_U : \right. \\ \left. da' = \pm 1 \bmod p\,, \quad b = 0 \bmod p, \quad c' = 0 \bmod p, \right\}, \tag{IV.2.43}$$

which is the group

$$(\mathbb{R} \times \mathbb{Z}_2) \ltimes \left(\hat{\Delta}^1(p) \times \hat{\Delta}_1(p) \right)\,, \tag{IV.2.44}$$

where $\hat{\Delta}^1(p)$ is defined by

$$\hat{\Delta}^1(p) = \left\{ \begin{pmatrix} a & b \\ c & d \end{pmatrix} \in \mathrm{SL}(2,\mathbb{R}) : \quad d = \pm 1 \bmod p\,, \quad b = 0 \bmod p \right\}. \tag{IV.2.45}$$

Then in the supergravity theory, $\mathrm{Spin}(6,6)$ is broken to the product of this group with $\mathcal{C}$.

We now turn to the breaking of the S-duality group $\mathrm{SL}(2)_S$. Under $\mathrm{SL}(2)_S$, the perturbative 4-vector v transforms into a non-perturbative 4-vector of NS5-brane charges and KK monopole charges. Then the shift vector transforms as the **2** representation under $\mathrm{SL}(2)_S$, so that it can be regarded as part of an 8-vector transforming as the $(\mathbf{4},\mathbf{2})$ representation of $\mathrm{Spin}(2,2) \times \mathrm{SL}(2)_S$. However, this $\mathrm{Spin}(2,2)$ factorises as $\mathrm{Spin}(2,2) = \mathrm{SL}(2)_T \times \mathrm{SL}(2)_U$, so that $\mathrm{Spin}(2,2) \times \mathrm{SL}(2)_S = \mathrm{SL}(2)_T \times \mathrm{SL}(2)_U \times \mathrm{SL}(2)_S$ and under this the shift vector transforms as a $(\mathbf{2},\mathbf{2},\mathbf{2})$. The non-zero component of (IV.2.11) is then part of an $\mathrm{SL}(2)_S$ doublet of the form (IV.2.19). From the earlier discussion, the subgroup of $\mathrm{SL}(2,\mathbb{Z})_S$ preserving this up to a sign and up to a lattice vector is $\hat{\Gamma}^1(p)_S$, so that the S-duality is broken to this subgroup. Then $\mathrm{SL}(2,\mathbb{Z})_T \times \mathrm{SL}(2,\mathbb{Z})_U \times \mathrm{SL}(2,\mathbb{Z})_S$ is broken to the subgroup $\hat{\Gamma}^1(p)_T \times \hat{\Gamma}_1(p)_U \times \hat{\Gamma}^1(p)_S$ and we have the final result that the U-duality group is broken to

$$\mathcal{K}(\mathbb{Z}) = \hat{\Gamma}^1(p)_T \times \hat{\Gamma}_1(p)_U \times \hat{\Gamma}^1(p)_S \times \mathcal{C}(\mathbb{Z})\,. \tag{IV.2.46}$$

For the supergravity limit, the subgroup of $\mathrm{SL}(2)_S$ preserving the shift up to a sign and a lattice vector is $\hat{\Delta}^1(p)$. However, the subgroup of $\mathrm{SL}(2)_T \times \mathrm{SL}(2)_U \times \mathrm{SL}(2)_S$ preserving the shift is slightly larger than the product of the T-duality

group given above. It is the group of matrices

$$\left\{ \begin{pmatrix} a & b \\ c & d \end{pmatrix} \in \mathrm{SL}(2,\mathbb{R})_T,\ \begin{pmatrix} a' & b' \\ c' & d' \end{pmatrix} \in \mathrm{SL}(2,\mathbb{R})_U,\ \begin{pmatrix} a'' & b'' \\ c'' & d'' \end{pmatrix} \in \mathrm{SL}(2,\mathbb{R})_S : \right.$$
$$\left. da'd'' = \pm 1 \bmod p\,,\ b = 0 \bmod p,\ c' = 0 \bmod p,\ b'' = 0 \bmod p \right\}. \tag{IV.2.47}$$

The supergravity duality group is then the product of this with $\mathcal{C}$.

IV.3 An STU-like $\mathbb{Z}_6$ model

In this section we discuss an $\mathcal{N} = 2, D = 4$ model, with three vector multiplets and two hypermultiplets arising in the massless untwisted orbifold sector. This model can be obtained from a circle reduction of an $\mathcal{N} = 2, D = 5$ freely acting $\mathbb{Z}_6$ orbifold model of IIB string theory on T^5 studied in [4]. We consider a $\mathbb{Z}_6$ orbifold with the following mass parameters

$$m_1 = \pi\ , \qquad m_2 = \frac{\pi}{3}\ , \qquad m_3 = \frac{2\pi}{3}\ , \qquad m_4 = 0\ . \tag{IV.3.1}$$

The corresponding twist vectors are (cf. (IV.2.9))

$$\tilde{u} = \left(\frac{5}{6}, \frac{1}{6}\right)\ , \qquad u = \left(\frac{1}{6}, \frac{1}{6}\right)\ , \tag{IV.3.2}$$

which satisfy (IV.2.13) (for this model $p = 6$), and the appropriate lattice is $\Gamma^{4,4}(A_2 \oplus A_2) \oplus \Gamma^{2,2}$. It is easy to verify that (IV.2.14) is also satisfied, as

$$p_{\mathrm{L}} \mathcal{N}_{\mathrm{L}}^3 p_{\mathrm{L}} - p_{\mathrm{R}} \mathcal{N}_{\mathrm{R}}^3 p_{\mathrm{R}} = -(p_{\mathrm{L}}^2 - p_{\mathrm{R}}^2) \in 2\mathbb{Z}\ . \tag{IV.3.3}$$

As a result, the theory is modular invariant. Notice that $\Gamma^{2,2}$ is left invariant under the twist. We picked this model because it has only NS-NS massless scalars and vectors. Consequently, the classical moduli space can be determined by simply computing the subgroup of the T-duality group that preserves the orbifold twist and shift, as explained in Subsection IV.2.2.

In the following, we will discuss the massless spectrum of our model in the untwisted sector, and the spectrum of the lightest states in the twisted sectors. Due to the orbifold shift, states in the twisted sectors are generically massive. However, there exist special lines in the bulk of the moduli space in which a finite number of massive twisted states become massless, which will be discussed in Subsection IV.4.2. Also, there exist points at infinite distance, where infinite towers of states become massless, and we will analyse these in Subsection IV.4.3.

IV.3.1 Untwisted sector

The massless spectrum in the untwisted sector of our $\mathbb{Z}_6$ model can be obtained by circle reduction of a five-dimensional model, with the same mass parameters

and twist vectors, that was studied in [4]. The untwisted massless spectrum of the five-dimensional model consists of the $\mathcal{N} = 2$ gravity multiplet, two vector multiplets, and two hypermultiplets, and all the fields come from the NS-NS and NS-R sectors. On reduction on a circle we simply get one additional vector multiplet. Then the massless untwisted orbifold spectrum consists of the $\mathcal{N} = 2$, $D = 4$ gravity multiplet coupled to 3 vector multiplets and 2 hypermultiplets; this can also be seen from the detailed analysis of the spectrum below.

The untwisted orbifold spectrum can be obtained from the partition function, which can be expanded as [2]

$$Z[0,l] = (q\bar{q})^{-\frac{1}{2}} \sum_{\{n_i,w_i\}\in\mathbb{Z}^4} e^{\frac{2\pi i l n_1}{p}}\, \bar{q}^{\frac{1}{2}p_{\rm L}^2(0)}\, q^{\frac{1}{2}p_{\rm R}^2(0)} \sum_{r,\tilde{r}} q^{\frac{1}{2}r^2}\, \bar{q}^{\frac{1}{2}\tilde{r}^2}\, e^{2\pi i l(\tilde{r}\cdot\tilde{u}-r\cdot u)}\, (1+\cdots)\,. \tag{IV.3.4}$$

Here, $r = (r_1, r_2, r_3, r_4)$ (and similarly $\tilde{r}$) is an SO(8) weight vector with each component $r_i \in \mathbb{Z}$ in the NS-sector and $r \in \mathbb{Z} + \frac{1}{2}$ in the R-sector, while the left- and right-moving momenta, $p^2_{\rm L/R}(k)$ are given in (IV.2.38). The GSO projection is $\sum_{i=1}^4 r_i \in 2\mathbb{Z}+1$ in the NS-sector and $\sum_{i=1}^4 r_i \in 2\mathbb{Z}$ in the R-sector. Finally, the dots denote contributions to the partition function from higher excited bosonic oscillator states.

Now, string states are constructed by tensoring left- and right-movers, and a generic state is characterised by the product $\tilde{r} \times r$. In order to implement the orbifold projection we need to sum over l and divide by the orbifold rank p. Then, the degeneracy of a state in the untwisted sector will be given by

$$D(k=0) = \frac{1}{p}\sum_{l=0}^{p-1} e^{2\pi i l\left[(\tilde{r}\cdot\tilde{u}-r\cdot u)+\frac{n_1}{p}\right]}\,. \tag{IV.3.5}$$

Note that states with trivial orbifold charge, i.e. trivial phase $e^{2\pi i l[(\tilde{r}\cdot\tilde{u}-r\cdot u)]}$, will survive the orbifold projection and will have degeneracy 1. States with non-trivial orbifold charge will survive the orbifold projection with the addition of appropriate momentum number n_1, such that they will become massive and will come with degeneracy 1.

The masses of left- and right-moving states can be read off from the exponents of $\bar{q}$ and q, respectively. In particular, the mass formulae read

$$\begin{aligned} \frac{\alpha' m_{\rm L}^2(0)}{2} &= \frac{1}{2}\tilde{r}^2 + \frac{1}{2}p_{\rm L}^2(0) - \frac{1}{2} + \widetilde{N}\,, \\ \frac{\alpha' m_{\rm R}^2(0)}{2} &= \frac{1}{2}r^2 + \frac{1}{2}p_{\rm R}^2(0) - \frac{1}{2} + N\,. \end{aligned} \tag{IV.3.6}$$

Here, $\widetilde{N}$ and N are integers, which refer to the bosonic occupation number of higher excited left- and right-moving oscillator states, respectively. In the untwisted sector, the lightest states satisfy $\widetilde{N} = N = 0$.

Let us now move on to the construction of massless states in the untwisted sector. First, we list in Table IV.1 the NS and R-sector SO(8) weight vectors for

the lightest left- and right-moving states that survive the GSO projection; all of these are massless in the absence of momentum and/or winding modes.

Sector	SO(8) weight
NS	$(\pm1,0,0,0),(0,\underline{0,0,\pm1})$
R	$\pm\left(\frac{1}{2},\frac{1}{2},\frac{1}{2},\frac{1}{2}\right),\pm\left(-\frac{1}{2},-\frac{1}{2},\frac{1}{2},\frac{1}{2}\right),\pm\left(\frac{1}{2},-\frac{1}{2},\frac{1}{2},-\frac{1}{2}\right),\pm\left(-\frac{1}{2},\frac{1}{2},\frac{1}{2},-\frac{1}{2}\right)$

Table IV.1: Here we list the weight vectors of the lightest left- and right-moving states in the untwisted sector. Underlying denotes permutation; e.g. $(0,\underline{0,0,1})$ denotes the states $(0,1,0,0)$, $(0,0,1,0)$ and $(0,0,0,1)$.

Massless string states in the untwisted sector must have a trivial orbifold charge, i.e. they must be invariant under $\mathbb{Z}_6$, and can be classified based on their helicity in 4D. The helicity of a state $(\tilde{r}_1,\tilde{r}_2,\tilde{r}_3,\tilde{r}_4)\times(r_1,r_2,r_3,r_4)$ is equal to $\tilde{r}_1-r_1$ [33]. As we can see from (IV.3.2) and (IV.3.5), massless states should satisfy $5\tilde{r}_3+\tilde{r}_4-(r_3+r_4)=0 \bmod 6$, which is the case only in the NS-NS and NS-R sectors. In the NS-NS sector we find the following massless states

$$\begin{aligned}
(\pm1,0,0,0)\times(\pm1,0,0,0) &: (\pm2)+2\times(0)\,,\\
(\pm1,0,0,0)\times(0,\pm1,0,0) &: 2\times(\pm1)\,,\\
(0,\pm1,0,0)\times(\pm1,0,0,0) &: 2\times(\pm1)\,,\\
(0,\pm1,0,0)\times(0,\pm1,0,0) &: 4\times(0)\,,\\
\pm[(0,0,1,0)\times(0,0,\underline{-1,0})] &: 4\times(0)\,,\\
\pm[(0,0,0,1)\times(0,0,\underline{1,0})] &: 4\times(0)\,.
\end{aligned} \tag{IV.3.7}$$

In total, we find the helicities that correspond to the graviton, (±2), 4 massless vectors, $4\times(\pm1)$, and 14 scalars, $14\times(0)$. The massless states in the NS-R sector can be constructed in a similar way. We find 2 gravitini, $2\times(\pm\frac{3}{2})$, and 10 dilatini, $10\times(\pm\frac{1}{2})$. Together the fields from the NS-NS and NS-R sectors form the $\mathcal{N}=2$, $D=4$ gravity multiplet, 3 vector multiplets and 2 hypermultiplets.

Note that the scalars in the 3 vector multiplets are the complex S, T and U moduli, where T and U are the T^2 moduli, defined in (IV.2.28), and S is defined by

$$S=a+ie^{-2\phi_4}\,, \tag{IV.3.8}$$

Here a is a scalar that is dual to the NS-NS B-field in four dimensions, and is usually referred to as the axion, and ϕ_4 is a scalar parametrising the four-dimensional string coupling by $\lambda_4=\langle e^{\phi_4}\rangle$. There are also 4 complex scalars in the two hypermultiplets.

Of course, all the aforementioned states in the NS-NS and NS-R sectors come with infinite towers of momentum and winding modes along T^2, and their masses

are given by (cf. (IV.2.31) and (IV.3.6))

$$\begin{aligned}\frac{\alpha' m_{\rm L}^2(0)}{2} &= \frac{1}{2}p_{\rm L}^2(0) = \frac{1}{4T_2U_2}|n_2 - Un_1 + \bar{T}w_1 + \bar{T}Uw_2|^2\,,\\ \frac{\alpha' m_{\rm R}^2(0)}{2} &= \frac{1}{2}p_{\rm R}^2(0) = \frac{1}{4T_2U_2}|n_2 - Un_1 + Tw_1 + TUw_2|^2\,.\end{aligned} \tag{IV.3.9}$$

Note that in these formulae the momentum number n_1 should obey $n_1 = 0$ mod 6, such that the states are invariant under the orbifold symmetry. Physical states should also satisfy the level-matching condition, $m_{\rm L}^2 = m_{\rm R}^2$, which in this case reads

$$n_1w_1 + n_2w_2 = 0\,. \tag{IV.3.10}$$

IV.3.2 Twisted sectors

As in the untwisted sector, the spectrum of lightest states in each twisted sector can be obtained from the partition function, which can be expanded as [2]

$$\begin{aligned}Z[k,l] =& \chi[k,l]\,\tilde{\chi}[k,l](q\bar{q})^{-\frac{1}{2}}\,e^{i(\tilde{\varphi}-\varphi)}q^{E_k}\,\bar{q}^{\widetilde{E}_k}\sum_{\{n_i,w_i\}\in\mathbb{Z}^4} e^{\frac{2\pi i l n_1}{p}}\,\bar{q}^{\frac{1}{2}p_{\rm L}^2(k)}\,q^{\frac{1}{2}p_{\rm R}^2(k)}\times\\ &\sum_{r,\tilde{r}} q^{\frac{1}{2}(r+ku)^2}\,\bar{q}^{\frac{1}{2}(\tilde{r}+k\tilde{u})^2}\,e^{2\pi i l(\tilde{r}\cdot\tilde{u}-r\cdot u)}\,e^{2\pi i l k(\tilde{u}^2-u^2)}\,(1+\cdots)\,.\end{aligned} \tag{IV.3.11}$$

Here, as in the untwisted sector, the dots denote contributions to the partition function from higher excited bosonic oscillator states, while

$$\chi[k,l] = \prod_{i=3}^{4} 2\sin(\pi\gcd(k,l)u_i)\,, \tag{IV.3.12}$$

is the number of "chiral" fixed points[11]. We note here that equation (IV.3.12) is valid for $ku_{3,4} \notin \mathbb{Z}$. If there exists $j \in [3,4]$ such that $ku_j \in \mathbb{Z}$, $\chi[k,l]$ should be divided by $2\sin(\pi l u_j)$ for $l \neq 0$, and replaced by $\prod_{i\neq j, ku_i\notin\mathbb{Z}} 2\sin(\pi k u_i)$ for $l = 0$ (see [34] for a relevant discussion). In addition, from the expansion of the bosonic piece of the partition function we obtain the phase factor

$$\varphi = 2\pi\sum_{u_i\notin\mathbb{Z}}\left(\frac{1}{2} - ku_i\right)lu_i\,, \tag{IV.3.13}$$

and a shift to the zero point energy given by

$$E_k = \sum_{u_i\notin\mathbb{Z}}\frac{1}{2}ku_i(1-ku_i)\,. \tag{IV.3.14}$$

[11] The orbifolds that we consider have fixed points on T^4. However, due to the shift along the one circle of T^2, there are no points left invariant under the full orbifold action. Also, $\gcd(k,l)$ denotes the greatest common divisor of k, l with the convention $\gcd(a,0) = \gcd(0,a) = a$.

Note that if $ku_i > 1$, we should substitute ku_i to $ku_i - \lfloor ku_i \rfloor$ in (IV.3.14), so that we actually compute the energy of the lowest order terms. This leads to the same modification of the phase factor in (IV.3.13), together with an overall shift $\varphi \to \varphi + \pi$. Regarding the expressions for $\tilde{\chi}[k,l], \tilde{\varphi}$ and $\widetilde{E}_k$, these can be simply obtained from (IV.3.12)–(IV.3.14) by substituting $u \to \tilde{u}$. The expressions for the left- and right-moving momenta, $p^2_{\rm L/R}(k)$, are given in (IV.2.38). We mention here that in the formulae (IV.3.12)–(IV.3.14) we consider $u_i > 0$, as sending $u_i \to -u_i$, for $i = 3$ and/or 4, leaves the bosonic piece of the partition function invariant.

Finally, in order to implement the orbifold projection, we fix k, sum over l and divide by the orbifold rank. Then, the degeneracy of a state with no bosonic oscillator excitations in the k-th twisted sector is given by (see also [35, 36] for a relevant discussion)

$$D(k) = \frac{1}{p}\sum_{l=0}^{p-1} \chi[k,l]\,\tilde{\chi}[k,l] e^{2\pi i l\left[(\tilde{r}\cdot\tilde{u} - r\cdot u) + k(\tilde{u}^2 - u^2) + \frac{n_1}{p}\right] + i(\tilde{\varphi}-\varphi)}\,. \tag{IV.3.15}$$

In the twisted sectors the mass formulae read

$$\begin{aligned} \frac{\alpha' m^2_{\rm L}(k)}{2} &= \frac{1}{2}(\tilde{r} + k\tilde{u})^2 + \frac{1}{2}p^2_{\rm L}(k) + \widetilde{E}_k - \frac{1}{2} + \widetilde{N}\,, \\ \frac{\alpha' m^2_{\rm R}(k)}{2} &= \frac{1}{2}(r + ku)^2 + \frac{1}{2}p^2_{\rm R}(k) + E_k - \frac{1}{2} + N\,, \end{aligned} \tag{IV.3.16}$$

where $p^2_{\rm L}$, $p^2_{\rm R}$ are defined in (IV.2.38). As in the untwisted sector, $\widetilde{N}$ and N refer to the bosonic occupation number of higher excited left- and right-moving oscillator states, respectively. However, in the twisted sectors $\widetilde{N}$ and N are not integers because the twisted boundary conditions of the T^4 coordinates (IV.2.8) result in a shift of the moding of the corresponding oscillators. In particular, the modings of the bosonic oscillators along the torus directions read (see e.g. [33])

$$\begin{aligned} &\tilde{\alpha}^1_{n-k\tilde{u}_3}\,, \quad \bar{\tilde{\alpha}}^1_{n+k\tilde{u}_3}\,, \quad \alpha^1_{n+ku_3}\,, \quad \bar{\alpha}^1_{n-ku_3}\,, \qquad n \in \mathbb{Z}\,, \\ &\tilde{\alpha}^2_{n-k\tilde{u}_4}\,, \quad \bar{\tilde{\alpha}}^2_{n+k\tilde{u}_4}\,, \quad \alpha^2_{n+ku_4}\,, \quad \bar{\alpha}^2_{n-ku_4}\,, \qquad n \in \mathbb{Z}\,. \end{aligned} \tag{IV.3.17}$$

Here, the left-movers are denoted by a tilde, and a bar denotes the complex conjugate. As an example, consider a generic state in a k twisted sector denoted by $|\tilde{r}, r\rangle_k$. We can act on this state with a left-moving creation operator, i.e. $\tilde{\alpha}^i_{-k\tilde{u}_i}|\tilde{r}, r\rangle_k$. Then, $\widetilde{N} = k\tilde{u}_i$, and the degeneracy of the state (IV.3.15) is modified by the addition of a phase $e^{2\pi i l \tilde{u}_i}$ (see e.g. [33]).

$k = 1$ sector

Let us now work out the spectrum of lightest states in the $k = 1$ sector of our orbifold model. We mention here that, in general, the spectrum in an orbifold k-twisted sector is identical with the spectrum of the $(p-k)$-twisted sector. This is due to the fact that the partition function of the k-twisted sector is equal to

the partition function of the $(p-k)$-twisted sector. As a result, the spectrum in the $k=1$ sector is the same as in the $k=5$ sector.

First, we compute the shift in the zero point energies (cf. (IV.3.2), (IV.3.14))

$$\widetilde{E}_1 = E_1 = \frac{5}{36}\,, \tag{IV.3.18}$$

together with the degeneracy of a state characterised by generic weight vectors $\tilde{r}$ and r and without bosonic oscillator excitations (cf. (IV.3.2), (IV.3.12), (IV.3.13), (IV.3.15)), which is given by

$$D(1) = \frac{1}{6}\sum_{l=0}^{5} e^{\frac{2\pi i l}{6}[5\tilde{r}_3+\tilde{r}_4-(r_3+r_4)+2+n_1]}\,. \tag{IV.3.19}$$

(We use the notation $D(k)$ for the degeneracy in the k'th twisted sector.) We list the weight vectors for the lightest left- and right-moving states in the $k=1$ sector in Table IV.2.

Sector	$\tilde{r}$	r
NS	$(0,0,-1,0)$	$(0,0,\underline{0,-1})$
R	$\left(\frac{1}{2},\frac{1}{2},-\frac{1}{2},-\frac{1}{2}\right), \left(-\frac{1}{2},-\frac{1}{2},-\frac{1}{2},-\frac{1}{2}\right)$	

Table IV.2: The weight vectors of the lightest left- and right-moving states in the $k=1$ twisted sector.

Let us start with the construction of states in the R-R sector, in which we have

$$\begin{aligned}
&\left(\tfrac{1}{2},\tfrac{1}{2},-\tfrac{1}{2},-\tfrac{1}{2}\right)\times\left(\tfrac{1}{2},\tfrac{1}{2},-\tfrac{1}{2},-\tfrac{1}{2}\right):(0)\,,\\
&\left(\tfrac{1}{2},\tfrac{1}{2},-\tfrac{1}{2},-\tfrac{1}{2}\right)\times\left(-\tfrac{1}{2},-\tfrac{1}{2},-\tfrac{1}{2},-\tfrac{1}{2}\right):(1)\,,\\
&\left(-\tfrac{1}{2},-\tfrac{1}{2},-\tfrac{1}{2},-\tfrac{1}{2}\right)\times\left(\tfrac{1}{2},\tfrac{1}{2},-\tfrac{1}{2},-\tfrac{1}{2}\right):(-1)\,,\\
&\left(-\tfrac{1}{2},-\tfrac{1}{2},-\tfrac{1}{2},-\tfrac{1}{2}\right)\times\left(-\tfrac{1}{2},-\tfrac{1}{2},-\tfrac{1}{2},-\tfrac{1}{2}\right):(0)\,.
\end{aligned} \tag{IV.3.20}$$

Here we denote a state of helicity h by (h). Using (IV.3.19), we can see that the above states are orbifold invariant for $n_1 = 0 \bmod 6$, and have degeneracy 1. From the spacetime point of view, we have the helicities that correspond to 1 massive vector $(\pm 1, 0)$ and 1 scalar (0). Also, from the mass formulae (IV.3.16) we get (for $\widetilde{N} = N = 0$)

$$\begin{aligned}
\frac{\alpha' m_{\mathrm{L}}^2(1)}{2} &= \frac{1}{2}p_{\mathrm{L}}^2(1) = \frac{1}{4T_2U_2}\left|n_2 - Un_1 + \overline{T}\left(w_1+\frac{1}{6}\right) + \overline{T}Uw_2\right|^2\,,\\
\frac{\alpha' m_{\mathrm{R}}^2(1)}{2} &= \frac{1}{2}p_{\mathrm{R}}^2(1) = \frac{1}{4T_2U_2}\left|n_2 - Un_1 + T\left(w_1+\frac{1}{6}\right) + TUw_2\right|^2\,,
\end{aligned} \tag{IV.3.21}$$

where now $n_1 = 0 \bmod 6$. Of course, physical states should also satisfy level-matching, that is $m_{\rm L}^2(1) = m_{\rm R}^2(1)$, which yields

$$n_1\left(w_1 + \frac{1}{6}\right) + n_2 w_2 = 0\,. \tag{IV.3.22}$$

In the R-NS sector we find the following states

$$\begin{aligned}&(\tfrac{1}{2},\tfrac{1}{2},-\tfrac{1}{2},-\tfrac{1}{2}) \times (0,0,\underline{0,-1}) : 2 \times (\tfrac{1}{2})\,,\\ &(-\tfrac{1}{2},-\tfrac{1}{2},-\tfrac{1}{2},-\tfrac{1}{2}) \times (0,0,\underline{0,-1}) : 2 \times (-\tfrac{1}{2})\,.\end{aligned} \tag{IV.3.23}$$

Similarly with the R-R sector, these states are orbifold invariant for $n_1 = 0 \bmod 6$, and have degeneracy 1. They correspond to 2 dilatini with helicity $(\pm\frac{1}{2})$ and mass given in (IV.3.21). The fields from the R-R and R-NS sectors form 1 tower of 4D massive vector multiplets, with mass (IV.3.21).

Let us now move on to the NS-NS sector, in which we have

$$(0,0,-1,0) \times (0,0,\underline{0,-1}) : 2 \times (0)\,. \tag{IV.3.24}$$

From (IV.3.19), we can see that the above states are orbifold invariant for $n_1 = 2 \bmod 6$, and have degeneracy 1. So, in the NS-NS sector we find 2 scalars, denoted by $2 \times (0)$. From the mass formulae (IV.3.16) we get (for $\widetilde{N} = N = 0$)

$$\begin{aligned}\frac{\alpha' m_{\rm L}^2(1)}{2} &= \frac{1}{2}p_{\rm L}^2(1) - \frac{1}{3} = \frac{1}{4T_2U_2}\left|n_2 - Un_1 + \overline{T}\left(w_1 + \frac{1}{6}\right) + \overline{T}Uw_2\right|^2 - \frac{1}{3}\,,\\ \frac{\alpha' m_{\rm R}^2(1)}{2} &= \frac{1}{2}p_{\rm R}^2(1) = \frac{1}{4T_2U_2}\left|n_2 - Un_1 + T\left(w_1 + \frac{1}{6}\right) + TUw_2\right|^2\,,\end{aligned} \tag{IV.3.25}$$

and the level-matching condition becomes

$$n_1\left(w_1 + \frac{1}{6}\right) + n_2 w_2 = \frac{1}{3}\,, \tag{IV.3.26}$$

which gives $n_1 = 2 \bmod 6$.

In the NS-R sector we find the following states

$$\begin{aligned}&(0,0,-1,0) \times (\tfrac{1}{2},\tfrac{1}{2},-\tfrac{1}{2},-\tfrac{1}{2}) : (-\tfrac{1}{2})\,,\\ &(0,0,-1,0) \times (-\tfrac{1}{2},-\tfrac{1}{2},-\tfrac{1}{2},-\tfrac{1}{2}) : (\tfrac{1}{2})\,.\end{aligned} \tag{IV.3.27}$$

As in the NS-NS sector, these states are orbifold invariant for $n_1 = 2 \bmod 6$, and have degeneracy 1. They correspond to 1 dilatino $(\pm\frac{1}{2})$ with mass (IV.3.25). The fields from the NS-NS and NS-R sectors in the $k = 1$ sector, constitute half of the field content of a hypermultiplet[12].

Now, we can also act on the NS-NS states (IV.3.24) with the left-moving creation operators $\tilde{a}^2_{-1/6}$ or $\bar{\tilde{a}}^1_{-1/6}$ (cf. (IV.3.17), (IV.3.2)). These will contribute

[12]The other half arises from the $k = 5$ twisted sector, which, as we have already mentioned, is equivalent to the $k = 1$ sector.

to $m_{\rm L}^2(1)$ in (IV.3.25) by a factor of $\widetilde{N} = 1/6$, and to the degeneracy of those states (IV.3.19) by a factor $e^{2\pi i l/6}$. So, these states will be orbifold invariant for $n_1 = 1 \bmod 6$. Putting everything together, we find 4 scalars with mass

$$\begin{aligned}\frac{\alpha' m_{\rm L}^2(1)}{2} &= \frac{1}{2}p_{\rm L}^2(1) - \frac{1}{3} + \frac{1}{6} = \frac{1}{4T_2U_2}\left|n_2 - Un_1 + \overline{T}\left(w_1 + \frac{1}{6}\right) + \overline{T}Uw_2\right|^2 - \frac{1}{6}\,,\\ \frac{\alpha' m_{\rm R}^2(1)}{2} &= \frac{1}{2}p_{\rm R}^2(1) = \frac{1}{4T_2U_2}\left|n_2 - Un_1 + T\left(w_1 + \frac{1}{6}\right) + TUw_2\right|^2\,,\end{aligned} \tag{IV.3.28}$$

and the level-matching condition becomes

$$n_1\left(w_1 + \frac{1}{6}\right) + n_2 w_2 = \frac{1}{6}\,, \tag{IV.3.29}$$

with $n_1 = 1 \bmod 6$. The above discussion also applies to the NS-R states (IV.3.27), where we find 2 dilatini with mass (IV.3.28). So, in the $k = 1$ sector we also find 1 tower of massive hypermultiplets with mass (IV.3.28).

Finally, we can act on the NS-NS states (IV.3.24) with combinations of two left-moving creation operators $\tilde{a}^2_{-1/6}$ and/or $\bar{\tilde{a}}^1_{-1/6}$ (cf. (IV.3.17), (IV.3.2)). These will contribute to $\alpha' m^2(1)_{\rm L}/2$ in (IV.3.25) by a factor of $\widetilde{N} = 1/3$, and to the degeneracy of those states (IV.3.19) by a factor $e^{2\pi i l/3}$. So, these states will be orbifold invariant for $n_1 = 0 \bmod 6$. Putting everything together, we find 6 scalars with mass

$$\begin{aligned}\frac{\alpha' m_{\rm L}^2(1)}{2} &= \frac{1}{2}p_{\rm L}^2(1) - \frac{1}{3} + \frac{1}{3} = \frac{1}{4T_2U_2}\left|n_2 - Un_1 + \overline{T}\left(w_1 + \frac{1}{6}\right) + \overline{T}Uw_2\right|^2\,,\\ \frac{\alpha' m_{\rm R}^2(1)}{2} &= \frac{1}{2}p_{\rm R}^2(1) = \frac{1}{4T_2U_2}\left|n_2 - Un_1 + T\left(w_1 + \frac{1}{6}\right) + TUw_2\right|^2\,,\end{aligned} \tag{IV.3.30}$$

and the level-matching condition becomes

$$n_1\left(w_1 + \frac{1}{6}\right) + n_2 w_2 = 0\,, \tag{IV.3.31}$$

with $n_1 = 0 \bmod 6$. Similarly, we can act with the left-moving oscillators $\tilde{a}^2_{-1/6}$ and $\bar{\tilde{a}}^1_{-1/6}$ on the NS-R states (IV.3.27). Then we find 3 dilatini with mass (IV.3.30). In this case, the fields from the NS-NS and NS-R sectors constitute the field content of 1 and a half hypermultiplet[13].

$k = 2$ sector

Now we move on to the construction of states in the $k = 2$ sector, which is equivalent to the $k = 4$ sector. The shift in the zero point energies is (cf. (IV.3.14))

$$\widetilde{E}_2 = E_2 = \frac{2}{9}\,, \tag{IV.3.32}$$

[13]The other 1 and a half hypermultiplet arises from the $k = 5$ twisted sector.

and the degeneracy of a generic state is given by[14] (cf. (IV.3.12), (IV.3.13), (IV.3.15))

$$D(2) = \frac{1}{6}\sum_{l=0}^{5} \chi[2,l]\,\tilde{\chi}[2,l] e^{\frac{2\pi i l}{6}[5\tilde{r}_3+\tilde{r}_4-(r_3+r_4)-2+n_1]}\,, \tag{IV.3.33}$$

where

$$\chi[2,l]\,\tilde{\chi}[2,l] = \begin{cases} 9 & \text{for} \quad l=0,2,4\,. \\ 1 & \text{for} \quad l=1,3,5\,. \end{cases} \tag{IV.3.34}$$

We list the weight vectors for the lightest left- and right-moving states of the $k=2$ sector in Table IV.3.

Sector	$\tilde{r}$	r
NS	$(0,0,-1,0),(0,0,-2,-1)$	$(0,0,-1,0),(0,0,0,-1)$
R	$(\frac{1}{2},-\frac{1}{2},-\frac{3}{2},-\frac{1}{2}),(-\frac{1}{2},\frac{1}{2},-\frac{3}{2},-\frac{1}{2})$	$(\frac{1}{2},\frac{1}{2},-\frac{1}{2},-\frac{1}{2}),(-\frac{1}{2},-\frac{1}{2},-\frac{1}{2},-\frac{1}{2})$

Table IV.3: The weight vectors of the lightest left- and right-moving states in the $k=2$ twisted sector.

Now, we take tensor products between left- and right-movers from Table IV.3. In the NS-NS sector we find

$$\begin{aligned} &(0,0,-1,0)\times(0,0,\underline{0,-1}) : 2\times(0) \\ &(0,0,-2,-1)\times(0,0,\underline{0,-1}) : 2\times(0)\,. \end{aligned} \tag{IV.3.35}$$

From (IV.3.33) and (IV.3.34), we see that these states survive the orbifold projection for $n_1 = 0 \bmod 6$, and have degeneracy 5. So, we find 20 scalars (0) with mass (cf. (IV.3.16), with $\widetilde{N}=N=0$)

$$\begin{aligned} \frac{\alpha' m_{\rm L}^2(2)}{2} &= \frac{1}{2}p_{\rm L}^2(2) = \frac{1}{4T_2U_2}\left|n_2 - Un_1 + \overline{T}\left(w_1+\frac{1}{3}\right)+\overline{T}Uw_2\right|^2\,, \\ \frac{\alpha' m_{\rm R}^2(2)}{2} &= \frac{1}{2}p_{\rm R}^2(2) = \frac{1}{4T_2U_2}\left|n_2 - Un_1 + T\left(w_1+\frac{1}{3}\right)+TUw_2\right|^2\,, \end{aligned} \tag{IV.3.36}$$

where $n_1 = 0 \bmod 6$, and the level-matching condition reads

$$n_1\left(w_1+\frac{1}{3}\right)+n_2w_2 = 0\,. \tag{IV.3.37}$$

Note that the states in (IV.3.35), can also survive the orbifold projection for $n_1 = 3 \bmod 6$, and, in this case, they come with degeneracy 4. The construction

[14] Here, we have introduced an additional phase factor $e^{\pi i l}$, in order to account for an extra minus sign arising from the fixed points.

of the lightest states in the NS-R sector is similar with the NS-NS sector, so we omit the details. We find 10 dilatini $(\pm\frac{1}{2})$ with mass (IV.3.36). So, from the NS-NS and NS-R sectors we obtain 5 towers of hypermultiplets with mass (IV.3.36), where $n_1 = 0 \bmod 6$, and 4 towers of hypermultiplets with mass (IV.3.36), where $n_1 = 3 \bmod 6$.

Let us now discuss the spectrum in the R-R sector, in which we have

$$\begin{aligned}
&(\tfrac{1}{2},-\tfrac{1}{2},-\tfrac{3}{2},-\tfrac{1}{2})\times(\tfrac{1}{2},\tfrac{1}{2},-\tfrac{1}{2},-\tfrac{1}{2}):(0)\,,\\
&(\tfrac{1}{2},-\tfrac{1}{2},-\tfrac{3}{2},-\tfrac{1}{2})\times(-\tfrac{1}{2},-\tfrac{1}{2},-\tfrac{1}{2},-\tfrac{1}{2}):(1)\,,\\
&(-\tfrac{1}{2},\tfrac{1}{2},-\tfrac{3}{2},-\tfrac{1}{2})\times(\tfrac{1}{2},\tfrac{1}{2},-\tfrac{1}{2},-\tfrac{1}{2}):(-1)\,,\\
&(-\tfrac{1}{2},\tfrac{1}{2},-\tfrac{3}{2},-\tfrac{1}{2})\times(-\tfrac{1}{2},-\tfrac{1}{2},-\tfrac{1}{2},-\tfrac{1}{2}):(0)\,.
\end{aligned} \tag{IV.3.38}$$

From (IV.3.33) and (IV.3.34), we see that these states survive the orbifold projection for $n_1 = 0 \bmod 6$, and have degeneracy 4. So, we find 4 vectors $(\pm 1, 0)$ and 4 scalars (0) with the same mass and level-matching condition as in (IV.3.36) and (IV.3.37). Similarly with the NS-NS (and NS-R) sector, the states in (IV.3.38) can also survive the orbifold projection for $n_1 = 3 \bmod 6$, and then, they have degeneracy 5. States in the R-NS sector are constructed similarly with the R-R sector. In the R-NS sector we find 8 dilatini $(\pm\frac{1}{2})$. In total, the lightest states from the R-R and R-NS sectors form 4 towers of vector multiplets with mass (IV.3.36), where $n_1 = 0 \bmod 6$, and 5 towers of vector multiplets with mass (IV.3.36), where $n_1 = 3 \bmod 6$.

$k = 3$ sector

Finally, we discuss the spectrum in the $k = 3$ sector. The shift in the zero point energies is (cf. (IV.3.14))

$$\widetilde{E}_3 = E_3 = \frac{1}{4}\,, \tag{IV.3.39}$$

and the degeneracy of a generic state is given by (cf. (IV.3.12), (IV.3.13), (IV.3.15))

$$D(3) = \frac{1}{6}\sum_{l=0}^{5} \chi[3,l]\,\tilde{\chi}[3,l] e^{\frac{2\pi i l}{6}[5\tilde{r}_3+\tilde{r}_4-(r_3+r_4)+n_1]}\,, \tag{IV.3.40}$$

where

$$\chi[3,l]\,\tilde{\chi}[3,l] = \begin{cases} 16 & \text{for} \quad l = 0,3\,. \\ 1 & \text{for} \quad l = 1,2,4,5\,. \end{cases} \tag{IV.3.41}$$

We list the weight vectors for the lightest left- and right-moving states of the $k = 3$ sector in Table IV.4.

Let us start with the construction of states in the NS-NS sector, in which we find

$$\begin{aligned}
&(0,0,-3,0)\times(0,0,\underline{0,-1}):2\times(0)\,,\\
&(0,0,-2,-1)\times(0,0,\underline{0,-1}):2\times(0)\,.
\end{aligned} \tag{IV.3.42}$$

Sector	$\tilde{r}$	r
NS	$(0,0,-3,0),(0,0,-2,-1)$	$(0,0,-1,0),(0,0,0,-1)$
R	$(\frac{1}{2},\frac{1}{2},-\frac{5}{2},-\frac{1}{2}),(-\frac{1}{2},-\frac{1}{2},-\frac{5}{2},-\frac{1}{2})$	$(\frac{1}{2},\frac{1}{2},-\frac{1}{2},-\frac{1}{2}),(-\frac{1}{2},-\frac{1}{2},-\frac{1}{2},-\frac{1}{2})$

Table IV.4: The weight vectors of the lightest left- and right-moving states in the $k=3$ twisted sector.

As we can see from (IV.3.40) and (IV.3.41), these states survive the orbifold projection for $n_1 = 0 \bmod 6$, and have degeneracy 5. So, we find 20 scalars (0) with mass (cf. (IV.3.16) with $\widetilde{N} = N = 0$)

$$\begin{aligned}\frac{\alpha' m_{\rm L}^2(3)}{2} &= \frac{1}{2}p_{\rm L}^2(3) = \frac{1}{4T_2U_2}\left|n_2 - Un_1 + \overline{T}\left(w_1+\frac{1}{2}\right) + \overline{T}Uw_2\right|^2 ,\\ \frac{\alpha' m_{\rm R}^2(3)}{2} &= \frac{1}{2}p_{\rm R}^2(3) = \frac{1}{4T_2U_2}\left|n_2 - Un_1 + T\left(w_1+\frac{1}{2}\right) + TUw_2\right|^2 ,\end{aligned} \tag{IV.3.43}$$

where $n_1 = 0 \bmod 6$, and the level-matching condition reads

$$n_1\left(w_1+\frac{1}{2}\right) + n_2 w_2 = 0\,. \tag{IV.3.44}$$

As in the $k=2$ twisted sector, the states in (IV.3.42) can also survive the orbifold projection for $n_1 = 2 \bmod 6$ and $n_1 = 4 \bmod 6$ and, in these cases, they come with degeneracy 5 or 6.

The construction of the lightest states in the NS-R sector is similar with the NS-NS sector, and we find 10 dilatini $(\pm\frac{1}{2})$ with mass (IV.3.43). So, from the NS-NS and NS-R sectors we obtain 5 towers of hypermultiplets with mass (IV.3.43), when $n_1 = 0 \bmod 6$, and 11 towers of hypermultiplets with mass (IV.3.43), from both $n_1 = 2 \bmod 6$ and $n_1 = 4 \bmod 6$.

Now, we move on to the R-R sector, in which we find

$$\begin{aligned}&(\tfrac{1}{2},\tfrac{1}{2},-\tfrac{5}{2},-\tfrac{1}{2})\times(\tfrac{1}{2},\tfrac{1}{2},-\tfrac{1}{2},-\tfrac{1}{2}) : (0)\,,\\ &(\tfrac{1}{2},\tfrac{1}{2},-\tfrac{5}{2},-\tfrac{1}{2})\times(-\tfrac{1}{2},-\tfrac{1}{2},-\tfrac{1}{2},-\tfrac{1}{2}) : (1)\,,\\ &(-\tfrac{1}{2},-\tfrac{1}{2},-\tfrac{5}{2},-\tfrac{1}{2})\times(\tfrac{1}{2},\tfrac{1}{2},-\tfrac{1}{2},-\tfrac{1}{2}) : (-1)\,,\\ &(-\tfrac{1}{2},-\tfrac{1}{2},-\tfrac{5}{2},-\tfrac{1}{2})\times(-\tfrac{1}{2},-\tfrac{1}{2},-\tfrac{1}{2},-\tfrac{1}{2}) : (0)\,.\end{aligned} \tag{IV.3.45}$$

From (IV.3.40) and (IV.3.41), we can see that these states survive the orbifold projection for $n_1 = 0 \bmod 6$, and have degeneracy 6. So, we find 6 vectors $(\pm 1, 0)$ and 6 scalars (0) with the same mass and level-matching condition as in (IV.3.43) and (IV.3.44). States in the R-NS sector are constructed similarly with the R-R sector. In the R-NS sector we find 12 dilatini $(\pm\frac{1}{2})$. In total, the lightest states from the R-R and R-NS sectors form 6 towers of vector multiplets with mass

(IV.3.43) and $n_1 = 0 \bmod 6$. Finally, we mention here that the states in the R-R and R-NS sectors can also survive the orbifold projection with the addition of momentum number $n_1 = 2$ or $4 \bmod 6$ and in these cases they come with degeneracy 5. So, we also find 10 towers of vector multiplets with mass (IV.3.43) and $n_1 = 2$ or $4 \bmod 6$.

IV.4 Moduli space and the Swampland

In this section we first discuss the classical moduli space of the *STU*-like $\mathbb{Z}_6$ model studied in Section IV.3. Then we determine the locations in the moduli space where generically massive states become massless. There are points at infinite distance where infinite towers of states become massless, as well as special lines and points in the interior of the (classical) moduli space where only a finite number of states become massless.

IV.4.1 Classical moduli space

In this subsection we will determine the vector multiplet and hypermultiplet moduli space of our $\mathbb{Z}_6$ orbifold model. First, we recall some classical aspects of the moduli spaces of the 5D $\mathbb{Z}_6$ model studied in [4]. In five dimensions, the vector multiplet moduli space is given by

$$\mathcal{M}_V^{(5)} = \mathbb{R}^+ \times \mathbb{R}^+ \,, \tag{IV.4.1}$$

where $\mathbb{R}^+ = \mathrm{SO}(1,1)/\mathbb{Z}_2$. This moduli space is parametrized by the five-dimensional string coupling λ_5 and the radius of the circle $\mathcal{R}_5$ along which the fields have non-trivial monodromy. The corresponding d-symbols are (up to an overall normalization)

$$d_{122} = 1 \,, \qquad d_{133} = -1 \,. \tag{IV.4.2}$$

The hypermultiplet scalars form the quaternion-Kähler manifold of real dimension 8 (with $\mathrm{SU}(2,2) \simeq \mathrm{SO}(4,2)$),

$$\mathcal{M}_H = \frac{\mathrm{SU}(2,2)}{\mathrm{SU}(2) \times \mathrm{SU}(2) \times \mathrm{U}(1)} \simeq \frac{\mathrm{SO}(4,2)}{\mathrm{SO}(4) \times \mathrm{SO}(2)} \,. \tag{IV.4.3}$$

The moduli space of the 5D orbifold was found by computing the commutant of the twist matrix in the 5D T-duality group $\mathrm{SO}(5,5)$. For this case, the commutant is [4]

$$\mathcal{C}^{(5)} = \mathrm{SO}(1,1) \times \mathrm{SU}(2,2) \times \mathrm{U}(1) \,. \tag{IV.4.4}$$

In order to find the moduli space of the 4D model, we have to compute the commutant of the twist matrix in the 4D T-duality group $\mathrm{SO}(6,6)$. But since the orbifold acts as a symmetry of T^4 together with a shift on $S^1_{\mathcal{R}_5}$, it is straightforward to verify that the commutant is enhanced as follows

$$\mathcal{C}^{(5)} \to \mathcal{C}^{(4)} = \mathrm{SO}(2,2) \times \mathrm{SU}(2,2) \times \mathrm{U}(1) \,. \tag{IV.4.5}$$

Since the monodromy is in the T-duality group, it also commutes with the classical 4D S-duality group $\mathrm{SL}(2)_S$. Then, using $\mathrm{SO}(2,2) \sim \mathrm{SL}(2) \times \mathrm{SL}(2)$, the vector multiplet moduli space is

$$\mathcal{M}_V^{(4)} = \frac{\mathrm{SL}(2)}{\mathrm{U}(1)} \times \frac{\mathrm{SL}(2)}{\mathrm{U}(1)} \times \frac{\mathrm{SL}(2)}{\mathrm{U}(1)} \,, \tag{IV.4.6}$$

and consists of 3 complex NS-NS scalar fields, which are the S, T and U moduli. This is all consistent with the supergravity dimensional reduction of the 5D theory to four dimensions, and is given by the so-called r-map. As we have explained in Subsection IV.2.2, the duality group of our $\mathbb{Z}_6$ orbifold is further broken to a subgroup

$$\hat{\Gamma}^1(6)_S \times \hat{\Gamma}^1(6)_T \times \hat{\Gamma}_1(6)_U \,, \tag{IV.4.7}$$

due to the orbifold shift. Therefore, each of the SL(2) factors in (IV.4.6) should be modded out by the corresponding congruence subgroup of $\mathrm{SL}(2,\mathbb{Z})$.

Now, the action of an $\mathcal{N} = 2$ supergravity theory coupled to n vector multiplets in 4D can be specified by the prepotential $F(X)$, which is a holomorphic and homogeneous function of second degree in the variables X^I, $I = 0, \ldots, n$. For the model at hand, the corresponding prepotential governing the 4D vector multiplets is given by

$$F(X) = i d_{ABC} \frac{X^A X^B X^C}{X^0} \,. \tag{IV.4.8}$$

Here $A, B, C = 1, 2, 3$, and the d-symbols are the same as in (IV.4.2). So, we obtain

$$F(X) = 3i \frac{X^1}{X^0} \left[(X^2)^2 - (X^3)^2 \right] \,. \tag{IV.4.9}$$

The complex coordinates X^1, X^2, X^3 are the complexifications of the 5D real coordinates denoted by h^1, h^2, h^3 in [4], as any 5D vector yields a scalar in 4D which pairs up with the 5D real scalar (reduced to 4D) to make up the complex variables as part of the 4D vector multiplet [37]. By applying a symplectic transformation we can bring the prepotential to the equivalent form

$$F(X) = i \frac{X^1 X^2 X^3}{X^0} \,. \tag{IV.4.10}$$

In this basis the only non-vanishing d-symbol is $d_{123} = 1/6$. Identifying

$$S = \frac{X^1}{X^0} \,, \qquad T = \frac{X^2}{X^0} \,, \qquad U = \frac{X^3}{X^0} \,, \tag{IV.4.11}$$

yields the classical prepotential

$$F(X) = i S T U (X^0)^2 \,. \tag{IV.4.12}$$

From the prepotential, one can also compute the Kähler potential K, which is given by

$$K = -\ln Y = -\ln \left(\frac{1}{2} X^I \overline{F}_I + \frac{1}{2} \overline{X}^I F_I \right) \,, \tag{IV.4.13}$$

where $F_I = \partial F/\partial X^I$ and $I = 0, \ldots, 3$. In our case, we find

$$Y = \frac{1}{2i}(S-\bar{S})(T-\bar{T})(U-\bar{U})\left|X^0\right|^2 . \tag{IV.4.14}$$

The vector multiplet moduli space is a Kähler manifold, and its metric is determined by the second derivative of the Kähler potential (IV.4.13), which is

$$\begin{aligned} K_{I\bar{J}}\,\mathrm{d}z^I\mathrm{d}\bar{z}^{\bar{J}} &= -\frac{1}{(S-\bar{S})^2}\mathrm{d}S\mathrm{d}\bar{S} - \frac{1}{(T-\bar{T})^2}\mathrm{d}T\mathrm{d}\bar{T} - \frac{1}{(U-\bar{U})^2}\mathrm{d}U\mathrm{d}\bar{U} \\ &= -\frac{1}{4S_2^2}\left(\mathrm{d}S_1^2+\mathrm{d}S_2^2\right) - \frac{1}{4T_2^2}\left(\mathrm{d}T_1^2+\mathrm{d}T_2^2\right) - \frac{1}{4U_2^2}\left(\mathrm{d}U_1^2+\mathrm{d}U_2^2\right) \\ &= -\frac{1}{4}e^{-2\sqrt{2}\phi_S}\mathrm{d}S_1^2 - \frac{1}{2}\mathrm{d}\phi_S^2 - \frac{1}{4}e^{-2\sqrt{2}\phi_T}\mathrm{d}T_1^2 - \frac{1}{2}\mathrm{d}\phi_T^2 - \frac{1}{4}e^{-2\sqrt{2}\phi_U}\mathrm{d}U_1^2 - \frac{1}{2}\mathrm{d}\phi_U^2 . \end{aligned} \tag{IV.4.15}$$

Here ϕ_I, $I = S, T, U$, are the corresponding normalized moduli, defined by

$$S_2 = e^{\sqrt{2}\phi_S}, \quad T_2 = e^{\sqrt{2}\phi_T}, \quad U_2 = e^{\sqrt{2}\phi_U} . \tag{IV.4.16}$$

These give the normalized classical moduli space metric.

IV.4.2 Massless states at finite distance

In this section we will analyse the special lines and points at finite distance in the interior of the moduli space where massive states become massless. It is important to mention here that in the interior of the moduli space only a finite number of states become massless and no infinite towers become massless.

Recall that in the $k = 1$ sector we found half a hypermultiplet[15] with mass

$$\begin{aligned} \frac{\alpha' m_{\mathrm{L}}^2(1)}{2} &= \frac{1}{2}p_{\mathrm{L}}^2(1) - \frac{1}{3} = \frac{1}{4T_2U_2}\left|n_2 - Un_1 + \bar{T}\left(w_1+\frac{1}{6}\right) + \bar{T}Uw_2\right|^2 - \frac{1}{3}, \\ \frac{\alpha' m_{\mathrm{R}}^2(1)}{2} &= \frac{1}{2}p_{\mathrm{R}}^2(1) = \frac{1}{4T_2U_2}\left|n_2 - Un_1 + T\left(w_1+\frac{1}{6}\right) + TUw_2\right|^2 , \end{aligned} \tag{IV.4.17}$$

with the constraint $n_1 = 2 \bmod 6$, and the level-matching condition

$$n_1\left(w_1+\frac{1}{6}\right) + n_2w_2 = \frac{1}{3} . \tag{IV.4.18}$$

From the mass formulae (IV.4.17), we see that massless states can appear if

$$T = \frac{n_1U - n_2}{w_2U + (w_1+\frac{1}{6})} , \tag{IV.4.19}$$

[15] The other half arises in the $k = 5$ sector.

where $n_1 = 2 \bmod 6$ and the level-matching constraint (IV.4.18) should be satisfied. We can rewrite the above expression together with the level-matching condition in a more convenient form as follows

$$\frac{T}{6} = \frac{n_1 U - n_2}{6w_2 U + (6w_1 + 1)}\,, \qquad \frac{n_1}{2}(6w_1 + 1) + 3n_2 w_2 = 1\,. \tag{IV.4.20}$$

By setting $\alpha = \frac{n_1}{2} \in 1+3\mathbb{Z}$, $\beta = -n_2 \in \mathbb{Z}$, $\gamma = 3w_2 \in 3\mathbb{Z}$ and $\delta = 1+6w_1 \in 1+6\mathbb{Z}$, we obtain

$$\frac{T}{6} = \frac{\alpha 2U + \beta}{\gamma 2U + \delta}\,, \qquad \alpha\delta - \beta\gamma = 1\,. \tag{IV.4.21}$$

Then massless states will appear when

$$\frac{T}{6} = g(2U)\,, \quad g \in \mathcal{S} \equiv \{\alpha\delta - \beta\gamma = 1 :\ \alpha \in 1+3\mathbb{Z},\, \beta \in \mathbb{Z},\, \gamma \in 3\mathbb{Z},\, \delta \in 1+6\mathbb{Z}\}\,. \tag{IV.4.22}$$

It can be easily proven that all solutions of (IV.4.22) can be obtained from the solution $\frac{T}{6} = 2U$ by applying $\Gamma^1(6)_T \times \Gamma_1(6)_U$ transformations. Starting from the solution $\frac{T}{6} = 2U$ and applying a generic $\Gamma^1(6)_T \times \Gamma_1(6)_U$ transformation we obtain (cf. (IV.2.39) and (IV.2.40))

$$\frac{a\frac{T}{6} + \frac{b}{6}}{cT + d} = \frac{a' 2U + 2b'}{c' U + d'} \implies \frac{a\frac{T}{6} + \frac{b}{6}}{6c\frac{T}{6} + d} = \frac{a' 2U + 2b'}{\frac{c'}{2} 2U + d'}\,. \tag{IV.4.23}$$

Here $a, d, a', d' \in 1+6\mathbb{Z}$, $b, c' \in 6\mathbb{Z}$ and $c, b' \in \mathbb{Z}$. Solving for $\frac{T}{6}$ yields

$$\frac{T}{6} = \frac{(da' - \frac{bc'}{12})2U + (2db' - \frac{bd'}{6})}{(\frac{ac'}{2} - 6a'c)2U + (ad' - 12b'c)}\,. \tag{IV.4.24}$$

Now, we note that

$$\begin{aligned} &\alpha \equiv da' - \frac{bc'}{12} \in 1+3\mathbb{Z}\,, \qquad \beta \equiv 2db' - \frac{bd'}{6} \in \mathbb{Z}\,, \\ &\gamma \equiv \frac{ac'}{2} - 6a'c \in 3\mathbb{Z}\,, \qquad \delta \equiv ad' - 12b'c \in 1+6\mathbb{Z}\,, \qquad \alpha\delta - \beta\gamma = 1\,. \end{aligned} \tag{IV.4.25}$$

So, we can rewrite (IV.4.24) as

$$\frac{T}{6} = \frac{\alpha 2U + \beta}{\gamma 2U + \delta}\,, \qquad \alpha\delta - \beta\gamma = 1\,, \tag{IV.4.26}$$

which exactly reproduces (IV.4.22).

As we have already discussed, the sectors $k = 1$ and $k = 5$ are equivalent. So, we conclude that at the critical line $\frac{T}{6} = 2U$, modulo $\Gamma^1(6)_T \times \Gamma_1(6)_U$ transformations, 1 hypermultiplet becomes massless.

Now, as in heterotic string constructions (see e.g. [38]), whenever two (or more) critical lines intersect, two (or more) hypermultiplets will become massless.

Starting from (IV.4.22), it is easy to show that the only lines intersecting inside the fundamental domain of $\Gamma^1(6)_T \times \Gamma_1(6)_U$ are the lines $\frac{T}{6} = 2U$ and $\frac{T}{6} = -(4U+1)/(6U+1)$. These lines intersect at the point $(T,U) = (12U^*, U^*)$, where $U^* = -\frac{1}{4} + i\frac{\sqrt{3}}{12}$, and it is depicted in Figure IV.1. Hence, at this point two hypermultiplets become massless.

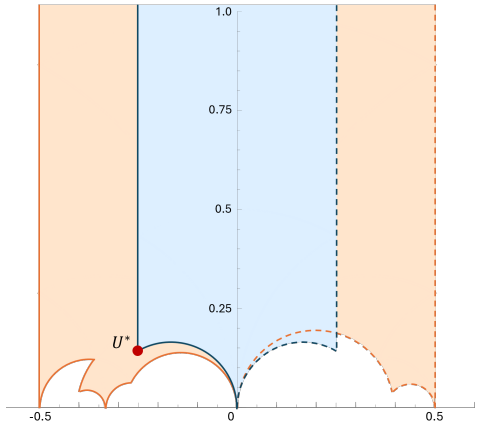

Figure IV.1: The location of U^*, represented by the red dot. The orange region is the fundamental domain of $\Gamma_1(6)_U$, whereas the blue region is the fundamental domain of $\Gamma_1(3)_{2U}$. The shapes of the fundamental domains are obtained via `DrawFunDoms.m`.

Finally, in the $k=1$ sector we also found one tower of hypermultiplets with mass

$$\begin{aligned}\frac{\alpha' m_{\rm L}^2(1)}{2} &= \frac{1}{2}p_{\rm L}^2(1) - \frac{1}{3} + \frac{1}{6} = \frac{1}{4T_2U_2}\left|n_2 - Un_1 + \overline{T}\left(w_1 + \frac{1}{6}\right) + \overline{T}Uw_2\right|^2 - \frac{1}{6}\,,\\ \frac{\alpha' m_{\rm R}^2(1)}{2} &= \frac{1}{2}p_{\rm R}^2(1) = \frac{1}{4T_2U_2}\left|n_2 - Un_1 + T\left(w_1 + \frac{1}{6}\right) + TUw_2\right|^2\,,\end{aligned} \tag{IV.4.27}$$

with the constraint $n_1 = 1 \bmod 6$ and the level-matching condition

$$n_1\left(w_1 + \frac{1}{6}\right) + n_2 w_2 = \frac{1}{6}\,. \tag{IV.4.28}$$

From the mass formulae (IV.4.27), we see that massless states can appear if

$$T = \frac{n_1 U - n_2}{w_2 U + (w_1 + \frac{1}{6})}\,, \tag{IV.4.29}$$

where $n_1 = 1 \bmod 6$ and the level-matching constraint (IV.4.28) should be satisfied. Again, we can rewrite the above expression together with the level-matching

condition in a more convenient form as follows

$$\frac{T}{6}=\frac{n_1U-n_2}{6w_2U+(6w_1+1)}\,,\qquad n_1(6w_1+1)+6n_2w_2=1\,. \tag{IV.4.30}$$

By setting $a=n_1\in 1+6\mathbb{Z}$, $b=-n_2\in\mathbb{Z}$, $c=6w_2\in 6\mathbb{Z}$, and $d=1+6w_1\in 1+6\mathbb{Z}$ we obtain

$$\frac{T}{6}=\frac{aU+b}{cU+d}\,,\qquad ad-bc=1\,. \tag{IV.4.31}$$

So, massless states will appear when

$$\frac{T}{6}=gU\,,\qquad g\in\Gamma_1(6)_U\,. \tag{IV.4.32}$$

or, equivalently,

$$hT=6U\,,\qquad h\in\Gamma^1(6)_T\,. \tag{IV.4.33}$$

We mention here that for the branch of solutions (IV.4.31), there are no intersecting lines. As we have already mentioned the sectors $k=1$ and $k=5$ are equivalent. Thus, at $\frac{T}{6}=U$ (mod $\Gamma^1(6)_T\times\Gamma_1(6)_U$) we get another massless hypermultiplet from the $k=5$ sector.

Concluding, we have found that there exist 2 special lines and 1 special point in the bulk of the moduli space, where massive hypermultiplets become massless. In particular, at $\frac{T}{6}=U$, modulo $\Gamma^1(6)_T\times\Gamma_1(6)_U$ transformations, 2 hypermultiplets become massless, and at $\frac{T}{6}=2U$, modulo $\Gamma^1(6)_T\times\Gamma_1(6)_U$ transformations, 1 hypermultiplet becomes massless. At the special point $(T,U)=(12U^*,U^*)$, where $U^*=-\frac{1}{4}+i\frac{\sqrt{3}}{12}$, two critical lines intersect, and 2 hypermultiplets become massless. Note that the hypermultiplets that become massless carry momentum and winding numbers along the T^2 directions, so they are charged under the corresponding vector fields.

The appearance of massless states in the bulk of the moduli space has significant consequences for the structure of the moduli space at the quantum level. As it was shown in [39, 40], the one-loop prepotential exhibits logarithmic singularities exactly at the lines in the moduli space where generically massive, charged states become massless. Hence, the classical moduli space is modified by quantum corrections. The computation of such corrections in our model relies on modularity properties of the prepotential under the congruence subgroups of $\mathrm{SL}(2,\mathbb{Z})$. We will discuss this issue in detail in Appendix IV.C, as a part of an upcoming work.

IV.4.3 Massless states at infinite distance

In this section we will study the spectrum of states at all different asymptotic limits in the $T-U$ plane of the moduli space. First, we will discuss these limits separately for T and U, i.e. we will fix U in the bulk of the moduli space and we will consider the infinite distance points in the T-plane and vice-versa. These will be referred to as single cusps. Then we will consider the asymptotic limits simultaneously for both T and U, which will be referred to as double cusps.

Single cusps as 6D limits

The fundamental domains of $\Gamma^1(6)_T$ and $\Gamma_1(6)_U$ are shown in Figure IV.2. There are 4 inequivalent cusps in the fundamental domain of $\Gamma^1(6)_T$, at the points $T = -3, -2, 0$ and $i\infty$. Similarly, there exist 4 inequivalent cusps in the fundamental domain of $\Gamma_1(6)_U$, at the points $U = -\frac{1}{2}, -\frac{1}{3}, 0$ and $i\infty$.

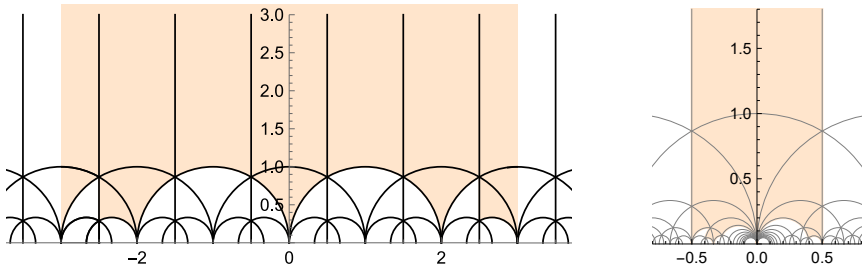

Figure IV.2: The fundamental domains of the congruence subgroups $\Gamma^1(6)_T$ and $\Gamma_1(6)_U$. The shaded region of the left and right figures corresponds to the fundamental domain of $\Gamma^1(6)_T$ and $\Gamma_1(6)_U$, respectively. The figures are obtained by the Mathematica package `DrawFunDoms.m`.

The cusp points correspond to singular geometric structures of the torus. In the limit $T_2 \to 0$, with U constant and finite, the volume of T^2 goes to zero, while the complex structure remains regular. This implies that the torus shrinks to a point. For the limit $U_2 \to 0$, with T constant and finite, the torus, as an elliptic curve, has zero discriminant and divergent modular invariants, so that it becomes a nodal curve. In the special case in which $U_1 = 0$, the nodal curve is described by $\mathcal{R}_4 \to 0$ and $\mathcal{R}_5 \to \infty$.

We should highlight here that all cusp points are at the asymptotic boundary of the fundamental domain. Hence, it is worth studying the spectrum and physical interpretation around these infinite distance points, and investigating whether the Swampland Distance Conjecture [41] is valid. Recall that in Subsection I.5.1, when approaching an asymptotic limit on the moduli space, the decreasing mass scale of the tower of states in the SDC is

$$m = m_0 e^{-\lambda|\Delta\phi|}\,, \tag{IV.4.34}$$

where ϕ is a normalized modulus and $\lambda \sim \mathcal{O}(1)$. To verify this conjecture, let us analyse the spectrum of the lightest states of all sectors with $N = \widetilde{N} = 0$.

The mass formulae for the lightest states that we found in the previous section (cf. (IV.3.9), (IV.3.21), (IV.3.36), and (IV.3.43)) can be summarized as follows:

$$\begin{aligned}
\frac{\alpha' m_{\rm L}^2}{2} &= \frac{1}{4T_2U_2}\left|n_2 - Un_1 + \overline{T}\,(\hat{w}_1 + Uw_2)\right|^2 = \frac{1}{4T_2U_2}\left|n_2 + T\hat{w}_1 + \overline{U}\,(-n_1 + Tw_2)\right|^2\,,\\
\frac{\alpha' m_{\rm R}^2}{2} &= \frac{1}{4T_2U_2}\left|n_2 - Un_1 + T\,(\hat{w}_1 + Uw_2)\right|^2 = \frac{1}{4T_2U_2}\left|n_2 + T\hat{w}_1 + U\,(-n_1 + Tw_2)\right|^2\,,
\end{aligned} \tag{IV.4.35}$$

and the level matching condition reads

$$n_1\hat{w}_1 + n_2 w_2 = 0\,, \quad \text{where} \quad \hat{w}_1 \equiv w_1 + \frac{k}{6}\,, \qquad k = 0, 1, \ldots, 5\,. \tag{IV.4.36}$$

Utilising this level matching condition, it can be derived from (IV.4.35) that

$$\alpha' m^2 = \frac{1}{T_2 U_2 w_2^2}\left|-n_1 + T w_2\right|^2 \left|\hat{w}_1 + U w_2\right|^2 = \frac{1}{T_2 U_2 n_2^2}\left|n_2 + T\hat{w}_1\right|^2 \left|-n_2 + U n_1\right|^2 . \tag{IV.4.37}$$

Given these, we can solve the equation $m^2 = m_{\rm L}^2(k) + m_{\rm R}^2(k) = 0$, as we approach the infinite distance points in the $T-U$ moduli space. There are 4 inequivalent sets of solutions:

- $T_2 \to 0$: $T = T_1 = \frac{n_1}{w_2} = -\frac{n_2}{\hat{w}_1}$, while U is in the bulk.
- $U_2 \to 0$: $U = U_1 = \frac{n_2}{n_1} = -\frac{\hat{w}_1}{w_2}$, while T is in the bulk.
- $T_2 \to \infty$: $\hat{w}_1 = w_2 = 0$, while U is in the bulk.
- $U_2 \to \infty$: $n_1 = w_2 = 0$, while T is in the bulk.

In Table IV.5, we list all towers of states that become massless as $T_2 \to 0$ or $U_2 \to 0$. Note that there are multiple towers of states becoming massless as $T_2 \to 0$ or $U_2 \to 0$. By using (IV.4.16), comparing (IV.4.34) with the last column of Table IV.5 and identifying $|\Delta\phi| = |\phi_T|$ or $|\phi_U|$, we can see that for all towers $\lambda = \frac{1}{\sqrt{2}}$. Then, as $T_2 \to 0$ or $U_2 \to 0$, that is $\phi_T \to -\infty$ or $\phi_U \to -\infty$ the masses of all towers decrease as[16]

$$m = m_0\, e^{-\frac{1}{\sqrt{2}}|\phi_I|}\,, \qquad I = T, U\,. \tag{IV.4.38}$$

In the limit $T_2 \to \infty$, that is $\phi_T \to \infty$, it is easy to see that there exist towers of KK states only in the untwisted sector whose masses decay as

$$m = \frac{1}{\sqrt{\alpha' U_2}}\left|n_2 - U n_1\right| e^{-\frac{1}{\sqrt{2}}|\phi_T|}\,. \tag{IV.4.39}$$

Finally, in the limit $U_2 \to \infty$, namely $\phi_U \to \infty$, there exist towers of states in all sectors whose masses decay exponentially fast. For example, in the untwisted sector we find towers with mass

$$m = \frac{1}{\sqrt{\alpha' T_2}}\left|n_2 + T w_1\right| e^{-\frac{1}{\sqrt{2}}|\phi_U|}\,. \tag{IV.4.40}$$

[16] We express mass scales in the string frame. In the Einstein frame in d dimensions, $m^{(\rm E)} = e^{2\phi_d/(d-2)} m$ (cf. [42–44]). In our case, $m^{(\rm E)} = S_2^{-1/2} m$. When analyzing limits in moduli space involving the axio-dilaton S, one encounters both decompactification limits and tensionless string limits. Note that in the limit $T_2 \to \infty$ with fixed g_s, $m^{(\rm E)} \propto g_s T_2^{-1/2} m \propto T_2^{-1}$, which is consistent with the decompactification SDC ratio in [43]. The same scaling holds at other sing-cusps by taking T-duality, as well as at double-cusp limits of $T-U$ moduli space, which we will discuss later.

Sector	Cusp		Lattice constraints	Mass of tower
$k=0$	$T_2 \to 0$	$T_1 = 0$	$n_1 = n_2 = 0$	$\frac{1}{\sqrt{\alpha' U_2}} \lvert w_1 + U w_2 \rvert \sqrt{T_2}$
		$T_1 = -2$	$n_1 = -2w_2,\ n_2 = 2w_1$	
		$T_1 = -3$	$n_1 = -3w_2,\ n_2 = 3w_1$	
	$U_2 \to 0$	$U_1 = 0$	$n_2 = w_1 = 0$	$\frac{1}{\sqrt{\alpha' T_2}} \lvert n_1 - T w_2 \rvert \sqrt{U_2}$
		$U_1 = -\frac{1}{3}$	$n_1 = -3n_2,\ w_2 = 3w_1$	
		$U_1 = -\frac{1}{2}$	$n_1 = -2n_2,\ w_2 = 2w_1$	
$k=1$	$T_2 \to 0$	$T_1 = 0$	$n_1 = n_2 = 0$	$\frac{1}{\sqrt{\alpha' U_2}} \lvert \hat{w}_1 + U w_2 \rvert \sqrt{T_2}$
$k=2$	$T_2 \to 0$	$T_1 = 0$	$n_1 = n_2 = 0$	$\frac{1}{\sqrt{\alpha' U_2}} \lvert \hat{w}_1 + U w_2 \rvert \sqrt{T_2}$
		$T_1 = -3$	$n_1 = -3w_2,\ n_2 = 3\hat{w}_1$	
	$U_2 \to 0$	$U_1 = -\frac{1}{3}$	$n_1 = -3n_2,\ w_2 = 3\hat{w}_1$	$\frac{1}{\sqrt{\alpha' T_2}} \lvert n_1 - T w_2 \rvert \sqrt{U_2}$
$k=3$	$T_2 \to 0$	$T_1 = 0$	$n_1 = n_2 = 0$	$\frac{1}{\sqrt{\alpha' U_2}} \lvert \hat{w}_1 + U w_2 \rvert \sqrt{T_2}$
		$T_1 = -2$	$n_1 = -2w_2,\ n_2 = 2\hat{w}_1$	
	$U_2 \to 0$	$U_1 = -\frac{1}{2}$	$n_1 = -2n_2,\ w_2 = 2\hat{w}_1$	$\frac{1}{\sqrt{\alpha' T_2}} \lvert n_1 - T w_2 \rvert \sqrt{U_2}$
$k=4$	$T_2 \to 0$	$T_1 = 0$	$n_1 = n_2 = 0$	$\frac{1}{\sqrt{\alpha' U_2}} \lvert \hat{w}_1 + U w_2 \rvert \sqrt{T_2}$
		$T_1 = -3$	$n_1 = -3w_2,\ n_2 = 3\hat{w}_1$	
	$U_2 \to 0$	$U_1 = -\frac{1}{3}$	$n_1 = -3n_2,\ w_2 = 3\hat{w}_1$	$\frac{1}{\sqrt{\alpha' T_2}} \lvert n_1 - T w_2 \rvert \sqrt{U_2}$
$k=5$	$T_2 \to 0$	$T_1 = 0$	$n_1 = n_2 = 0$	$\frac{1}{\sqrt{\alpha' U_2}} \lvert \hat{w}_1 + U w_2 \rvert \sqrt{T_2}$

Table IV.5: All towers of states that become massless for $T_2 \to 0$ and U fixed in the bulk of the moduli space, or $U_2 \to 0$ and T fixed in the bulk of the moduli space.

Hence, regarding the single cusps on the $T-U$ moduli space, the SDC is satisfied due to the existence of all the aforementioned towers of states.

Recall that the Emergent String Conjecture [45] (see Subsection I.5.1) proposes that each infinite distance limit on the moduli space corresponds to either a decompactification in which an infinite tower of Kaluza–Klein modes becomes massless, or a limit in which a string becomes tensionless and an infinite tower of string modes becomes massless. For our compactification, we will demonstrate that there exist decompactification limits as the infinite distance limits on the

$T-U$ moduli space.

Asymptotic supersymmetry enhancement

In our 4-dimensional $\mathcal{N}=2$ theory, there are 6 massive gravitini and 2 massless gravitini. These gravitini are in the multiplets of the untwisted sector. The massless gravitini arise in the NS-R sector and survive the orbifold projection if $n_1 = 0 \bmod 6$. The massive gravitini come from the NS-R and R-NS sector and carry non-trivial orbifold charge, as can be easily checked by using Table IV.1 and the formula (IV.3.5). This charge can be cancelled by the addition of an appropriate momentum number n_1, which makes the gravitini massive. This indicates that supersymmetry is spontaneously broken from $\mathcal{N}=8$ to $\mathcal{N}=2$. The weight vectors of the 6 massive gravitini and their corresponding momentum numbers are:

$$\begin{aligned}
&(\pm 1,0,0,0)\times(\pm\tfrac{1}{2},\pm\tfrac{1}{2},\tfrac{1}{2},\tfrac{1}{2}):\left(\pm\tfrac{3}{2},\pm\tfrac{1}{2}\right)\,, && n_1 = 1 \bmod 6\,,\\
&(\pm 1,0,0,0)\times(\pm\tfrac{1}{2},\pm\tfrac{1}{2},-\tfrac{1}{2},-\tfrac{1}{2}):\left(\pm\tfrac{3}{2},\pm\tfrac{1}{2}\right)\,, && n_1 = 5 \bmod 6\,,\\
&(\pm\tfrac{1}{2},\pm\tfrac{1}{2},\tfrac{1}{2},\tfrac{1}{2})\times(\pm 1,0,0,0):\left(\pm\tfrac{3}{2},\pm\tfrac{1}{2}\right)\,, && n_1 = 3 \bmod 6\,,\\
&(\pm\tfrac{1}{2},\pm\tfrac{1}{2},-\tfrac{1}{2},-\tfrac{1}{2})\times(\pm 1,0,0,0):\left(\pm\tfrac{3}{2},\pm\tfrac{1}{2}\right)\,, && n_1 = 3 \bmod 6\,,\\
&(\pm\tfrac{1}{2},\mp\tfrac{1}{2},\tfrac{1}{2},-\tfrac{1}{2})\times(\pm 1,0,0,0):\left(\pm\tfrac{3}{2},\pm\tfrac{1}{2}\right)\,, && n_1 = 4 \bmod 6\,,\\
&(\pm\tfrac{1}{2},\mp\tfrac{1}{2},-\tfrac{1}{2},\tfrac{1}{2})\times(\pm 1,0,0,0):\left(\pm\tfrac{3}{2},\pm\tfrac{1}{2}\right)\,, && n_1 = 2 \bmod 6\,.
\end{aligned} \tag{IV.4.41}$$

In summary, 1 gravitino survives the orbifold projection if $n_1 = 1 \bmod 6$, 1 gravitino survives if $n_1 = 2 \bmod 6$, 2 gravitini survive if $n_1 = 3 \bmod 6$, 1 gravitino survives if $n_1 = 4 \bmod 6$ and 1 gravitino survives if $n_1 = 5 \bmod 6$.

The masses of the gravitini can be easily computed using (IV.3.6). We find

$$\begin{aligned}
\frac{\alpha' m_{\rm L}^2(0)}{2} &= \frac{1}{2}p_{\rm L}^2(0) = \frac{1}{4T_2U_2}|n_2 - Un_1 + \overline{T}w_1 + \overline{T}Uw_2|^2\,,\\
\frac{\alpha' m_{\rm R}^2(0)}{2} &= \frac{1}{2}p_{\rm R}^2(0) = \frac{1}{4T_2U_2}|n_2 - Un_1 + Tw_1 + TUw_2|^2\,.
\end{aligned} \tag{IV.4.42}$$

Also, the level-matching condition reads

$$n_1 w_1 + n_2 w_2 = 0\,. \tag{IV.4.43}$$

It is important to stress here that the quantum number n_1 in (IV.4.42) and (IV.4.43) is constrained, according to (IV.4.41).

Now, as we approach the various cusps in the $T-U$ moduli space, all gravitini may remain massive, or some (or all) of them may become massless, as can be easily verified by using (IV.4.41), (IV.4.42) and Table IV.5. In addition, all these infinite distance points can be interpreted as decompactification limits in type IIB theory or in a dual type IIA picture. These limits can be understood by studying the behaviour of the T^2 partition function at all cusps; a detailed analysis can be found in Appendix IV.A. This is consistent with the Gravitini Mass (Swampland)

Conjecture [46, 47]. This conjecture proposes that a massive gravitino can only become massless with an infinite tower of states at an infinite distance on the moduli space, and the gravitino mass is proportional to some power of the KK (or string excitation) mass scale. The power is between 1 and 3; in our case, it is 1.

Moreover, the effective supergravity theory becomes six-dimensional. The massless spectrum follows immediately from the analysis of Section IV.3, with the only difference that all fields fall in representations of the massless little group $\mathrm{SU}(2) \times \mathrm{SU}(2)$ in 6D. For the supergravity multiplets in 6D and our conventions we refer to Appendix IV.B.

We first discuss the cusps of the modulus T and we keep U fixed:

- $T \to i\infty$: All gravitini become massless and supersymmetry in enhanced from $\mathcal{N} = 2$ to $\mathcal{N} = 8$. The resulting theory is type IIB theory on $\mathbb{R}^{1,5} \times T^4$. The massless fields make up the $\mathcal{N} = 8$ gravity multiplet is 6D.

- $T \to 0$: All gravitini remain massive. The theory becomes type IIB on a non-freely acting asymmetric orbifold $\mathbb{R}^{1,5} \times T^4/\mathbb{Z}_6$, characterized by the twist vectors $\tilde{u} = \left(\frac{5}{6}, \frac{1}{6}\right)$ and $u = \left(\frac{1}{6}, \frac{1}{6}\right)$. The massless fields make up the $\mathcal{N} = 2$ gravity multiplet in 6D coupled to 9 tensor multiplets, 8 vector multiplets and 20 hypermultiplets, satisfying the gravitational anomaly cancellation condition $n_{\mathrm{H}} - n_{\mathrm{V}} = 273 - 29n_{\mathrm{T}}$.

- $T \to -2$: The two R-NS gravitini carrying momentum number $n_1 = 2 \bmod 6$ and $n_1 = 4 \bmod 6$ become massless and supersymmetry in enhanced from $\mathcal{N} = 2$ to $\mathcal{N} = 4$. At this cusp we obtain type IIB on a non-freely acting symmetric orbifold $\mathbb{R}^{1,5} \times T^4/\mathbb{Z}_2$, characterized by the twist vectors $\tilde{u} = u = \left(\frac{1}{2}, \frac{1}{2}\right)$. The massless fields make up the $\mathcal{N} = 4\,(0,2)$ gravity multiplet and 21 tensor multiplets in 6D. The same spectrum could also be obtained from type IIB on $\mathbb{R}^{1,5} \times \mathrm{K3}$. Also, note that the resulting number of tensor multiplets is exactly the number that is required for the gravitational anomalies to cancel in a chiral $\mathcal{N} = 4\,(0,2)$ theory in 6D [48].

- $T \to -3$: The two R-NS gravitini carrying momentum number $n_1 = 3 \bmod 6$ become massless and supersymmetry in enhanced from $\mathcal{N} = 2$ to $\mathcal{N} = 4$. In this case, we get type IIB theory on a non-freely acting asymmetric orbifold $\mathbb{R}^{1,5} \times T^4/\mathbb{Z}_3$, characterized by the twist vectors $\tilde{u} = \left(-\frac{1}{3}, \frac{1}{3}\right)$ and $u = \left(\frac{1}{3}, \frac{1}{3}\right)$. The massless fields make up the $\mathcal{N} = 4\,(1,1)$ gravity multiplet and 20 vector multiplets in 6D.

We continue with the cusps of the modulus U and we keep T fixed:

- $U \to i\infty$: All gravitini remain massive. The theory becomes type IIA on a non-freely acting asymmetric orbifold $\mathbb{R}^{1,5} \times T^4/\mathbb{Z}_6$, characterized by the twist vectors $\tilde{u} = \left(\frac{5}{6}, \frac{1}{6}\right)$ and $u = \left(\frac{1}{6}, \frac{1}{6}\right)$. The massless fields make up the $\mathcal{N} = 2$ gravity multiplet in 6D coupled to 9 tensor multiplets, 8 vector multiplets and 20 hypermultiplets, satisfying the gravitation anomaly cancellation condition $n_{\mathrm{H}} - n_{\mathrm{V}} = 273 - 29n_{\mathrm{T}}$.

- $U \to 0$: All gravitini become massless and supersymmetry in enhanced from $\mathcal{N}=2$ to $\mathcal{N}=8$. The resulting theory is type IIA theory on $\mathbb{R}^{1,5}\times T^4$. The massless fields make up the $\mathcal{N}=8$ gravity multiplet is 6D.
- $U \to -1/2$: The two R-NS gravitini carrying momentum number $n_1 = 2 \bmod 6$ and $n_1 = 4 \bmod 6$ become massless and supersymmetry in enhanced from $\mathcal{N}=2$ to $\mathcal{N}=4$. At this cusp we obtain type IIA on a non-freely acting symmetric orbifold $\mathbb{R}^{1,5}\times T^4/\mathbb{Z}_2$, characterized by the twist vectors $\tilde{u}=u=\left(\frac{1}{2},\frac{1}{2}\right)$. The massless fields make up the $\mathcal{N}=4\,(1,1)$ gravity multiplet and 20 vector multiplets in 6D. The same spectrum could also be obtained from type IIA on $\mathbb{R}^{1,5}\times \mathrm{K3}$.
- $U \to -1/3$: The two R-NS gravitini carrying momentum number $n_1 = 3 \bmod 6$ become massless and supersymmetry in enhanced from $\mathcal{N}=2$ to $\mathcal{N}=4$. In this case, we get type IIA theory on a non-freely acting asymmetric orbifold $\mathbb{R}^{1,5}\times T^4/\mathbb{Z}_3$, characterized by the twist vectors $\tilde{u}=\left(-\frac{1}{3},\frac{1}{3}\right)$ and $u=\left(\frac{1}{3},\frac{1}{3}\right)$. The massless fields make up the $\mathcal{N}=4\,(2,0)$ gravity multiplet and 21 tensor multiplets in 6D, ensuring that gravitational anomalies cancel.

It is easy to see that the various cusp points of the modulus T can be mapped to those of U by the following transformation

$$\gamma: \quad T \leftrightarrow \frac{1}{\overline{U}}\,, \qquad U \leftrightarrow \frac{1}{\overline{T}}\,. \tag{IV.4.44}$$

Such a transformation is an element in $\mathrm{O}(2,2;\mathbb{Z})$, but not in $\mathrm{SO}(2,2;\mathbb{Z})$, so it also maps type IIB to type IIA. The construction and action on the lattice of this element is written at the end of Appendix IV.A. Note that this transformation changes the chirality of the right-moving Ramond vacuum; this is important for understanding the representations of the various supergravity fields in 6D.

Double cusps as 5D limits

So far, we have discussed the single cusps on the $T-U$ plane of the moduli space. However, there are limits on the boundary of both spaces: the double cusps. The analysis of these double cusps is similar to the analysis of the single cusps. Hence, we will omit most of the details and we will simply present our results, which we collect in Table IV.6. Note that at all double cusps the effective supergravity theory becomes five-dimensional. Regarding our conventions for the massless spectra at each of the double cusps we refer to [2].

There are four T-cusps and four U-cusps, and by combination there are 16 double-cusp infinite distance limits on the moduli space. The masses of the towers of states that become massless as we approach each double cusp can be derived from (IV.4.37). As an example, we consider the limit $T \to i\infty$ and $U \to -1/2$. In this case we find a KK tower with mass

$$m^2 = \frac{n_1^2 U_2}{\alpha' T_2} = \frac{n_1^2}{\alpha'} e^{\sqrt{2}(\phi_U - \phi_T)} \propto e^{-2|\phi|}, \tag{IV.4.45}$$

T	U	$\alpha' m^2$	Compactification	Supersymmetry	Massless spectrum
0	0	$w_2^2 T_2 U_2$	$\left(T^4 \times S^1\right)/\mathbb{Z}_6$	$\mathcal{N}=2$ IIA	1GM + 2VM + xHM
0	$-\frac{1}{2}$		$\left(T^4 \times S^1\right)/\mathbb{Z}_6^{(3)}$	$\mathcal{N}=2$ IIA	1GM + 8VM + 7HM
0	$-\frac{1}{3}$		$\left(T^4 \times S^1\right)/\mathbb{Z}_6^{(2)}$	$\mathcal{N}=2$ IIA	1GM + 8VM + 10HM
-2	0		$\left(T^4 \times S^1\right)/\mathbb{Z}_2$	$\mathcal{N}=4\,(1,1)$ IIA	1GM + 5VM
-3	0		$\left(T^4 \times S^1\right)/\mathbb{Z}_3$	$\mathcal{N}=4\,(2,0)$ IIA	1GM + 3VM
-2	$-\frac{1}{2}$		$T^4/\mathbb{Z}_2 \times S^1$	$\mathcal{N}=4\,(1,1)$ IIA	1GM + 21VM
-3	$-\frac{1}{3}$		$T^4/\mathbb{Z}_3 \times S^1$	$\mathcal{N}=4\,(2,0)$ IIA	1GM + 21VM
-2	$-\frac{1}{3}$		$\left(T^4 \times S^1_{\sqrt{6}}\right)/\mathbb{Z}_6$	$\mathcal{N}=2$ IIA	1GM + 2VM + 4HM
-3	$-\frac{1}{2}$				
$i\infty$	$i\infty$	$\frac{n_2^2}{T_2 U_2}$	$\left(T^4 \times S^1\right)/\mathbb{Z}_6$	$\mathcal{N}=2$ IIB	1GM + 2VM + xHM
$i\infty$	0	$\frac{n_1^2 U_2}{T_2}$	T^5	$\mathcal{N}=8$ IIB	1GM
$i\infty$	$-\frac{1}{2}$		$\left(T^4 \times S^1\right)/\mathbb{Z}_2$	$\mathcal{N}=4\,(0,2)$ IIB	1GM + 5VM
$i\infty$	$-\frac{1}{3}$		$\left(T^4 \times S^1\right)/\mathbb{Z}_3$	$\mathcal{N}=4\,(1,1)$ IIB	1GM + 3VM
0	$i\infty$	$\frac{\hat{w}_1^2 T_2}{U_2}$	$T^4/\mathbb{Z}_6 \times S^1$	$\mathcal{N}=2$ IIA	1GM + 18VM + 20HM
-2	$i\infty$		$\left(T^4 \times S^1\right)/\mathbb{Z}_6^{(3)}$	$\mathcal{N}=2$ IIA	1GM + 8VM + 7HM
-3	$i\infty$		$\left(T^4 \times S^1\right)/\mathbb{Z}_6^{(2)}$	$\mathcal{N}=2$ IIA	1GM + 8VM + 10HM

Table IV.6: Here we present our results for all double cusps in the T-U moduli space. First, we list the double-cups. Then we specify the mass of the towers that become massless and the resulting decompactified theory at the corresponding cusp. In all cases there are five non-compact directions ($\mathbb{R}^{1,4}$) and five compact directions. Here, GM stands for gravity multiplet, VM stands for vector multiplet, and HM stands for hypermultiplet. Regarding the massless spectrum at the cusps $(T,U) \to (0,0)$ and $(i\infty, i\infty)$, if $T_2/U_2 = 6$, $x = 4$; if $T_2/U_2 = 12$, $x = 3$; and for all other cases $x = 2$.

for $\hat{w}_1 = w_2 = 0$, and $n_1 = -2n_2$. These constraints on the lattice of momenta and windings imply that this tower appears only in the untwisted sector, that is $k = 0$, and if $n_1 \in 2\mathbb{Z}$. Furthermore, there are two gravitini carrying momentum $n_1 \in 2\mathbb{Z}$, which become massless at this double-cusp limit. Hence, supersymmetry

is enhanced from $\mathcal{N}=2$ to $\mathcal{N}=4$ in 5D.[17] We collect all information about the masses of the towers that become zero, the constraints on the momentum and winding numbers and the sectors in which massless towers appear at each of the 16 double cusps in Table IV.7.

Note that at the cusps $(T,U)=(-2,-1/3)$, $(-3,-1/2)$, there are two additional towers of hypermultiplets that become massless, since we are exactly at the critical line $\frac{T}{6}=U$ (cf. (IV.4.31)). Regarding the cusps $(T,U)=(0,0)$ and $(i\infty,i\infty)$, if the ratio T_2/U_2 as we approach the cusp is 12, we obtain one extra tower of massless hypermultiplets (cf. (IV.4.22)), and if the ratio is 6 we get two towers of massless hypermultiplets (cf. (IV.4.31)).

Moreover, at the cusps $(T,U)=(0,-1/2)$, $(0,-1/3)$, $(-2,i\infty)$, $(-3,i\infty)$ the theory decompactifies to an orbifold of $\mathbb{R}^{1,4}\times S^1\times T^4$, which acts as a rotation of order 6 on the torus and as a shift of order 2 or 3 on the circle. Such that, the twist vector at cusps $(T,U)=(0,-1/2)$ and $(-2,i\infty)$ becomes $u=\left(0,\frac{1}{3}\right)$, and we denote the orbifold action as $\mathbb{Z}_6^{(3)}$ in Table IV.6; Similarly, the twist vector at cusps $(T,U)=(0,-1/3)$ and $(-3,i\infty)$ becomes $u=\left(0,\frac{1}{2}\right)$, and we denote the orbifold action as $\mathbb{Z}_6^{(2)}$. The fact that the shift is not of order 6 has important implications for the spectrum of the orbifold. Consider for example the case in which the rotation on the torus is of order 6 and the shift on the circle is of order 3. In this orbifold, the winding number along the circle direction will be shifted as $w\to w+k/3$, which implies that states in the $k=3$ twisted sector will not feel the shift. Consequently, there will be massless states coming from this twisted sector. Moreover, states with momentum number n along the circle direction will pick up a phase $e^{2\pi i n/3}$. So, states with orbifold charge $e^{\pi i/3}, e^{\pi i}$ or $e^{5\pi i/3}$ will be projected out of the spectrum, since such orbifold charge cannot be cancelled by adding momentum along the circle direction. The situation is similar if the shift along the circle is of order 2. In this case, states in the $k=2$ and 4 sectors will not feel the shift, and states with orbifold charge $e^{\pi i/3}, e^{2\pi i/3}, e^{4\pi i/3}$ or $e^{5\pi i/3}$ will be projected out of the spectrum.

Finally, as in the example (IV.4.45), the masses of all towers that become massless at the double cusps are proportional to both $\exp\left(\pm\frac{1}{\sqrt{2}}\phi_T\right)$ and $\exp\left(\pm\frac{1}{\sqrt{2}}\phi_U\right)$. Hence, the masses of the towers decrease exponentially with $\lambda=1$ (see (IV.4.34)), and the SDC is verified also in the case of double cusps in the $T-U$ moduli space.

IV.5 Conclusion and discussion

In this chapter we have checked that the Distance Conjecture holds for a particular non-geometric string compactification, which is a freely acting asymmetric $\mathbb{Z}_6$ orbifold of type IIB string theory with a classical *STU* moduli space. This was a non-trivial test, as the duality group of the orbifolded theory was reduced to subgroups of the modular group due to the shift along the circle coordinate. Hence, new points of infinite distance on the real axis of the moduli space needed

[17] In our notation, $\mathcal{N}=2$ supersymmetry in 5D means 8 supersymmetries.

T	U	Lattice constraints	$n_1 (\mathrm{mod} 6)$	Massless sectors
0	0	$n_1 = n_2 = \hat{w}_1 = 0$	0	$0\,(1,5)$
0	$-\frac{1}{2}$	$n_1 = -2n_2 = 0, 2\hat{w}_1 = w_2$	0	$0, 3$
0	$-\frac{1}{3}$	$n_1 = -3n_2 = 0, 3\hat{w}_1 = w_2$	0	$0, 2, 4$
-2	0	$2\hat{w}_1 = n_2 = 0, n_1 = -2w_2$	$0, 2, 4$	0
-3	0	$3\hat{w}_1 = n_2 = 0, n_1 = -3w_2$	$0, 3$	0
-2	$-\frac{1}{2}$	$-n_1 = 2n_2 = 4\hat{w}_1 = 2w_2$	$0, 2, 4$	$0, 3$
-3	$-\frac{1}{3}$	$-n_1 = 3n_2 = 9\hat{w}_1 = 3w_2$	$0, 3$	$0, 2, 4$
-2	$-\frac{1}{3}$	$-n_1 = 3n_2 = 6\hat{w}_1 = 2w_2$	0	$0, 1, 5$
-3	$-\frac{1}{2}$	$-n_1 = 2n_2 = 6\hat{w}_1 = 3w_2$		
$i\infty$	$i\infty$	$n_1 = \hat{w}_1 = w_2 = 0$	0	$0\,(1,5)$
$i\infty$	0	$\hat{w}_1 = w_2 = n_2 = 0$	All	0
$i\infty$	$-\frac{1}{2}$	$2\hat{w}_1 = w_2 = 0, n_1 = -2n_2$	$0, 2, 4$	0
$i\infty$	$-\frac{1}{3}$	$3\hat{w}_1 = w_2 = 0, n_1 = -3n_2$	$0, 3$	0
0	$i\infty$	$n_1 = w_2 = n_2 = 0$	0	All
-2	$i\infty$	$n_1 = -2w_2 = 0, n_2 = 2\hat{w}_1$	0	$0, 3$
-3	$i\infty$	$n_1 = -3w_2 = 0, n_2 = 3\hat{w}_1$	0	$0, 2, 4$

Table IV.7: Here we list the masses of towers that become massless, the constraints on the lattice of momenta and windings and the sectors in which massless states appear at each double cusp. For the cusps $(T, U) \to (0, 0)$ and $(i\infty, i\infty)$, there are extra towers of massless hypermultiplet arising from the $k = 1$ and 5 sectors, if $T = 6U$ or $T = 12U$ asymptotically.

to be examined. We chose this particular example because of its rich structure, but we expect our conclusions to hold more generally.

In our example, all infinite distance points corresponded to decompactification limits to either six or five dimensions. As we explicitly demonstrated by studying the orbifold partition function, at the cusps on the real axis of the moduli space a freely acting asymmetric orbifold could decompactify to a non-freely acting symmetric orbifold. Also, at some cusps, some or all gravitini became massless

and supersymmetry was enhanced from $\mathcal{N}=2$ to $\mathcal{N}=4$ or $\mathcal{N}=8$.

Beyond the geometric moduli space of the T^2 orbifold analyzed in this work, a complete picture must include the axio-dilaton S, which governs the string coupling constant and transforms under the S-duality group $\hat{\Gamma}_1(6)$. A natural extension of this research is therefore to classify the infinite-distance limits associated with the cusps of the axio-dilaton moduli space. As S-duality often corresponds to a string-string duality, these limits will reveal new tensionless string theories. Furthermore, a comprehensive analysis of the combined (S,T,U) moduli space would involve classifying numerous double- and triple-cusp limits. Such an investigation would be crucial for further testing the Emergent String Conjecture and distinguishing between decompactification and tensionless string limits in this more intricate setting.

In addition to the distance conjecture, there are conjectures that the volume of moduli space should be finite or that its asymptotic growth be restricted [41]. For a recent discussion on this and the relation to dualities, see [49, 50]. The volume of the classical moduli space for our model is indeed finite, because the hypermultiplet moduli space is a Narain moduli space with a finite volume and the vector multiplet moduli space is the triple product of the fundamental domains of $\hat{\Gamma}^1(6)$ (or $\hat{\Gamma}_1(6)$). The index of $\hat{\Gamma}^1(6)$ is $[\mathrm{SL}(2,\mathbb{Z}):\hat{\Gamma}^1(6)]=12$ (same as $\hat{\Gamma}_1(6)$), so that the volume of the classical vector multiplet moduli space is $(12\mathrm{Vol}(\mathbb{H}/\mathrm{SL}(2,\mathbb{Z})))^3=64\pi^3$.

Finally, we also found that a finite number of massive and charged hypermultiplets could become massless at special lines or points in the interior of the moduli space, which indicates that the classical prepotential could be modified by quantum effects[18]. The computation of such quantum corrections will be the subject of a future work, and our current process is presented in Appendix IV.C.

IV.A Details on the partition function

The orbifold partition function takes the general form

$$Z(\tau,\bar{\tau})=\frac{1}{p}\sum_{k,l=0}^{p-1}Z[k,l](\tau,\bar{\tau})\ , \tag{IV.A.1}$$

where $\tau=\tau_1+i\tau_2$ is the complex structure modulus of the torus[19], and

$$Z[k,l]=Z_{\mathbb{R}^{1,3}}\,Z_{T^2}[k,l]Z_{T^4}[k,l]Z_F[k,l]\,. \tag{IV.A.2}$$

Here $Z_{\mathbb{R}^{1,3}}$ is the contribution to the partition function from the non-compact bosons, $Z_{T^2}[k,l]$ and $Z_{T^4}[k,l]$ refer to the compact bosons on T^2 and T^4 respectively and $Z_F[k,l]$ is the fermionic contribution to the partition function. Recall

[18] On the volume finiteness of the quantum corrected moduli space, because the geodesic distance to the singularities $\frac{T}{6}=U$ and $\frac{T}{6}=2U$ is finite, the volume also remains finite.

[19] The modulus τ should not be confused with the modulus U, which is the complex structure modulus of the worldsheet T^2.

that p is the orbifold rank and k labels the untwisted and twisted sectors. In addition, l implements the orbifold projection in each sector.

Also, it is useful to mention that, in general, the partition function can be factorized into left- and right-moving pieces as[20]

$$Z[k,l] = \widetilde{\mathcal{Z}}[\tilde{\theta}^k, \tilde{\theta}^l] \otimes \mathcal{Z}[\theta^k, \theta^l] \,. \tag{IV.A.3}$$

Here θ is the generator of the orbifold group; θ^k refers to twisted sectors where the torus coordinates obey boundary conditions of the form $W_{\rm R}^i(\sigma^0, \sigma^1 + 2\pi) = \theta^k\, W_{\rm R}^i(\sigma^0, \sigma^1)$ and θ^l characterizes the orbifold action: $W_{\rm R}^i \to \theta^l\, W_{\rm R}^i$ ($\tilde{\theta}^k, \tilde{\theta}^l$ correspond to the left-movers). In this appendix we will focus mostly on the behaviour of the T^2 partition function in the various infinite distance points. For more details on the partition function we refer to [2].

Recall that the T^2 partition function reads

$$Z_{T^2}[k,l] = \frac{1}{(\eta\bar{\eta})^2} \sum_{\{n_i,w_i\}\in\mathbb{Z}^4} e^{\frac{2\pi i l n_1}{p}}\, \bar{q}^{\frac{1}{2}p_{\rm L}^2(k)}\, q^{\frac{1}{2}p_{\rm R}^2(k)} \,, \qquad i = 1,2 \,, \tag{IV.A.4}$$

where

$$\begin{aligned} p_{\rm L}^2(k) &= \frac{1}{2T_2U_2}\left| n_2 - Un_1 + \overline{T}\left(w_1 + \frac{k}{p}\right) + \overline{T}Uw_2 \right|^2 \,, \\ p_{\rm R}^2(k) &= \frac{1}{2T_2U_2}\left| n_2 - Un_1 + T\left(w_1 + \frac{k}{p}\right) + TUw_2 \right|^2 \,. \end{aligned} \tag{IV.A.5}$$

We can rewrite the left- and right-moving momenta in terms of the background fields of T^2, i.e. the metric g_{ij} and antisymmetric tensor b_{ij}, as

$$\begin{aligned} p_{\rm L}^2(k) &= \frac{\alpha'}{2} n_i g^{-1}_{ij} n_j + \frac{1}{2\alpha'} \hat{w}_i (g - bg^{-1}b)_{ij} \hat{w}_j + \hat{w}_i (bg^{-1})_{ij} n_j + n_i \hat{w}_i \,, \\ p_{\rm R}^2(k) &= \frac{\alpha'}{2} n_i g^{-1}_{ij} n_j + \frac{1}{2\alpha'} \hat{w}_i (g - bg^{-1}b)_{ij} \hat{w}_j + \hat{w}_i (bg^{-1})_{ij} n_j - n_i \hat{w}_i \,, \end{aligned} \tag{IV.A.6}$$

where, $i,j = 1,2$ and summation over repeated indices is implied. Also, we have defined $\hat{w}_i \equiv w_i + k_i/p$, where $\vec{k} = (k_1, k_2) = (k, 0)$. Also, let us define $\vec{l} = (l_1, l_2) = (l, 0)$. Then, by performing a Poisson resummation over the momentum vector $\vec{n} = (n_1, n_2)$ we can bring (IV.A.4) to the equivalent form

$$Z_{T^2}[k,l] = \frac{\sqrt{\det g}}{\alpha'\, \tau_2\, (\eta\,\bar{\eta})^2} \sum_{\{n_i,w_i\}\in\mathbb{Z}^4} e^{\frac{-\pi}{\alpha'\tau_2}\left[n_i - \frac{l_i}{p} + \left(w_i + \frac{k_i}{p}\right)\tau\right](g_{ij} - b_{ij})\left[n_j - \frac{l_j}{p} + \left(w_j + \frac{k_j}{p}\right)\bar{\tau}\right]} \,. \tag{IV.A.7}$$

Recall that the D-dimensional Poisson resummation formula is given by

$$\sum_{n_i\in\mathbb{Z}^d} e^{-\pi n_i A_{ij} n_j + \pi B_i n_i} = (\det A)^{-\frac{1}{2}} \sum_{n_i\in\mathbb{Z}^d} e^{-\pi\left(n_i + i\frac{B_i}{2}\right)(A^{-1})ij\left(n_j + i\frac{B_j}{2}\right)} \,. \tag{IV.A.8}$$

[20] The bosonic zero modes along the compact directions require special treatment, as infinite sums over quantized momenta and windings may appear. The bosonic zero modes along the T^4 are irrelevant for our discussion but those along the T^2 will be discussed in detail.

Also,

$$g_{ij} = \alpha' \frac{T_2}{U_2} \begin{pmatrix} 1 & U_1 \\ U_1 & |U|^2 \end{pmatrix}, \qquad \text{and} \qquad b_{ij} = \alpha' \begin{pmatrix} 0 & T_1 \\ -T_1 & 0 \end{pmatrix}. \tag{IV.A.9}$$

Let us now focus on the cusps of the modulus T, and keep the modulus U fixed in the bulk. For convenience, we set $U_1 = 0$. Then, $T_2 = \mathcal{R}_5\mathcal{R}_4/\alpha'$ and $U_2 = \mathcal{R}_4/\mathcal{R}_5$. First we study the limit $T_2 \to \infty$, that is $\mathcal{R}_5 \to \infty$ and $\mathcal{R}_4 \to \infty$. In this limit, $g_{ij} \to \infty$ and the only term that contributes to the sum in (IV.A.7) is the term with $n_1 = n_2 = w_1 = w_2 = k = l = 0$. So, we find

$$\lim_{T_2\to\infty} Z_{T^2}[0,0] = \frac{\mathcal{R}_4\mathcal{R}_5}{\alpha'\,\tau_2\,(\eta\,\bar\eta)^2}\,, \tag{IV.A.10}$$

while for k and/or $l \neq 0$ the limit is exponentially suppressed. Using that the string length ℓ_s is given by $\ell_s = 2\pi\sqrt{\alpha'}$, we can rewrite the above expression as

$$\lim_{T_2\to\infty} Z_{T^2}[0,0] = \frac{4\pi^2\mathcal{R}_4\mathcal{R}_5}{\ell_s^2\,\tau_2\,(\eta\,\bar\eta)^2} = \frac{V}{\ell_s^2}\frac{1}{\tau_2\,(\eta\,\bar\eta)^2}\,, \tag{IV.A.11}$$

where V is the volume of a very large two-torus. Now, we recognize that the expression (IV.A.11) is the properly normalized partition function of two non-compact bosons (see e.g. [28] or [51]). Combining this result with the orbifold partition function (IV.A.1)–(IV.A.3), we conclude that in the limit $T \to i\infty$, the resulting theory is type IIB on $\mathbb{R}^{1,5} \times T^4$.

We mention here that there is a subtlety regarding the volume of the torus that becomes very large. Since the orbifold partition function is divided by the orbifold rank p, the volume of the torus that decompactifies is actually $4\pi^2\mathcal{R}_4\mathcal{R}_5/p$. Moreover, it is interesting to note that the radius $\mathcal{R}_5$ on which the orbifold acts by a shift is related to the radius R_5 of the corresponding Scherk–Schwarz effective supergravity theory by $\mathcal{R}_5 = pR_5$.

Now we focus on the limit $T_2 \to 0$, i.e $\mathcal{R}_4 \to 0$ and $\mathcal{R}_5 \to 0$. Here, we have three different cusps, namely the cusps at $T = 0, -2$ and -3. We start from the cusp $T_1 = 0$. In this case, the partition function (IV.A.7) reads

$$Z_{T^2}[k,l] = \frac{\mathcal{R}_4\mathcal{R}_5}{\alpha'\,\tau_2\,(\eta\,\bar\eta)^2} \sum_{\{n_i,w_i\}\in\mathbb{Z}^4} e^{\frac{-\pi\mathcal{R}_5^2}{\alpha'\tau_2}\left|n_1 - \frac{l}{p} + \left(w_1 + \frac{k}{p}\right)\tau\right|^2} e^{\frac{-\pi\mathcal{R}_4^2}{\alpha'\tau_2}|n_2 + w_2\tau|^2}\,. \tag{IV.A.12}$$

By performing a multiple Poisson resummation over all momentum and winding numbers we can bring (IV.A.12) to the equivalent form

$$Z_{T^2}[k,l] = \frac{\alpha'}{\mathcal{R}_5\mathcal{R}_4}\frac{1}{\tau_2\,(\eta\,\bar\eta)^2} \sum_{\{n_i,w_i\}\in\mathbb{Z}^4} e^{\frac{2\pi i}{p}(n_1 l + w_1 k)} e^{\frac{-\pi\alpha'}{\mathcal{R}_5^2\tau_2}|w_1 + n_1\tau|^2} e^{\frac{-\pi\alpha'}{\mathcal{R}_4^2\tau_2}|w_2 + n_2\tau|^2}\,. \tag{IV.A.13}$$

It is easy to verify that the above result could also be obtained by performing the T-duality transformation $\mathcal{R}_5 \to \alpha'/\mathcal{R}_5$, $\mathcal{R}_4 \to \alpha'/\mathcal{R}_4$, $n_1 \leftrightarrow w_1$, $n_2 \leftrightarrow w_2$.

Note that this transformation changes the shift vector $u = (1/p, 0, 0, 0)$ to $\tilde{u} = (0, 0, 1/p, 0)$. As we can see from (IV.A.13), in the limit $\mathcal{R}_4 \to 0$ and $\mathcal{R}_5 \to 0$ all terms are exponentially suppressed except for the terms with $n_1 = n_2 = w_1 = w_2 = 0$ and $k, l = 0, \ldots, p$. In particular, we find that for all k, l

$$\lim_{T_2 \to 0} Z_{T^2}[k,l] = \frac{\alpha'}{\mathcal{R}_5 \mathcal{R}_4} \frac{1}{\tau_2 \, (\eta\, \bar{\eta})^2} \,, \tag{IV.A.14}$$

or, by defining the dual radii $\widetilde{\mathcal{R}}_5 = \alpha'/\mathcal{R}_5$, $\widetilde{\mathcal{R}}_4 = \alpha'/\mathcal{R}_4$

$$\lim_{T_2 \to 0} Z_{T^2}[k,l] = \frac{\widetilde{\mathcal{R}}_4 \widetilde{\mathcal{R}}_5}{\alpha' \tau_2 \, (\eta\, \bar{\eta})^2} \,. \tag{IV.A.15}$$

So, in the limit $T \to 0$ we obtain the partition function of two non-compact bosons, for all values of k and l. Then, from (IV.A.1)-(IV.A.3) we can see that in the limit $T \to 0$ the theory becomes type IIB on a non-freely acting asymmetric orbifold $\mathbb{R}^{1,5} \times T^4/\mathbb{Z}_6$, characterized by the twist vectors $\tilde{u} = \left(\frac{5}{6}, \frac{1}{6}\right)$ and $u = \left(\frac{1}{6}, \frac{1}{6}\right)$.

We continue with the cusp $T_1 = -2$, for which we use the partition function given in (IV.A.4)-(IV.A.6). After a bit of algebra, it is easy to verify that, in the limit $T_2 \to 0$, all terms in the partition function are exponentially suppressed unless

$$n_1 = -2w_2 \qquad \text{and} \qquad n_2 = 2w_1 + \frac{k}{3} \,. \tag{IV.A.16}$$

Here, in order to make contact with the model studied in Section IV.3, we have used that $p = 6$. Note that (IV.A.16) has solutions only for $k = 0$ and 3. Now, by plugging (IV.A.16) back in (IV.A.4)-(IV.A.6) we obtain

$$\lim_{\substack{T_2 \to 0 \\ T_1 = -2}} Z_{T^2}[k,l] = \lim_{T_2 \to 0} \frac{1}{(\eta\bar{\eta})^2} \sum_{\{w_1, w_2\} \in \mathbb{Z}^2} e^{\frac{-2\pi i l w_2}{3}} e^{-\pi\alpha' \tau_2 (\tilde{w}_1^2 \mathcal{R}_5^2 + w_2^2 \mathcal{R}_4^2)} \,. \tag{IV.A.17}$$

By performing a double Poisson resummation over the winding numbers w_1 and w_2 we find

$$\lim_{\substack{T_2 \to 0 \\ T_1 = -2}} Z_{T^2}[k,l] = \lim_{\substack{\mathcal{R}_5 \to 0 \\ \mathcal{R}_4 \to 0}} \frac{\alpha'}{\mathcal{R}_5 \mathcal{R}_4} \frac{1}{\tau_2 \, (\eta\, \bar{\eta})^2} \sum_{\{w_1, w_2\} \in \mathbb{Z}^2} e^{\frac{\pi i k w_1}{3}} e^{\frac{-\pi\alpha'}{\mathcal{R}_5^2 \tau_2} w_1^2} e^{\frac{-\pi\alpha'}{\mathcal{R}_4^2 \tau_2} (w_2 + \frac{l}{3})^2} \,. \tag{IV.A.18}$$

From this expression we see that all terms are exponentially suppressed unless

$$w_1 = 0 \qquad \text{and} \qquad w_2 + \frac{l}{3} = 0 \,, \tag{IV.A.19}$$

which is satisfied only for $l = 0$ and 3. Putting everything together, we conclude that if $[k,l] = [0,0], [0,3], [3,0]$ or $[3,3]$

$$\lim_{\substack{T_2 \to 0 \\ T_1 = -2}} Z_{T^2}[k,l] = \frac{\alpha'}{\mathcal{R}_5 \mathcal{R}_4} \frac{1}{\tau_2 \, (\eta\, \bar{\eta})^2} \,, \tag{IV.A.20}$$

while for all other values of $[k,l]$ the limit is exponentially suppressed. Now, from (IV.A.1)–(IV.A.3) we can see that we obtain type IIB on a non-freely acting symmetric orbifold $\mathbb{R}^{1,5}\times T^4/\mathbb{Z}_2$, characterized by the twist vectors $\tilde{u}=u=\left(\frac{1}{2},\frac{1}{2}\right)$.

Finally, the analysis of the cusp $T_1=-3$ is completely analogous to the case $T_1=-2$, so we omit the details. We find that if $[k,l]=[0,0]$, $[0,2]$, $[0,4]$, $[2,0]$, $[2,2]$, $[2,4]$, $[4,0]$, $[4,2]$ or $[4,4]$,

$$\lim_{\substack{T_2\to 0\\ T_1=-3}} Z_{T^2}[k,l]=\frac{\alpha'}{\mathcal{R}_5\mathcal{R}_4}\frac{1}{\tau_2\,(\eta\,\bar{\eta})^2}\,, \tag{IV.A.21}$$

while for all other values of $[k,l]$ the limit is exponentially suppressed. In this case we obtain type IIB on a non-freely acting asymmetric orbifold $\mathbb{R}^{1,5}\times T^4/\mathbb{Z}_3$, characterized by the twist vectors $\tilde{u}=\left(-\frac{1}{3},\frac{1}{3}\right)$ and $u=\left(\frac{1}{3},\frac{1}{3}\right)$.

Now, we discuss the cusps of the modulus U and we keep T constant. Also, for convenience, we set $T_1=0$. We start from the limit $U_2\to\infty$, and without loss of generality, we set $U_1=0$. Then, $U_2\to\infty$ implies that $\mathcal{R}_4\to\infty$ and $\mathcal{R}_5\to 0$. In order to study this limit, we start from (IV.A.12) and we perform a double Poisson resummation over the momentum number n_1 and the winding number w_1. We find

$$Z_{T^2}[k,l]=\frac{\mathcal{R}_4/\mathcal{R}_5}{\tau_2\,(\eta\,\bar{\eta})^2}\sum_{\{n_i,w_i\}\in\mathbb{Z}^4} e^{\frac{2\pi i}{p}(n_1 l+w_1 k)}e^{\frac{-\pi\alpha'}{\mathcal{R}_5^2\tau_2}|w_1+n_1\tau|^2}e^{\frac{-\pi\mathcal{R}_4^2}{\alpha'\tau_2}|n_2+w_2\tau|^2}\,. \tag{IV.A.22}$$

From this expression it is easy to see that for all k,l

$$\lim_{U_2\to\infty} Z_{T^2}[k,l]=\frac{\mathcal{R}_4/\mathcal{R}_5}{\tau_2\,(\eta\,\bar{\eta})^2}\,. \tag{IV.A.23}$$

We continue with the limit $U_2\to 0$. Here we have three different cusps at $U_1=0$, $-\frac{1}{3}$ and $-\frac{1}{2}$. We start from the cusp $U_1=0$. Now, $U_2\to 0$ implies that $\mathcal{R}_4\to 0$ and $\mathcal{R}_5\to\infty$. In order to analyse this limit we start from (IV.A.12) and we perform a double Poisson resummation over the momentum number n_2 and the winding number w_2. We obtain

$$Z_{T^2}[k,l]=\frac{\mathcal{R}_5/\mathcal{R}_4}{\tau_2\,(\eta\,\bar{\eta})^2}\sum_{\{n_i,w_i\}\in\mathbb{Z}^4} e^{\frac{-\pi\mathcal{R}_5^2}{\alpha'\tau_2}\left|n_1-\frac{l}{p}+\left(w_1+\frac{k}{p}\right)\tau\right|^2}e^{\frac{-\pi\alpha'}{\mathcal{R}_4^2\tau_2}|w_2+n_2\tau|^2}\,. \tag{IV.A.24}$$

From the above expression it is clear that the only term that is not exponentially suppressed is the term with $n_1=n_2=w_1=w_2=k=l=0$. Thus, we obtain

$$\lim_{U_2\to 0} Z_{T^2}[0,0]=\frac{\mathcal{R}_5/\mathcal{R}_4}{\tau_2\,(\eta\,\bar{\eta})^2}\,. \tag{IV.A.25}$$

while for k and/or $l\neq 0$ the limit is exponentially suppressed.

Let us now consider the limit $U_2 \to 0$, with $U_1 = -\frac{1}{2}$. In this case, $g_{ij} \to \infty$, as we can see from (IV.A.9). After a bit of algebra, it is easy to see that the sum in (IV.A.7) is exponentially suppressed unless the following condition is met (recall that the model of Section IV.3 is a $\mathbb{Z}_6$ orbifold, so $p = 6$):

$$n_2 = 2n_1 - \frac{l}{3} \qquad \text{and} \qquad w_2 = 2w_1 + \frac{k}{3}\,. \tag{IV.A.26}$$

First of all, it is clear that for l and/or $k = 1, 2, 4$ and 5, the condition (IV.A.26) can never be met. Moreover, if $[k, l] = [0, 0], [0, 3], [3, 0]$ or $[3, 3]$, (IV.A.26) fixes n_2 and w_2 in terms of n_1 and w_1, respectively. By substituting (IV.A.26) back in (IV.A.7), we obtain

$$\lim_{\substack{U_2\to 0\\ U_1=-1/2}} Z_{T^2}[k,l] = \frac{T_2}{\tau_2\,(\eta\,\bar\eta)^2} \lim_{U_2\to 0} \sum_{n_1,w_1\in\mathbb{Z}} e^{\frac{-\pi 4T_2U_2}{\tau_2}\left|n_1-\frac{l}{6}+\left(w_1+\frac{k}{6}\right)\tau\right|^2}\,. \tag{IV.A.27}$$

By performing a double Poisson resummation on n_1 and w_1 we get

$$\lim_{\substack{U_2\to 0\\ U_1=-1/2}} Z_{T^2}[k,l] = \frac{1}{\tau_2\,(\eta\,\bar\eta)^2} \lim_{U_2\to 0} \frac{1}{4U_2} \sum_{n_1,w_1\in\mathbb{Z}} e^{\frac{2\pi i}{6}(n_1 l + w_1 k)} e^{\frac{-\pi}{4\tau_2 T_2 U_2}|w_1+n_1\tau|^2}\,. \tag{IV.A.28}$$

So, all terms are exponentially suppressed unless $n_1 = w_1 = 0$, which yields

$$\lim_{\substack{U_2\to 0\\ U_1=-1/2}} Z_{T^2}[k,l] = \frac{1}{4U_2}\frac{1}{\tau_2\,(\eta\,\bar\eta)^2}\,. \tag{IV.A.29}$$

The analysis of the limit $U_2 \to 0$, with $U_1 = -\frac{1}{3}$ and T constant, proceeds in a similar way. In this case, we find that the sum in (IV.A.7) is exponentially suppressed unless

$$n_2 = 3n_1 - \frac{l}{2} \qquad \text{and} \qquad w_2 = 3w_1 + \frac{k}{2}\,. \tag{IV.A.30}$$

This condition can be solved if $[k, l] = [0, 0], [0, 2], [0, 4], [2, 0], [2, 2], [2, 4], [4, 0], [4, 2]$ or $[4, 4]$. For these values of $[k, l]$ we find

$$\lim_{\substack{U_2\to 0\\ U_1=-1/3}} Z_{T^2}[k,l] = \frac{1}{9U_2}\frac{1}{\tau_2\,(\eta\,\bar\eta)^2}\,. \tag{IV.A.31}$$

We would like to mention here that the results for the cusps of the modulus U can be simply obtained from those of T by performing the T-duality transformation $T \to 1/\overline{U}$. To be precise, let us denote the element of $\mathrm{O}(2, 2; \mathbb{Z})$ that exchanges the moduli T and U by γ_e; this element also exchanges type IIB with type IIA theory. Furthermore, we denote the coordinate reflection $Z_1 \to -Z_1$, which acts on the moduli as $(T, U) \to (-\overline{T}, -\overline{U})$, by γ_r. These two $\mathbb{Z}_2$'s act on a vector of

the lattice $\Gamma^{2,2}$ as

$$(T,U)\to(U,T):\begin{pmatrix}0&0&1&0\\0&-1&0&0\\1&0&0&0\\0&0&0&-1\end{pmatrix},\quad (T,U)\to(-\overline{T},-\overline{U}):\begin{pmatrix}-1&0&0&0\\0&1&0&0\\0&0&-1&0\\0&0&0&1\end{pmatrix}. \tag{IV.A.32}$$

Finally, we denote the transformation $(T,U)\to(-1/T,U)$ of $\mathrm{SL}(2,\mathbb{Z})_T$ as γ_i. Then, the T-duality element $\gamma=\gamma_i\gamma_e\gamma_r\gamma_i$ acts as

$$T\leftrightarrow\frac{1}{\overline{U}},\quad U\leftrightarrow\frac{1}{\overline{T}},\qquad \begin{pmatrix}w_1\\w_2\\n_1\\n_2\end{pmatrix}\leftrightarrow\begin{pmatrix}w_1\\n_2\\n_1\\w_2\end{pmatrix}. \tag{IV.A.33}$$

Note that this duality element leaves the shift vector invariant, and it exchanges the cusps of T and U as follows:

$$\begin{aligned}U\to 0\quad&\leftrightarrow\quad T\to i\infty\,,\\ T\to 0\quad&\leftrightarrow\quad U\to i\infty\,,\\ U\to -\tfrac{1}{2}\quad&\leftrightarrow\quad T\to -2\,,\\ U\to -\tfrac{1}{3}\quad&\leftrightarrow\quad T\to -3\,,\end{aligned} \tag{IV.A.34}$$

Finally it is easy to see that $\det(\gamma)=-1$. Hence, the T-duality element γ exchanges type IIB with type IIA theory. Concluding, we can see that the cusps of the modulus T can be interpreted as various decompactification limits of the type IIB theory, while the cusps of the modulus U can be interpreted as various decompactification limits of the type IIA theory.

IV.B Supergravity multiplets in 6D

In this appendix we discuss the various supergravity fields, and supergravity multiplets in 6D. First of all, we list in Table IV.8 the weight vectors of the lightest left- and right-moving states in the untwisted orbifold sector, and their representations under the massless little group $\mathrm{SU}(2)\times\mathrm{SU}(2)$ in 6D.

Also, for the construction of states, we use the rule $\mathbf{2}\otimes\mathbf{2}=\mathbf{3}\oplus\mathbf{1}$, for tensoring SU(2) representations. In addition, we tabulate the massless representations that correspond to the various supergravity fields in six dimensions in Table IV.9.

Now, we can present the various supergravity multiplets.

$\mathcal{N}=8$

All massless fields fit in the gravity multiplet, in the representations

$$(\mathbf{3},\mathbf{3})\oplus 4(\mathbf{3},\mathbf{2})\oplus 4(\mathbf{2},\mathbf{3})\oplus 5(\mathbf{3},\mathbf{1})\oplus 5(\mathbf{1},\mathbf{3})\oplus 16(\mathbf{2},\mathbf{2})\oplus 20(\mathbf{2},\mathbf{1})\oplus 20(\mathbf{1},\mathbf{2})\oplus 25(\mathbf{1},\mathbf{1})\,. \tag{IV.B.1}$$

Sector	$\tilde{r}, r$	SU(2) × SU(2) rep
NS	$(\underline{\pm 1, 0}, 0, 0)$	$(\mathbf{2}, \mathbf{2})$
	$(0, 0, \pm 1, 0)$	$2 \times (\mathbf{1}, \mathbf{1})$
	$(0, 0, 0, \pm 1)$	$2 \times (\mathbf{1}, \mathbf{1})$
R	$(\pm\frac{1}{2}, \pm\frac{1}{2}, \frac{1}{2}, \frac{1}{2})$	$(\mathbf{2}, \mathbf{1})$
	$(\pm\frac{1}{2}, \pm\frac{1}{2}, -\frac{1}{2}, -\frac{1}{2})$	$(\mathbf{2}, \mathbf{1})$
	$(\underline{\frac{1}{2}, -\frac{1}{2}}, \frac{1}{2}, -\frac{1}{2})$	$(\mathbf{1}, \mathbf{2})$
	$(\underline{\frac{1}{2}, -\frac{1}{2}}, -\frac{1}{2}, \frac{1}{2})$	$(\mathbf{1}, \mathbf{2})$

Table IV.8: The weight vectors of the lightest left- and right-moving states in the untwisted sector, and their representations under the massless little group SU(2) × SU(2) in 6D. Underlying denotes permutation.

Massive field	SU(2) × SU(2) rep
$B^+_{\mu\nu}$ / $B^-_{\mu\nu}$	$(\mathbf{3}, \mathbf{1})$ / $(\mathbf{1}, \mathbf{3})$
ψ^+_μ / ψ^-_μ	$(\mathbf{2}, \mathbf{3})$ / $(\mathbf{3}, \mathbf{2})$
A_μ	$(\mathbf{2}, \mathbf{2})$
χ^+ / χ^-	$(\mathbf{1}, \mathbf{2})$ / $(\mathbf{2}, \mathbf{1})$
ϕ	$(\mathbf{1}, \mathbf{1})$

Table IV.9: Here we show the various massless 6D supergravity fields and their representations under the massless little group.

$\mathcal{N} = 4$ $(0, 2)$

There are two types of multiplets. The gravity multiplet

$$(\mathbf{3}, \mathbf{3}) \oplus 4 \times (\mathbf{2}, \mathbf{3}) \oplus 5 \times (\mathbf{1}, \mathbf{3}) \,, \tag{IV.B.2}$$

and the tensor multiplet

$$(\mathbf{3}, \mathbf{1}) \oplus 4 \times (\mathbf{2}, \mathbf{1}) \oplus 5 \times (\mathbf{1}, \mathbf{1}) \,. \tag{IV.B.3}$$

$\mathcal{N} = 4$ $(1, 1)$

Again, we have two types of multiplets. The gravity multiplet

$$(\mathbf{3}, \mathbf{3}) \oplus 2 \times (\mathbf{3}, \mathbf{2}) \oplus 2 \times (\mathbf{2}, \mathbf{3}) \oplus (\mathbf{3}, \mathbf{1}) \oplus (\mathbf{1}, \mathbf{3}) \oplus 4 \times (\mathbf{2}, \mathbf{2}) \oplus 2 \times (\mathbf{2}, \mathbf{1}) \oplus 2 \times (\mathbf{1}, \mathbf{2}) \oplus (\mathbf{1}, \mathbf{1}) \,, \tag{IV.B.4}$$

and the vector multiplet

$$(\mathbf{2},\mathbf{2}) \oplus 2 \times (\mathbf{2},\mathbf{1}) \oplus 2 \times (\mathbf{1},\mathbf{2}) \oplus 4 \times (\mathbf{1},\mathbf{1})\,. \tag{IV.B.5}$$

$\mathcal{N} = 2$

There exist four types of multiplets. The gravity multiplet

$$(\mathbf{3},\mathbf{3}) \oplus 2 \times (\mathbf{2},\mathbf{3}) \oplus (\mathbf{1},\mathbf{3})\,, \tag{IV.B.6}$$

the tensor multiplet

$$(\mathbf{3},\mathbf{1}) \oplus 2 \times (\mathbf{2},\mathbf{1}) \oplus (\mathbf{1},\mathbf{1})\,, \tag{IV.B.7}$$

the vector multiplet

$$(\mathbf{2},\mathbf{2}) \oplus 2 \times (\mathbf{1},\mathbf{2})\,. \tag{IV.B.8}$$

and the hypermultiplet

$$2 \times (\mathbf{2},\mathbf{1}) \oplus 4 \times (\mathbf{1},\mathbf{1})\,. \tag{IV.B.9}$$

IV.C Quantum corrections to the moduli space

The moduli space metric is determined by the prepotential, as we demonstrated in (IV.4.8) for the classical moduli space. This classical prepotential can be modified at the quantum level. For $\mathcal{N} = 2$ theories, non-renormalization theorems [52–54] dictate that, regarding spacetime effects, all quantum corrections to the prepotential can arise by one-loop and non-perturbative contributions. So, the exact prepotential is of the form

$$F(X) = F^{(0)}(X) + F^{(1)}(X) + F^{(\mathrm{np})}(X)\,. \tag{IV.C.1}$$

Here $F^{(0)}(X)$ is the classical prepotential, given by (IV.4.12), and $F^{(1)}(X)$ is the perturbative, in string coupling $\sim 1/S_2$, one-loop correction to the prepotential. Hence, this term should be independent of the axio-dilaton field S. Also, $F^{(\mathrm{np})}(X)$ denotes non-perturbative, in string coupling, corrections to the prepotential, which may arise by instantons from the NS5-brane wrapped on $T^4 \times T^2$; such terms will be proportional to $e^{2\pi i S}$. Note that both $F^{(1)}(X)$ and $F^{(\mathrm{np})}(X)$ can contain perturbative and non-perturbative terms in α'. In particular, non-perturbative terms in α' can arise by instantons from the closed string worldsheet wrapped on T^2 and by worldline instantons of a particle with mass[21] $m \sim 1/\mathcal{R}_5$ wrapped around the cycle of T^2 with radius $\mathcal{R}_4$. These terms will be of the form $e^{2\pi i T}$ and $e^{2\pi i U}$, respectively.

The prepotential satisfies useful identities, such as the homogeneous condition

$$F = \tfrac{1}{2} F_I X^I\,, \tag{IV.C.2}$$

[21] Recall that in a freely acting orbifold, states become massive instead of being projected out of the spectrum. The masses are inversely proportional to the radius of the circle on which the orbifold acts as a shift.

where derivatives of $F(X)$ with respect to X^I are denoted by F_I. Also, the prepotential is defined up to symplectic transformations. Such transformations can be represented by a $(2n+2)\times(2n+2)$ real matrix $\mathscr{S}\in \mathrm{Sp}(2n+2;\mathbb{R})$

$$\mathscr{S}=\begin{pmatrix} A & B\\ C & D\end{pmatrix}\,, \tag{IV.C.3}$$

satisfying

$$\mathscr{S}^T\Omega\mathscr{S}=\Omega\,,\qquad \Omega=\begin{pmatrix} 0 & \mathbf{1}_{n+1}\\ -\mathbf{1}_{n+1} & 0\end{pmatrix}. \tag{IV.C.4}$$

This definition imposes the following constraints on the $(n+1)\times(n+1)$ real sub-matrices A,B,C and D:

$$A^TC-C^TA=\mathbf{0}_{n+1}\,,\quad B^TD-D^TB=\mathbf{0}_{n+1}\,,\quad A^TD-C^TB=\mathbf{1}_{n+1}\,. \tag{IV.C.5}$$

Constant $\mathrm{Sp}(2n+2;\mathbb{R})$ transformations of the form

$$\begin{pmatrix}\widetilde{X}^I\\ -\frac{i}{2}\widetilde{F}_I\end{pmatrix}=\begin{pmatrix} A & B\\ C & D\end{pmatrix}\begin{pmatrix} X^I\\ -\frac{i}{2}F_I\end{pmatrix}\,, \tag{IV.C.6}$$

leave the set of equations of motion and Bianchi identities invariant and thus, constitute dualities of the theory. Note that if the transformation

$$\widetilde{X}^I=A^I{}_JX^J-\tfrac{i}{2}B^{IJ}F_J\,, \tag{IV.C.7}$$

is invertible, $\widetilde{F}_I$ can be written as the derivative of a new prepotential, $\widetilde{F}(\widetilde{X})$, with respect to $\widetilde{X}^I$, that is

$$\widetilde{F}_I=\frac{\partial\widetilde{F}(\widetilde{X})}{\partial\widetilde{X}^I}\,. \tag{IV.C.8}$$

Moreover, a symplectic transformation (IV.C.6) is a symmetry of the action, if $B=0$ (see e.g. [40, 55]). Also, for $C\neq 0$ the Lagrangian changes by a total derivative, while for $C=0$ the Lagrangian is invariant. These, combined with (IV.C.5) imply that symmetries of the action can be represented by a constant matrix $\hat{\mathscr{S}}\in\mathrm{Sp}(2n+2;\mathbb{R})$ of the form

$$\hat{\mathscr{S}}=\begin{pmatrix} A & 0\\ A^{-T}W & A^{-T}\end{pmatrix}\,, \tag{IV.C.9}$$

where W is any real, symmetric matrix.

IV.C.1 One-loop quantum corrections

Let us now focus on the one-loop corrected prepotential by taking the weak coupling limit $S\to i\infty$, which takes the form

$$F(X)=F^{(0)}(X)+F^{(1)}(X)\,. \tag{IV.C.10}$$

It will be convenient to work in a basis $\left(\widetilde{X}^I, -\frac{i}{2}\widetilde{F}_I\right)$ which has the $\mathrm{Sp}(8;\mathbb{R})$ transformation rule:

$$\widetilde{X}^I = X^I\,, \widetilde{F}_I = F_I\,, \quad I = 0,2,3; \qquad \widetilde{X}^1 = -iF_1\,, \quad \widetilde{F}_1 = -iX^1\,. \tag{IV.C.11}$$

Now, let us present some useful relations in the $\left(\widetilde{X}^I, -\frac{i}{2}\widetilde{F}_I\right)$ basis. We start from the classical properties of this basis with $F^{(1)}(X) = 0$. We substitute the value of F_1 in the equation $\widetilde{X}^1 = -iF_1$ to obtain the following constraint

$$-\widetilde{X}^0\widetilde{X}^1 + \widetilde{X}^2\widetilde{X}^3 = 0\,. \tag{IV.C.12}$$

It will be convenient to rewrite the above constraint as

$$\widetilde{X}^I\widetilde{\eta}_{IJ}\widetilde{X}^J = 0\,, \qquad \text{where} \qquad \widetilde{\eta}_{IJ} = \begin{pmatrix} 0 & -\frac{1}{2} & 0 & 0 \\ -\frac{1}{2} & 0 & 0 & 0 \\ 0 & 0 & 0 & \frac{1}{2} \\ 0 & 0 & \frac{1}{2} & 0 \end{pmatrix}. \tag{IV.C.13}$$

Using the matrix η, we can express $\widetilde{F}_I$ as

$$\widetilde{F}_I = 2iS\eta_{IJ}\widetilde{X}^J\,, \qquad \text{where} \qquad S = \frac{X^1}{X^0}\,. \tag{IV.C.14}$$

Then let us go to the one-loop level $F = F^{(0)} + F^{(1)}$ (from now on we omit writing down explicitly the dependence of $F(X)$ on X). Since $\widetilde{X}^1 = -i\left(F_1^{(0)} + F_1^{(1)}\right)$, and $F^{(1)}$ is independent of S, it follows that $F_1^{(1)} = 0$. So, the expressions for $\widetilde{X}^I$ remain the same as in the classical theory. This implies that the constraint (IV.C.13) is valid also at one-loop. On the other hand, the expressions for $\widetilde{F}_I$, $I = 0,2,3$, change at the one-loop level. Specifically, we have

$$\widetilde{F}_I = F_I^{(0)} + F_I^{(1)}\,, \quad I = 0,2,3 \qquad \widetilde{F}_1 = -iX^1\,. \tag{IV.C.15}$$

Using the classical result (IV.C.14), we can rewrite the above equation as

$$\widetilde{F}_I = 2iS\eta_{IJ}\widetilde{X}^J + F_I^{(1)}. \tag{IV.C.16}$$

By multiplying the above equation by $\widetilde{X}^I$, and using the constraint (IV.C.13), we get

$$\widetilde{F}_I\widetilde{X}^I = F_I^{(1)}\widetilde{X}^I\,. \tag{IV.C.17}$$

Now, recall that $F_1^{(1)} = 0$ and $\widetilde{X}^I = X^I\,, I = 0,2,3$. Hence, we can write

$$\widetilde{F}_I\widetilde{X}^I = F_I^{(1)}X^I\,. \tag{IV.C.18}$$

Finally, as $F^{(1)}$ is a homogeneous function of second degree in X^I, it satisfies $2F^{(1)} = F_I^{(1)}X^I$ as in (IV.C.2). Then, it follows that

$$F^{(1)} = \frac{1}{2}\widetilde{F}_I\widetilde{X}^I\,. \tag{IV.C.19}$$

So, we have expressed the one-loop correction to the prepotential $F^{(1)}$ in the basis $\left(\widetilde{X}^I, -\frac{i}{2}\widetilde{F}_I\right)$. This will help us to study how $F^{(1)}$ transforms under general symplectic transformations.

Of particular interest are symplectic transformations that leave the action invariant. These transformations are of the form (cf. (IV.C.9))

$$\begin{aligned}\widetilde{X}^I &\longrightarrow A^I{}_J\widetilde{X}^J\,,\\ \widetilde{F}_I &\longrightarrow 2i(A^{-t}W)_{IJ}\widetilde{X}^J + (A^{-t})_I{}^J\widetilde{F}_J\,,\end{aligned} \tag{IV.C.20}$$

which, combined, yield

$$\widetilde{F}_I\widetilde{X}^I \longrightarrow \widetilde{F}_I\widetilde{X}^I + 2iW_{IJ}\widetilde{X}^I\widetilde{X}^J\,. \tag{IV.C.21}$$

This, together with (IV.C.19) gives

$$F^{(1)} \longrightarrow F^{(1)} + iW_{IJ}\widetilde{X}^I\widetilde{X}^J\,. \tag{IV.C.22}$$

We mention here that $F^{(1)}$ might be shifted, even if $\widetilde{X}^I \to \widetilde{X}^I$. This indicates that $F^{(1)}$ has singularities, which when encircled by closed monodromies lead to a shift of $F^{(1)}$. The shift in the prepotential changes the action by a total derivative; thus constitutes a symmetry of the theory. Also, the singularities of $F^{(1)}$ occur at special lines in the moduli space, where generically massive states become massless. We will come back to these issues later in this appendix section. Finally, we mention here that the matrix W should be integer-valued but not necessarily in the basis $(\widetilde{X}^I, -\frac{i}{2}\widetilde{F}_I)$ [39]. As we have already mentioned above, $F^{(1)}$ is independent of the axio-dilaton field S, so we may write

$$F^{(1)}(X) = \left(X^0\right)^2 f^{(1)}(T,U) = \left(\widetilde{X}^0\right)^2 f^{(1)}(T,U)\,. \tag{IV.C.23}$$

Then, we can combine this with (IV.C.20) and (IV.C.22) to obtain

$$f^{(1)}(T,U) \longrightarrow \frac{f^{(1)}(T,U) + iW_{IJ}\frac{\widetilde{X}^I}{\widetilde{X}^0}\frac{\widetilde{X}^J}{\widetilde{X}^0}}{A^0{}_I A^0{}_J \frac{\widetilde{X}^I}{\widetilde{X}^0}\frac{\widetilde{X}^J}{\widetilde{X}^0}}\,. \tag{IV.C.24}$$

IV.C.2 Attempted computation

Let us now focus on the T-duality group of our model. First of all, the classical T-duality group $\mathrm{SL}(2,\mathbb{R})_T \times \mathrm{SL}(2,\mathbb{R})_U$ is broken to $\Gamma^1(p)_T \times \Gamma_1(p)_U$ at the quantum level. Also, we have seen that in the classical theory, the action is manifestly invariant under T-dualities, which is reflected to the embedding of $\mathrm{SL}(2,\mathbb{R})_T \times \mathrm{SL}(2,\mathbb{R})_U$ in $\mathrm{Sp}(8,\mathbb{R})$. However, as we have explained, in the quantum theory the action can be modified by a total derivative due to shifts of the prepotential.

Specifically, under $\Gamma^1(p)_T$ $\widetilde{X}^I$ and $\widetilde{F}_I$ transform as in (IV.C.20) with

$$A = \begin{pmatrix} d & 0 & c & 0 \\ 0 & a & 0 & b \\ b & 0 & a & 0 \\ 0 & c & 0 & d \end{pmatrix}, \qquad a, d = 1 \bmod p\,, \quad b = 0 \bmod p\,, \qquad ad - bc = 1\,, \tag{IV.C.25}$$

while under $\Gamma_1(p)_U$ we have

$$A = \begin{pmatrix} d' & 0 & 0 & c' \\ 0 & a' & b' & 0 \\ 0 & c' & d' & 0 \\ b' & 0 & 0 & a' \end{pmatrix} \qquad a', d' = 1 \bmod p\,, \quad c' = 0 \bmod p\,, \qquad a'd' - b'c' = 1\,. \tag{IV.C.26}$$

Note that at one-loop level, the axio-dilaton field S is not invariant under the T-duality group.

Under $\Gamma^1(p)_T$ transformations (IV.C.25), the transformation (IV.C.24) can be expressed as

$$f^{(1)}(T,U) \longrightarrow \frac{f^{(1)}(T,U) + \mathcal{P}(T,U)}{(d+cT)^2}\,, \quad \mathcal{P}(T,U) = iW_{IJ}\frac{\widetilde{X}^I}{\widetilde{X}^0}\frac{\widetilde{X}^J}{\widetilde{X}^0}\,. \tag{IV.C.27}$$

$\mathcal{P}(T,U)$ is a quadratic polynomial of T and U. To make contact with the literature of modular forms, we rewrite the above transformation of $f^{(1)}(T,U)$ in the more suitable form

$$f^{(1)}\left(\frac{aT+b}{cT+d}, U\right) = (d+cT)^{-2}\left[f^{(1)}(T,U) + \mathcal{P}(T,U)\right]\,. \tag{IV.C.28}$$

So, we see that under $\Gamma^1(p)_T$ transformations the function $f^{(1)}(T,U)$ would transform as a modular form of weight -2, if the quadratic polynomial $\mathcal{P}(T,U)$ was absent. By using $\partial_T^3\mathcal{P}(T,U) = 0$, it is straightforward to show that

$$\partial_T^3 f^{(1)}\left(\frac{aT+b}{cT+d}, U\right) = (d+cT)^4\,\partial_T^3 f^{(1)}(T,U)\,, \tag{IV.C.29}$$

which shows that $\partial_T^3 f^{(1)}(T,U)$ transforms as a modular form of weight 4 under $\Gamma^1(p)_T$ transformations. Moreover, it is easy to see that

$$\partial_T^3 f^{(1)}\left(T, \frac{a'U+b'}{c'U+d'}\right) = (d'+cU')^{-2}\,\partial_T^3 f^{(1)}(T,U)\,, \tag{IV.C.30}$$

So, $\partial_T^3 f^{(1)}(T,U)$ transforms as a modular form of weight -2 under $\Gamma_1(p)_U$ transformations. Of course, similar results can be obtained for $\partial_U^3 f^{(1)}(T,U)$, which transforms as a modular form with weights -2 and 4 under $\Gamma^1(p)_T$ and $\Gamma_1(p)_U$ transformations, respectively.

The function $f^{(1)}(T,U)$ has singularities at special areas in the moduli space, where massive fields become massless. As we have mentioned in Subsection IV.4.2,

for our model there are two such lines at $T = 6U$ and $T = 12U$ (cf. (IV.4.31) and (IV.4.22)). It was shown in [39] that if massless charged hypermultiplets arise at $\phi = 0$, where ϕ is a modulus of the theory, then the one-loop prepotential around $\phi = 0$ is given by[22]

$$f^{(1)}(\phi) = -\frac{b_\phi}{8\pi^2}\phi^2 \log \phi + \text{regular}\,, \tag{IV.C.31}$$

where b_ϕ is the β-function coefficient of the gauge group under which the massless hypermultiplets are charged. For 1 massless hypermultiplet charged under a U(1) gauge group this coefficient is $+2$ [56].

Recall that at $T = 6U$ two charged hypermultiplets become massless. Then, if we identify $\phi = \frac{1}{2}(T - 6U)$, we can see that near $T - 6U = 0$ the function $f^{(1)}(T, U)$ takes the form

$$f^{(1)}(T \approx 6U) = -\frac{1}{8\pi^2}\,(T - 6U)^2 \log(T - 6U) + \text{regular}\,, \tag{IV.C.32}$$

A similar analysis applies for $T = 12U$, where 1 charged hypermultiplet becomes massless. In this case we find that near $T - 12U = 0$ the prepotential takes the form

$$f^{(1)}(T \approx 12U) = -\frac{1}{16\pi^2}\,(T - 12U)^2 \log(T - 12U) + \text{regular}\,. \tag{IV.C.33}$$

Finally, recall that there is a special point $(T, U) = (12U^*, U^*)$, where $U^* = -\frac{1}{4} + i\frac{\sqrt{3}}{12}$ as shown in Figure IV.1. At this point, two critical lines intersect, namely the lines $T = 12U$ and $T = -(24U + 6)/(6U + 1)$, such that 2 hypermultiplets become massless. Hence, for $(T, U) \approx (12U^*, U^*)$ the prepotential should take the form

$$f^{(1)}(T \approx 12U^*) = -\frac{1}{8\pi^2}\,(T - 12U^*)^2 \log(T - 12U^*) + \text{regular}\,. \tag{IV.C.34}$$

From the above, we can also determine the behavior of $\partial_T^3 f^{(1)}(T, U)$ near the critical lines and critical point. We find that

$$\begin{aligned}
&\text{near} \quad T = 6U \;: && \partial_T^3 f^{(1)} \to -\frac{1}{4\pi^2}\frac{1}{T - 6U} + \text{regular}\,, \\
&\text{near} \quad T = 12U \neq 12U^* \;: && \partial_T^3 f^{(1)} \to -\frac{1}{8\pi^2}\frac{1}{T - 12U} + \text{regular}\,, \\
&\text{near} \quad T = 12U = 12U^* \;: && \partial_T^3 f^{(1)} \to -\frac{1}{4\pi^2}\frac{1}{T - 12U^*} + \text{regular}\,.
\end{aligned} \tag{IV.C.35}$$

Similarly, around the critical lines and critical point, $\partial_U^3 f^{(1)}(T, U)$ behaves as

[22] The same expression holds also for massless vector multiplets.

follows

$$\begin{aligned}
&\text{near} \quad T = 6U \ : && \partial_U^3 f^{(1)} \to \frac{6^3}{4\pi^2}\frac{1}{T-6U} + \text{regular}\,, \\
&\text{near} \quad T = 12U \neq 12U^* \ : && \partial_U^3 f^{(1)} \to \frac{12^3}{8\pi^2}\frac{1}{T-12U} + \text{regular}\ , \\
&\text{near} \quad T = 12U = 12U^* \ : && \partial_U^3 f^{(1)} \to \frac{12^3}{4\pi^2}\frac{1}{T-12U^*} + \text{regular}\,.
\end{aligned} \tag{IV.C.36}$$

In addition, near the singular cusps $T = 6U \to 0, i\infty$ and $T = 12U \to 0, i\infty$,

$$\partial_T^3 f^{(1)}(T,U),\ \partial_U^3 f^{(1)}(T,U) \quad \propto \quad \frac{\infty}{T-6U} \quad \text{or} \quad \frac{\infty}{T-12U}\,. \tag{IV.C.37}$$

Putting everything together, we see that $\partial_T^3 f^{(1)}(T,U)$ ($\partial_U^3 f^{(1)}(T,U)$) should transform as a modular form with weights $(4,-2)$ ($(-2,4)$) under $\Gamma^1(6)_T \times \Gamma_1(6)_U$. This function should have a simple pole at the lines $T = 6U$ and $T = 12U$, and a simple pole at the special point $(T,U) = (12U^*, U^*)$. Note that these must be the only singularities of $\partial_{T,U}^3 f^{(1)}(T,U)$.

Besides the properties of the 1-loop prepotential near the singularity lines, the derivatives have asymptotic restrictions when $T \to i\infty$ or $U \to i\infty$. To avoid the divergence of the prepotential at the $T \to i\infty$, we required the T-derivative $\partial_T^3 f^{(1)}(T,U) \to 0$; similarly, $\partial_U^3 f^{(1)}(T,U) \to 0$ when $U \to i\infty$. In addition, as $U \to i\infty$, $\partial_T^3 f^{(1)}(T,U) \to$ constant and as $T \to i\infty$, $\partial_U^3 f^{(1)}(T,U) \to$ constant [39, 57].

These singular and asymptotic behaviours are necessary to constrain the expressions of the third derivatives. For example, for 1-loop quantum corrections of the prepotential under $\mathrm{SL}(2,\mathbb{Z})_T \times \mathrm{SL}(2,\mathbb{Z})_U$ duality group, the singular line appears at $T = U$. The third derivative is uniquely determined by the asymptotic properties at $T \to i\infty$ and $U \to i\infty$ and the divergence at $T = U$, up to the number of massless multiplets there. The expression can be generated by the derivatives of the moduli function of $\mathrm{SL}(2,\mathbb{Z})$:

$$\partial_T^3 f^{(1)}(T,U) \propto -\frac{2i}{\pi}\frac{j_T(T)}{j(T)-j(U)}\frac{j_T(T)}{j_U(U)}\frac{j(U)-j(i)}{j(T)-j(i)}\frac{j(U)-j(\rho)}{j(T)-j(\rho)}\,, \tag{IV.C.38}$$

where the j-function is the moduli function of $\mathrm{SL}(2,\mathbb{Z})$. There is one double fixed point i and one triple fixed point ρ on the boundary of $\mathrm{SL}(2,\mathbb{Z})$ fundamental domain, and $j(\rho) = 0$.

Following this logic, in our model with duality group $\Gamma^1(6) \times \Gamma_1(6)$, the third derivatives of the 1-loop prepotential should be expressed in terms of the modular functions and moduli forms of $\Gamma_1(6)$ (and $\Gamma_1(3)$ due to the location of U^*). In Appendix IV.D, we find many interesting relations between the Hauptmoduln of $\Gamma_1(6)$ and $\Gamma_1(3)$, J_6 and J_3, and modular forms. Combining with the asymptotic and singular properties above, and the integrability condition near (and not at) the singularities

$$\partial_U^3 \partial_T^3 f^{(1)} = \partial_T^3 \partial_U^3 f^{(1)}\,, \tag{IV.C.39}$$

we can fairly restrict the expression of the 1-loop prepotential. However, due to the additional cusps (fixed points) in our model, these conditions are not enough to uniquely determine the result.

The continuing work based on an ansatz

Here we present the unfinished work, which has not yet yielded conclusive results, but offers intriguing insights that warrant further investigation.

In order to find a function that satisfies all the above criteria, we start with the following ansatz

$$\partial_T^3 f^{(1)}(T,U) = \frac{g_{(4,-2)}(T,U)}{\left[J_6\left(\frac{T}{6}\right) - J_6(U)\right]\left[J_3\left(\frac{T}{6}\right) - J_3(2U)\right]}\,, \tag{IV.C.40}$$

where $g_{(4,-2)}(T,U)$ is a modular form with weight $(4,-2)$ under $(\Gamma^1(6)_T,\Gamma_1(6)_U)$, which is T-holomorphic and U-meromorphic. Also $J_3(2U)$ and $J_6(U)$ are modular functions of $\Gamma_1(6)_U$, and similarly for $J_{3,6}\left(\frac{T}{6}\right)$. Note that the singularities of the prepotential, which are located at the lines $T = 6U$ and $T = 12U$, are captured by the denominator of (IV.C.40).

Let us now study the behavior of $\partial_T^3 f(T,U)$ near the line $T = 6U$. Using the residue theorem and the first line of (IV.C.35) we find

$$\operatorname*{Res}_{T\to 6U} \partial_T^3 f^{(1)}(T,U) = \frac{g_{(4,-2)}(6U,U)}{\partial_T J_6\left(\frac{T}{6}\right)|_{T=6U}\left[J_3\left(U\right) - J_3(2U)\right]} \stackrel{!}{=} -\frac{1}{4\pi^2}\,. \tag{IV.C.41}$$

Similarly, near $T = 12U$ we find

$$\operatorname*{Res}_{T\to 12U} \partial_T^3 f^{(1)}(T,U) = \frac{g_{(4,-2)}(12U,U)}{\left[J_6\left(2U\right) - J_6(U)\right]\partial_T J_3\left(\frac{T}{6}\right)|_{T=12U}} \stackrel{!}{=} -\frac{1}{8\pi^2}\,. \tag{IV.C.42}$$

Given the above and using the fact that the derivative of a modular invariant function is a modular function of weight 2, without loss of generality, we can bring (IV.C.40) to the form

$$\partial_T^3 f^{(1)}(T,U) = -\frac{1}{4\pi^2}\frac{h_{(2,-2)}(T,U)\partial_T J_6\left(\frac{T}{6}\right)}{J_6\left(\frac{T}{6}\right) - J_6(U)} - \frac{1}{8\pi^2}\frac{\tilde{h}_{(2,-2)}(T,U)\partial_T J_3\left(\frac{T}{6}\right)}{J_3\left(\frac{T}{6}\right) - J_3(2U)}\,, \tag{IV.C.43}$$

where $h_{(2,-2)}(T,U)$ is a function with weight $(2,-2)$ under $(\Gamma^1(6)_T,\Gamma_1(6)_U)$, subject to the constraints $h_{(2,-2)}(6U,U) = 1$ and $h_{(2,-2)}(12U,U)$ regular. Similarly, $\tilde{h}_{(2,-2)}(T,U)$ is a function with weight $(2,-2)$ under $(\Gamma^1(6)_T,\Gamma_1(6)_U)$, subject to the constraints $\tilde{h}_{(2,-2)}(12U,U) = 1$ and $\tilde{h}_{(2,-2)}(6U,U)$ regular. Also, in the limit $T \to i\infty$, $h_{(2,-2)}(T,U) \to 0$ and $\tilde{h}_{(2,-2)}(T,U) \to 0$. Finally, in the limit $U \to i\infty$, $h_{(2,-2)}(T,U)/J_6(U) \to$ constant, and $\tilde{h}_{(2,-2)}(T,U)/J_6(U) \to$ constant.

Let us now focus on the first term of (IV.C.43), for which we need to specify the function $h_{(2,-2)}(T,U)$. According to $h_{(2,-2)}(6U,U) = 1$, a natural assumption

similar as (IV.C.52) is that

$$h_{(2,-2)}(T,U)=\frac{h_{(2)}\left(\frac{T}{6}\right)}{h_{(2)}(U)}, \tag{IV.C.44}$$

where $h_{(2)}$ is a weight 2 modular form and can generally be expressed using Hauptmoduln and derivatives. However, by computation, $h_{(2)}$ cannot solve the integrability condition near the $T=6U$ singularity:

$$\partial_U^3\partial_{\frac{T}{6}}^3 f(\frac{T}{6},U)=\partial_{\frac{T}{6}}^3\partial_U^3 f(\frac{T}{6},U)=\partial_U^3\partial_{\frac{T}{6}}^3 f(U,\frac{T}{6}),\quad \text{when } \frac{T}{6}\neq U\,. \tag{IV.C.45}$$

Hence we focus on another possible ansatz of the form of $h_{(2,-2)}(T,U)$. Note that its q-series in terms of T must start with $\mathcal{O}(q_T)$ because $\partial_T^3 f^{(1)}(T\to i\infty,U)\to 0$. The graded ring of modular forms of $\Gamma_1(6)$ is generated by two weight 1 modular forms $X_1(\tau)$ and $X_2(\tau)\equiv X_1(2\tau)$ which we define in (IV.D.6) in the next subsection, which are finite as $q=e^{2\pi i\tau}\to 0$. With these at hand, we can expand the function $h_{(2,-2)}(T,U)$ as follows

$$h_{(2,-2)}(T,U)=g_1(U)X_1\left(\tfrac{T}{6}\right)^2+g_2(U)X_1\left(\tfrac{T}{6}\right)X_2\left(\tfrac{T}{6}\right)+g_3(U)X_2\left(\tfrac{T}{6}\right)^2\,. \tag{IV.C.46}$$

Now, the condition $h_{(2,-2)}(T\to i\infty,U)\to 0$ yields $g_3(U)=-g_1(U)-g_2(U)$. Also, from the constraint $h_{(2,-2)}(6U,U)=1$, we obtain

$$g_1(U)\left[X_1(U)^2-X_2(U)^2\right]+g_2(U)\left[X_1(U)X_2(U)-X_2(U)^2\right]=1\,. \tag{IV.C.47}$$

Hence, we only need to determine the weight -2 form $g_2(U)$, and $g_1(U)$ can be expressed as

$$g_1(U)=\frac{1-g_2(U)\left[X_1(U)X_2(U)-X_2(U)^2\right]}{X_1(U)^2-X_2(U)^2}. \tag{IV.C.48}$$

In the $U\to i\infty$ limit, $\partial_T^3 f^{(1)}$ must be finite and non-zero, such that the q-expansion of $g_2(U)$ starts at the $1/q_U$-order. Unfortunately we cannot determine the expression of g_2. According to the exchanging identity of third derivatives (IV.C.45), if our ansatz is correct, the q-expansion of $g_2(U)$ can be written as

$$\begin{aligned}g_2=&\frac{a}{q}+b+\left(\frac{3}{8}-9a+\frac{b}{4}\right)q+\left(\frac{2}{3}-\frac{140a}{9}+\frac{44b}{9}\right)q^2+\left(\frac{31}{96}-\frac{413a}{36}+\frac{305b}{144}\right)q^3\\&+\left(-\frac{43}{200}+\frac{2053a}{375}-\frac{6553b}{1500}\right)q^4+\left(-\frac{569}{400}+\frac{27299a}{750}-\frac{33299b}{3000}\right)q^5+\cdots\,,\end{aligned} \tag{IV.C.49}$$

where $a,b\in\mathbb{R}$ are to be determined and keep $g_1(U),g_2(U)$ finite everywhere on the fundamental domain except for $U=i\infty$.

Regarding the function $\tilde{h}_{(2,-2)}(T,U)$ we can work in a similar way and consider the following expansion

$$\tilde{h}_{(2,-2)}(T,U)=\tilde{g}_1(U)X_1\left(\tfrac{T}{6}\right)^2+\tilde{g}_2(U)X_1\left(\tfrac{T}{6}\right)X_2\left(\tfrac{T}{6}\right)+\tilde{g}_3(U)X_2\left(\tfrac{T}{6}\right)^2\,. \tag{IV.C.50}$$

First, note that the condition $\tilde{h}_{(2,-2)}(12U,U)=1$ yields

$$\tilde{g}_1(U)X_1\left(2U\right)^2+\tilde{g}_2(U)X_1\left(2U\right)X_2\left(2U\right)+\tilde{g}_3(U)X_2\left(2U\right)^2=1\,. \tag{IV.C.51}$$

Now, the function $X_2\left(2U\right)$ is not a modular function of $\Gamma_1(6)_U$. So, in order to get a proper $\Gamma_1(6)_U$ modular function we should set $\tilde{g}_2(U)=\tilde{g}_3(U)=0$. Then, the condition $\tilde{h}_{(2,-2)}(12U,U)=1$ is easily satisfied by setting $\tilde{g}_1(U)=X_1(2U)^{-2}=X_2(U)^{-2}$. This would, in principle, fix $\tilde{h}_{(2,-2)}(T,U)$. However, the function $X_1(2U)$ has a zero at $X_1(2U^*)$, which would indicate an unphysical singularity in the prepotential. In order to remove this undesired singularity we consider the following modification

$$\begin{aligned}\tilde{h}_{(2,-2)}(T,U)&=\frac{X_1\left(\frac{T}{6}\right)^2}{X_1\left(2U\right)^2}\frac{J_3(2U)-J_3(2U^*)}{J_3\left(\frac{T}{6}\right)-J_3(2U^*)}\\&=\frac{J_3'\left(\frac{T}{6}\right)}{J_3'(2U)}\frac{J_3(2U)-J_3(0)}{J_3\left(\frac{T}{6}\right)-J_3(0)}\frac{J_3(2U)-J_3(2U^*)}{J_3\left(\frac{T}{6}\right)-J_3(2U^*)}\,.\end{aligned} \tag{IV.C.52}$$

Here $J_3'\left(\frac{T}{6}\right)\equiv\frac{\mathrm{d}J_3\left(\frac{T}{6}\right)}{\mathrm{d}T/6}$, $J_3'\left(2U\right)\equiv\frac{\mathrm{d}J_3(2U)}{\mathrm{d}2U}$. Also,

$$J_3(0)=12,\qquad J_3(2U^*)=-15\,. \tag{IV.C.53}$$

Combining everything together we arrive at the following result

$$\tilde{h}_{(2,-2)}(T,U)\partial_T J_3\left(\tfrac{T}{6}\right)=-18\pi i\frac{X_1\left(\frac{T}{6}\right)\left[X_1^3\left(\frac{T}{6}\right)-3X_1^2\left(\frac{T}{6}\right)X_2\left(\frac{T}{6}\right)+4X_2^3\left(\frac{T}{6}\right)\right]}{X_2^{-1}(U)\left[X_1^3\left(U\right)-3X_1\left(U\right)X_2^2\left(U\right)+2X_2^3\left(U\right)\right]}\,. \tag{IV.C.54}$$

The above result satisfies the integrability condition

$$\partial_{2U}^3\partial_{\frac{T}{6}}^3 f(\frac{T}{6},2U)=\partial_{\frac{T}{6}}^3\partial_{2U}^3 f(\frac{T}{6},2U)=\partial_{2U}^3\partial_{\frac{T}{6}}^3 f(2U,\frac{T}{6}),\quad \text{when } \frac{T}{6}\neq 2U\,. \tag{IV.C.55}$$

However, this result indicates incorrect behaviour near $T=12U=12U^*$. Specifically, the value is three times that near $T=12U\neq 12U^*$, rather than twice. Actually, (IV.C.54) is the unique (up to a constant) expression of the 1-loop prepotential under duality group $\Gamma^1(3)_{T/2}\times\Gamma_1(3)_{2U}$. And the point $2U^*$ is a triple fixed point of $\Gamma_1(3)_{2U}$, which we show in (IV.D.17). Hence, further work is required to determine the quantum corrections to the moduli space. On the future direction of this research, we will discuss in Chapter V, at the end of this thesis.

IV.D Modular forms of congruence subgroups

Here we discuss modular forms of congruence subgroups of $\mathrm{SL}(2,\mathbb{Z})$. The basic reference for this section is [58]. Also, for explicit computations we use [59].

One way to construct modular forms of congruence subgroups is by starting with an $\mathrm{SL}(2,\mathbb{Z})$ modular form $f(\tau)$ and define $f'(\tau)\equiv f(d\tau)$, where d is a positive

integer.[23] Then $f'(\tau)$ is a modular form of $\Gamma_0(d)$. In the same way we can take modular forms of $\Gamma_0(p)$ to forms of $\Gamma_0(dp)$ and forms of $\Gamma_1(p)$ to forms of $\Gamma_1(dp)$. Moreover, if $g(\tau)$ is a modular form of $\Gamma_1(p)$, then $g'(\tau) \equiv g(\tau/p)$ is a modular form of $\Gamma^1(p)$. Note that $\Gamma_1(p) \subset \Gamma_0(p)$ for $p > 2$, and $\Gamma_0(2) \cong \Gamma_1(2)$. Also, if N is a divisor of p, $\Gamma_1(p) \subset \Gamma_1(N)$.

For later reference, we remind here the Dedekind η-function defined in Subsection I.2.1:

$$\eta(\tau) = q^{\frac{1}{24}} \prod_{n=1}^{\infty} (1-q^n)\,, \quad q = e^{2\pi i \tau}\,. \tag{IV.D.1}$$

Also, the Jacobi ϑ-function with characteristics α, β is given by

$$\vartheta\begin{bmatrix}\alpha\\ \beta\end{bmatrix}(\tau) = \sum_{n\in\mathbb{Z}} q^{\frac{1}{2}(n+\alpha)^2} e^{2\pi i (n+\alpha)\beta}\,. \tag{IV.D.2}$$

Particular ϑ-functions that we will use in the next are

$$\vartheta_2(\tau) \equiv \vartheta\begin{bmatrix}1/2\\ 0\end{bmatrix}(\tau), \quad \vartheta_3(\tau) \equiv \vartheta\begin{bmatrix}0\\ 0\end{bmatrix}(\tau)\,. \tag{IV.D.3}$$

Now, for any congruence subgroup $\Gamma \subset \mathrm{SL}(2,\mathbb{Z})$ and any integer k, the weight k Eisenstein space is defined as the quotient space of the modular forms by the cusp forms

$$\mathcal{E}_k(\Gamma) = \mathcal{M}_k(\Gamma)/\mathcal{S}_k(\Gamma)\,. \tag{IV.D.4}$$

In particular, for $\Gamma_1(6)$ we have

$$\dim\left(\mathcal{M}_k(\Gamma_1(6))\right) = k+1\,, \qquad \dim\left(\mathcal{S}_k(\Gamma_1(6))\right) = \begin{cases} 0 & \text{for} \quad k<3 \\ k-3 & \text{for} \quad k\geq 3 \end{cases}. \tag{IV.D.5}$$

The graded ring of modular forms of $\Gamma_1(6)$ is generated by two weight 1 forms, which we denote by $X_1(\tau)$ and $X_2(\tau) \equiv X_1(2\tau)$, where [60]

$$X_1(\tau) = \vartheta_3(2\tau)\vartheta_3(6\tau) + \vartheta_2(2\tau)\vartheta_2(6\tau) = 1 + 6q + 6q^3 + 6q^4 + 12q^7 + \mathcal{O}(q^8)\,. \tag{IV.D.6}$$

Note that $X_1(\tau)$ coincides with the theta series of the SU(3) root lattice [61]. $X_1(\tau)$ has a unique zero at $\tau = \frac{1}{2} + i\frac{\sqrt{3}}{6}$. Also, $X_1(\tau)$ diverges at the cusps $\tau = 0, -\frac{1}{3}, -\frac{1}{2}$.[24] Specifically, $X_1(\tau) \propto 1/\tau_2$ when approaching to the cusps along the imaginary axis.

The derivatives of $X_1(\tau)$ and $X_2(\tau)$ obey the identity:

$$\begin{aligned} &\frac{1}{2\pi i}\frac{\mathrm{d}}{\mathrm{d}\tau}\frac{X_2(\tau)}{X_1(\tau)} \\ =&\frac{1}{6X_1^2(\tau)}\left[X_1(\tau)+X_2(\tau)\right]\left[X_1(\tau)-X_2(\tau)\right]\left[X_1(\tau)+2X_2(\tau)\right]\left[X_1(\tau)-2X_2(\tau)\right]. \end{aligned} \tag{IV.D.7}$$

[23] Note that here τ is an arbitrary number, rather than the worldsheet complex structure. In our model, this τ may represent $\frac{T}{6}$, U, $2U$ and so on.

[24] These divergences can be regularised by Ramanujan summation. For example, $X_1^2(0) = -1/3$.

We can also construct modular functions for $\Gamma_1(6)$ by taking quotients of the above forms. A particularly interesting quotient is

$$J_6(\tau) = \frac{7X_2(\tau) - X_1(\tau)}{X_1(\tau) - X_2(\tau)} = 5 + \frac{\eta(\tau)^5\eta(3\tau)}{\eta(2\tau)\eta(6\tau)^5} = \frac{1}{q} + 6q + 4q^2 - 3q^3 - 12q^4 + \mathcal{O}(q^5)\,, \tag{IV.D.8}$$

which is a modular invariant function with respect to $\Gamma_0(6)$ [60]. The function $J_6(\tau)$ is usually referred to as the *Hauptmodul* of $\Gamma_0(6)$; this is the analog of the $\mathrm{SL}(2,\mathbb{Z})$ modular function $J(\tau) = j(\tau) - 744$ (see e.g. [62]). As shown in [63], [64], the series (IV.D.8), which is actually the McKay–Thompson series of class 6E [65], is also the Hauptmodul of $\Gamma_1(6)$. Using the results of [66], the derivative of $J_6(\tau)$ can be expressed in terms of $X_1(\tau)$ and $X_2(\tau)$ as

$$\begin{aligned}\frac{1}{2\pi i}\frac{\mathrm{d}J_6(\tau)}{\mathrm{d}\tau} &= \frac{[X_1(\tau) + X_2(\tau)]\,[X_1(\tau) + 2X_2(\tau)]\,[X_1(\tau) - 2X_2(\tau)]}{X_1(\tau) - X_2(\tau)} \\ &= -\frac{[X_1(\tau) - X_2(\tau)]^2}{36}\,[J_6(\tau) - J_6(0)]\left[J_6(\tau) - J_6\left(-\tfrac{1}{3}\right)\right]\left[J_6(\tau) - J_6\left(-\tfrac{1}{2}\right)\right]\,,\end{aligned} \tag{IV.D.9}$$

where the values of $J_6(\tau)$ at these cusps are

$$J_6(0) = 5, \quad J_6\left(-\tfrac{1}{3}\right) = -3, \quad J_6\left(-\tfrac{1}{2}\right) = -4. \tag{IV.D.10}$$

Another modular invariant function with respect to $\Gamma_1(6)$ is the Hauptmodul of $\Gamma_1(3)$, given by

$$J_3(\tau) = 12 + \left(\frac{\eta(\tau)}{\eta(3\tau)}\right)^{12} = \frac{1}{q} + 54q - 76q^2 - 243q^3 + 1188q^4 + \mathcal{O}(q^5)\,, \tag{IV.D.11}$$

which is the McKay–Thompson series of class 3B [67]. Using the results of [66], we can rewrite $J_3(\tau)$ as follows

$$J_3(\tau) = 12 + 27\frac{[X_1(\tau) + X_2(\tau)]\,[X_1(\tau) - 2X_2(\tau)]^2}{[X_1(\tau) - X_2(\tau)]\,[X_1(\tau) + 2X_2(\tau)]^2}\,. \tag{IV.D.12}$$

In order to compute the derivative of $J_3(\tau)$ we use [58]

$$\frac{\mathrm{d}\eta(\tau)}{\mathrm{d}\tau} = \frac{\pi i}{12}\eta(\tau)E_2(\tau)\,, \tag{IV.D.13}$$

where $E_2(\tau)$ is the $\mathrm{SL}(2,\mathbb{Z})$ weight 2 normalized Eisenstein series. Then, it is straightforward to compute

$$\frac{1}{2\pi i}\frac{\mathrm{d}J_3(\tau)}{\mathrm{d}\tau} = \frac{1}{2}\left(\frac{\eta(\tau)}{\eta(3\tau)}\right)^{12}[E_2(\tau) - 3E_2(3\tau)]\,. \tag{IV.D.14}$$

Using that

$$X_1^2(\tau) = -\frac{1}{2}[E_2(\tau) - 3E_2(3\tau)]\,, \tag{IV.D.15}$$

we arrive at

$$\frac{1}{2\pi i}\frac{\mathrm{d}J_3(\tau)}{\mathrm{d}\tau} = -27X_1^2(\tau)\frac{[X_1(\tau)+X_2(\tau)]\,[X_1(\tau)-2X_2(\tau)]^2}{[X_1(\tau)-X_2(\tau)]\,[X_1(\tau)+2X_2(\tau)]^2} \\ = -X_1^2(\tau)\,[J_3(\tau)-J_3(0)]\,, \tag{IV.D.16}$$

where we used that $J_3(0) = 12$. We mention here that $\Gamma_1(3)$ has a triple fixed point at

$$\tau_* = -\frac{1}{2} + i\frac{\sqrt{3}}{6} : \qquad \tau_* = \frac{-2\tau_*-1}{3\tau_*+1} = \frac{\tau_*+1}{-3\tau_*-2}\,. \tag{IV.D.17}$$

Moreover, $X_1(\tau_*) = 0$, so

$$J_3'(\tau_*) = J_3''(\tau_*) = 0\,. \tag{IV.D.18}$$

Note that $J_3(\tau_*) = -15$. Finally, $J_3(2\tau)$ is also a modular function of $\Gamma_1(6)$ (but not of $\Gamma_1(3)$) and is given by

$$J_3(2\tau) = 12 - 27\frac{[X_1(\tau)+X_2(\tau)]^2\,[X_1(\tau)-2X_2(\tau)]}{[X_1(\tau)-X_2(\tau)]^2\,[X_1(\tau)+2X_2(\tau)]}\,. \tag{IV.D.19}$$

The derivative of $J_3(2\tau)$ reads

$$\frac{1}{2\pi i}\frac{\mathrm{d}J_3(2\tau)}{\mathrm{d}\tau} = 54X_2^2(\tau)\frac{[X_1(\tau)+X_2(\tau)]^2\,[X_1(\tau)-2X_2(\tau)]}{[X_1(\tau)-X_2(\tau)]^2\,[X_1(\tau)+2X_2(\tau)]} \\ = -2X_2^2(\tau)\,[J_3(2\tau)-J_3(0)]\,. \tag{IV.D.20}$$

References

[1] M. Bianchi, G. Bossard and D. Consoli, *Perturbative higher-derivative terms in N= 6 asymmetric orbifolds*, *Journal of High Energy Physics* **2022** (2022) 1–96.

[2] G. Gkountoumis, C. Hull, K. Stemerdink and S. Vandoren, *Freely acting orbifolds of type IIB string theory on T^5*, *JHEP* **08** (2023) 089, [2302.09112].

[3] Z. K. Baykara, Y. Hamada, H.-C. Tarazi and C. Vafa, *On the String Landscape Without Hypermultiplets*, 2309.15152.

[4] G. Gkountoumis, C. Hull and S. Vandoren, *Exact moduli spaces for $\mathcal{N} = 2$, $D = 5$ freely acting orbifolds*, *JHEP* **07** (2024) 126, [2403.05650].

[5] G. Gkountoumis, *Asymmetric $\mathbb{Z}_4$ orbifolds of type IIB string theory revisited*, *JHEP* **11** (2024) 136, [2404.12962].

[6] Z. K. Baykara, H.-C. Tarazi and C. Vafa, *Quasicrystalline string landscape*, *Phys. Rev. D* **111** (2025) 086025, [2406.00129].

[7] Z. K. Baykara, H.-C. Tarazi and C. Vafa, *New Non-Supersymmetric Tachyon-Free Strings*, 2406.00185.

[8] C. Angelantonj, I. Florakis, G. Leone and D. Perugini, *Non-supersymmetric non-tachyonic heterotic vacua with reduced rank in various dimensions*, *JHEP* **10** (2024) 216, [2407.09597].

[9] G. Aldazabal, E. Andrés, A. Font, K. Narain and I. G. Zadeh, *Asymmetric Orbifolds, Rank Reduction and Heterotic Islands*, 2501.17228.

[10] Z. K. Baykara, H. P. De Freitas and H.-C. Tarazi, *String islands, discrete theta angles and the 6D $\mathcal{N} = (1, 1)$ string landscape*, 2502.19468.

[11] A. Dabholkar and C. Hull, *Duality twists, orbifolds, and fluxes*, *JHEP* **09** (2003) 054, [hep-th/0210209].

[12] A. Sen and C. Vafa, *Dual pairs of type II string compactification*, *Nuclear Physics B* **455** (1995) 165–187.

[13] T. W. Grimm, E. Palti and I. Valenzuela, *Infinite Distances in Field Space and Massless Towers of States*, *JHEP* **08** (2018) 143, [1802.08264].

[14] P. Corvilain, T. W. Grimm and I. Valenzuela, *The Swampland Distance Conjecture for Kähler moduli*, *JHEP* **08** (2019) 075, [1812.07548].

[15] R. Rohm, *Spontaneous Supersymmetry Breaking in Supersymmetric String Theories*, *Nucl. Phys. B* **237** (1984) 553–572.

[16] S. Ferrara, C. Kounnas and M. Porrati, *Superstring Solutions With Spontaneously Broken Four-dimensional Supersymmetry*, *Nucl. Phys. B* **304** (1988) 500–512.

[17] C. Kounnas and M. Porrati, *Spontaneous Supersymmetry Breaking in String Theory*, *Nucl. Phys. B* **310** (1988) 355–370.

[18] S. Ferrara, C. Kounnas, M. Porrati and F. Zwirner, *Superstrings with Spontaneously Broken Supersymmetry and their Effective Theories*, *Nucl. Phys. B* **318** (1989) 75–105.

[19] C. Hull and P. Townsend, *Unity of superstring dualities*, *Nucl. Phys.* **B438** (1995) 109–137, [hep-th/9410167].

[20] H. S. Tan, *T-duality twists and asymmetric orbifolds*, *Journal of High Energy Physics* **2015** (2015) 1–62.

[21] Y. Satoh and Y. Sugawara, *Lie algebra lattices and strings on T-folds*, *Journal of high energy physics* **2017** (2017) 1–27.

[22] K. Narain, M. Sarmadi and C. Vafa, *Asymmetric Orbifolds*, *Nucl. Phys.* **B288** (1987) 551.

[23] K. Narain, M. Sarmadi and C. Vafa, *Asymmetric orbifolds: Path integral and operator formulations*, *Nuclear Physics B* **356** (1991) 163–207.

[24] K. Narain, *New heterotic string theories in uncompactified dimensions < 10*, in *Current Physics–Sources and Comments*, vol. 4, pp. 246–251. Elsevier, 1989.

[25] W. Lerche, A. Schellekens and N. Warner, *Lattices and strings*, *Physics Reports* **177** (1989) 1–140.

[26] C. Vafa, *Modular invariance and discrete torsion on orbifolds*, *Nuclear Physics B* **273** (1986) 592–606.

[27] J. Harvey and G. Moore, *An Uplifting Discussion of T-Duality*, *JHEP* **05** (2018) 145, [1707.08888].

[28] R. Blumenhagen, D. Lüst and S. Theisen, *Basic concepts of string theory*. Theoretical and Mathematical Physics. Springer, Heidelberg, Germany, 2013, 10.1007/978-3-642-29497-6.

[29] D. Bailin, A. Love, W. Sabra and S. Thomas, *Duality symmetries of threshold corrections in orbifold models*, *Phys. Lett. B* **320** (1994) 21–28, [hep-th/9309133].

[30] E. Kiritsis and C. Kounnas, *Perturbative and nonperturbative partial supersymmetry breaking: N=4 —> N=2 —> N=1*, *Nucl. Phys. B* **503** (1997) 117–156, [hep-th/9703059].

[31] A. Gregori, E. Kiritsis, C. Kounnas, N. Obers, P. M. Petropoulos and B. Pioline, *R^2 corrections and nonperturbative dualities of N=4 string ground states*, *Nucl. Phys. B* **510** (1998) 423–476, [hep-th/9708062].

[32] H. Itoyama, Y. Koga and S. Nakajima, *Target space duality of non-supersymmetric string theory*, *Nuclear Physics B* **975** (2022) 115667.

[33] A. Font and S. Theisen, *Introduction to string compactification*, in *Geometric and Topological Methods for Quantum Field Theory*, pp. 101–181. Springer, 2005.

[34] Y. Katsuki, Y. Kawamura, T. Kobayashi, N. Ohtsubo, Y. Ono and K. Tanioka, *Z_N orbifold models*, *Nuclear Physics B* **341** (1990) 611–640.

[35] L. Ibanez, J. Mas, H.-P. Nilles and F. Quevedo, *Heterotic strings in symmetric and asymmetric orbifold backgrounds*, *Nuclear Physics B* **301** (1988) 157–196.

[36] A. Font, L. Ibanez, F. Quevedo and M. Sierra, *The construction of "realistic" four-dimensional strings through orbifolds*, *Nuclear Physics B* **331** (1990) 421–474.

[37] M. Gunaydin, G. Sierra and P. Townsend, *Exceptional Supergravity Theories and the MAGIC Square*, *Phys. Lett. B* **133** (1983) 72–76.

[38] G. Lopes Cardoso, D. Lust and T. Mohaupt, *Threshold corrections and symmetry enhancement in string compactifications*, *Nucl. Phys. B* **450** (1995) 115–173, [hep-th/9412209].

[39] B. de Wit, V. Kaplunovsky, J. Louis and D. Lust, *Perturbative couplings of vector multiplets in N=2 heterotic string vacua*, *Nucl. Phys. B* **451** (1995) 53–95, [hep-th/9504006].

[40] I. Antoniadis, S. Ferrara, E. Gava, K. Narain and T. R. Taylor, *Perturbative prepotential and monodromies in N=2 heterotic superstring*, *Nucl. Phys. B* **447** (1995) 35–61, [hep-th/9504034].

[41] H. Ooguri and C. Vafa, *On the Geometry of the String Landscape and the Swampland*, *Nucl. Phys. B* **766** (2007) 21–33, [hep-th/0605264].

[42] B. Valeixo Bento, D. Chakraborty, S. Parameswaran and I. Zavala, *A guide to frames, 2π's, scales and corrections in string compactifications*, *Int. J. Mod. Phys. D* **34** (2025) 2530003, [2301.05178].

[43] D. van de Heisteeg, C. Vafa and M. Wiesner, *Bounds on Species Scale and the Distance Conjecture*, *Fortsch. Phys.* **71** (2023) 2300143, [2303.13580].

[44] F. Revello and G. Villa, *Cosmic (super)strings with a time-varying tension*, *JCAP* **04** (2025) 049, [2411.04186].

[45] S.-J. Lee, W. Lerche and T. Weigand, *Emergent strings from infinite distance limits*, *JHEP* **02** (2022) 190, [1910.01135].

[46] N. Cribiori, D. Lust and M. Scalisi, *The gravitino and the swampland*, *JHEP* **06** (2021) 071, [2104.08288].

[47] A. Castellano, A. Font, A. Herraez and L. E. Ibáñez, *A gravitino distance conjecture*, *JHEP* **08** (2021) 092, [2104.10181].

[48] P. Townsend, *A new anomaly free chiral supergravity theory from compactification on K3*, *Physics Letters B* **139** (1984) 283–287.

[49] M. Delgado, D. van de Heisteeg, S. Raman, E. Torres, C. Vafa and K. Xu, *Finiteness and the Emergence of Dualities*, 2412.03640.

[50] T. W. Grimm, D. Prieto and M. van Vliet, *Tame Embeddings, Volume Growth, and Complexity of Moduli Spaces*, 2503.15601.

[51] E. Kiritsis, *String Theory in a Nutshell: Second Edition*. Princeton University Press, USA, 4, 2019.

[52] M. Grisaru and W. Siegel, *Supergraphity. 2. Manifestly Covariant Rules and Higher Loop Finiteness*, *Nucl. Phys. B* **201** (1982) 292.

[53] P. Howe, K. Stelle and P. C. West, *A Class of Finite Four-Dimensional Supersymmetric Field Theories*, *Phys. Lett. B* **124** (1983) 55–58.

[54] N. Seiberg, *Supersymmetry and Nonperturbative beta Functions*, *Phys. Lett. B* **206** (1988) 75–80.

[55] S. Cecotti, S. Ferrara and L. Girardello, *Geometry of Type II Superstrings and the Moduli of Superconformal Field Theories*, *Int. J. Mod. Phys. A* **4** (1989) 2475.

[56] Y. Gautier and D. Israël, *Moduli spaces of non-geometric type II/heterotic dual pairs*, *JHEP* **09** (2020) 082, [2005.01816].

[57] J. Louis and K. Foerger, *Holomorphic couplings in string theory*, *Nucl. Phys. B Proc. Suppl.* **55** (1997) 33–64, [hep-th/9611184].

[58] F. Diamond and J. Shurman, *A first course in modular forms*, *Graduate Texts in Mathematics/Springer-Verlag* **436** (2005) .

[59] The Sage Developers, *SageMath, the Sage Mathematics Software System (Version 10.4)*, 2024.

[60] A. Sebbar, *Modular subgroups, forms, curves and surfaces*, *Canadian Mathematical Bulletin* **45** (2002) 294–308.

[61] J. H. Conway and N. J. A. Sloane, *Sphere packings, lattices and groups*, vol. 290. Springer Science & Business Media, 2013.

[62] J. McKay and A. Sebbar, *Fuchsian groups, automorphic functions and schwarzians*, *Mathematische Annalen* **318** (2000) 255–275.

[63] C.-H. Kim and J.-K. Koo, *Super-replicable functions $N(j_{1,N})$ and periodically vanishing property*, *Journal of the Korean Mathematical Society* **44** (2007) 343–371.

[64] C. Kim and J. K. Koo, *Generators of function fields of the modular curves $X_1(5)$ and $X_1(6)$*, *Mathematics of computation* **79** (2010) 1047–1066.

[65] *The on-line encyclopedia of integer sequences*, *https://oeis.org* .

[66] K. Matsuda, *Cubic theta functions and modular forms of level six*, *The Ramanujan Journal* **62** (2023) 469–532.

[67] C.-H. Kim and J.-K. Koo, *Arithmetic of the modular functions $j_{1,2}$ and $j_{1,3}$*, *Bulletin of the Korean Mathematical Society* **44** (2007) 47–59.

Chapter V

Conclusion and Outlook

V.1 Summary

Three research projects are presented in this thesis. Based on the Swampland program, non-geometric compactifications, and string dualities, these research projects investigate cosmological phenomenology and the asymptotic properties of moduli spaces from both bottom-up and top-down perspectives.

Chapter I presents the motivations and lays a firm theoretical foundation of this thesis, by reviewing string theory and its compactifications, the role of moduli and dualities, string cosmology, and the Swampland program. In light of the Swampland conjectures, it argues that non-geometric backgrounds and duality structures are practical tools for probing dark energy and the asymptotic geometry of moduli spaces. The chapter thereby equips the remainder of the thesis with the concepts and criteria that organize the three research projects.

Chapter II tests the compatibility of accelerated cosmic expansion in a multi-field setting with current Swampland conjectures. Applying the Swampland Distance Conjecture to scalar potentials, we analyze field dynamics near infinite distance limits of moduli space. Focusing on asymptotic hyperbolic geometries, which are ubiquitous in compactifications such as Calabi–Yau, we derive an upper bound on the turning rate of non-geodesic trajectories close to the boundary of field space. A large turning rate is expected as a way to reconcile acceleration with the de Sitter conjecture. However, we show that this mechanism fails in asymptotic regions, where the turning rate in quasi-de Sitter evolution must be small. The resulting constraint implies an upper bound on the potential gradient that conflicts with the asymptotic de Sitter Conjecture:

$$\frac{|\nabla V|}{V} \sim \mathcal{O}(\sqrt{\epsilon}) \lesssim \mathcal{O}(1)\,. \tag{V.1.1}$$

Therefore, assuming the validity of the asymptotic de Sitter Conjecture, which aligns with many known string theory constructions, it follows that a universe with eternal or asymptotically accelerated expansion lies in the Swampland, i.e., viable cosmic acceleration can likely only occur in the interior of the scalar field space.

Chapter III develops a string-theoretic realization of the Dark Dimension Scenario, which is a recent proposal inspired by Swampland conjectures, and posits that our Universe has exactly one extra dimension of mesoscopic size. We investigate the classical viability of this picture using a non-geometric compactification, in which the internal space is a $T^5 \times S^1$ toroidal T-fold with non-trivial H-, f- and Q-fluxes. These NS-NS fluxes implement a T-duality twist along T^5, such that the effective theory arises from a Scherk–Schwarz reduction from 5D to 4D on S^1 with this twist. This construction breaks supersymmetry and generates a potential for the moduli, stabilizing the T^5 volume together with several geometric moduli. The resulting theory fixes most moduli and leaves two runaway

directions, one of which is the S^1 radion. After further stabilization, the effective potential scales as $V \propto m_{\mathrm{KK}}^4$, where m_{KK} is the Kaluza–Klein mass associated with S^1. The m_{KK}^4 scaling precisely matches the requirement of the Dark Dimension scenario and identifies S^1 as the mesoscopic Dark Dimension, providing a classical realization of the proposal.

Chapter IV analyzes the moduli spaces of freely acting asymmetric orbifolds and tests Swampland conjectures in a non-geometric setting. We construct four-dimensional models by compactifying type IIB string theory on $\left(T^4 \times T^2\right)/\mathbb{Z}_p$ orbifolds, with asymmetric rotations on T^4 and a shift on T^2. By adjusting the twist parameters, supersymmetry can be spontaneously broken from $\mathcal{N} = 8$ to $\mathcal{N} = 6, 4, 2, 0$. We focus on an $\mathcal{N} = 2$ model with $p = 6$ and analyze its mass spectrum and duality group in detail, which shows that it is an STU-like model. Compared to the full toroidal duality, the duality group reduces to a congruence subgroup, such that the moduli space enlarges. In particular, the STU-moduli space is $\hat{\Gamma}^1(6)_S \times \hat{\Gamma}^1(6)_T \times \hat{\Gamma}_1(6)_U$, which is the fundamental domain of the congruence subgroup. Its cusps represent new infinite distance limits, which we verify satisfy the Swampland Distance Conjecture. Especially, each infinite distance point in the geometric T^2 moduli space corresponds to a decompactification limit. Classifying these limits, we find:

- Eight single-cusp limits, yielding 6-dimensional theories with 8, 16, or 32 supercharges;
- Sixteen double-cusp limits, corresponding to 5-dimensional theories exhibiting various orbifold constructions with different amounts of supersymmetry;

consistent with the Emergent String Conjecture.

Our investigation of the mass spectrum reveals the presence of additional massless hypermultiplets at specific loci in the interior of the moduli space. These states render the moduli space metric singular, corresponding to quantum corrections. In Appendices IV.C–IV.D, we present an initial calculation of one-loop quantum corrections. The corrections are constrained by the reduced duality symmetry and can be written in terms of modular forms of the relevant congruence subgroups. Several identities among these modular forms are derived in Appendix IV.D.

V.2 Outlook

We conclude by highlighting further research directions and open questions motivated by this thesis.

Cosmic acceleration and the Swampland

Realizing dark energy within a controlled string compactification remains a central challenge at the interface of cosmology and the Swampland program. Swampland

criteria, including the de Sitter Conjecture, highlight the difficulty of obtaining even metastable de Sitter vacua. Our work in Chapter II takes a further step in this direction: it provides strong evidence that viable cosmic acceleration is realized in the *interior* of field space, driven by multi-field dynamics that support large-turn, non-geodesic motion. In this picture, constructing transient large-turn trajectories in the bulk of moduli space offers a concrete and promising route to string model building of quintessence.

String cosmology in non-geometric compactifications

Non-geometric compactifications provide a powerful framework for engineering string vacua with diverse scalar potentials, including de Sitter candidates, multi-field quintessence, and the Dark Dimension Scenario. As reviewed in Subsection I.4.2, several constructions suggest that turning on non-geometric fluxes can yield tachyon-free, metastable de Sitter vacua. Besides, [1] analyzes a quasi-crystal asymmetric-orbifold compactification that produces a tachyon-free, non-supersymmetric theory whose quantum corrections generate a positive runaway potential. In Chapter III we propose a possible route to de Sitter model building: within T-fold flux compactifications, and at parametrically large flux quanta, the scalar potential develops a positive saddle point (cf. (III.4.22)) that stabilizes the torus volume. If additional fluxes or non-perturbative effects further stabilize the Scherk–Schwarz radion, this saddle might be promoted to a metastable de Sitter minimum. We aim to develop this approach in future work.

Dark Dimension and cosmic acceleration

In light of the No Global Symmetry Conjecture, the global $B-L$ symmetry of the Standard Model suggests that our Universe may reside near an asymptotic region of field space. The Dark Dimension proposal builds on this observation and motivates a closer look at its particle physics implications. The original work [2] already links the Dark Dimension KK tower to sterile neutrinos and to addressing the Higgs hierarchy problem. Further particle physics implications require systematic investigation; see [3–8] for recent progress.

Phenomenologically, the Dark Dimension scenario must be compatible with cosmological observations. This appears to be in tension with our conclusion from Chapter II that cosmic acceleration is in the interior of field space. A central challenge is that the relevant potential typically scales as $V \sim m_{\mathrm{KK}}^4$, which is much steeper than in standard single-field quintessence, $V \sim e^{-\lambda\phi}$ with $\lambda < \sqrt{2}$, as discussed in Appendix III.B. One might try to invoke quantum fluctuations to generate metastable de Sitter vacua along the tail of the potential, but this sits uneasily with the de Sitter conjecture and is difficult to realize in a controlled manner. A more promising avenue is multi-field dynamics. Recent work [9] proposes realizing quintessence and the Dark Dimension along orthogonal directions in field space: quintessence from the axio-dilaton in the interior and the Dark Dimension from the radion near the boundary. This indicates that nontrivial multi-field

dynamics can reconcile the Dark Dimension with viable cosmic acceleration.

Quantum corrections and duality group

A complete understanding of the moduli space requires a thorough investigation of the quantum corrections to its metric. In Appendix IV.C, we present an initial calculation of the one-loop quantum corrections for a freely acting asymmetric orbifold. However, this analysis remains incomplete because the quantum-corrected prepotential is constrained only by its asymptotics at the cusps $T \to i\infty$ and $U \to i\infty$. A systematic treatment should incorporate the behavior at the remaining inequivalent cusps, in particular $T \to -2, -3$ and $U \to -1/2, -1/3$, which can supply the additional modular data needed to fix the functional form of the prepotential. In addition, non-perturbative corrections from $e^{2\pi i S}$ instantons must also be considered. As discussed at the end of Subsection I.3.3, the Sen–Vafa duality exchanges the S and T moduli and therefore maps perturbative T-dependent corrections to the non-perturbative S sector. By combining these approaches, the properties of this non-geometric construction can be completely determined. More broadly, this inspires us that in supergravity theories arising from string compactifications, quantum corrections may be fully fixed by duality symmetry.

Moduli spaces in the Swampland

This thesis highlights the central role of moduli spaces in the Swampland program. Chapter IV analyzes the moduli space of freely acting asymmetric orbifolds as a computable and controllable representation for non-geometric compactifications, a regime that has received comparatively little attention in Swampland tests. Compared to geometric internal spaces, asymmetric orbifolds often yield fewer massless and light states, providing a more realistic low-energy effective theory. Systematic exploration of asymmetric orbifolds can provide sharper tests of Swampland conjectures and examine constraints on conjecture parameters such as the SDC exponent.

The top-down construction of the moduli space in Chapter IV is classical, and quantum corrections to the metric were not included. These corrections can modify geodesic distances and, in some cases, bend infinite-distance directions to finite length, challenging the generality of the SDC and the ESC. Related analyses in geometric compactifications include [10–12]. Extending to non-geometric settings is a natural next step and will be pursued in future work.

In Chapter IV the decompactification limits exhibit supersymmetry enhancement, as a consequence of the freely acting orbifold that lifts the gravitini masses. The construction thereby links theories with different numbers of supercharges. This suggests a global picture in which moduli spaces from distinct compactifications glue together, pointing toward a unified perspective on moduli space geometry that warrants systematic study.

V.3 Samenvatting

Drie onderzoeksprojecten worden in dit proefschrift gepresenteerd. Op basis van het Swampland-programma, niet-geometrische compactificaties en snaardualiteiten onderzoeken deze projecten, vanuit zowel bottom-up- als top-downperspectief, kosmologische fenomenologie en de asymptotische eigenschappen van moduliruimten.

Hoofdstuk I presenteert de motivaties en legt een stevig theoretisch fundament voor dit proefschrift, door een overzicht te geven van de snaartheorie en haar compactificaties, de rol van moduli en dualiteiten, snaarkosmologie en het Swampland-programma. In het licht van de Swampland-conjecturen wordt betoogd dat niet-geometrische achtergronden en dualiteitsstructuren praktische instrumenten zijn om donkere energie en de asymptotische geometrie van moduliruimten te onderzoeken. Het hoofdstuk voorziet de rest van het proefschrift van de begrippen en criteria die de drie onderzoeksprojecten structureren.

Hoofdstuk II toetst de verenigbaarheid van versnelde kosmische expansie in een multiveldkader met de huidige Swampland-conjecturen. Door de Swampland Distance Conjecture toe te passen op scalaire potentialen analyseren we de veldendynamica nabij limieten op oneindige afstand in de moduliruimte. Met de focus op asymptotisch hyperbolische geometrieën, die alomtegenwoordig zijn in Calabi–Yau-compactificaties, leiden we een bovengrens af voor de draaisnelheid (turning rate) van niet-geodetische trajecten dicht bij de rand van de veldruimte. Een grote draaisnelheid wordt vaak gezien als een manier om versnelling te verzoenen met de De Sitter-conjectuur. Wij laten echter zien dat dit mechanisme faalt in asymptotische regio's, waar de draaisnelheid in quasi-De Sitter-evolutie klein moet zijn. De resulterende beperking impliceert een bovengrens op de potentiaalgradiënt die in strijd is met de asymptotische De Sitter-conjectuur:

$$\frac{|\nabla V|}{V} \sim \mathcal{O}(\sqrt{\epsilon}) \lesssim \mathcal{O}(1)\,. \tag{V.3.1}$$

Daarom volgt, uitgaande van de geldigheid van de asymptotische De Sitter-conjectuur, die strookt met veel bekende snaartheorieconstructies, dat een universum met eeuwige of asymptotisch versnelde expansie in de Swampland ligt; met andere woorden, realiseerbare kosmische versnelling kan waarschijnlijk alleen plaatsvinden in het binnengebied van de scalaire veldruimte.

Hoofdstuk III ontwikkelt een snaartheoretische realisatie van het Dark Dimension-scenario, een recent voorstel geïnspireerd door Swampland-conjecturen, dat stelt dat ons heelal exact één extra dimensie van mesoscopische grootte heeft. We onderzoeken de klassieke haalbaarheid van dit beeld met behulp van een niet-geometrische compactificatie, waarin de interne ruimte een toroïdaal T-fold $T^5 \times S^1$ is met niet-triviale H-, f- en Q-fluxen. Deze NS-NS-fluxen implementeren een T-dualiteitstwist langs T^5, zodanig dat de effectieve theorie voortkomt uit een

Scherk–Schwarz-reductie van 5D naar 4D op S^1 met deze twist. Deze constructie breekt supersymmetrie en genereert een potentiaal voor de moduli, waarbij het T^5-volume samen met verschillende geometrische moduli wordt gestabiliseerd. De resulterende theorie fixeert het merendeel van de moduli en laat twee runaway-richtingen over, waarvan er één de S^1-radion is. Na verdere stabilisatie schaalt het effectieve potentiaal als $V \propto m_{\mathrm{KK}}^4$, waarbij m_{KK} de Kaluza–Klein-massa is die met S^1 is geassocieerd. Het m_{KK}^4-schaalgedrag komt precies overeen met de eis van het Dark Dimension-scenario en identificeert S^1 als de mesoscopische Donkere Dimensie, waarmee een klassieke realisatie van het voorstel wordt geleverd.

Hoofdstuk IV analyseert de moduliruimten van vrij opererende asymmetrische orbifolds en test Swampland-conjecturen in een niet-geometrische setting. We construeren vierdimensionale modellen door type-IIB-snaartheorie te compactificeren op $\left(T^4 \times T^2\right)/\mathbb{Z}_p$-orbifolds, met asymmetrische rotaties op T^4 en een verschuiving op T^2. Door de twistparameters aan te passen kan supersymmetrie spontaan worden gebroken van $\mathcal{N} = 8$ naar $\mathcal{N} = 6, 4, 2, 0$. We richten ons op een $\mathcal{N} = 2$-model met $p = 6$ en analyseren het massaspectrum en de dualiteitsgroep in detail, waaruit blijkt dat het een *STU*-achtig model is. Vergeleken met de volledige toroidale dualiteit reduceert de dualiteitsgroep tot een congruentiesubgroep, waardoor de moduliruimte vergroot. In het bijzonder is de *STU*-moduliruimte $\hat{\Gamma}^1(6)_S \times \hat{\Gamma}^1(6)_T \times \hat{\Gamma}_1(6)_U$, wat het fundamentele domein van de congruentiesubgroep is. De cusps ervan vertegenwoordigen nieuwe limieten op oneindige afstand, waarvan we verifiëren dat ze voldoen aan de Swampland Distance Conjecture. In het bijzonder correspondeert elk punt op oneindige afstand in de geometrische T^2-moduliruimte met een decompactificatielimiet. Door deze limieten te classificeren vinden we:

- Acht enkelvoudige cusp-limieten, die 6-dimensionale theorieën opleveren met 8, 16 of 32 superladingen;

- Zestien dubbele cusp-limieten, corresponderend met 5-dimensionale theorieën die uiteenlopende orbifold-constructies vertonen met verschillende hoeveelheden supersymmetrie;

in overeenstemming met de Emergent String-conjectuur.

Ons onderzoek van het massaspectrum onthult de aanwezigheid van extra massaloze hypermultiplets op specifieke loci in het binnengebied van de moduliruimte. Deze toestanden maken de moduliruimtemetriek singulier, hetgeen correspondeert met kwantumcorrecties. In Bijlagen IV.C–IV.D presenteren we een eerste berekening van één-luskwantumcorrecties. De correcties worden begrensd door de gereduceerde dualiteitssymmetrie en kunnen worden uitgedrukt in termen van modulaire vormen van de relevante congruentiesubgroepen. Verscheidene identiteiten tussen deze modulaire vormen worden afgeleid in Bijlage IV.D.

References

[1] Z. K. Baykara, H.-C. Tarazi and C. Vafa, *New Non-Supersymmetric Tachyon-Free Strings*, 2406.00185.

[2] M. Montero, C. Vafa and I. Valenzuela, *The dark dimension and the Swampland*, *JHEP* **02** (2023) 022, [2205.12293].

[3] E. Gonzalo, M. Montero, G. Obied and C. Vafa, *Dark dimension gravitons as dark matter*, *JHEP* **11** (2023) 109, [2209.09249].

[4] L. A. Anchordoqui, I. Antoniadis and J. Cunat, *Dark dimension and the standard model landscape*, *Phys. Rev. D* **109** (2024) 016028, [2306.16491].

[5] N. Gendler and C. Vafa, *Axions in the dark dimension*, *JHEP* **12** (2024) 127, [2404.15414].

[6] J. J. Heckman, C. Vafa, T. Weigand and F. Xu, *Dark dimension and the grand unification of forces*, *Phys. Rev. D* **111** (2025) 046014, [2409.01405].

[7] L. A. Anchordoqui, I. Antoniadis, D. Lust and K. P. Castillo, *Cosmological constraints on dark neutrino towers*, *Phys. Rev. D* **111** (2025) 015024, [2411.07029].

[8] H.-J. Li, *QCD axion dark matter in the dark dimension*, *JHEP* **05** (2025) 139, [2412.19426].

[9] L. A. Anchordoqui, I. Antoniadis, N. Cribiori, A. Hasar, D. Lust, J. Masias et al., *Bulk/boundary Modular Quintessence and DESI*, 2506.02731.

[10] F. Baume, F. Marchesano and M. Wiesner, *Instanton Corrections and Emergent Strings*, *JHEP* **04** (2020) 174, [1912.02218].

[11] D. Klaewer, S.-J. Lee, T. Weigand and M. Wiesner, *Quantum corrections in 4d $N = 1$ infinite distance limits and the weak gravity conjecture*, *JHEP* **03** (2021) 252, [2011.00024].

[12] M. Delgado, D. van de Heisteeg, S. Raman, E. Torres, C. Vafa and K. Xu, *Finiteness and the Emergence of Dualities*, 2412.03640.

Acknowledgements

Time has flown. The four years of my PhD journey have passed in an instant. While I still ponder my ability as an independent researcher, the inexorable current of time pushes me towards the next phase of my life. Looking back on these four years, there have been both achievements and regrets, with various experiences remaining vivid, as if they occurred only yesterday. With these reflections in mind, I dedicate the following pages to express my sincerest acknowledgment for the invaluable support, guidance, and encouragement that have shaped my experience and enabled the completion of this thesis.

飞光，飞光，劝尔一杯酒。吾不识青天高、黄地厚，唯见月寒日暖，来煎人寿。（李贺《苦昼短》）

Fleeting light, fleeting light, please drink a cup of wine. I know not the sky's height nor the earth's depth; I only see the chill moonshine and warm sunshine, unceasingly frying the remnant of human life. (Li He, "*Lamenting the brevity of the day*")

First and foremost, I am deeply grateful to my supervisor, Stefan Vandoren, for his steady guidance, generous time, and invaluable insights throughout my PhD. He taught me how to do research and shared his expertise in supergravity and non-geometric compactifications. He always encouraged me and gave me wise advice. His approachability and openness created a supportive, collegial environment. Many discussions with him shaped this thesis. His example set the standards of clarity, rigor, and patience that I have tried to follow throughout my research.

I am also very thankful to my second supervisor, Thomas Grimm. His profound knowledge and prolific insights, shared through valuable discussions during lunch, coffee breaks, journal clubs, and seminars, were incredibly beneficial. From him, I gained a significant understanding of string phenomenology and various other areas of physics. I am also grateful to Umut Gürsoy. He was truly the most friendly professor I have ever met. I sincerely miss his caring conversations and inspiring discussions, both within the institute and at restaurants. His passing is an extreme loss to our community, and I feel deep sorrow at his absence.

I extend my thanks to Erik Plauschinn and Wilke van der Schee for their enlightening discussions during our daily lunch time, coffee breaks, and contributions to journal clubs and seminars. I also thank Ro Jefferson and Tomislav Prokopec for

sharing knowledge and insights in seminars, discussions, and coffee breaks.

高山仰止，景行行止。（《诗经 · 小雅 · 车辖》）

A lofty mountain invites admiration from afar; a noble path inspires us to walk in its footsteps. ("*The Classic of Poetry: The Linchpin*")

I am truly grateful to my colleagues in our research group for the insightful exchange of ideas and opinions during our lunchtime conversations, and for the engaging talks, paper discussions, and questions-and-answers during our Journal Clubs. Their intelligence, friendliness and professionalism have created a collaborative and productive working environment. My sincere thanks extend to: Cesar Alfonso Agón, Ibra Akal, Maaike Bakker, Casey Cartwright, Tuna Demircik, Nava Gaddam, George Gkountoumis, Javier Gomez Subils, Nico Groenenboom, Damian van de Heisteeg, Arno Hoefnagels, Stefano Lanza, Chongchuo Li, Jeroen Monnee, Claire Moran, Guim Planella I Planas, Erik Plauschinn, Edwan Préau, David Prieto Rodríguez, Shradha Ramakrishnan, Filippo Revello, Thorsten Schimannek, Lorenz Schlechter, Koen Stemerdink, Pedro Vicente Marto, Mick van Vliet, Raúl Wolters.
I also thank George Gkountoumis, Arno Hoefnagels, Guim Planella I Planas, Iris van Gemeren, and Sofia Canevarolo for our collaborative efforts as teaching assistants for the master courses.

君子尊德性而道问学，致广大而尽精微。（子思等《礼记 · 中庸》）

Junzi (the noble exemplars) honor their moral nature, and pursue inquiry and study; extend understanding to the broadest, and fathom details to the finest. (Confucians, "*Book of Rites: Doctrine of the Mean*")

I feel honored to have shared my research journey with all the individuals mentioned above at the Institute for Theoretical Physics of Utrecht University.

I sincerely thank my collaborators Julian Freigang, George Gkountoumis, Chris Hull, Dieter Lüst, Marco Scalisi, and of course, my supervisor Stefan Vandoren. I truly appreciate the collaborative efforts, insightful discussions, and shared ideas with each of them, which were absolutely fundamental to the successful realization of the works presented in this thesis. Dieter and Marco are my master's thesis supervisors, and I particularly thank their invaluable guidance. A special note of thanks is reserved for George: the extensive face-to-face discussions held in our office proved to be fruitful and essential to our work.
My collaborators and I thank all those who had helpful discussions with us: for Chapter II, José Calderón-Infante, Michele Cicoli, Niccolò Cribiori, Joaquin Masias, Francisco Gil Pedro, and Ivonne Zavala; for Chapter III, Ivano Basile, George Gkountoumis, Thomas Grimm, and Dieter Lüst; for Chapter IV, Thomas Grimm, Thorsten Schimannek, and Cumrun Vafa.

I thank ChatGPT and Gemini large language models for their assistance in polishing my English expressions, troubleshooting LaTeX issues, providing technical

clarifications in physics, and translating the English Summary of this thesis into Dutch.

I thank Max Wiesner for his enthusiastic help, insightful advice, and comforting support through the String Theory Mentoring Program.

I thank Yinan Wang for supporting me with a postdoctoral position at Peking University.

I am profoundly grateful to my parents and my grandfather. Their unconditional love has been the bedrock of my life and the driving force propelling me forward. My decision to study physics, and to continue my studies in Europe, was not an easy situation for my family. Both my parents are manual workers. My studies in Europe meant an extra financial strain for them, and my time abroad prevented me from celebrating Chinese New Years with my family. Nevertheless, they always believed in me and supported my decisions, even if the content of my PhD work was distant from their everyday lives.
Since childhood I was frail and often ill. Even amid ceaseless busyness, my mother tended to me every day with devoted care; it is thanks to her that I grew up at all. I know she too was once young and liked to look her best, but years of work for the family took the smoothness from her skin and drew wrinkles on her face. I can never truly repay such selfless devotion.

见面怜清瘦，呼儿问苦辛。低徊愧人子，不敢叹风尘。（蒋士铨《岁暮到家》）

She sees my face, pained by my gauntness; she calls my name and asks if I have suffered. Head bowed, ashamed in my duty as a son, I dare not speak of my hardships. (Jiang Shiquan, "*Back Home at the End of the Year*")

I want to express my special thanks to my girlfriend, Yanjie Du. Our relationship began at the end of my master's studies, and since then she has been a constant source of support and joy throughout these past four demanding PhD years. Although she lives in Munich, roughly an eight-hour train journey from Utrecht, we commuted to each other countless times. Her steadfast encouragement and support, and heartfelt understanding and comfort, provided immense solace, especially during the difficult periods of my anxiety disorder. She shared in both the triumphs and frustrations of this journey, and provided a constant reminder of life beyond the research. Our shared adventures, especially our travels around Europe, were a wonderful balance to the academic intensity. Furthermore, the playful presence of her cat, Amber, consistently brought moments of pure joy and therapeutic distraction. I am truly thankful for her love and companionship.

此时相望不相闻，愿逐月华流照君。（张若虚《春江花月夜》）

At this hour we gaze toward one another from a distance unheard; I would follow the moonlight to shine upon you. (Zhang Ruoxu, "*The Moon over the River on a Spring Night*")

During my PhD, being an introvert, I primarily formed new friendships with my colleagues, including George, Arno, Nico, Jeroen, Filippo, and others, to whom I extend my sincere gratitude. Their collective warmth has shaped my perception of European friendliness and openness. I am deeply thankful for the unique bond shared with George, Arno, and Nico, who began their PhDs concurrently with me. Our four-year journey since the Solvay school has been marked by continuous daily discussions and chats, providing essential mutual support and camaraderie. Especially, George, as my officemate and fellow advisee of Stefan, has been a constant source of intellectual exchange and companionship during our daily insightful chats and shared lunches, especially as we collaborated on asymmetric orbifolds. My particular thanks go to Jeroen for the kind discussions in our shared research area on string phenomenology, and his crucial help with my postdoctoral application.

My only Chinese friends in the Netherlands are Chongchuo Li and his wife, Yiran Zhao. I am truly grateful for the invaluable life advice and encouragement they provided, and for the many joyful moments we shared. I am also deeply grateful to friends from my master's period who still keep in touch with me: Zhizhen Wang, Zhen Gao, Gongrui Cheng, and others. Their humor, engaging intellectual discussions, and consistent affirmation were highly valued. A special appreciation is reserved for Zhizhen Wang. We both embarked on our PhDs and navigated the challenging postdoc application process in the same academic years. Our research areas are relatively close, and we attended conferences together many times. Through this journey, we shared impressive academic information and rumors, exchanged various emotional and dramatic life experiences, and provided crucial mutual support and encouragement.

永结无情游，相期邈云汉。（李白《月下独酌》）

Bind an eternal friendship, transcending all emotion, and meet amid the distant Milky Way. (Li Bai, "*Drinking Alone under the Moon*")

I extend my profound gratitude to the **China Scholarship Council** (CSC) for their foundational financial support throughout my PhD period. Their indispensable contribution made it possible for me to pursue this enriching and significant PhD position at Utrecht University.

I am also thankful to the Ministry of Finance of the Netherlands for providing the rent allowance, which significantly eased my financial burden of the high room rents in Utrecht.

The four years of my PhD journey presented various health problems. I am grateful to all the medical professionals who provided care, including family doctors, psychotherapists, and psychologists, in both the Netherlands and China. Furthermore, my appreciation goes to AON Insurance for covering the majority of my

medical expenses.

Finally, I would like to thank the Universe, which is so attractive as to capture my curiosity, so mysterious as to sustain my lifelong exploration, and so fine-tuned as to allow my fleeting stay in this small patch of spacetime.

吾生也有涯，而知也无涯。（庄周《庄子 · 养生主》）

My life is finite, while knowledge is infinite. (Zhuang Zhou, "*Zhuangzi: Nurturing Life*")

哀吾生之须臾，羡长江之无穷。挟飞仙以遨游，抱明月而长终。知不可乎骤得，托遗响于悲风。（苏轼《赤壁赋》）

Grieving my life's brief instant, I envy the river's endless flow. I would roam with winged immortals, embrace the lucid moon and dwell forever. Knowing such dreams are not won, I consign these lingering notes to the sorrowing wind. (Su Shi, "*Ode on the Red Cliff*")

About the author

Guoen Nian (念国恩) was born on 19 September (the 7th of the 8th lunar month) 1996 in Liaocheng, Shandong, China.

From 2014 to 2018, he studied physics at Taishan College of Shandong University, earning his bachelor's degree. His bachelor's thesis was under the supervision of Shiyuan Li, focusing on an algorithm for QCD jets.

From 2018 to 2021, he pursued a master's degree in physics at LMU Munich, graduating with master's thesis *Field Geometry, Scalar Potentials and the Swampland Distance Conjecture*, supervised by Dieter Lüst and Marco Scalisi.

From 2021 to 2025, he conducted his PhD research at the Institute for Theoretical Physics of Utrecht University, under the supervision of Stefan Vandoren. His work focused on string phenomenology, including string compactifications, the Swampland program, and string cosmology. The main results of this period are presented in this dissertation.

He will continue as a postdoctoral researcher at Peking University.